

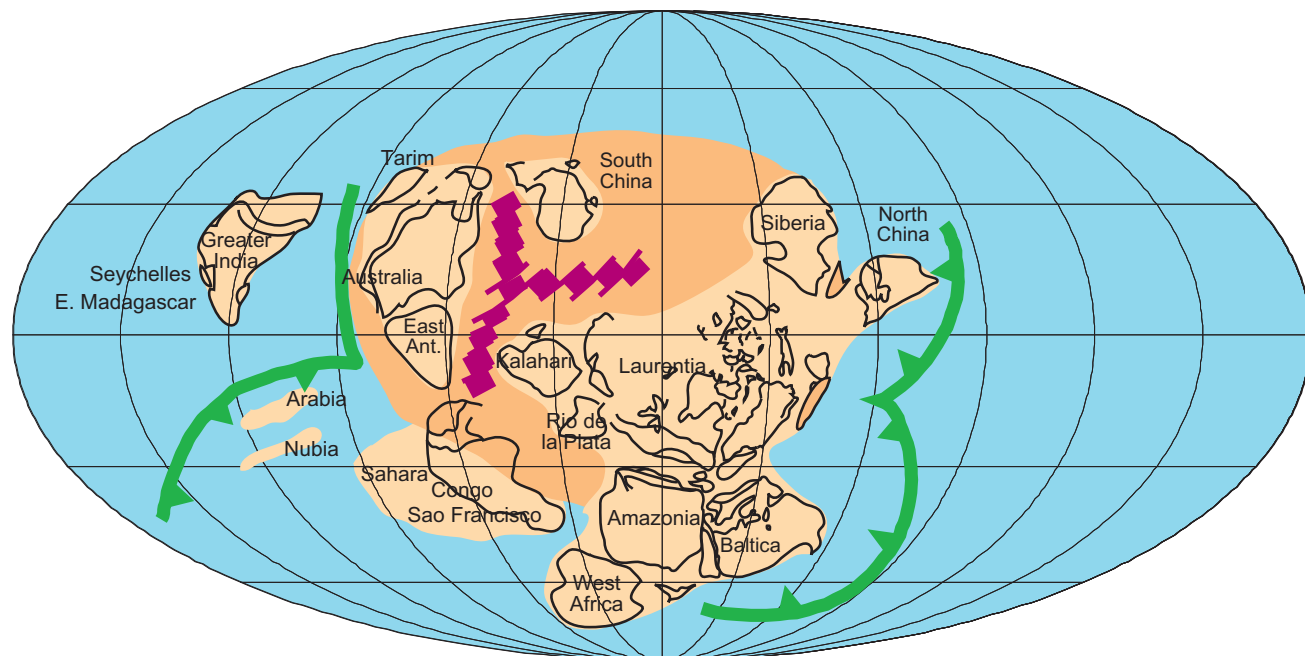
c0016 A Chronostratigraphic Division of the Precambrian:

Possibilities and Challenges

Martin J. Van Kranendonk

Contributors: Wladyslaw Altermann, Brian L. Beard, Paul F. Hoffman, Clark M. Johnson, James F. Kasting, Victor A. Melezhik, Allen P. Nutman, Dominic Papineau and Franco Pirajno

720 Ma Precambrian



Chapter Outline

16.1. Introduction	314	
16.1.1. Rationale	315	
16.2. Historical Review	317	
16.2.1. Timescale Divisions and Stratigraphic Principles	317	
16.2.2. Historical and Current Subdivisions of the Precambrian	318	
		16.2.2.1. Logan's (1857) Laurentian-Huronian Boundary and Stockwell's 'Kenoran' Event 318
		16.2.2.2. Many Countries, Many Timescales 319
		16.2.2.3. Cloud's Timescale and the Hadean 319
		16.2.2.4. The Current Precambrian Timescale 321

16.2.2.5. The Geon Concept	321	16.3.3.4. Breakout Magmatism, the Lomagundi-Jatuli Carbon Isotopic Excursion, and the First Eukaryotes (2.25–2.06 Ga)	350
16.2.2.6. More Recent Suggestions	323	16.3.3.5. Global Orogenesis, Re-Appearance of BIF, Natural Uranium Reactors, and Shungite (c. 2.06–1.78 Ga)	359
16.2.3. Problems with Past and Current Precambrian Timescales	323	16.3.4. Adult Earth (~1.78–present)	360
16.2.3.1. Cloud's Timescale	323	16.3.4.1. Canfield Ocean (1.78 Ga–750 Ma)	363
16.2.3.2. The Current Precambrian Timescale	323	16.3.4.2. Eukaryote Diversification	363
16.2.4. Recent Advances in Precambrian Stratigraphy	326	16.3.4.3. Late Proterozoic Environmental Instability (850–582 Ma)	363
16.3. Precambrian Earth History		16.3.4.4. Increasing Oxygen, the Rise of Animals, and Post-Glacial Phosphorites	367
– A Progress Report	326	16.4. A Linked, Causative Series of Events in Precambrian Earth Evolution	368
16.3.1. Nascent Earth (4.567–4.03 Ga)	327	16.4.1. The Late Archean Superevent	370
16.3.1.1. Accretion of the Solar System (4.567–4.40 Ga)	327	16.4.2. The Rise in Atmospheric O ₂ and the LJE	372
16.3.1.2. Isotopic Evidence for an Early Basaltic Protocrust	329	16.4.3. Linked Events and GSSPs	373
16.3.1.3. Hadean Zircons from Jack Hills	330	16.5. A Revised Precambrian Timescale	373
16.3.1.4. Origins and Early Evolution of Life	330	16.5.1. A Hadean Eon	374
16.3.2. Juvenile Earth (4.03–2.78 Ga)	331	16.5.2. The Archean Eon	374
16.3.2.1. Early Crustal Remnants (4.03–3.53 Ga)	331	16.5.2.1. Paleoarchean Era: 4030–3490 Ma	374
16.3.2.2. Stable Cratonic Lithosphere and the First Signs of Life (3.49–2.82 Ga)	333	16.5.2.2. Mesoarchean Era: 3490–2780 Ma	374
16.3.2.3. Early Atmosphere and Climate	333	16.5.2.3. Neoarchean Era: 2780–2420 Ma	376
16.3.2.4. Early Life	338	16.5.3. The Archean-Proterozoic Boundary	377
16.3.3. Adolescent Earth (2.78–1.78 Ga)	340	16.5.4. The Proterozoic Eon	377
16.3.3.1. The Late Archean Superevent: Rapid Crust Formation and Explosion of Microbial Life (2.78–2.63 Ga)	340	16.5.4.1. Paleoproterozoic Era: 2420–1780 Ma	377
16.3.3.2. Continental Maturation, Rusting of the Oceans and the Widespread Microbial Production of Oxygen (2.63–2.42 Ga)	345	16.5.4.2. Mesoproterozoic Era: 1780–850 Ma	377
16.3.3.3. Mantle Slowdown, Global Cooling and the Great Oxygenation Event (2.42–2.25 Ga)	347	16.5.4.3. Neoproterozoic Era: 850–541 Ma	378
		16.5.5. Summary of Proposed Changes and GSSPs	378
		Acknowledgments	379
		References	379

s0010 16.1. INTRODUCTION

p0045 One of the principal current activities of the International Commission on Stratigraphy (ICS) is to erect Global Stratotype Section and Points (GSSPs) for the standard geological timescale, as a way of formalizing global chronostratigraphy. Once a complete and mature proposal for a GSSP is in place and (generally) published, that GSSP is subsequently ratified by IUGS. The intended outcomes of this task are an enhanced understanding of Earth evolution, a common language for geological research, and a means of communication with the general public about Earth Science issues. GSSPs have been identified and formally ratified through much of the Phanerozoic Eon at the Erathem (Era), System (Period), Series (Epoch), and Stage (Age) levels (paired names refer to chronostratigraphic (chronometric) divisions), including the first Precambrian GSSP defined for the Ediacaran Period at the top of the Neoproterozoic (Figure 16.1; Knoll et al., 2004).

p0050 The formal recognition of GSSPs through the rest of the Precambrian is more problematic, since current divisions are

chronometric and based on round number averages of minima of geotectonic activity, as compiled from an early 1980s summary of global geological data (Figure 16.1 and Table 16.1; Plumb and James, 1986; Plumb, 1991). Although this scheme has served the geosciences community over the past 30 years, and has helped to emphasize some of the significant changes on Earth in Precambrian time, it is out of date and fails to do justice to the wealth of detail we now know about Precambrian Earth history.

The shortcomings of the current geotectonics-based p0055 chronometric division of Precambrian time are demonstrated in three principal ways. The main problem is that the chronometric boundaries are not tied to the actualistic rock record and thus do not represent *chronostratigraphic* divisions with which we can achieve the goals stated above (Bleeker, 2004a; Van Kranendonk, 2008; Van Kranendonk et al., 2008a). Indeed, successions show little, or no, significant changes in lithostratigraphy in cases where continuous stratigraphic records are preserved across existing timescale boundaries. For example in the Hamersley Basin of Western Australia, the

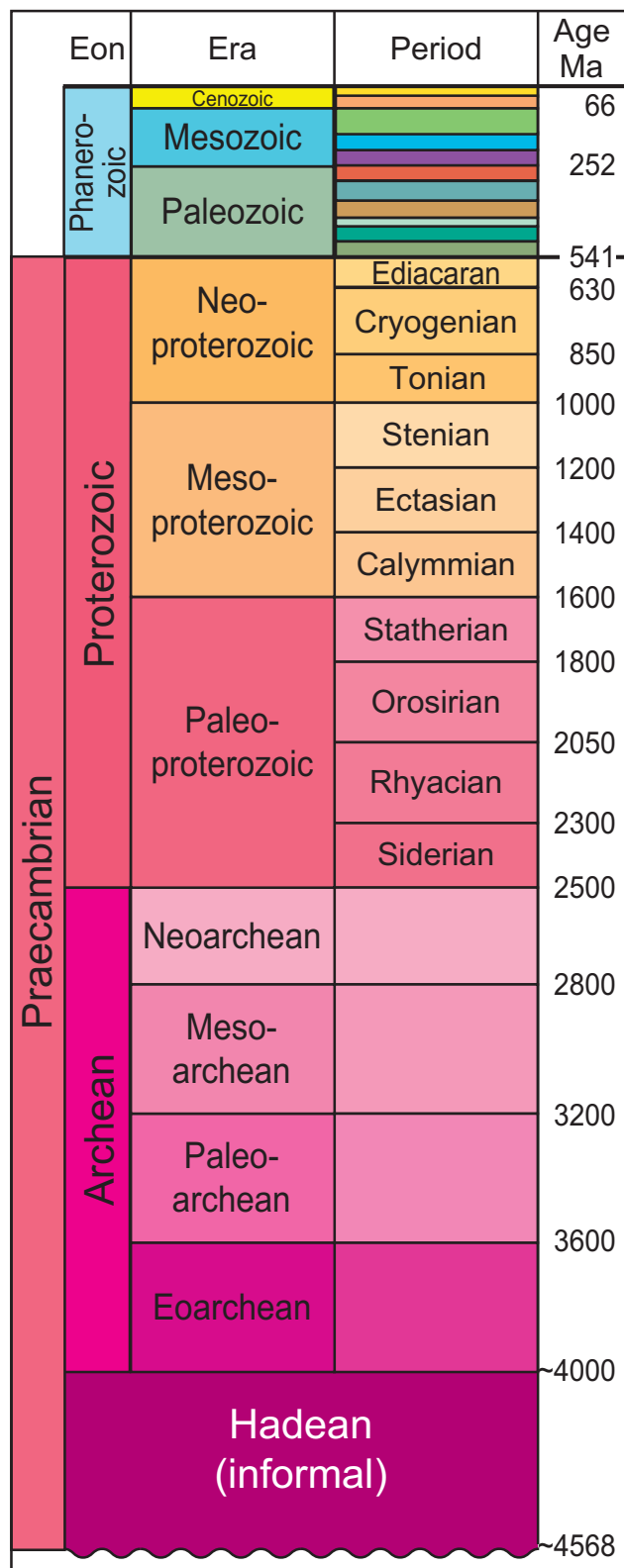


FIGURE 16.1 The current Precambrian timescale, from the International Commission on Stratigraphy, based on Plumb and James (1986) and Plumb (1991). Note that Precambrian is not a formal timescale unit and that all divisions of the Precambrian are chronometric except for the base of the Ediacaran, which is chronostratigraphic and marked by a GSSP. Only the ages of era boundaries are shown in the Phanerozoic (Ph), for simplicity.

Archean-Proterozoic boundary falls within the middle of a thick succession of shales and banded iron-formations (BIF), with no apparent lithologic changes on either side (Figure 16.2). The stratigraphic unsuitability of current timescale boundaries applies particularly to the 200–250 Ma long Period boundaries of the Proterozoic, which are rarely used in the literature as a result.

The second main problem with the current Precambrian timescale is that the global tectonic events on which the current scheme is based are known to be highly diachronous and thus cannot be used to accurately reflect changes on all continents equally well (Figure 16.3). The global diachroneity of the supercontinent cycle, for example, is well demonstrated by late Precambrian and Phanerozoic supercontinents, which were dispersing in some places at the same time as they were aggregating in others, so that the geotectonic record preserved in one continent differs dramatically from that in another (e.g., Rodinia: Li et al., 2008).

The third major shortcoming of the current Precambrian timescale is the lack of any formal representation of the very early history of the Earth, from the time of planetary formation to the undefined base of the Archean (Figure 16.1). However, we now have a much more thorough understanding of the first 500 Ma period of Earth history, including an age for the formation of the Earth and other planets of the solar system, a mechanism and age for the Moon-forming event, and the formation and destruction of early crust up to the age of the oldest solid rock on Earth, as described in Section 16.3.1.

As a result of these shortcomings, and because of a veritable explosion of new information on both the geological development and biological evolution of Precambrian Earth, the time is right to review the Precambrian and utilize the wealth of new information to erect a revised, more naturalistic, Precambrian timescale. In this chapter, I present a review of the 4 billion-year history of the Precambrian (Section 16.3) and develop a proposal for a chronostratigraphic division of Precambrian time, based principally on geobiological events that are recorded in the stratigraphic record, but also linked to global geodynamics in a whole-Earth model of planetary development (Sections 16.4 and 16.5).

16.1.1. Rationale

The proposed scheme developed herein follows the rationale of Cloud (1972: 538), who wrote in regards to the division of Precambrian time that:

“...we seek trend-related events that have affected the entire Earth over relatively short intervals of time and left recognizable signatures in the rock sequences of the globe. Such attributes are more likely to result from events in atmospheric, climatic, or biologic

t0010

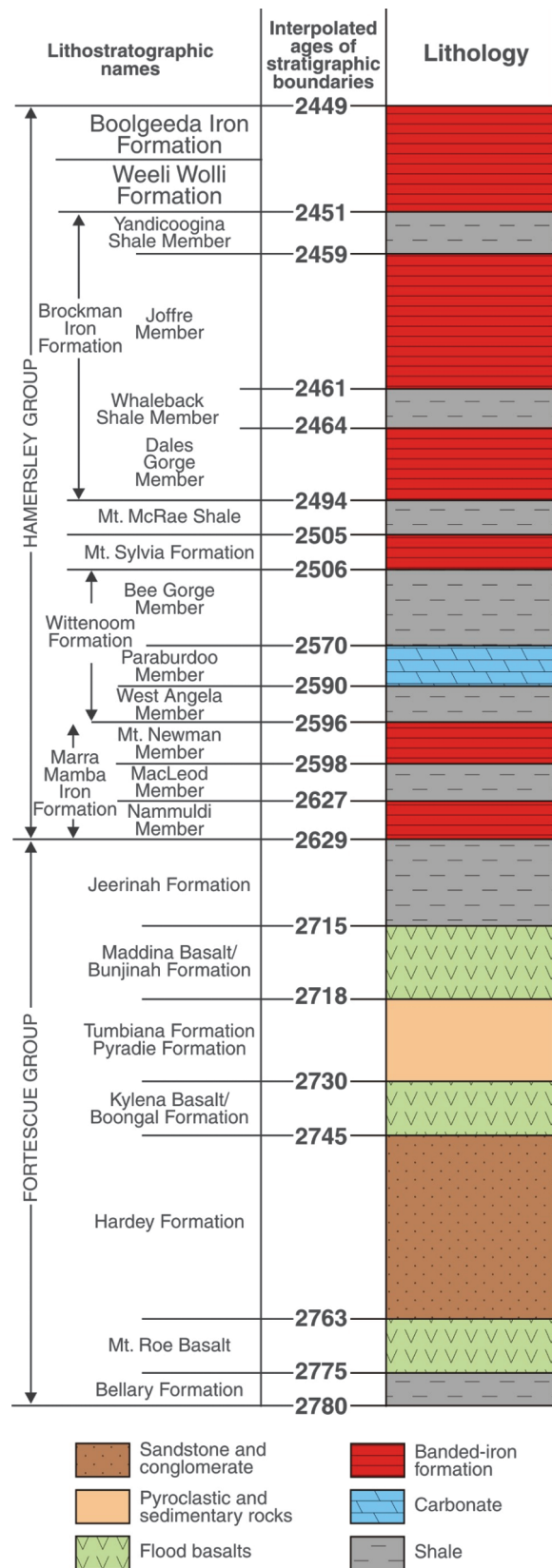
TABLE 16.1 Explanation of Nomenclature Used at the Period Level in the Proterozoic Eon in the Current ICS Geologic Time Scale

Period Name	Base	Derivation	Geological Process
EDIACARAN	GSSP, ~620 Ma	Ediacara = from Australian Aboriginal term for place near water	"Evolution of first megascopic marine animals"
		Oldest record of megascopic marine life. GSSP in Australia coincides with termination of glaciations and a pronounced carbon-isotope excursion	
CRYOGENIAN	–850 Ma	Cryos = ice; Genesis = birth	"Global glaciation"
		Glacial deposits, which typify the late Proterozoic, are most abundant during this interval	
TONIAN	–1000 Ma	Tonas = stretch	
		Further major platform cover expansion (e.g., Upper Riphean, Russia.; Qingbaikou, China; basins of Northwest Africa), following final cratonization of polymetamorphic mobile belts, below.	
STENIAN	–1200 Ma	Stenos = narrow	"Narrow belts of intense metamorphism & deformation"
		Narrow polymetamorphic belts, characteristic of the mid-Proterozoic, separated the abundant platforms and were orogenically active at about this time (e.g., Grenville, Central Australia)	
ECTASIAN	–1400 Ma	Ectsis = extension	"Continued expansion of platform covers"
		Platforms continue to be prominent components of most shields	
CALYMMIAN	–1600 Ma	Calymma = cover	"Platform covers"
		Characterised by expansion of existing platform covers, or by new platforms on recently cratonized basement (e.g. Riphean of Russia)	
STATHERIAN	–1800 Ma	Statheros = stable, firm	"Stabilisation of cratons; Cratonization"
		This period is characterized on most continents by either new platforms (e.g. North China, North Australia) or final cratonization of fold belts (e.g. Baltic Shield, North America)	
OROSIRIAN	–2050 Ma	Orosira = mountain range	"Global orogenic period"
		The interval between about 1900 Ma and 1850 Ma was an episode of orogeny on virtually all continents;	
RHYACIAN	–2300 Ma	Rhyax = stream of lava	"Injection of layered complexes"
		The Bushveld Complex (and similar layered intrusions) is an outstanding event of this time; the age of the Bushveld seems unlikely to change dramatically	
SIDERIAN	–2500 Ma	Sideros = iron	"Banded iron formations"
		The earliest Proterozoic is widely recognized for an abundance of BIF, which peaked just after the Archaean-Proterozoic boundary	

evolution than plutonic evolution and hence should be more characteristic of the sedimentary record than of the igneous or metamorphic record, although the latter must be included in any meaningful global assessment."

p0085 This rationale is based on the observation that biological evolution operates at a rate several orders of magnitude faster than crust-forming events; i.e. tens of years to a million years for biological evolution (e.g., Grant and Grant, 2008), versus 100s of millions of years for crust-forming events

(e.g., Condie, 1998). Thus, a change in Precambrian atmosphere composition, or balance of the global carbon budget, will be recorded in the rock record as a near-instantaneous horizon in comparison with changes in geotectonic development and, importantly, across a range of depositional environments. But we must also recognize that the biogeochemical cycles defined in the ancient rock record by variations in C, S, O and Sr and their isotopes, are controlled by tectonics of plate re-organization through orogeny, which provides nutrients to the oceans through weathering; ultimately, these changes are



f0015 **FIGURE 16.2** Stratigraphic column of Hamersley Basin, showing available geochronology (adapted from Trendall et al., 2004). Note that the current Archean-Proterozoic boundary lies within a continuous section of alternating iron-formation, shale and carbonate, within the Mt McRae Shale (tip of bold arrow, at right).

driven by changes in heat flow coming out of the mantle (Cameron, 1982; Des Marais et al., 1992; Veizer et al., 1999; Godderis and Veizer, 2000; Lindsay and Brasier, 2002; Squire et al., 2006; Campbell and Allen, 2008).

A critical aspect in the perspective of any historical p0090 analysis is the recognition of causative mechanisms behind change, as outlined by Gould (1994, p. 5):

“The organizing principles of history are directionality and contingency. Directionality is the quest to explain (not merely document) the primary character of any true history as a complex, but causally connected series of unique events, giving an arrow to time by their unrepeatability and sensible sequence. Contingency is the recognition that such sequences do not unfold as predictable arrays under timeless laws of nature, but that each step is dependent (contingent) upon those that came before, and that explanation therefore requires a detailed knowledge of antecedent particulars.”

With these guiding principles in mind, this Precambrian p0100 Chapter contains five major sections. Section 16.1 is an Introduction; Section 16.2 presents a review of the history of Precambrian timescale division; Section 16.3 discusses the series of major events in Precambrian Earth history; Section 16.4 proposes a model for the causative links behind changes in Precambrian Earth history; and Section 16.5 presents a proposal for a revised, chronostratigraphic division of Precambrian time. This new proposal better reflects the developmental stages of the early Earth and the processes through the whole of Precambrian time that gave rise to our modern Earth and the complex biosphere it supports.

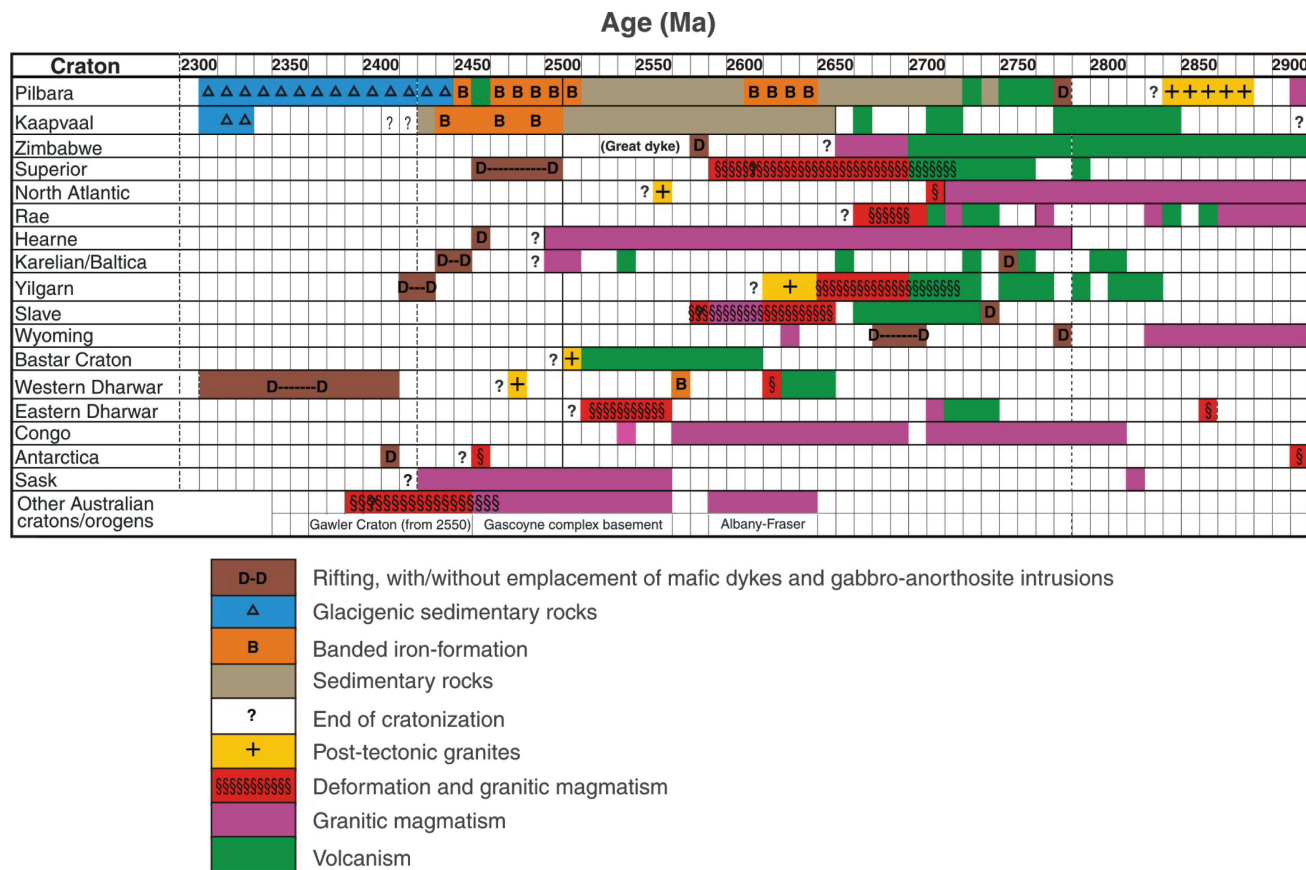
16.2. HISTORICAL REVIEW s0020

16.2.1. Timescale Divisions and Stratigraphic Principles s0025

As outlined in Chapter 1 of this volume, the main benefit of p0105 a geological time scale is that it provides geologists with a common and precise language to discuss geologic time and unravel Earth’s history. A primary goal of the ICS is to unite the individual regional scales by reaching consensus on a standardized nomenclature and hierarchy for stages defined by precise GSSP’s, wherever possible; in this “correlation precedes definition” (Remane, 2003: 8).

Most GSSPs coincide with a single primary marker, which p0110 is generally a biostratigraphic event, but other events with widespread correlation – such as a rapid change in isotope values or a geomagnetic reversal – also bracket or define GSSP’s. Unconformities or hiatuses near the boundary interval must be avoided.

Following the principle of communication, the major p0115 geologic time scale divisions (Eons, Eras, and perhaps System/Periods) must also be applicable to making geological maps. And at some level, the timescale should permit



f0020 **FIGURE 16.3** Compilation of events for a selection of cratons, showing diachroneity in the ages of cratonization and emplacement of mafic dykes.

clear and concise communication with the general public, to give some idea of the events that led to modern Earth.

s0030 **16.2.2. Historical and Current Subdivisions of the Precambrian**

s0035 **16.2.2.1. Logan's (1857) Laurentian-Huronian Boundary and Stockwell's 'Kenoran' Event**

p0120 For several decades prior to the advent of precise geochronology and widespread dating of rocks, it was considered that the rock record showed a principal division between mobilist cratonic areas and stable continental platform successions. Early results from K-Ar dating indicated that this transition occurred at roughly 2.5 Ga, an age that continues to be used as the division between the Archean and Proterozoic eons.

p0125 The earliest division of Precambrian rocks was made by Sir William E. Logan, who divided what at the time were referred to as the Azoic rocks of Canada into two "stratigraphical groups". These included an older Laurentian series of gneiss, with generally steep dips of layering, and a younger, overlying Huronian Series of sedimentary rocks that are characterized by low dips of bedding and include conglomerates that contain pebbles and boulders of the adjacent gneiss (Logan, 1857).

In this short paper, Logan correctly inferred that the Huronian series had not been deposited until the Laurentian series had been transformed into gneiss. Significantly in terms of time scale issues, Logan also recognized a distinct and important feature of the Huronian series, in that it contained red feldspar and blood-red jasper pebbles, which subsequent studies have shown relate to the onset of an oxidizing atmosphere (see Section 16.3.3).

More than a century later, Stockwell (1961, 1973) identified a cluster of K-Ar dates around 2480 Ma in the Superior Province of Canada. He used this data to identify a late Archean "Kenoran" event of mountain building, accompanied by folding. This event correlates with the orogenic event that Logan identified as having affected the older Laurentian series prior to deposition of the Huronian series (now the Huronian Supergroup). It is this relationship and this age that continues to influence the Precambrian timescale to this day, as the current Archean-Proterozoic boundary.

Subsequently, the advent of more precise U-Pb zircon dating led Stockwell (1982) to subdivide the Kenoran orogeny into an early phase around 2650 Ma (based on U-Pb zircon and titanite ages), and a later phase near 2555 Ma (mostly based on Rb-Sr whole rock isochron ages). These events are recognized in the middle to lower crustal section

exposed in the Kapuskasing uplift, where U-Pb dates on metamorphic monazite and titanate indicate that Superior Province crust continued to deform and cool through to ~2594 Ma (Krogh, 1993; Krogh and Moser, 1994). However, more recent work has shown that ca. 2512 Ma growth of zircons is, in fact, related to emplacement of the Matachewan dyke swarm and the onset of deposition of the Huronian Supergroup during continental rifting (Moser and Heaman, 1997; Moser et al., 2008).

s0040 16.2.2.2. *Many Countries, Many Timescales*

p0140 Until recently (but continuing through the present), many countries have used their own variations on the Precambrian timescale, based on geological observations within their national boundaries. Generally, this is true only for the countries having the largest areas (e.g., Russia, Canada, China), where a large amount of geology and a sufficient amount of work has provided a basis for timescale divisions. Significantly, this work has revealed that the geodynamic history differs between continents, making global correlations of geodynamic events near impossible. For example, Canada has historically used the names Aphebian (2500–1750 Ma), Helikian (1750–1000 Ma), and Hadrynian (1000–542 Ma) to subdivide the Proterozoic, and has employed ages of 3400 Ma and 3000 Ma to subdivide the Archean (Okulitch, 2004).

p0145 In eastern Europe, a major difference with the internationally approved timescale (Gradstein et al., 2004) is the widespread use of Vendian to describe both a fossil assemblage and a timescale division in the latest Precambrian (see review by McCall, 2006), both of which are now officially referred to as the Ediacaran, based on the type section in South Australia (Knoll et al., 2004).

p0150 Others have weighed in to the timescale debate on more local and theoretical grounds. For example, Moorbath (2005) suggested that the base of the Archean be placed at the age of the oldest known mafic and ultramafic lavas from the North Atlantic Craton, West Greenland, at c. 3.82 Ga (based on data in Nutman et al., 1997, 1999 and Crowley 2003). He further suggested that the Hadean be recognized as an Eon that extends from the formation of Earth to the end of the late heavy meteor bombardment at 3.85 Ga, and that the intervening period, from 3.85–3.82 Ga, be referred to as a transitional Hadeo-Archaean interval, during which Earth was resurfaced by global volcanism and sediment transport (Figure 16.4).

p0155 A key aim of the ICS is to overcome regional differences and decide upon sections and time scale events that are global and useful in terms of lithostratigraphic nomenclature and understanding the history of the Earth.

s0045 16.2.2.3. *Cloud's Timescale and the Hadean*

p0160 Preston Cloud (1972) devised one of the first holistic timescale divisions for the Precambrian, based on four broad modal trends in Earth history prior to the onset of the

Phanerozoic (representing geologically “modern” times; see Figure 16.5).

Cloud identified the oldest modality as the *Hadean*, p0165 a period of obscure geological record, from the formation of Earth to the age “...of the oldest confidently dated rocks”. Hadean is derived from the Greek word, Hades, the ancient Greek underworld, and misty abode of the (God of the) Dead (Hades), where all mortals go.

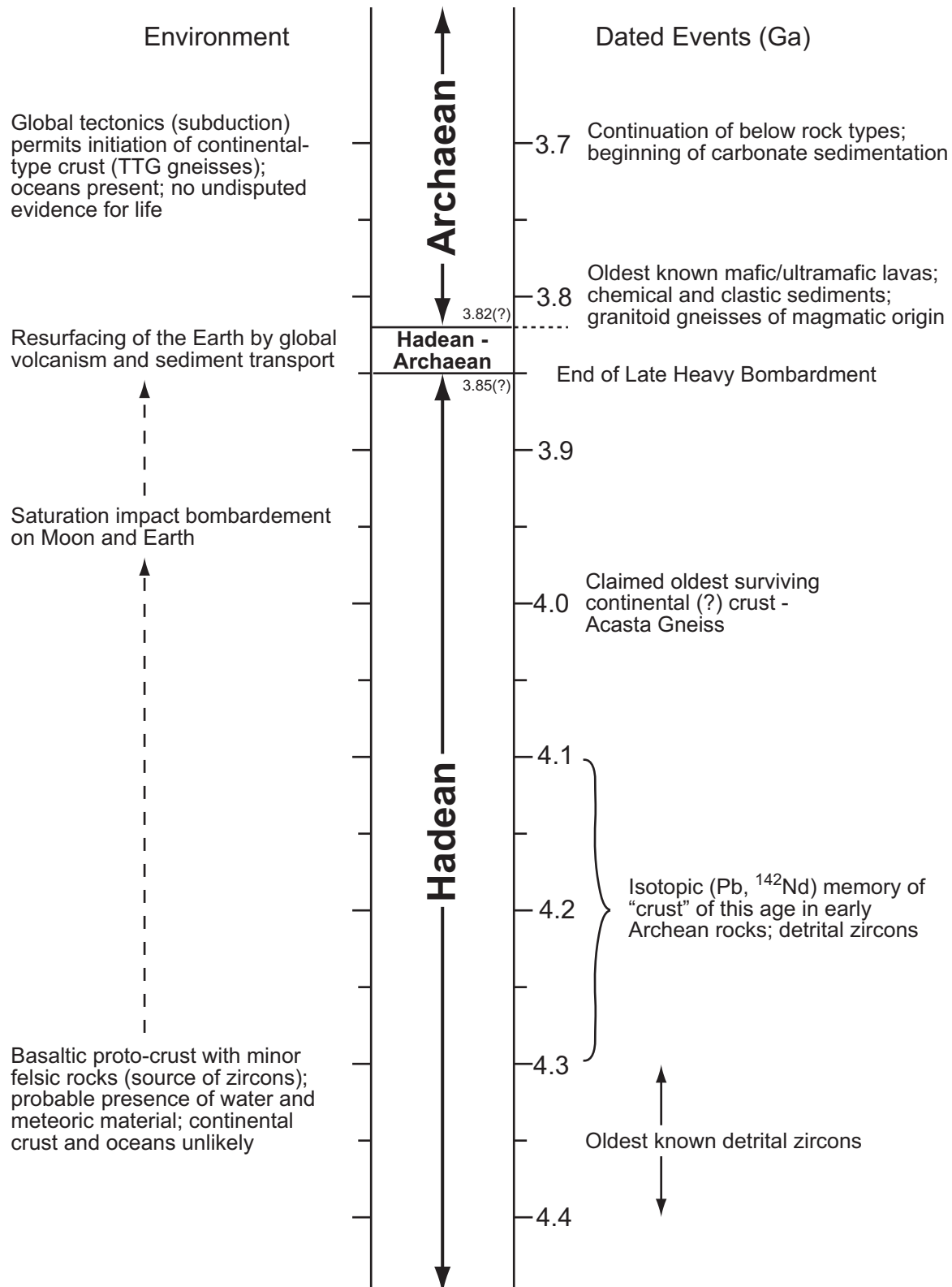
The second great modality was recognized as the *Archean* p0170 (derived from the ancient Greek word Arkhe, meaning beginning, or origin), from roughly 3.6–2.6 Ga, which includes dominantly granitic (granodioritic) rocks and gneisses with low K to Na ratios, enclosed or embedded in belts of greenstones and volcanoclastic graywacke-like sediments. He recognized that there was no free O₂ and that the first autotrophs produced complex organic compounds, such as carbohydrates, fats, and proteins, from simple inorganic molecules, using energy from light (by photosynthesis) or inorganic chemical reactions (chemosynthesis).

The third modality was an interval during which plutonic p0175 rocks became more potassic and sedimentary rocks more [AU1] cratonal (platformal), including plenty of clean quartzites and thick carbonate sections near the top of sequences that were terminated by great thicknesses of BIF. He stated that platform sediments of this modality were not subaerially oxidized, in contrast to those of the following (Proterozoic) mode. Cloud named this modality the *Proterophytic*, acknowledging “...the evolution of primitive plants (blue-green algae and bacteria)” (now called cyanobacteria), and he suggested that it covered the time interval of 2.6–1.9 Ga, or most of what is now the Paleoproterozoic.

The youngest modality was named the *Proterozoic* p0180 (derived from the Greek for ‘early life’, coined by S.F. Emmons in 1888, according to Windley, 1995), and characterized by oxidized platformal sediments, rarity of gypsum, and a preponderance of dolomite over calcite. The Proterozoic was also characterized by the absence of Metazoan fossils, tracks, burrows, or after-death imprints, and thus Cloud (1972) placed the upper boundary at c. 680 Ma, near the end of major glaciations and before the appearance of fossil evidence for multicellular life.

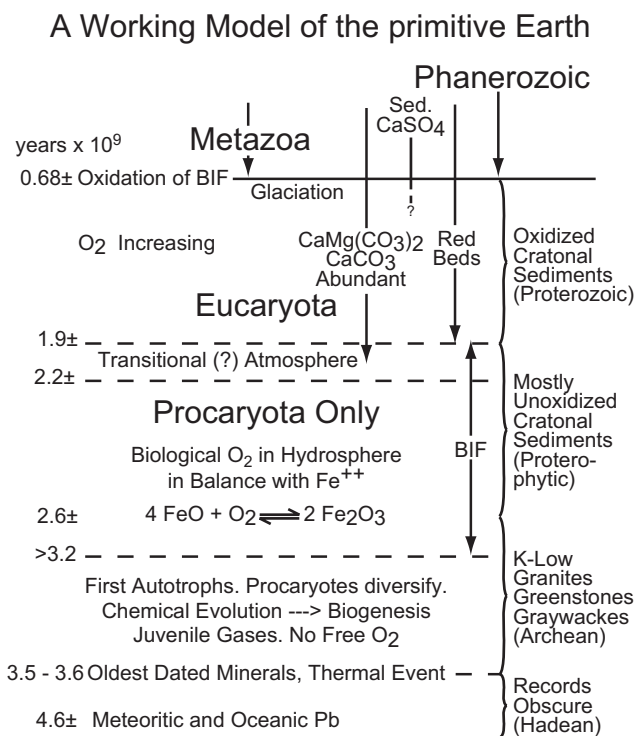
A principal observation in this scheme was that deposition p0185 of BIF ceased at nearly the same time as oxidized redbed deposits appeared in the geologic record, reflecting the onset of oxygenation of the atmosphere. Cloud (1972) also recognized that oxygenic photosynthesis was the main source of free oxygen in Earth’s atmosphere and oceans and he argued that the deposition of widespread BIF before c. 1.9 Ga was probably the result of biological O₂ production in the hydrosphere that was in fluctuating balance with a sink of ferrous iron in solution in seawater, an idea rejuvenated by Brake et al. (2002) and Konhauser et al. (2002). Another important observation was that O₂ could accumulate no faster than a chemically equivalent mass of carbon is sequestered,

Mantle Differentiation (c. 4.45 Ga)



f0025

FIGURE 16.4 Sketch of dated events, environments, and suggested timescale divisions for early Earth according to Moorbath (2005).



f0030 **FIGURE 16.5** Cloud's (1972) view of the evolution of the early Earth, showing the principle characteristics relating to biological change.

and recognized that the first appearance of significant carbonaceous deposits (metacoal or shungite deposits in Russia) equated with this time interval and related to oxygenation of the atmosphere (see Melezhik et al., 2005a).

p0190 The Plumb and James (1986) chronometric timescale for the Precambrian, which was adopted by the ICS in 1990 (Plumb, 1991, see next section), subsumes this fundamental transition to an oxygenated atmosphere within the Paleoproterozoic Era, whose upper boundary was placed at 1600 Ma.

s0050 16.2.2.4. The Current Precambrian Timescale

p0195 Plumb and James (1986) provided the basis for the current Precambrian timescale (Figure 16.1), in which:

"...Precambrian time...shall be divided according to the chronometric division...in which time boundaries have been selected so as to enclose or delimit principal cycles of sedimentation, orogeny, and magmatism, but in which boundaries are defined in years without specific reference to any bodies of rock....Rock units should be assigned into that timescale only on the basis of the interpretation or perception of the unit's isotopic age..."

(Plumb, 1991, p. 139).

p0210 The Plumb and James (1986) timescale reflects global geodynamic events that are based on a compilation of "comprehensive time-rock charts" completed in the early 1980s, near the start of the precise U-Pb zircon-dating

revolution that has since transformed Earth Science and our understanding of the planet in so many ways. This timescale was based on comparing events in different cratons and choosing appropriate chronometric (round number) boundaries at times of minimal activity or actual gaps in the known geological record that suited most, or at least the best-known, cases. In this way, the boundaries represent averages of processes that are gradational over periods of hundreds of millions of years.

The Precambrian is not a formal stratigraphic unit, but p0215 simply refers to all rocks that formed prior to the beginning of the Cambrian Period (base of Phanerozoic) and by its very nature therefore includes the full period of time back to the formation of the Earth. The current scheme reaffirmed the pre-existing Archean and Proterozoic Eons, but at the time of publication, the age of the Earth was not well defined and the knowledge concerning Earth's oldest rocks was poorly constrained. This is reflected in the current timescale by an undefined base of the Archean Eon, although it is roughly indicated at about 4.0 Ga. The Archean Eon is currently subdivided into four eras; the c. 4.0–3.6 Ga Eoarchean, 3.6–3.2 Ga Paleoarchean, 3.2–2.8 Ga Mesoarchean, and 2.8–2.5 Ga Neoarchean (Figure 16.1).

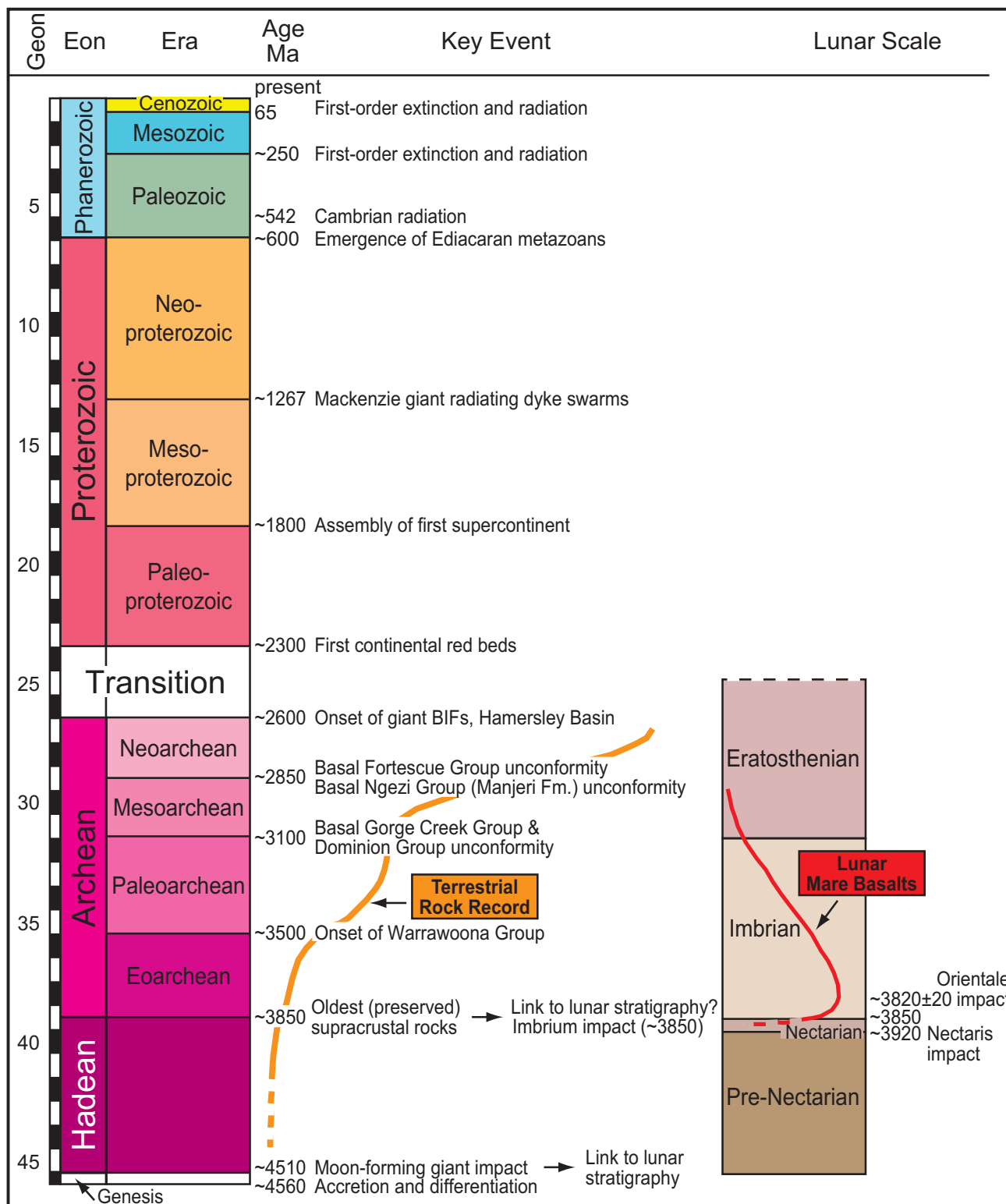
The Proterozoic Eon begins at 2.5 Ga, which is the p0220 approximate time by which most granite-greenstone crust had formed. The Proterozoic Eon is subdivided into 10 periods, generally of 200-Ma duration, grouped into three eras: the 2.5–1.6 Ga Paleoproterozoic, 1.6–1.0 Ga Mesoproterozoic, and 1.0 Ga–542 Ma Neoproterozoic (Figure 16.1). Except for the Ediacaran Period, the Proterozoic periods were chosen to reflect large-scale tectonic or sedimentary features (Plumb, 1991). The base of the Cryogenian Period/System is currently not defined, but estimated to be around 850 Ma.

16.2.2.5. The Geon Concept

The Geon (*geological eon*) concept has been advocated by p0225 Hofmann (1990) as a way of overcoming regional differences in stratigraphy and nomenclature, and the problems associated with an imperfect geological record. The idea is to use a universal calendar system with numerical units appropriately large enough to encompass major geological developments (basin formation, orogenic belts, etc.), but independent of regional variations in these events. Geons are specified 100-million-year intervals of geological time, counted backwards from the present and numbered after the first integer of each 100-million-year period (Figure 16.6); e.g., 65 million years ago belongs in Geon 0, 180 million years ago belongs in Geon 1, 3465 million years ago belongs in Geon 34.

According to Hofmann (1990), benefits of the Geon p0230 concept include:

1. it is numerical, direct and simple u0020
2. it is easy to learn, remember and apply o0015
3. it is necessary to learn only one word o0020



f0035

FIGURE 16.6 Suggested Precambrian timescale proposed by Bleeker (2004a). Geon scale after Hofmann (1990).

- o0025 4. it transcends language barriers
- o0030 5. it is geopolitically neutral
- o0035 6. it is a logical extension of the calendar system
- o0040 7. it provides time slices of equal duration
- o0045 8. it is versatile and facilitates quantitative studies
- o0050 9. it is applicable beyond Earth to planets and stars
- o0055 10. it is helpful in communicating with non-geologists.

p0285 Although there are some advantages to a purely chronometric, Geon-based timescale, it fails as a primary timescale in the same way and for the same reasons that the current Precambrian timescale fails – it is based on round numbers and has no basis in real Earth rocks. This does not mean that Precambrian time cannot, or should not, be divided into Geons and used in parallel with a chronostratigraphic timescale: it can, and geochronologists and many geologists will always talk about Precambrian rocks in terms of their age (e.g., “The 2720–2650 Ma granite-greenstone belts of the Yilgarn Craton, Western Australia were deformed at 2630 Ma during orogeny related to...”). And certainly, for purposes of quantitative (areal, volumetric, and temporal) analysis, the Geon timescale may provide a useful tool. But dividing the history of the Earth into 100-million-year time bins does nothing to convey the nature and rates of evolutionary changes of our planet and the life upon it, nor does it indicate the contingency of history in the development of these changes, and thus the Geon concept fails as a means to communicate with non-geologists, one of the principal requirements of any timescale. Furthermore, a Geon-based timescale would be impractical for mapping purposes.

s0060 16.2.2.6. *More Recent Suggestions*

p0290 Bleeker (2004a, b) suggested a more naturalistic approach to the Precambrian timescale (Figure 16.6). He suggested the use of a period of accretion and differentiation, in addition to a Hadean Eon for the early history of the Earth (following Cloud, 1972). In addition, and also following Cloud (1987), Bleeker (2004a) suggested that a transitional period between the Archean and Proterozoic be established, from the base of giant iron formations to the first appearance of bona fide redbeds, thus recognizing the transition to an oxygenated atmosphere (Figure 16.6). He suggested that features such as the Great Dyke of Zimbabwe might be a useful time marker, if equivalents could be found in stratified rocks, and since then he has attempted to “barcode” the geological history of continents in terms of their mafic magmatic events (Bleeker and Ernst, 2006).

p0295 Robb et al. (2004) suggested using stable isotope stratigraphy (C, O, Sr and S) in the Precambrian to denote periods of significant change, specifically for the Neoproterozoic, but potentially also for the period of oxygenation of the atmosphere.

p0300 Zalasiewicz et al. (2004) suggested ending the distinction between the dual stratigraphic terminology of time-rock units

(of chronostratigraphy) and geologic time units (of geochronology). In their view, chronostratigraphy should be used to define eons, eras, and periods, etc., whereas geochronology should be used to refer to numerical age dating. They also suggested the use of early and late as subdivisions of chronostratigraphic units, rather than lower and upper.

As mentioned earlier, Moorbath (2005) advocated that a Hadean Eon extend from the time of formation of the solar system (denoted as T_0) until what he inferred was the end of the Late Heavy Bombardment at 3850 Ma (Figure 16.4). He also envisaged a transitional Hadeo-Archean period, during which Earth was resurfaced by global volcanism and sediment transport prior to the formation and stabilization of the oldest intact piece of crust in Western Greenland. He envisaged this period as lasting only a few tens of millions of years and regarded this as “...the most influential and exciting part of Earth’s entire geological time scale.” (Moorbath, 2005: 822).

Nisbet (1991) suggested the upper boundary of a “Hadean Eon” be placed at the moment of the first self-replication on Earth, but noted that we do not know when that moment was, a situation which is likely to remain for some time and thus renders this suggestion impractical. Goldblatt et al. (2009a) proposed a Chaotian Eon for the period of planet formation, and a Hadean Eon for the following, early period of Earth history up to 4.0 Ga. These authors further proposed subdivision of the Hadean into three eras (Paleo-, Meso- and Neo-) and each era into two periods, based on aspects of the geological record. These aspects will be further discussed below (see Section 16.5).

16.2.3. Problems with Past and Current Precambrian Timescales s0065

16.2.3.1. *Cloud’s Timescale* s0070

Although elegant in its broad outline, Cloud’s (1972) timescale has some difficulties in practical terms, the most significant of which is the diachronous timing of cratonization of Archean terrains and the appearance of platformal sedimentary successions (transition from modality 2 to 3 of Cloud, 1972). It is now known that this process was highly diachronous from one craton to the next, with some cratonic nuclei having formed by 2.83 Ga with a 2.78–2.63 Ga platformal cover sequence (Pilbara Craton and Mount Bruce Supergroup, Australia), others with 2.65 Ga cratonization ages and 2.45–2.2 Ga cover sequences (e.g., Superior Craton and Huronian Supergroup, Canada), and still others with 2.0 Ga granite-greenstone type crust and still younger cover sequences (e.g., Fennoscandian Shield) (Figure 16.3).

16.2.3.2. *The Current Precambrian Timescale* s0075

Several features of the current ICS stratigraphic chart relating to the Precambrian timescale have raised concern within the geological community, primary among which is the

chronometric scheme used for Eon, Era and System/Period boundaries that are based purely on round-number chronometric divisions and ignore stratigraphy (Cloud, 1987; Bleeker, 2004a, b).

p0325 The current chronometric scheme for Precambrian time was partly chosen because of a relative paucity of potential biological criteria. Round number divisions of the scheme has worked reasonably well because there was relatively little precise geochronological information available at the time of compilation (more than 30 years ago) to disprove these broad divisions. The existing chronometric scheme is now unsatisfactory because there has been a veritable explosion of new geoscientific information on the geodynamic evolution of Precambrian terrains and on the geobiological evolution of the planet. In addition, there are now thousands of precise U-Pb zircon age dates, and many detailed isotopic studies of stratigraphic sections. The new data has revealed that many of the current divisions are either misplaced in terms of global geodynamic events, impractical in terms of global correlation, or meaningless in terms of significant lithostratigraphic, biogeological, and biogeochemical changes that have since been recognized and critically assessed to a significant degree across the globe.

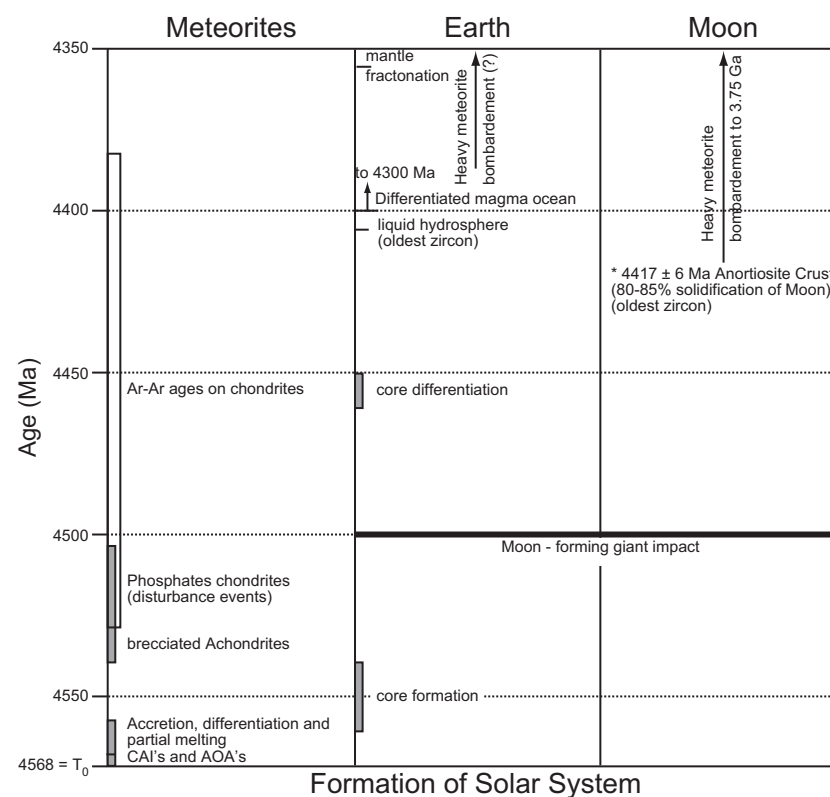
s0080 **Undefined Base of the Archean**

p0330 One of the most unsatisfactory aspects of the current ICS timescale is the undefined lower boundary of the Archean

and un-ascribed nature of events in the early history of the Earth (Figure 16.1). One of the key advances in understanding Earth evolution has been the discovery of truly ancient zircon crystals in Archean conglomerates at Jack Hills in Western Australia, which extend back to 4404 Ma and contain a wealth of information about conditions on very early Earth (Mojzsis et al., 2001; Wilde et al., 2001; Valley et al., 2002; Crowley et al., 2005; Cavosie et al., 2007; Ushikubo et al., 2008). Also significant has been the discovery of a number of very old terrains (older than 3.6 Ga) in cratons around the world, including what is currently Earth's oldest dated rock, the ca. 4030 Ma Acasta Gneiss in northern Canada (Bowring and Williams, 1999; see Van Kranendonk, 2007a). These discoveries, together with age dating of the Moon and meteorites, have yielded a great deal of knowledge about the early history of our solar system that is completely missing from the current timescale (Figure 16.7).

Critically, the current timescale does not include any p0335 reference to these early events, a time which is widely referred to in the literature as "the Hadean", following the initial definition by Cloud (1972). Currently, any use of Hadean is informal as it has not been defined, but its widespread and general usage suggests it should be considered for a formal subdivision of Precambrian time, as applied to the time period from around 4.0 Ga back to the age of formation of the Earth/solar system.

f0040 **FIGURE 16.7** Summary of early solar system events (compiled from the literature cited in Section 16.3.1).



s0085 Archean Eras

p0340 The Eoarchean (?–3.6 Ga), Paleoarchean (3.6–3.2 Ga), Mesoarchean (3.2–2.8 Ga), and Neoarchean (2.8–2.5 Ga) eras of the Archean Eon broadly correspond to peaks in the amount of preserved crust. This is particularly so for the Neoarchean Era, when a great deal of highly mineralized granite-greenstone crust was formed (Barley et al., 1998; Condie, 1998, 2004). These divisions have been useful, in part because they each cover a considerable amount of time (300–400 Ma) in relation to geodynamic cycles and the cooling rate of the Earth, which is on the order of 50–100°C/Ga (Pollack, 1997; Herzberg et al., 2007). In geobiological terms, the Archean Eon is characterized by microbial life, with varied claims as to whether or not each of the three main branches of life (Archea, Bacteria, and Eukarya) had evolved during this time (see below). What is clear is that life left traces in the rock record as far back as 3.8–3.5 Ga and became much more widespread and varied in the rock record from 3.0 Ga onwards, in part because of the better preservation of younger rocks, and in part because of the wider development of shallow-water environments on stable, larger continents after this time. Ever more complete and detailed knowledge regarding the evolution of early life and continents has allowed for the better division of Archean time, as described below (see Section 16.3.2).

s0090 Archean-Proterozoic Boundary

p0345 Since the definition of the Archean-Proterozoic boundary at 2.5 Ga, it has become apparent that this age does not reflect a unique time of synchronous global change in tectonic style from mobile, soft and weak continental crust to stable, cold and rigid continental lithosphere, as was previously believed. Rather, it is now well understood that this process was highly diachronous on Earth, with stabilization of continental crust happening at different times in different places. For example, in the Pilbara Craton, the deposition of “post-tectonic” sedimentary and volcanic rocks of the Fortescue Group occurred at 2.78–2.63 Ga, at the same time as most “mobilist” Archean granite-greenstone crust formed on other cratons, including such large continental nuclei as the Superior (Canada) and Yilgarn (Australia) cratons (Percival, 2007; Kositcin et al., 2008) (Figure 16.3). And whereas most typical Archean granite-greenstone crust had formed by about 2.6 Ga, this is not the case everywhere. For example, the Dharwar Craton of India contains voluminous granites at 2.5 Ga, whose intrusion was accompanied by greenstone sagduction and formation of typical granite-greenstone patterns (Chardon et al., 1996, 1998). Furthermore, granite-greenstone type crust, including komatiites (an ultramafic extrusive igneous rock widely considered typical of the Archean and to erupt from hotter-than-present mantle; Arndt et al., 2008), continued to form until c. 2.1 Ga in West Africa (Abouchami et al., 1990; Boher et al., 1992; Sylvester and Attoh, 1992)

and the Guiana Shield (Capdevila et al., 1999), and until 2.0–1.9 Ga in the Central Lapland greenstone belt (Hanski et al., 2001) and in parts of the Trans-Hudson Orogen in Canada (e.g., the Flin Flon Belt: Stern et al., 1999; Syme et al., 1999) (see Section 16.3.3.4).

Another widely cited example of a possibly geodynamically significant event across the Archean-Proterozoic boundary is the emplacement of mafic dyke swarms during what has been interpreted as a global period of mafic magmatism at 2.45 Ga (Heaman, 1997). Indeed, Nisbet (1982) suggested that the Great Dyke of Zimbabwe could be used as a rock definition for the Archean-Proterozoic boundary. However, this so-called global event is in reality highly diachronous, as indicated by the fact that the first large mafic dyke swarm was emplaced into the Pilbara Craton at 2772 Ma, followed by emplacement of the Great Dyke of Zimbabwe at 2574 Ma, 2505–2490 Ma dykes in Karelia, 2496–2450 Ma dykes in Superior Craton (Matachewan dykes), 2445–2436 Ma dykes in Karelia, and a dyke swarms of a range of ages continuing thereafter (Figure 16.3; Wingate and Giddings, 1999; Wingate, 2000; Bleeker and Ernst, 2006).

A third major, and possibly the most significant, problem with the current Archean-Proterozoic boundary is that, in the few places where a continuous stratigraphic section is preserved that spans this boundary, the currently defined age of 2.5 Ga does not correspond with a major change in lithology. This is shown by the stratigraphy of the Hamersley (Australia) and Transvaal (South Africa) basins, which shows that 2.5 Ga falls in the middle of a long period of continuous BIF and alternating shale deposition that extends from 2.63–2.42 Ga (Figure 16.2). One criterion that does appear to change across this boundary, however, is the appearance of a negative Europium anomaly in shales, reflecting a dramatic increase in the (exposure and) weathering of granitic rocks (Taylor and McLennan, 1985). However, it is yet to be determined whether this is a temporally discrete, or a gradual, change, and whether or not this feature can be used as an effective chronostratigraphic time marker.

In summary, comparisons of global geodynamic and stratigraphic data show that the Archean-Proterozoic boundary, as currently defined, does not correspond precisely and uniquely with a global change in tectonic style, the onset of global mafic magmatism and rifting, or a distinct change in lithostratigraphy. For these reasons, it must be considered whether or not the current Archean-Proterozoic boundary should be redefined.

Proterozoic Eras

The Paleoproterozoic (2.5–1.6 Ga), Mesoproterozoic (1.6–1.0 Ga), and Neoproterozoic (1.0 Ga–542 Ma) eras vary significantly in duration (460–900 Ma) and encompass major changes both in Earth history and biological evolution.

For example, the Paleoproterozoic spans the rifting, amalgamation and rifting of supercontinents, as well as the re-appearance of significant volumes of BIF, the oxygenation of the Earth, the first appearance of Eukaryotes, and a number of other significant geobiological revolutions that are indicated by excursions in several different isotopic systems (see Section 16.3.3). There is concern that the Paleoproterozoic Era, in particular, is too long, and should be subdivided to better reflect some of these major changes in Earth history. Another aspect is that many significant tectonic and/or geodynamic aspects of Earth evolution are *not* reflected in the current timescale; for example, the appearance of the first ophiolites at c. 2.0 Ga (Kontinen, 1987; Scott et al., 1991), which some consider to mark the onset of truly modern plate tectonic processes (e.g., Hamilton, 1998, 2003, 2007; Stern, 2005).

p0370 There has also been criticism that the end of the Paleoproterozoic (1.6 Ga) does not tie in well with global geodynamic events and should better be placed nearer to 1.7 Ga, the end of most tectonic activity associated with amalgamation of the supercontinent Nuna (Columbia). The end of the Mesoproterozoic corresponds roughly with the terminal amalgamation of the supercontinent Rodinia (Li et al., 2008). However, Rodinia continued to amalgamate until c. 900 Ma, so the 1.0 Ga age for the end of the Mesoproterozoic is therefore also suspect in terms of practical use.

s0100 Proterozoic Systems/Periods

p0375 The round number subdivision of the Proterozoic into several Systems/Periods based on broad orogenic characteristics (Figure 16.1; Plumb, 1991) has not met with success and is only rarely used in the literature. Partly this is because the duration of each System/Period (200–250 Ma) is too short for geodynamic cycles (225–300 Ma, as reflected by worldwide cycles of eustatic sealevel change: Payton, 1977; Krapez, 1993), and partly because the suggested events do not occur on all continents.

s0105 16.2.4. Recent Advances in Precambrian Stratigraphy

p0380 Since the previous compilation of events relating to the division of Precambrian time was made in the 1980s, there has been a veritable explosion of geoscientific information, particularly in regard to the acquisition of high-precision U-Pb zircon dates of rocks and magmatic, metamorphic, exogenic, exoplanetary, and hydrothermal events, as well as rates of change (e.g., Krogh, 1973; Compston et al., 1984; Kröner et al., 1991; Krogh et al., 1993; Condie, 1998; Rasmussen and Fletcher, 2002; Davis, D. W. et al., 2003; Ireland et al., 2008). There have also been major advances in terms of high quality, detailed map coverage of large areas (Heather and Shore, 1999; Van Kranendonk, 1999; Percival et al., 2006; Van

Kranendonk et al., 2007a). Even more importantly, there has been the recognition and delineation of major global geobiological events (Fedonkin, 1996), most specifically the stepwise rise in atmospheric O₂ (e.g., Holland, 1984, 1994, 2002; Des Marais et al., 1992; Farquhar et al., 2000; Catling et al., 2001; Pavlov and Kasting, 2002; Farquhar and Wing, 2003), changes in the global carbon and sulfur cycles (e.g., Cameron, 1982; Hayes et al., 1992; Hayes, 1994; Mojzsis, 2007), extremes in global temperature over time (e.g., Kirschvink, 1992; Fedo et al., 1997; Hoffman et al., 1998; Kirschvink et al., 2000), and the interaction between mantle dynamics, geotectonics, geochemistry, and geobiology (e.g., Föllmi, 1995; Lindsay and Brasier, 2002; Squire et al., 2006; Pearson et al., 2007; Campbell and Allen, 2008). All of this has led to a more thorough understanding of Precambrian Earth and, particularly, to the causes behind changes preserved in the rock record. It is these major new advances – and there are several new, important papers every month! – that now gives the opportunity to construct a revised chronostratigraphic division of Precambrian time. What follows below is based on the published literature available to the beginning of 2011.

16.3. PRECAMBRIAN EARTH HISTORY – A PROGRESS REPORT

s0110

Ever since Earth formed from the accumulation of dust and gas as part of the solar system at T₀ (= 4567 Ma), our planet has undergone secular change. This was the result of slow cooling and compositional differentiation from a sphere of molten silicate material after the Moon-forming giant impact event at 4.50 Ga, to a planet with a core, mantle, and crust, and an atmosphere and oceans. Somewhere along the way – and quite early in its development – Earth also acquired a biological community of living organisms. These two components – the geodynamic and the geobiological – have co-evolved until the present day, with the additional influence of extra-terrestrial events which were more important early in Earth history, but that continued to affect biological evolution through to the Phanerozoic.

p0385

For almost four billion years prior to the Cambrian explosion of multicellular animals, life on Earth was dominated by single-celled organisms. This period of time is referred to as The Precambrian, an informal name that refers to the period of Earth history from the base of the Cambrian, at c. 541 Ma (see Chapter 19; Amthor et al., 2003; but see also Bowring et al., 2007), back to the formation of the planet at T₀ = 4567 Ma (see Section 16.3.1.1).

p0390

The lack of a diverse and well-preserved fossil record going back in time through the Precambrian, the generally decreasing volume of preserved crust, and increasing degree of metamorphism and tectonic disturbance of that crust over this time period, as well as the uncertainties in the

p0395

configuration of the continents, all contribute to making the establishment of a chronostratigraphic time scale for the Precambrian more challenging. Nevertheless, we have progressed a long way in our understanding of Earth evolution over its 4.5 billion year history, and have recognized a number of significant changes over time, not only in how the planet operated and why, but also in terms of how and when major evolutionary developments of the biosphere were achieved.

p0400 In this review, Precambrian Earth history is divided into four main stages of planetary development, based on rates of change as preserved in the rock record: *Nascent Earth* (4.56–4.03 Ga), *Juvenile Earth* (4.03–2.78 Ga), *Adolescent Earth* (2.78–1.78 Ga), and *Mature Earth* (1.78–present). Each of these stages contains a series of temporally distinct events, or periods, with characteristic rock (or in the earliest stage, isotopic and mineral) associations.

s0115 16.3.1. Nascent Earth (4.567–4.03 Ga)

s0120 16.3.1.1. Accretion of the Solar System (4.567–4.40 Ga)

p0405 Dating of meteorites using a wide array of isotope systems – including short-lived, now-extinct radionuclides – show that condensation and accretion of rocky components within the inner solar nebula occurred at $T_0 = 4567 \pm 1$ Ma, from material already depleted in the volatile elements that had earlier been swept by the solar wind to the outer nebula and incorporated into the giant gas planets (Figure 16.7; Allègre et al., 1995; Amelin et al., 2002; Bevan, 2007; Burkhardt et al., 2008; Nyquist et al., 2009; Bouvier and Wadhwa, 2010). The cited errors in this chapter section are those published by the original studies, but a new study by Brennecka et al. (2010) shows that the actual errors of early solar system events may be ± 5 Ma.

p0410 Ca-Al-rich refractory inclusions (CAIs) and amoeboid olivine aggregates were the first solids to form in the solar nebula, at between 4567.1 and 4568.3 ± 0.7 Ma, when the sun was an infalling (class 0) and evolved (class 1) protostar (Amelin et al., 2009; Kleine et al., 2009; Krot et al., 2009; Bouvier and Wadhwa, 2010). Chondrules and the fine-grained matrix of primitive chondrites formed 1–4 Ma after CAIs, as free-floating objects in the solar nebula, when the sun was a classical (class II) and weak-lined T-Tauri (class III) star (Baker et al., 2005; Hutcheon et al., 2009; Krot et al., 2009; Scott and Sanders, 2009). The subsequent process of collisional accretion to form protoplanetary bodies occurred in a stochastic fashion (Taylor, 2007), such that within only 500,000 years after T_0 , some protoplanetary bodies were fully accreted (Wadhwa et al., 2009). Most rocky bodies experienced core formation, differentiation and partial melting between 1–11 Ma after T_0 , while subsequent disturbance events continued to c. 4500 Ma, during late stages of accretion (Figure 16.7; Allègre et al., 1995; Carlson and Lugmair,

2000; Boyet et al., 2003; Walter and Trønnes, 2004; Baker et al., 2005; Bevan, 2007; Zahnle et al., 2007; Burkhardt et al., 2008; Krot et al., 2009).

Recent data from W isotopes suggests that Earth accretion p0415 initially progressed rapidly, over 10–30 Ma, through equilibrium accretion and metallic core segregation directly from the silicate mantle; the surface of Earth at this time would have been a magma ocean (Figure 16.7; Kleine et al., 2004; Jacobsen, 2005; Wood et al., 2008; Halliday and Wood, 2009). Mars differentiated within ~40 Ma of T_0 , and both it and the Earth are now thought to have formed from superchondritic bulk compositions (Caro et al., 2008; Kleine et al., 2009), although Walter and Trønnes (2004) have suggested that the non-chondritic Sm-Nd and Lu-Hf signature of upper mantle rocks on Earth may be accounted for by long-term isolation of Mg-perovskite, Ca-perovskite and ferropericlaite that crystallized and sank into the deep mantle during fractionation at c. 4356 Ma.

The discovery of isotopic similarity between Lunar and p0420 Earth rocks (Wiechert et al., 2001; Pahlevan and Stevenson, 2005; Toubol et al., 2007) discounted early models of Moon capture by Earth's gravitational field and led to the idea of their co-evolution through a Moon-forming giant impact event between a Mars-sized protoplanetary impactor, Theia (between 0.1–0.2 Earth masses), and nascent Earth that had attained 90% of its current mass (Figure 16.8; Jacobsen, 2005; Taylor, 2007; Zahnle et al., 2007). This giant impact event is now considered to have occurred late in the accretionary history, at ~4500 Ma, following a ~40 Ma hiatus in accretion: this event would have led once more to a magma ocean on early Earth (Kleine et al., 2004, 2009; Toubol et al., 2007; Halliday, 2008; Halliday and Wood, 2009).

Impact simulation models suggest that the vast majority of material in the Moon originated from the impactor, which p0425 collided with Earth with an impact angle near 45° (Figure 16.8; Canup, 2004, 2008). On Mars, a relatively large surface area is inferred to be ancient – c. 4500 Ma (Nyquist et al., 2001; Solomon et al., 2005), and recent studies suggest that the Martian hemispheric dichotomy occurred as the result of a late-accretionary giant impact, ~100 Ma after planetary accretion (Nimmo et al., 2008).

The weak gravity field of the Moon and dry accretion p0430 history led to development of its anorthositic crust, which formed through plagioclase flotation in a magma ocean, following solidification of 80–85% of the original melt within about 100 Ma of the impact event (4417 ± 6 Ma, Nemchin et al., 2009). This anorthositic crust insulated the molten mantle for a considerable period of time, leading to continuous magmatism from 4350–3900 Ma (Meyer et al., 1989). Interestingly, this age range is similar to that obtained from the Jack Hills detrital zircons on Earth (Figure 16.9; Pidgeon et al., 2010). On Earth, the greater gravitational energy allowed it to retain a water-rich atmosphere. The presence of water increases the solubility of plagioclase in

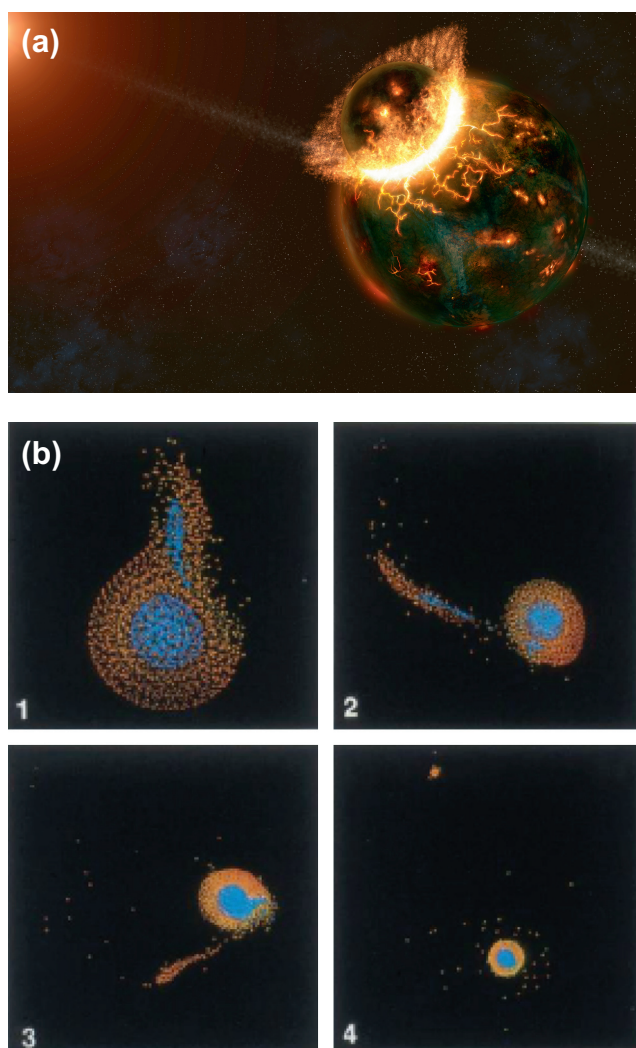


FIGURE 16.8 A) The Moon-forming giant impact event at c. 4.5 Ga, showing a Mars-sized protoplanetary body (Theia) colliding with a primitive Earth; B) Computer simulation model of the Moon-forming giant impact, in which oblique collision of protoplanet Theia with an already differentiated Earth (Blue core, orange mantle) causes the mantles of both to be vaporized. Some of this material ends up back in Earth orbit and forms a circumterrestrial disk from which the Moon coalesces shortly afterward. Both images from Spudis (1990).

melts and thus plagioclase did not crystallize within the early magma ocean and no anorthositic crust formed on Earth (Albarède and Blichert-Toft, 2007).

By 4.46–4.45 Ga, Earth had attained its present size, the core had differentiated, and the planet had retained its atmosphere (Allègre et al., 1995). The post-Moon forming magma ocean had completely differentiated by 4.4–4.3 Ga (Blichert-Toft and Arndt, 1999). Kramers (2007) suggested that freezing of the magma ocean would lead to a gravitationally unstable mantle, which overturned and led to the formation of a huge mafic crust. By 4 Ga, the mantle had already obtained its current redox state, due to loss of He^{2+} to

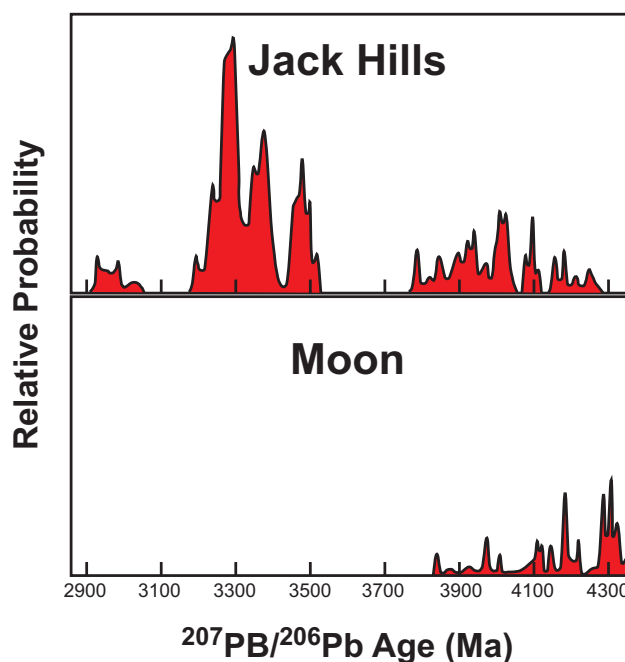


FIGURE 16.9 Comparative histogram of zircon ages from dated lunar samples and from detrital zircons from the Jack Hills greenstone belt. (redrafted from Pidgeon et al., 2010).

space and mixing of oxidants, such as ferric iron (Fe^{3+}), water, and carbonate (Arculus and Delano, 1980; Catling et al., 2001; Delano, 2001).

Xenon isotopes suggest that heat escaped much faster on early Earth than today, driven by magmatism, rather than conduction through the lithospheric lid, and that the surface was renewed over a time-scale on the order of 1–10 Ma for the first billion years of Earth history (Coltice et al., 2009). These results strongly argue against modern-style plate tectonics occurring prior to c. 3.5 Ga, or to significant formation of continental crust prior to this time (e.g., Bennett et al., 2010).

Heavy bombardment of the Moon continued, with the formation of many of the maria in the period 3.9–3.75 Ga, as a result of the impact of several large (100 km diameter) meteorites (Cohen et al., 2000). It is unclear, however, whether this period represents an unusual late heavy bombardment, or whether the spike in ages partly represents the effects of preservation potential and limited sampling of what was more likely a gradually decreasing intensity of meteorite bombardment since the Moon-forming impact event (Hartmann, 2003; Stöffler et al., 2006; Norman, 2009). Large impacts may have had a significant and long lasting thermal influence on the mantle, both on the Moon and Earth, causing widespread melting. Compositionally, too, these impactors may have added material as a “late veneer”, enriched in PGEs (platinum group elements), into the upper mantle (Maier et al., 2009). This, in combination with depletion of PGEs from lower mantle into the core, would

have led to an early mantle that was stratified in trace elements.

p0450 On Earth, only tiny zircon crystals and only a few small, scattered fragments of crust exist from the period 4.4–3.6 Ga. Given Earth's much greater mass, the continued meteorite bombardment that pummeled the lunar crust to 3.9 Ga must also have affected Earth. Evidence that Earth was affected by the late heavy bombardment is found in the form of Tungsten isotope heterogeneities from metasedimentary rocks of the Isua supracrustal belt, in western Greenland (Schoenberg et al., 2002). One possible reason for the lack of more direct evidence for this event (e.g., shocked zircons) is that along with its greater mass, Earth also contained more internal heat than the Moon and so contained a molten mantle and thinner crust than the Moon. Another possible factor is that the crust was largely basaltic and thus there were no zircons or quartz to be shocked by the impacts. The high energy and size of these late meteorites meant they would have penetrated Earth's crust and stirred the mantle, leading to resurfacing of much of the Earth by basaltic lavas. Thus, it is perhaps no coincidence that continental crust was not widely preserved on Earth until after the late heavy bombardment tailed off, after 3.9 Ga (Van Kranendonk, 2007a).

p0455 Early models envisaged the formation of Earth's atmosphere and oceans through volcanic outgassing of the mantle (Rubey and Poldervaart, 1955). However, it is now considered that delivery of these excess volatiles (H₂O, CO₂, N₂, HCl) to the surface proceeded through impact degassing during planetary accretion, such that the atmosphere and ocean should have started as the planet formed (Lange and Ahrens, 1982; Matsui and Abe, 1986a, b). Modeling studies show that accretion would have included material from the outer solar system (2.5–3.5 astronomical units), where icy planetesimals and meteorites have approximately the same deuterium/hydrogen ratio as do Earth's oceans: only ~10% of volatiles are considered to have been imported from comets (Morbidelli et al., 2000; Kasting and Catling, 2003).

p0460 Three possible sources of water on Earth have been proposed:

- o0060 1) Water-containing rocky planetesimals, similar to carbonaceous chondrites;
- o0065 2) Icy planetesimals, such as comets;
- o0070 3) The solar nebula.

p0480 However, the D/H ratio of water on Earth indicates that it did not come from comets. Rather, it is considered that Earth accreted in a dry state, and, although it may have had an early atmosphere, this would have been blasted off by the Giant Moon-forming impact event at 4.50 Ga, which created a magma ocean and vapor silicate atmosphere that lasted for several millions of years (Liu, 2004). It is now widely agreed that late addition of water was imported by icy asteroids, perturbed into Earth orbit by the gravitational effect of Jupiter (Albarède and Blichert-Toft, 2007; Kramers, 2007).

Solidification of the magma ocean resulted in outgassing p0485 of CO₂ and H₂O from the mantle, resulting in a CO₂-rich early atmosphere. The oceans formed later, with the onset of dense, supercritical H₂O condensation at 450 ± 20 °C. CO₂ was removed from the atmosphere as a dense supercritical H₂O-CO₂ mixture during ocean formation when surface temperatures had cooled to 300 °C (Liu, 2004).

Although the oceans and atmosphere probably formed p0490 early in planetary evolution, the last ocean-vaporizing impactor (≥440 km diameter) occurred around 4.3–4.1 Ga (Sleep et al., 1989), such that the origin of life (or at least the precursor to present life) was unlikely prior to this time (Kasting and Catling, 2003).

16.3.1.2. Isotopic Evidence for an Early Basaltic Protocrust s0125

The mineral and rock record of Earth's earliest crust begins at p0495 4404 ± 8 Ma, the age of the oldest detrital zircon grain from Jack Hills in Western Australia. Detrital zircons and Sm-Nd isochrons are the only record of crust-forming processes on Earth prior to 4404–4030 Ma, the age of the oldest dated rock from the Acasta gneiss complex (see Section 16.3.2.1).

Lead isotope patterns and anomalous ¹⁴²Nd/¹⁴⁴Nd ratios p0500 in early Archean metasedimentary rocks and ¹⁷⁶Hf/¹⁷⁷Hf ratios of 3.7–4.4 Ga old detrital zircons point to a vanished crust that persisted through much of early Earth history (Vervoort and Blichert-Toft, 1999; Kamber et al., 2003; Kamber, 2007; Kramers, 2007). Specifically, Pb-isotopic heterogeneity in 3.82–3.65 Ga rocks from West Greenland (North Atlantic Craton) has been used to infer the coexistence of enriched and depleted mantle domains, or, more likely, the separation of protocrust by 4.3–4.1 Ga (Kamber et al., 2003; Kamber, 2007; Blichert-Toft and Puchel, 2010). This protocrust may have formed by remelting or differentiation of even more ancient basaltic crust. Indeed, the presence and involvement of >4 Ga crustal remnants, including enriched basaltic protocrust, in the formation of other early Archean terrains is now much more widely recognized (Iizuka et al., 2006, 2008; O'Neil et al., 2008; Upadhyay et al., 2009; Tessalina et al., 2010). However, new isotopic evidence supports only a limited amount of *continental* crust on the early Earth (Bennett et al., 2010).

¹⁴²Nd excesses relative to modern basalts exist in p0505 a variety of 3.8–3.6 Ga rocks from southwest Greenland (North Atlantic Craton) and indicate Sm/Nd fractionation to have commenced before 4.35 Ga to form a strongly evolved crustal component (Harper and Jacobsen, 1992; Bennett et al., 1993; Caro et al., 2006; Kamber, 2007). This ¹⁴²Nd anomaly is absent from rocks younger than 3.7 Ga, and when combined with Hf isotopes of ancient zircons and Nb/Th evolution models, provides strong evidence that the reservoirs that resulted from Hadean silicate differentiation were homogenized by this time through effective and rapid

recycling of the crust (Collerson and Kamber, 1999; Kamber, 2007). However, evidence from combined Sm-Nd and Lu-Hf isotopic studies suggest that a depleted reservoir persisted though at least all of the Archean (Blichert-Toft and Puchel, 2010).

s0130 *16.3.1.3. Hadean Zircons from Jack Hills*

p0510 The oldest directly dated crustal materials on Earth are detrital zircons from low-grade Archean (c. 3.0 Ga) metaconglomerates and quartzites from the Jack Hills greenstone belt, and a variety of nearby belts in the northwestern part of the Yilgarn Craton, Australia (Froude et al., 1983; Compston and Pidgeon, 1986; Wilde et al., 2001; Wyche, 2007). These ≤ 3.05 Ga rocks contain detrital zircons with a range of ages from c. 3700 Ma back to astonishing 4404 ± 8 Ma (Wilde et al., 2001; Crowley et al., 2005; Cavosie et al., 2007).

p0515 Heterogeneous hafnium isotope values on 4.37–4.01 Ga Jack Hills detrital zircons was used to suggest the early formation of continental crust, probably as early as 4.45 ± 0.02 Ga (similar to on Mars) (Zhang, 2002; Harrison et al., 2005; Hopkins et al., 2008), supporting other work (Bennett et al., 1993; Blichert-Toft et al., 1999; Bizzarro et al., 2003; Harley and Kelly, 2007). Oxygen isotope values from these same zircons suggest crystallization from protoliths that were affected by low-temperature alteration, which has been used to suggest the presence of cool liquid water at 4.2 Ga (Mojzsis et al., 2001; Wilde et al., 2001; Cavosie et al., 2005; Valley et al., 2005). The oxygen isotope data has been used in combination with other results to infer the formation of continental crust by convergent margin magmatism at plate boundary interactions (i.e. subduction zones), and that this occurred essentially continuously from 4.5–4.2 Ga, with parts of the crust taking on continental characteristics by c. 4.35 Ga (Harrison et al., 2005, 2008; Ushikubo et al., 2008; Harrison, 2009). Rollinson (2008), however, cautioned that the Jack Hills zircons could have crystallized in granitic melts derived from hydrous partial melting of hornblende gabbros in the roof zone of axial magma chambers, as in modern oceanic crust, and Nutman and Heiss (2009) also pointed out that the low magmatic temperatures could simply relate to late-stage zircon crystallization in melts that were originally much hotter. Bennett et al. (2010) also caution against inference of significant volumes of Hadean continental crust, based on combined Hf and ^{142}Nd isotopic signatures from 3.87–3.63 Ga rocks from southwest Greenland and China. A more recent model suggests that the early Earth was characterized by a thick basaltic crust that underwent local partial melting to form relatively low volumes of tonalite (Kemp, 2010).

s0135 *16.3.1.4. Origins and Early Evolution of Life*

p0520 The origin(s) of life on Earth are not known and remain one of the biggest challenges facing science. Following the famous

Urey-Miller experiments of the early 1950s (Miller, 1953), which showed that it was relatively simple to create organic molecules from inorganic components, a major advance in understanding the origin(s) of life was made with the recognition that the tree of life is composed of three main branches and that the last common ancestor of all of these were thermophiles (Stetter, 1996; Pace, 1997). Furthermore, many hyperthermophilic, deep-branching organisms share the same metabolic pathway of reducing elemental sulfur to H_2S , with both H_2 and organic compounds as an electron donor (Stetter and Gaag, 1983; Stetter, 1996; Mojzsis, 2007): thus, it is most likely that life started in hydrothermal environments where seawater is circulated down along fractures deep into the Earth's crust, heated up, and returned to the surface in warm to hot vein systems (Russell, 1996; Nisbet and Sleep, 2001; Rothschild and Mancinelli, 2001; Kelley et al., 2005). Most researchers agree that in these systems, anaerobic metabolism arose first, as it derives energy from the oxidation of organic compounds faster and more efficiently than aerobic metabolisms using O_2 (Russell and Hall, 2006). What makes hydrothermal systems so exciting to early life studies is that they are natural reactors, where many types of complex chemical reactions occur as a result of the interaction between hot water and rocks of the Earth's crust (Russell and Hall, 2006; Wächtershäuser, 2006). Most of us are aware of these systems through spectacular on-land examples, where water that has been circulated down into the crust and heated by volcanic activity erupts back to the surface as hot springs and geysers, as, for example, in Geysir, Iceland, and Yellowstone, USA. But by far the more common are hydrothermal systems that erupt underwater in the marine environment, where hot water interacts with basaltic and/or ultramafic rocks of the oceanic crust. Most of these systems are high-temperature black smokers along the axis of mid-oceanic spreading centers. Cooler, white smokers occur off-axis and in other marine environments, where the heating of seawater within the crust is less extreme and the products of water-rock interactions are significantly different from those formed under higher-temperature regimes.

For many years, black smokers were considered a possible p0525 site for the origins of life (Russell et al., 1988; Russell, 1996; Nisbet, 2000). However, current thinking suggests that rather than high-temperature black smokers, where temperatures are commonly too high for even the most extreme hyperthermophiles (Miller and Bada, 1988), a more likely environment for the origin of life is in alkaline, low-temperature, hydrothermal systems in oceanic crust, where mineral reactions may form the purine coding elements of RNA and amino acids, all trapped within tiny iron sulfide cavities (Holm et al., 2006; Russell and Hall, 2006; Martin and Russell, 2007). Water-rock interactions in oceanic lithosphere have even been shown to produce HCN (Holm and Neubeck, 2009). Recently, the importance of the serpentinization of oceanic crust as a source of energy to promote the

development of life has been identified (Russell et al., 2010). According to Russell and Hall (2006), the fluxes of energy and nutrients available in hydrothermal mounds encouraged differentiation of the first microbes into Bacteria and Archea. It is widely considered that these two main branches of life — including most of the principal biochemical pathways that sustain the modern biosphere — had evolved early in Earth history, probably prior to 3.7 Ga (Russell and Hall, 2006), and almost certainly by 3.5 Ga (Nisbet and Sleep, 2001), when it appears from morphological and geological data that life was already diverse and occupied different niches (Van Kranendonk, 2006; Van Kranendonk et al., 2008b; see Section 16.3.2.4).

p0530 A promising technique for estimating the timescale of prokaryote evolution has been achieved using phylogenetic relationships. For example, Battistuzzi et al. (2004) have used phylogenetic results from the analysis of amino acid sequences from 32 proteins common to 72 species of prokaryotes and eukaryotes and estimated phylogenetic relationships and divergence times with a local clock method. These authors estimate an origin of life prior to 4.1 Ga, methanogenesis at 4.1–3.8 Ga, anaerobic methanotrophy after 3.1 Ga, phototrophy prior to 3.2 Ga, and aerobic methanotrophy by 2.8–2.5 Ga.

s0140 16.3.2. Juvenile Earth (4.03–2.78 Ga)

s0145 16.3.2.1. Early Crustal Remnants (4.03–3.53 Ga)

p0535 After the formation of the first crust(s) during the initial, chaotic, ~500 Ma period of Earth accretion, increasingly voluminous differentiated (felsic, continental) crust became preserved in an ever-increasing number of geological terrains over the period 4.03–3.53 Ga. Crustal remnants from this period are generally small (in terms of exposed surface area) and consist predominantly of highly metamorphosed and strongly deformed meta-igneous rocks, particularly sodic granitic rocks of the tonalite-trondhjemite-granodiorite (TTG) series (e.g., Bickford et al., 2007; Iizuka et al., 2007a, b; Kröner, 2007). However, some of these terrains, commencing at about 3.85 Ga, also include small remnants of very ancient supracrustal rocks, best known from the North Atlantic Craton and the northern part of the Superior Craton (Bridgwater and McGregor, 1974; Allaart, 1976; Nutman et al., 1997; Appel et al., 1998; O’Neil et al., 2007, 2008).

p0540 Xenon isotopes suggest that heat escaped much faster on early Earth than it does today, driven by magmatism rather than conduction through the lithospheric lid, and that the surface was renewed in a time-scale on the order of 1–10 Ma for the first billion years of Earth history (Coltice et al., 2009). A small volume of continental crust in early Earth is also indicated by initial Nd, Hf and Pb isotopic ratios from the oldest orthogneisses, which derive from essentially homogeneous early Archean mantle (Kamber et al., 2002). Models

based on Pb-Pb ratios, Sm-Nd and trace element modeling suggest that a basaltic protocrust existed prior to 3.8 Ga, but was recycled back into the mantle due to the lack of a stabilizing lithosphere (Figure 16.10; Vervoort and Blichert-Toft, 1999; Kamber et al., 2003; Kramers, 2007). McCulloch (1993) suggested that the more volatile-rich, less depleted mantle of the Archean would have been less viscous than in the Proterozoic. This behavior has been confirmed experimentally in olivine, whereby olivine’s yield strength decreases by as much as a factor of ~140 in the presence of H₂O at a confining pressure of 300 MPa (Hirth and Kohlstedt, 1996). Consequently, hot oceanic crust would be recycled and readily de-volatilized into the upper mantle, preserving a high viscosity hydrous layer above a more depleted, low viscosity, dry, lower mantle. As the mantle cooled into the Proterozoic and Phanerozoic, subduction processes allowed progressively deeper penetration of volatiles into the lower mantle — this factor may perhaps explain, in part, the change from submerged, to exposed continents at c. 2.5 Ga (Arndt, 1999).

These results strongly argue against *modern-style* plate tectonics prior to c. 3.5 Ga, or to significant formation of continental crust prior to this time (e.g., McCulloch and Bennett, 1994). A lack of early Precambrian plate tectonics is supported by thermal evolution models, which suggest that subduction of large plates did not occur prior to ~3 Ga, the time when Earth reached a thermal maximum; prior to this time, heat loss was smaller than heat production, meaning rapid mantle convection (Labrosse and Jaupart, 2007), thick, buoyant oceanic crust (Sleep and Windley, 1982), and smaller plates (e.g., de Wit and Hart, 1993). However, there is geological evidence that some form of plate tectonics had commenced by at least 3.8 Ga (Polat et al., 2002; Jenner et al., 2009), although quite likely in a style that differed significantly from modern-style plate tectonics (e.g., Davies, 1995; Martin and Moyen, 2002;

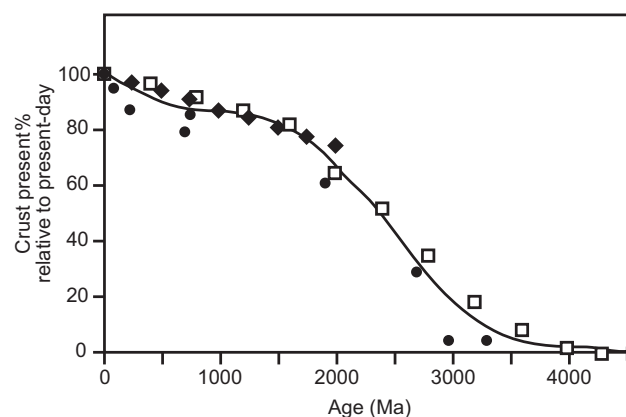


FIGURE 16.10 Crustal growth over time estimated from geophysical data by Reyer and Schubert (1984) (solid diamonds), transport-forward modeling (Kramers and Tolstikhin, 1997), and the Nb/Th evolution of the depleted mantle. (from Collerson and Kamber, 1999).

Smithies et al., 2003; Martin et al., 2005): by 3.1 Ga, there is agreement that modern-style subduction had commenced, at least locally (Smithies et al., 2005a; Van Kranendonk et al., 2007a, 2010; Pease et al., 2008).

s0150 **Acasta Gneiss Complex, Slave Craton, Canada**

p0550 The oldest dated rock on Earth is a 4031 ± 3 Ma tonalitic gneiss that forms part of the 4.03–3.94 Ga Acasta gneisses of the northwestern Canada Slave Craton (Stern and Bleeker, 1998; Bowring and Williams, 1999; Iizuka et al., 2007a, b). These rocks include a heterogeneous mixture of foliated to gneissic tonalite, granodiorite, trondhjemite, granite, amphibolites, diorite, and gabbroic rocks (Figure 16.11A; Bowring et al., 1990; Bowring and Williams, 1999; Iizuka et al., 2007a, b). A 4.2 Ga xenocrystic zircon discovered in these rocks combines with a 4.1 Ga Nd model age to indicate an even older history in the formation of this small, but ancient piece of crust (Bowring et al., 1989; Iizuka et al., 2008). Similarly cryptic, very ancient histories of Paleoproterozoic crustal remnants have been discovered in southeastern India and Western Australia (Pilbara and Yilgarn cratons) (Wyche, 2007; Upadhyay et al., 2009; Tesselina et al., 2010).

s0155 **Itsaq Gneiss Complex, North Atlantic Craton, Southwestern Greenland**

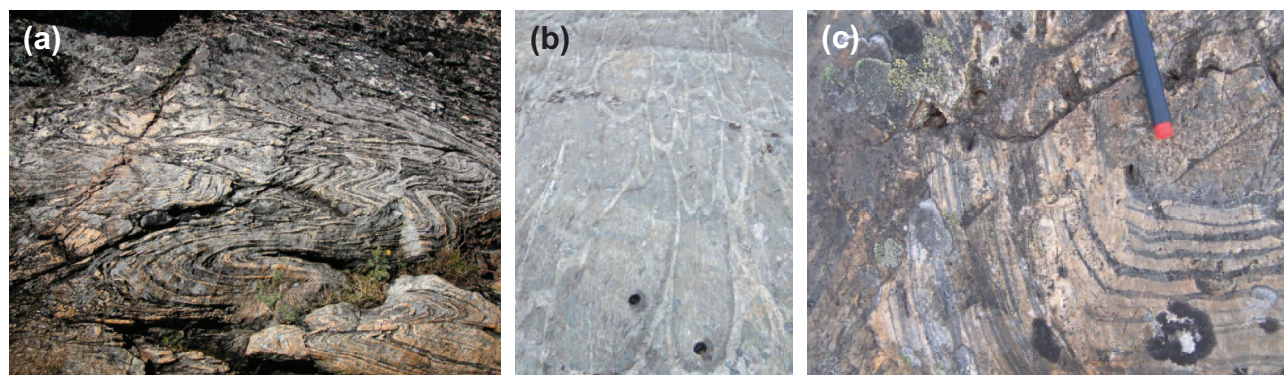
p0555 (with a contribution from A. P. Nutman)
p0560 The 3000 km² Itsaq Gneiss Complex (IGC) of southwestern Greenland forms one of several distinct terranes within the North Atlantic Craton, which extends from eastern Canada, across Greenland, and into Scotland (Nutman et al., 1989; 1996; 2002; 2007). The IGC contains the largest exposure of early Archean rocks in the world and is dominated by banded tonalitic gneiss, comprising tonalitic protoliths representing juvenile sialic crust emplaced at between 3870 and 3620 Ma, and later granitic bodies that formed by melting of that juvenile crust during subsequent orogenic

events (Nutman et al., 1999). A diverse suite of mafic, ultramafic and siliceous rocks occurs as enclaves and tectonic intercalations within the banded gneisses. Identified protoliths include metabasalts (mostly with island arc-like and MORB chemistry), layered gabbro-ultramafic complexes, rare slivers of depleted mantle, chemical sedimentary rocks, including BIF, and rare felsic volcanic and clastic sedimentary rocks. Supracrustal rocks are locally well preserved in the Isua supracrustal belt (Figures 16.11B,C), whereas older, more highly metamorphosed supracrustal rocks occur on the island of Akilia, in the southern part of the IGC (Bridgwater and McGregor, 1974; Allaart, 1976; Nutman et al., 1997; Appel et al., 1998).

Recent studies have demonstrated that the Isua Supracrustal Belt and surrounding granitic terrain is composed of two tectonically juxtaposed crustal slices, including c. 3810–3800 Ma supracrustal rocks and contemporaneous tonalities, and c. 3710–3690 Ma supracrustal rocks intruded by 3720–3690 Ma tonalitic rocks (Nutman et al., 2002; 2007; 2009). These crustal slices were juxtaposed at ca. 3650–3550 Ma, through terrane accretion at a convergent margin, and then intercalated with younger rocks during 2.8–2.7 Ga terrane accretion and collisional orogeny that affected the whole of the North Atlantic Craton (Nutman et al., 1999, 2002; Hanmer and Greene, 2002).

Nuvvuagittuq Supracrustal Belt, Superior Province, Canada

A small sliver of Eoarchean, or possibly Hadean, supracrustal rocks (Nuvvuagittuq supracrustal belt) is preserved in the northeastern part of the Superior Province, Canada. This isoclinally-folded belt contains predominantly mafic amphibolite rocks with rare felsic schists, oxide-rich and quartz-rich iron formations, and possible conglomeratic units, and metamorphosed gabbro and ultramafic sills (Dauphas et al., 2007; O’Neil et al., 2007, 2008; David et al., 2009). The dominant lithology is a heterogeneous, cummingtonite-rich



f0060 **FIGURE 16.11** A) Outcrop photograph of Earth’s oldest rock, the Acasta Gneiss (photograph courtesy of T. Iizuka); B, C) Photos of well preserved supracrustal rocks from the Isua supracrustal belt, including flattened pillow structures in 3720–3710 Ma boninitic metabasalts (B) and folded primary bedding in BIF from the c. 3750 Ma dividing metasedimentary unit C). Photographs courtesy of Allen Nutman.

(quartz-biotite-plagioclase±anthophyllite±garnet) amphibolite gneiss of uncertain protolith. With high MgO (4–16 wt %) and generally moderate silica (40–56 wt %) and iron contents (7–14 wt %), basaltic to andesitic compositions are favored, possibly derived from a suprasubduction zone setting (O’Neil et al., 2007, 2011).

p0575 The age of the belt is constrained by U-Pb ages of 3817 ± 16 Ma from a felsic schist within the belt, and by a 3661 ± 4 Ma age from surrounding tonalites; a Nd depleted mantle model age of c. 3.9 Ga appears to confirm the age of this belt (David et al., 2009). However, Nd data from the cummingtonite-amphibolite unit indicate that these rocks preserve lower $^{142}\text{Nd}/^{144}\text{Nd}$ ratios than the terrestrial standard ($\epsilon^{142}\text{Nd} = -0.07$ to -0.15) and produce a $^{146}\text{Sm}-^{142}\text{Nd}$ isochron with an age of $4280 + 53 / - 81$ Ma. Although this data has been interpreted as evidence that these rocks may represent the oldest preserved crustal section on Earth (O’Neil et al., 2008), the zircon and Nd model age data suggest that the Hadean isochron may reflect the age of the source from which the rocks were originally derived and not the actual age of the belt itself.

s0165 16.3.2.2. Stable Cratonic Lithosphere and the First Signs of Life (3.49–2.82 Ga)

p0580 Collerson and Kamber (1999) showed from analysis of Th-U-Nb systematics that the area of continental crust grew most rapidly from 3.5–2.0 Ga and has been broadly recycled since that time through subduction-erosion, a process that has balanced continental growth at island arcs since the Proterozoic (Scholl and von Huene, 2007). Major growth of continental crust at c. 3.0 Ga is supported by more recent studies of Hf in zircons, gold deposits, and Re-Os studies of sulfides from sub-continental mantle lithosphere (Griffin and O’Reilly, 2007a; Frimmel, 2008; Hawkesworth et al., 2010). At about 3 Ga, petrological estimates of mantle potential temperature suggest that the mantle may have been at its hottest temperature since the accretionary period of Earth history, due to the effects of internal heating exceeding surface heat loss (Labrosse and Jaupart, 2007; Herzberg et al., 2010). Modern-style plate tectonics was operational, at least locally, by 3.2 Ga (Smithies et al., 2005a; Van Kranendonk et al., 2007a; 2010), consistent with results from numerical modeling that shows the viability of Archean plate tectonics (Van Hunen and van den Berg, 2008).

p0585 The oldest well-preserved crustal remnants on Earth include two small (200 x 200 km) areas of 3.49–3.2 Ga, low strain and (generally) low metamorphic grade supracrustal rocks in the Pilbara Craton of Western Australia (East Pilbara Terrane) and the eastern Kaapvaal Craton in southern Africa (Barberton Greenstone Belt), sometimes referred to collectively as Vaalbara on account of their similar crustal histories (Figure 16.12). These crustal remnants formed on a foundation of still older crust, up to 3.82 Ga or even 4.1 Ga, at least

some of which was sialic in composition (Chavagnac, 2004; Van Kranendonk et al., 2007a, b; 2009; Tessalina et al., 2010). Greenstone successions in these two cratons consist of dominantly mafic-ultramafic volcanic rocks and subordinate felsic volcanic rocks, chert, and clastic sedimentary rocks that were deposited over similar intervals from 3.53–3.42 Ga, 3.35–3.32 Ga, and 3.27–3.22 Ga (Figure 16.10; Byerly et al., 1996; Lowe and Byerly, 2007; Van Kranendonk et al., 2007a, b; 2009). Deposition of each group was accompanied by the emplacement of widespread and voluminous, dominantly TTG, granitic rocks that became progressively more potassium rich through time, culminating with local A-type granites with rapakivi texture emplaced at 3.24 Ga (Smithies et al., 2003; Champion and Smithies, 2007; Moyen et al., 2007; Van Kranendonk et al., 2007a, b). Crust formation was coeval with the development of a thick, highly depleted, and buoyant subcontinental mantle lithosphere in these terrains, resulting from high degrees of melt extraction (Wilson et al., 2003; Griffin et al., 2004; Smithies et al., 2005b; Griffin and O’Reilly, 2007a, b).

By ~3 Ga, these stable pieces of cratonic lithosphere p0590 provided a basement for the development of widespread, thick platform successions, including the 3.02–2.94 Ga De Grey Supergroup in Australia and the 3.0–2.9 Ga Pongola and Witwatersrand supergroups in southern Africa (Figure 16.13; Hegner et al., 1984; Walraven and Pape, 1994; Gold, 2006; McCarthy, 2006; Van Kranendonk et al., 2007a). Each of these supergroups is several kilometers thick and deposited – at least in part – under subaerial conditions with evidence of terrestrial biological communities, including probable cyanobacterial mats (Mossman and Dyer, 1985; Hallbauer, 1986; Noffke et al., 2003, 2006, 2008; Marsh, 2006; McCarthy, 2006).

16.3.2.3. Early Atmosphere and Climate

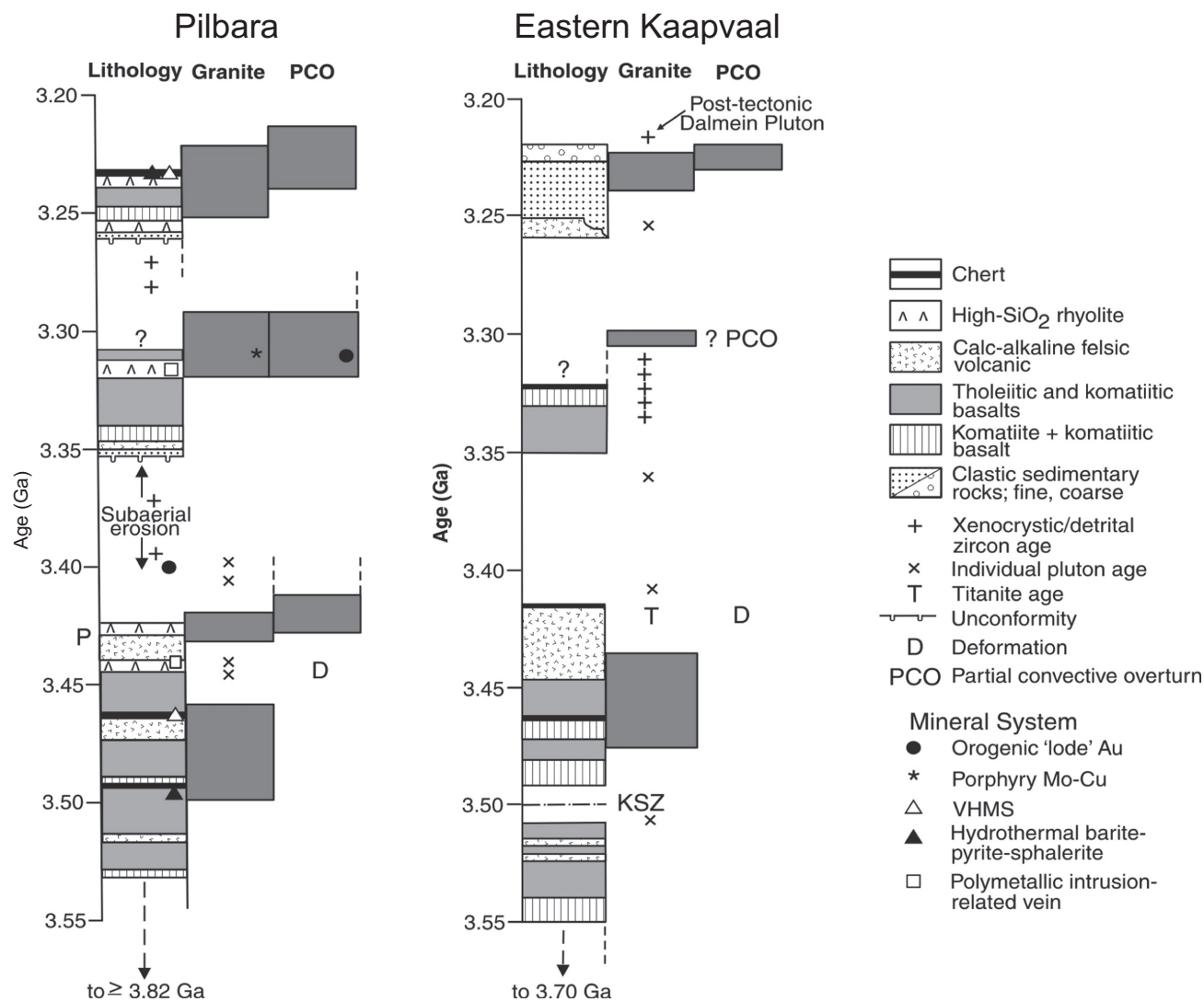
(with a contribution from J. Kasting)

The composition of the atmosphere on early Earth is much debated, with most supporting a reducing atmosphere, with little or no oxygen (Figure 16.14; Cloud, 1972; Holland, 1994; Krupp et al., 1994; Farquhar et al., 2000, 2007; Farquhar and Wing, 2003; Domagal-Goldman et al., 2008; Krull-Davatzes et al., 2010), and others supporting a limited amount of oxygen, at least periodically (Ohmoto et al., 2006; Ono et al., 2006; Hoashi et al., 2009; Smith et al., 2010). Debate concerning the composition of the early atmosphere goes back to 1924, when the Russian biologist, A. I. Oparin, wrote a book, later translated into English (Oparin, 1938), in which he suggested that the early atmosphere was rich in highly reduced gases, such as hydrogen (H_2), methane (CH_4), and ammonia (NH_3). This view was later supported by experiments performed by a US graduate student, Stanley Miller, under the tutelage of his advisor Harold Urey, in which they successfully synthesized amino acids and other biologically

s0170

p0595

p0600



f0065 **FIGURE 16.12** Comparative events between the Pilbara (Australia) and Eastern Kaapvaal (South Africa) cratons, showing their similar temporal evolution.

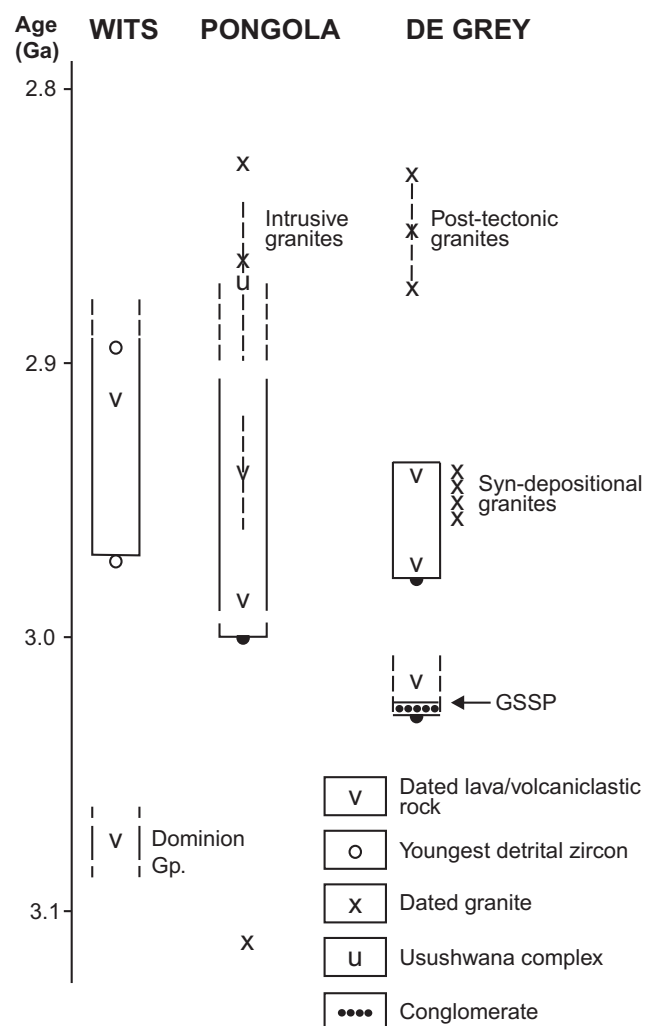
important organic compounds using spark discharge in a highly reduced atmosphere (Miller, 1953). So, the concept of a highly reduced primitive atmosphere became entrenched in the scientific community, particularly amongst biologists interested in the origin of life.

p0605 At nearly the same time as the famous Miller-Urey experiment, the geologist William Rubey began arguing that the early atmosphere was a weakly reduced mixture consisting mostly of N₂ and CO₂ (Rubey and Poldervaart, 1955). His reasoning was that the atmosphere was produced largely by volcanic outgassing, and modern volcanic gases are only weakly reduced. This model was later developed more fully by Walker (1977), who added the concept of redox balance: hydrogen and other reduced gases outgassed from volcanoes must be largely balanced by hydrogen lost to space. He assumed that the escape rate occurred at the diffusion-limited rate; i.e., as fast as it could possibly go, given the presence of

a static background atmosphere composed mostly of N₂ and CO₂. This generates atmospheric H₂ mixing ratios of the order of 10⁻⁴ to 10⁻³, depending on the magnitude of the assumed volcanic outgassing rate (Walker, 1977; Kasting, 1993; Holland, 2002; Canfield et al., 2006). The corresponding atmospheric O₂ concentrations, as calculated with photochemical models, vary with altitude from ~10⁻³ in the upper stratosphere (around 60 km), to ~10⁻¹³ near the surface (Kasting, 1993).

Since Walker's book was written, the concept of atmospheric redox balance has been more fully elaborated. Rainout of reduced and oxidized species from the atmosphere can also affect the atmospheric redox state. The full atmospheric hydrogen budget includes these terms, along with outgassing and escape of H₂ (or H), (Figure 16.14; Kasting, 1993; Kasting and Catling, 2003). The rainout terms are typically of the order of 10 percent of the budget if volcanic outgassing

p0610

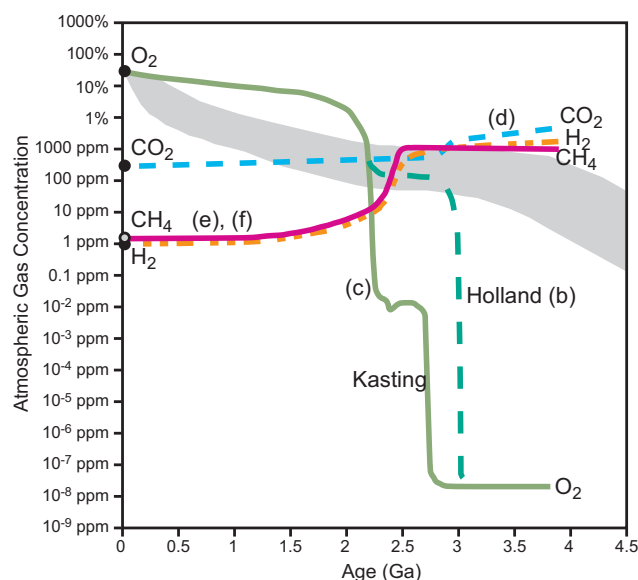


f0070 **FIGURE 16.13** Schematic histogram of depositional events in well-preserved, c. 3 Ga, cratonic basins of the Kaapvaal (Witwatersrand (Wits), and Pongola supergroups), and Pilbara (De Grey Supergroup) cratons: suggested GSSP for the base of the proposed Mesoarchean Era lies just above a basal conglomerate within the De Grey Supergroup.

rates were high, as calculated by Holland (2002). However, these terms can dominate the hydrogen budget if hydrogen outgassing rates were lower, as predicted by Sleep (2005) and Canfield et al. (2006). Importantly, rainout of oxidized species, such as H_2SO_4 and H_2O_2 , would have kept prebiotic O_2 concentrations low even if the volcanic outgassing rate of hydrogen was essentially negligible (Segura et al., 2007). Also keeping O_2 concentrations low was the reaction between O_2 and reducing components in the sulfate-poor Archean oceans, particularly dissolved, reduced iron (Cloud, 1972, 1973; Walker and Brimblecombe, 1985; Walker, 1987; Foriel et al., 2004).

p0615 CH_4 may also have been an important component of the early atmosphere, especially after methanogens started producing it (Figure 16.14). Kharecha et al. (2005) have explored the effects of a methanogenic Archean marine ecosystem on atmospheric CH_4 concentrations. Anoxygenic

photosynthesis, based on H_2 , Fe, and S, was also included in certain of their simulations. In their model, methane was produced by the (biologically mediated) reaction; $\text{CO}_2 + 4 \text{H}_2 \rightarrow \text{CH}_4 + 2 \text{H}_2\text{O}$, as well as by methanogenesis based on fermentation of organic matter produced from anoxygenic photosynthesis. The rate of methane production was found to be limited by the rate of gas transfer through the atmosphere-ocean surface, which can be estimated using arguments based on “piston velocities” (Broecker and Peng, 1982). Surprisingly, Kharecha et al. (2005) found that CH_4 should have been generated at rates that are comparable to today, even though the Archean ecosystem was entirely different from the modern one. The lifetime of CH_4 in a low- O_2 atmosphere is approximately 1000 times longer than today (10,000 yr versus 10 yr); hence, a flux of this magnitude could have produced an atmospheric CH_4 mixing ratio of 1000 ppmv or larger (Pavlov et al., 2001a). At these concentrations, CH_4 is



f0075 **FIGURE 16.14** The Cloud-Walker-Holland-Kasting model for the evolution of atmospheric chemistry. Grey area represents the range of pO₂ suggested by Holland (1966); curve (b) from Rye and Holland (1998); curve (c) from Kasting (1987, 2001); curves (d) through (f) from Kasting (2001) and Pavlov et al. (2001a). Adapted from Ohmoto (2004).

an effective greenhouse gas and could have helped warm the early climate, as described further below.

p0620 CH₄ could have been abundant on the prebiotic Earth, as well, if the impact rate from comets and asteroids was high. Models for impact degassing of comets and asteroids predict that CH₄ should have been the major carbon species generated under most circumstances (Kress and McKay, 2004; Hashimoto et al., 2007; Schaefer and Fegley, 2007). It is not expected to have been a major component of volcanic gases, at least after the upper mantle had achieved its present redox state, which occurred by 3.5 Ga or earlier (Frost and McCammon, 2008). CH₄ is destroyed by short-wavelength UV photolysis and by reaction with OH radicals produced from longer-wavelength H₂O photolysis. Hence, its concentration would have depended on the balance between the solar UV flux, which decreased with time (Ribas et al., 2005), and the impact rate of comets and asteroids. The latter number is highly uncertain. During the 1980s and 1990s, most modelers assumed that the impact rate declined exponentially with time (e.g., Sleep et al., 1989; Kasting, 1990). This assumption was based on the notion that the early Earth experienced a protracted period of heavy bombardment from 4.5 Ga until about 3.8 Ga. Geologists who studied Moon rocks, though, had long ago concluded that the Moon (and the Earth) experienced a pulse of bombardment around 3.8–3.9 Ga (Ryder, 2003 and references therein). This “pulse” hypothesis is supported by a new theoretical model (Gomes et al., 2005; Tsiganis et al., 2005), termed the “Nice model”, which shows how continued migration of the outer planets following accretion could have

led to just such a late pulse in the flux of small bodies through the inner Solar System. If the Nice model is correct, then the Hadean Earth between 4.4–4.0 Ga may have experienced a relatively small impact flux and, hence, should have contained relatively little CH₄.

Domagal-Goldman et al. (2008) have suggested that low p0625 Δ³³S values measured in the Mesoarchean (Figure 16.15) are the result of a thick organic haze in the absence of free oxygen. Significantly, the c. 2.9 Ga Pongola Supergroup contains the oldest evidence of glaciation on Earth, indicating at least locally cool atmospheric conditions at this time (Von Brunn and Gold, 1993; Young et al., 1998), and possibly even a weakly oxidized atmosphere (Ono et al., 2006; Smith et al., 2010), although alternative explanations for minor Δ³³S anomalies at this time have been proposed (Farquhar et al., 2007). Continental glaciation probably requires mean surface temperatures of 20°C or below, based on the more recent climate record (Kasting, 1987). Evidence from paleo-weathering profiles may also support a milder Archean climate (Holland, 1984; Condie et al., 2001; Sleep and Hessler, 2006), although some of this evidence is disputed (Lowe, 2007).

Claims of hot, fire-opal Archean oceans (Knauth and p0630 Lowe, 2003; Robert and Chaussidon, 2006) have been largely discounted, and the high temperatures re-interpreted as the effects of (in many cases seafloor) hydrothermal alteration (Kasting et al., 2006; Van Kranendonk, 2006; Shields and Kasting, 2007). More recent studies using oxygen and hydrogen isotopes in chert from the Barberton greenstone belt also supports a moderate climate (≤40 °C) at 3.42 billion years ago (Hren et al., 2009; Blake et al., 2010), similar to results from ancestral sequence reconstruction using amino acids in elongation factor proteins (Gaucher et al., 2008).

From a theoretical standpoint, it would be surprising if p0635 the early Earth was hot because the Sun is thought to have been significantly less bright at that time. Solar evolution models (e.g., Gough, 1981) predict that the Sun was originally ~30 percent less luminous at 4.6 Ga than today and that it has brightened more or less linearly with time (Kasting, 2005). If such models are correct – and nearly all astronomers agree that they are – then high concentrations of greenhouse gases (and N₂; Goldblatt et al., 2009b) would have been needed simply to keep the early oceans from freezing. A cooler early Earth would have resulted in less silicate weathering and a consequent buildup of volcanic-derived CO₂, which would have helped warm the planet (Figure 16.14). Climate model calculations for c. 2.9 Ga suggest that a combination of ~0.03 bars of CO₂ (100 times the present atmospheric level) and 1000 ppmv of CH₄ (600 times higher than present) could have kept the Earth warm at that time (Haqq-Misra et al., 2008).

Huston and Logan (2004) noted that the Archean rock p0640 record is characterized by the presence of barite in rocks

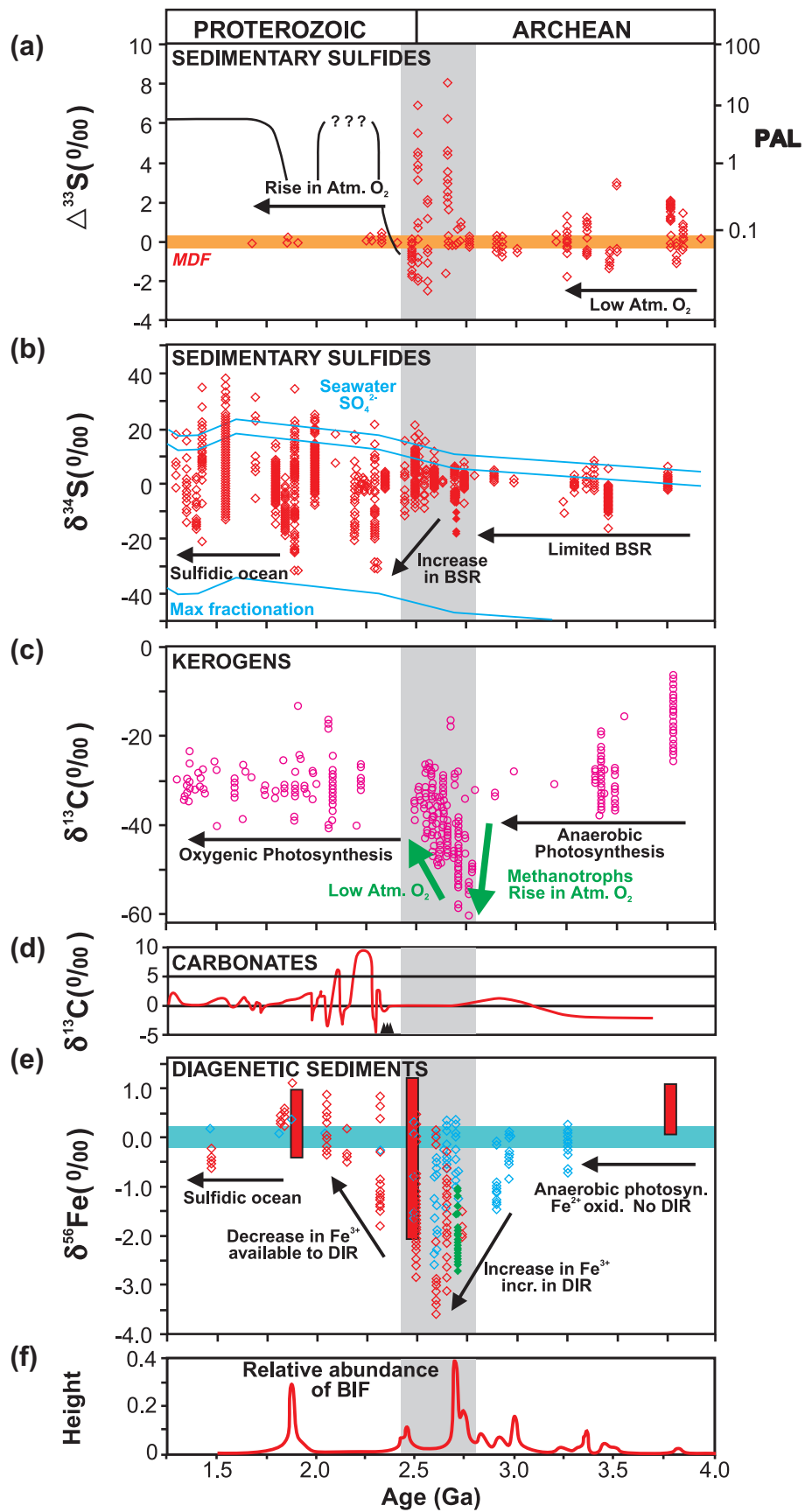


FIGURE 16.15 Temporal variations of S, C, and Fe isotopic systems through the Precambrian. **A)** $\Delta^{33}\text{S}$ of sedimentary sulfides (orange bar, MDF = range of mass-dependent fractionation); PAL = % of present atmospheric level of oxygen (logarithmic scale; from Canfield, 2005); **B)** $\delta^{34}\text{S}$ of sedimentary sulfides (red circles) and of seawater sulfate (blue lines); **C)** $\delta^{13}\text{C}$ of kerogens; **D)** $\delta^{13}\text{C}$ of carbonates (black triangles denote time of Paleoproterozoic glaciations); **E)** $\delta^{56}\text{Fe}$ of diagenetic sediments; **F)** relative abundance of BIF. Grey shade indicates time of instability in the biosphere. (Compiled from sources cited in the text).

>3.2 Ga and <1.8 Ga, and by abundant BIFs in the intervening interval (3.2–1.8 Ga). They ascribe the older occurrences of sulfates to the presence of an upper ocean layer (locally) enriched in sulfates that were produced through atmospheric photolytic reactions, rather than biological activity. From 3.2–2.4 Ga (actually 2.3 Ga), they ascribe low seawater sulfate to removal by the activity of bacterial sulfate reduction. After 2.3 Ga, the increase in atmospheric oxygen resulted in oxidative weathering of sulfides in continental rocks and an associated increase in seawater sulfate concentrations (see Section 16.3.3). Archean oceans are also regarded as having been significantly oversaturated in CaCO_3 (Grotzinger and Kasting, 1993), although their major ion concentrations and ratios were similar to modern oceans, reflecting the dominance of hydrothermal processes at mid-ocean ridges (Hardie, 2003; Foriel et al., 2004).

p0645 The zero to positive $\delta^{56}\text{Fe}$ values for rocks >3.1 Ga (Figure 16.15) is accepted to reflect partial oxidation of marine hydrothermal $\text{Fe}^{2+}_{\text{aq}}$, suggesting that the amount of oxidant was limited (e.g., Dauphas et al., 2004; Johnson and Beard, 2006; Whitehouse and Fedo, 2007a). Because it is generally (although not universally) thought that atmospheric O_2 contents were low in the Paleoproterozoic (Holland, 1984), the oxidant was most likely anaerobic photosynthetic $\text{Fe}^{2+}_{\text{aq}}$ oxidation, based on experimental data (Croal et al., 2004) and evidence that UV-photo oxidation is inhibited in experiments that used natural seawater fluid compositions (Konhauser et al., 2007a).

s0175 16.3.2.4. Early Life

p0650 (with contributions from W. Altermann, C.M. Johnson and B.L. Beard)

p0655 Possibly the oldest record of life is that occurring as carbon-isotopic signatures from 3.83–3.7 Ga, amphibolite facies metamorphosed supracrustal rocks from the Akilia enclave and Isua Supracrustal Belt in southwest Greenland (Schidlowski et al., 1979; Schidlowski, 1988; Mojzsis et al., 1996; Rosing, 1999), but most of these claims have been controversial (see Whitehouse and Fedo, 2007b). Schidlowski et al. (1979) reported $\delta^{13}\text{C}_{\text{PDB}}$ values between -6 and -25% in a variety of rock types, including what were considered to be metacarbonates, and considered this to be a signature of early life based on the principle that organisms preferentially sequester ^{12}C over ^{13}C during metabolic processes. However, the metacarbonate samples have since been shown to be the products of extensive metasomatism (Rose et al., 1996; Rosing et al., 1996) and the graphite to be a product of carbonate breakdown to reduced carbon during metamorphism and/or metasomatic processes (Naraoka et al., 1996; Van Zuilen et al., 2002, 2003; McCollom, 2003; McCollom and Seewald, 2006).

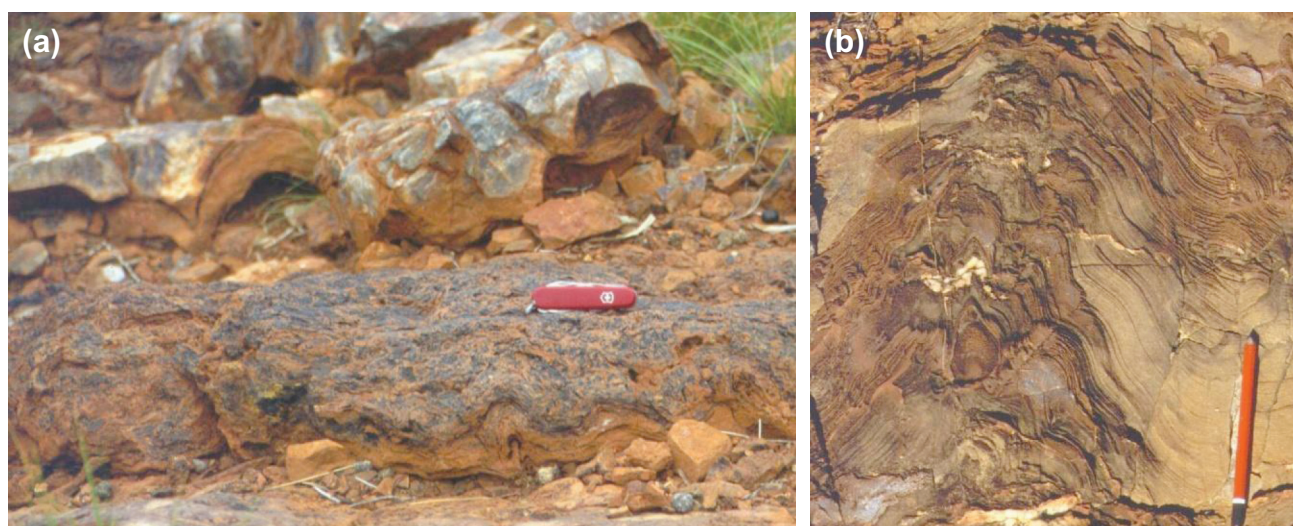
p0660 Rosing and Frei (2004) interpreted -25% $\delta^{13}\text{C}$ -values in some of the Isua rocks as typical organic content of pelagic

sediments, from planktonic prokaryotes, that released oxygen in the photic zone. However, geological uncertainties do not allow for an unequivocal interpretation of the environment in which the carbon analyzed by Rosing and Frei (2004) accumulated.

Mojzsis et al. (1996) described isotopically light graphite p0665 as inclusions in apatite crystals in amphibolite-facies Isua supracrustal rocks and in a granulite-facies BIF from Akilia Island, which they and a subsequent study (McKeegan et al., 2007) interpreted as indicative of biogenic carbon in sedimentary apatite. However, the significance of the Akilia supracrustal enclave as the host of ca. 3.83 Ga biogenic graphite has shown to be contentious because of – amongst other things (Lepland et al., 2002; 2005) – the typical occurrence of graphite in fluids inclusion trails and clusters together with CO_2 and CH_4 (Lepland et al., 2011). Such an association was interpreted to reflect abiogenic graphite precipitation from carbonic fluids during a poly-phase metamorphic history.

A different signature of life in Greenland rocks was suggested by Rosing (1999), who presented geological, petrographic, and carbon isotopic data regarding graphite globules p0670 in c. 3.8 Ga metaturbiditic and pelagic metasedimentary rocks from the Isua supracrustal belt that supports an interpretation as the metamorphosed remnants of biogenic detritus. Whereas the bulk of Isua graphite is formed by metamorphic alteration of Fe-carbonate, this mechanism is not applicable for the graphite globules described above (Van Zuilen et al., 2002; 2003). Thus, the original biogenic interpretation of graphite globules (Rosing, 1999) remains unchallenged, and it is possible that these represent the oldest currently known traces of terrestrial life.

Macroscopic fossil evidence of early life is preserved in p0675 a wide variety of rocks deposited during the second part of this time interval. The oldest, widely accepted evidence of life comes from the c. 3.49 Ga Dresser Formation in the Pilbara Craton, where stromatolites and possible microfossils are preserved in a thin succession of carbonates, sandstones and hydrothermal precipitates deposited under intermittently shallow-water conditions within a volcanic caldera setting (Figure 16.16; Walter et al., 1980; Buick and Dunlop, 1990; Ueno et al., 2001; 2004; Van Kranendonk, 2006; Van Kranendonk et al., 2008b; Tessalina et al., 2010). Chemical and isotopic evidence in support of a diverse microbial community has also been presented for this formation (Shen et al., 2001; Ueno et al., 2006; Philippot et al., 2007; Van Kranendonk et al., 2008), as well as for other, nearly contemporaneous rocks (e.g., Blake et al., 2010; Wacey et al., 2010). Possible cyanobacterial microfossils from the 3.46 Ga Apex chert (Schopf locality) are controversial (Schopf, 1993; Brasier et al., 2002, 2005; Schopf et al., 2002, 2007), but new discoveries of different forms of stromatolites, microfossils, and carbonaceous matter of biological origin in 3.35–3.0 Ga rocks from the Pilbara and Kaapvaal cratons are still being



f0085 **FIGURE 16.16 Earliest macroscopic evidence of life on Earth.** A) Wrinkly laminated microbial mats (black, foreground) and domical stromatolites of the c. 3.49 Ga Dresser Formation, Pilbara Craton (Australia); B) Cross-sectional view of incipiently branching, coniform stromatolite in finely bedded dolostone of the c. 3.4 Ga Strelley Pool Formation, Pilbara Craton (Australia).

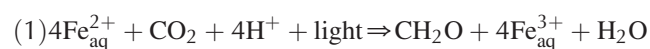
made (Figure 16.13; Walsh and Lowe, 1985; Hofmann et al., 1999; Tice and Lowe, 2004, 2006; Kiyokawa et al., 2006; Banerjee et al., 2007; Duck et al., 2007; Furnes et al., 2007; Marshall et al., 2007; Sugitani et al., 2007, 2010; Glikson et al., 2008; Javaux et al., 2010), some of which closely resemble earlier finds from similar-age rocks in South Africa (Walsh, 1992).

p0680 The existence of cyanobacteria in the earlier Archean was supported primarily by morphological indicators (Walsh, 1992; Schopf, 1993; Altermann and Schopf, 1995; Altermann, 2007a), but it was widely assumed that cyanobacterial metabolism was far too advanced for such early stages in the evolution of life, and simple morphological criteria for taxonomy were criticized as unreliable because of *post mortem* alterations. Others, however, have held to Schopf's (1993) original interpretation of cyanobacteria, with some restrictions because of diagenetic and thermal alteration (Kazmierczak and Kremer, 2002; Altermann, 2005, 2007b). More recent morphological and biomarker studies support the rare, though excellent, preservation of complex microbial morphologies by 3.2–3.0 Ga, if not 3.5 Ga, in a variety of geological settings (Mason and von Brunn, 1977; Rasmussen, 2000; Duck et al., 2007; Marshall et al., 2007; Schopf et al., 2007; Sugitani et al., 2007, 2010; Glikson et al., 2008).

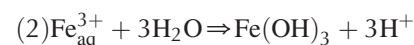
p0685 Although 3.49–3.35 Ga stromatolites already show phototactic behavior (Walter et al., 1980; Hofmann et al., 1999; Allwood et al., 2006; 2007; Van Kranendonk, 2010a), direct evidence for photosynthesis is difficult to prove and no direct irrefutable evidence for *oxygenic* photosynthesis in the early Archean exists. Olson (2006) proposed that there was no evolutionary pressure for the development of oxygenic photosynthesis in the presence of H₂ as the primary electron donor for carbon fixation in the early

Archean (see also Tice and Lowe, 2006). Early *anoxygenic* photosynthesis may have involved H₂ and H₂S as reductants, and experimental results support a key role of anoxygenic photosynthetic microbes in early stromatolite formation (Bosak et al., 2007). Only when the abundant source of H₂ was reduced by bacterial methanogenesis is it likely that sulfur-driven photosynthesis may have developed at around 3.5 Ga. This is consistent with the geological setting of Dresser Formation stromatolites within a sulfur-rich volcanic caldera (Van Kranendonk, 2006; Van Kranendonk et al., 2008b).

Another reductant for photosynthesis might have been p0690 ferrous iron, which would also support the deposition of BIFs (Catling et al., 2001; Kappler et al., 2005). Many workers have argued that the earliest photosynthesis was anoxygenic, specifically anaerobic photosynthetic Fe²⁺ oxidation, because Fe²⁺_{aq} was probably the most important electron donor in the early Archean oceans (e.g., Widdel et al., 1993; Canfield, 2005; Canfield et al., 2006; Olson, 2006). Anaerobic photosynthetic Fe²⁺ oxidation produces organic carbon and Fe³⁺:



which, at circum-neutral pH, produces ferric oxide/hydroxide p0695 precipitates:



Microbial methanogenesis has been traced by Ueno et al. p0700 (2006) in fluid inclusions in hydrothermal chert veins containing methane with carbon isotopic composition of –58‰, next to H₂O and CO₂. The authors discuss the possibility of thermophilic methanogens thriving above 80°C as being

responsible for this strong isotopic fractionation, and compare the preserved methane to that produced by CO₂ reduction or acetate fermentation in modern methanogens. This discovery fits nicely with the suggestion that methanogen niches were most abundant where CO₂-rich Archean ocean water flowed through serpentinites (Sleep and Bird, 2007). Bacterial depletion of ³⁴S in pyrite through sulfate reducing bacteria was found in the same rocks by Shen et al. (2001). The presence of sulfate-reducing bacteria was also inferred by Grassineau et al. (2006) for rocks c. 3.24 Ga. A new habitat for early life appears for the first time in the rock record at c. 3.2 Ga, with colonization of shallow sandy environments by photoautotrophic micro-organisms, likely to be cyanobacteria (Noffke et al., 2003; 2006, 2008; Noffke, 2008), although evidence for microbial mats in shallow sandy environments has also been described in older rocks from the Pilbara Craton (c. 3.4 Ga: Van Kranendonk, 2007b, 2010a).

p0705 The H₂-driven bacterial anoxygenic photosynthesis was certainly developed prior to the advanced chlorophyll α photosynthesis (Schopf, 1992). However, its geochemical isotopic signature would be almost indistinguishable from that of oxygenic photosynthesis in the fossil record because of the large range overlap in $\delta^{13}\text{C}$ values (Schidlowski, 1988; Mojzsis et al., 1996). Although the timing of the evolutionary steps in the development of different metabolisms is controversial, it seems reasonable that they were invented in the Archean and that oxygenic photosynthesis was present at least by the Neoproterozoic, if not earlier (3.2–2.9 Ga: e.g., Buick, 1992, 2008; Des Marais, 2000; Anbar et al., 2007; Nisbet et al., 2007). It is also probable that aerobic respiration may also have been initiated in the Archean (Towe, 1990). Battistuzzi et al. (2004) note that the evolution of phototrophy would be at risk of extensive damage by UV radiation in the absence of an ozone layer prior to the Great Oxidation Event at c. 2.3 Ga (see Section 6.3.3.4). Pigments such as carotenoids function as photoprotective compounds and are present in all the photosynthetic eubacteria and in groups that are partly or mostly associated with terrestrial habitats (e.g., actinobacteria, cyanobacteria, and *Deinococcus-Thermus*). These authors also point out that these three groups also share a high resistance to dehydration and that, as such, their common ancestor was adapted to land environments, which they suggest were colonized at 3.05 Ga, prior to the divergence of Actinobacteria from Cyanobacteria + *Deinococcus* at c. 2.78 Ga. They conclude that previous geological evidence for cyanobacteria prior to ~3.0 Ga should be re-evaluated.

p0710 Evidence for a rapid diversification of bacterial lineages in the Archean was provided by David and Alm (2011), who mapped the evolutionary history of gene families across the three domains of life onto a geological timeline. The results show a brief period of genetic innovation and de-novo gene family birth at between 3.33–2.85 Ga, which gave rise to 26.8 % of the extant gene families involved in electron transport

and respiratory pathways. After ~2.85 Ga, rates of gene loss and gene transfer stabilized at roughly modern-day levels.

16.3.3. Adolescent Earth (2.78–1.78 Ga) s0180

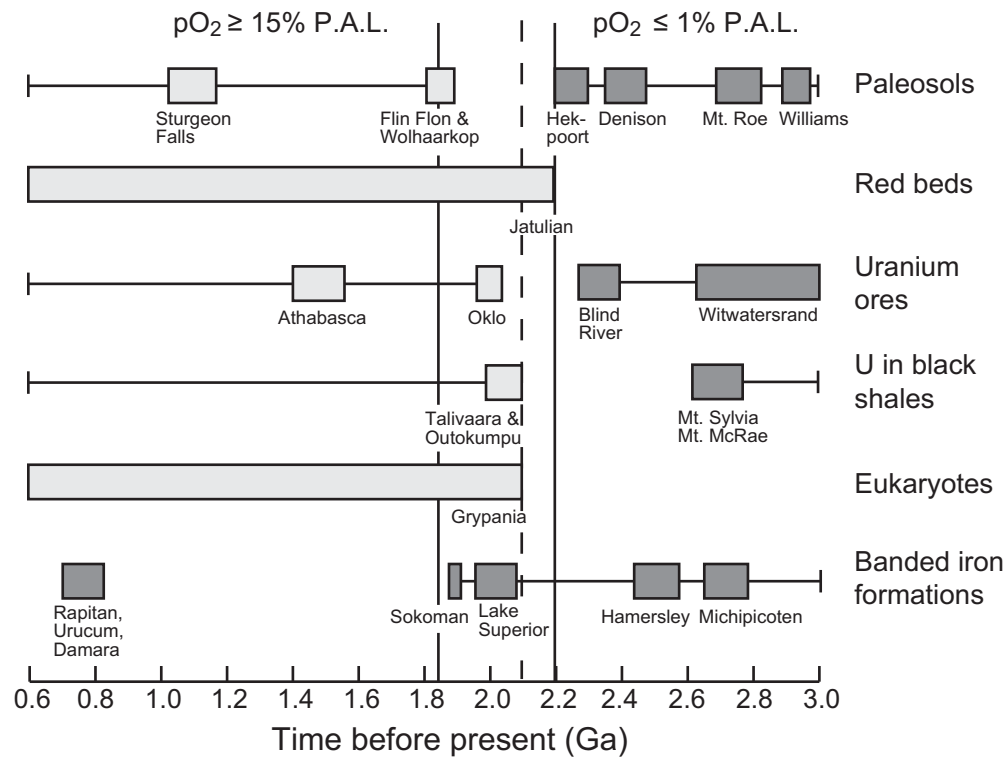
For almost a billion years, from 2.78–1.78 Ga, Earth experienced a tumultuous adolescence of irreversible change that transformed a hot, juvenile, rapidly convecting planet with small, mostly submerged protocontinents, nascent plate tectonics, and primitive life (prokaryotes) into a mature, cooler planet with large, rigid, emergent continental land masses, modern-style plate tectonics, a supercontinent cycle, and more complex life (eukaryotes) (e.g., Cloud, 1972; Holland, 1994; Condie, 1998; Rogers and Santosh, 2002; Parman, 2007). Significantly, these global *geological changes* were accompanied by *chaos in the biosphere*, as reflected by the largest excursions in chemical tracers of biological activity at any time in Earth history (Figure 16.15), and by the formation of many significant ore deposits, including vast resources of BIF. p0715

This combination of geological and biological changes p0720 was initiated by widespread mantle melting and crust formation (2.78–2.63 Ga) resulting in one or more supercontinents (Superia and Sclavia). These changes developed in concert with the gradual rise in atmospheric oxygen from c. 2.7 Ga, which culminated in the Great Oxidation Event at 2.3–2.2 Ga (Figure 16.17; Veizer et al., 1989; Holland, 1994, 2002; Farquhar et al., 2000; Bekker et al., 2004), and passed into a period of environmental stability after c. 1.78 Ga. As outlined below (see Section 16.4), this billion-year-long period of Earth history can be divided into a linked series of causative events, each of which is recorded in the geological rock record by a distinctive assemblage of rocks and/or isotopic characteristics (see Table 16.4).

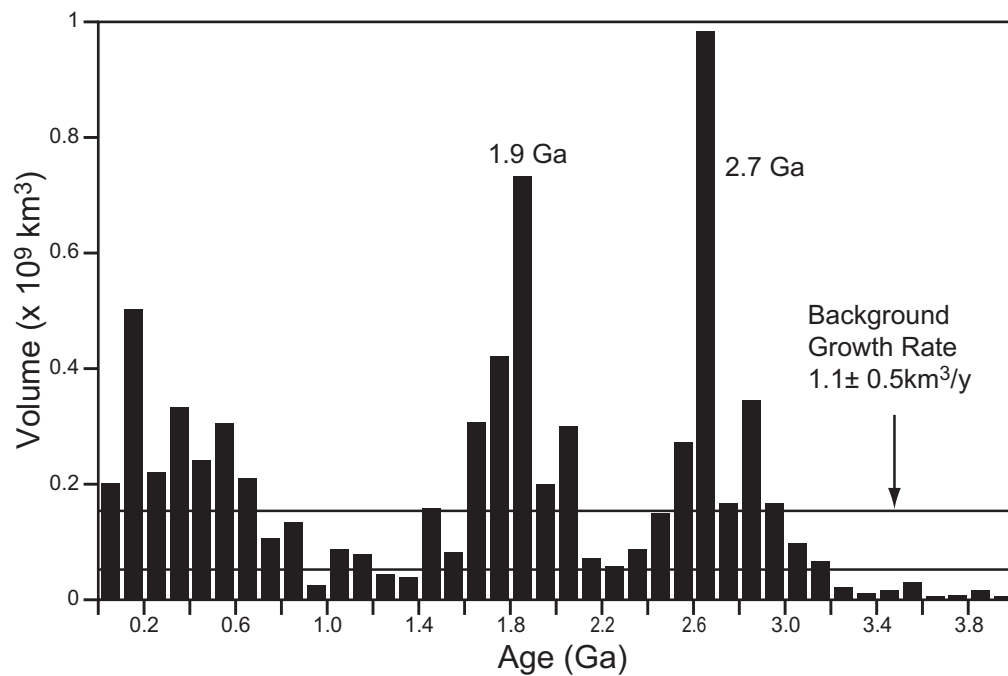
16.3.3.1. The Late Archean Superevent: Rapid Crust Formation and Explosion of Microbial Life (2.78–2.63 Ga) s0185

Rapid Crustal growth s0190

The period 2.78–2.63 Ga is distinguished by arguably the greatest volume of crust produced at any time in Earth history, possibly forming one or more supercontinents (Figure 16.18; Kenorland and Superia and/or Sclavia: Aspler and Chiarenzi, 1998; Condie, 1998; Isley and Abbott, 2002; Bleeker, 2003). This growth was most likely caused by a catastrophic overturn event (flush instability) in the mantle (Stein and Hofmann, 1994; Breuer and Spohn, 1995; Davies, 1995; Condie, 1998; 2000, 2004; Condie et al., 2001; O'Neill et al., 2007; Pearson et al., 2007; Maurice et al., 2009; Safanova et al., 2010). Some modeling suggests that nearly 100% of the continental crust had been formed by c. 2.5 Ga (or even earlier: Armstrong, 1981; 1991), with all subsequent growth balanced by the effects of subduction-erosion (Scholl and von Huene, 2007; Hawkesworth et al., 2010). p0725



f0090 **FIGURE 16.17** Changes in rock types and life forms across the Great Oxidation Event at c. 2.2 Ga. Dark shaded boxes indicate features indicative of a reducing atmosphere, whereas open boxes are features associated with an oxidized atmosphere. (adapted from Holland, 1994).



f0095 **FIGURE 16.18** Histogram of U-Pb zircon ages from juvenile crust through time, emphasizing the episodic nature of crust formation. (from Condie, 2000).

p0730 Whereas some have suggested that the zircon peaks through Earth history that were compiled by Condie (1998) reflect only a fluke of preservation (e.g., Kemp et al., 2006; Hawkesworth et al., 2009), this is discounted — at least for the 2.8–2.5 Ga peak in zircon ages — by evidence for a large mantle melting event associated with this peak in crustal growth, by a temperature change of the mantle, a possible a change in the style of subduction, and by well established indicators of major change in many different proxies for crustal composition, such as shale compositions (Taylor and McLennan, 1985; Richter, 1988; Condie and Wronkiewicz, 1990; Condie, 1993, 2008; Barley et al., 1998, 2005; Condie et al., 2001; Isley and Abbott, 2002; Pearson et al., 2007; Herzberg et al., 2010).

p0735 The 150 million-year-long period from 2.78–2.63 Ga witnessed the creation of large areas of granite-greenstone crust, as well as areas of high-grade gneiss (Windley and Bridgwater, 1971). Both of these types of terrain contain very good evidence of plate tectonics (e.g., Bridgwater et al., 1974; Nutman et al., 1989; Card, 1990; Calvert et al., 1995; Davis, 1998; Van Kranendonk, 2004, 2011; Percival, 2007; Windley and Garde, 2009), despite some differences with modern counterparts (Smithies, 2000; Martin et al., 2005) and skepticism by some researchers about any form of Archean plate tectonics (Hamilton, 1998; 2003, 2007; Stern, 2005). Studies have suggested that plate motions were as fast as, or up to five times faster, than any known from the Phanerozoic (Strik et al., 2003; Blake et al., 2004). In addition to crust that formed as a direct result of subduction-accretion processes, there is clear evidence that at least some late Archean granite-greenstone crust formed as a result of mantle plumes (Tomlinson and Condie, 2001; Bédard, 2006; Van Kranendonk et al., 2007b; Van Kranendonk, 2011) and some models suggest crust formation by the interaction between these two (plume and plate) superimposed tectonic processes (e.g., Nelson, 1998; Wyman et al., 2002).

p0740 Supracrustal sequences within crust that formed during this time interval commonly contain a relatively high volume of komatiites, a type of ultramafic lava or volcanoclastic rocks, with >18% MgO (Viljoen and Viljoen, 1969; Arndt et al., 2008). There are two geochemical types: Barberton, or Al-depleted, komatiites, and Munro, or Al-undepleted, komatiites (Arndt, 2003). Both are derived from melting an anhydrous, unusually hot (1700–1900°C) and deep, source, ~250°C hotter than ambient mantle (Herzberg et al., 2007; Berry et al., 2008). Barberton-type komatiites were derived through 30% fractional melting in the presence of garnet, at $P > 10$ GPa (300 km), within a rising mantle plume source (Arndt, 2003; Herzberg et al., 2007). Munro-type komatiites were derived from the melting of a cooler plume source, with 50% fractional melting, but without garnet being present and therefore derived from shallower in the mantle. A cooler source for Munro-type komatiites is consistent with their generally younger age (typically 2.7 Ga) than Barberton-type

komatiites (3.5 Ga), although both types are found in the Neoproterozoic Abitibi greenstone belt (Superior Province, Canada: Sproule et al., 2002), and recent petrological data suggest that the mantle may have been hotter during this younger part of the Archean (Herzberg et al., 2010). Significantly, komatiites do *not* represent oceanic crust, as they derive from too great a depth and commonly contain evidence of eruption onto (and contamination by and mixing with) older continental crust, as part of widespread cover sequences (Arndt and Jenner, 1986; Claoué-Long et al., 1988; Bleeker et al., 1999; Chavagnac, 2004; Trofimovs et al., 2004; Maurice et al., 2009).

The presence of widespread komatiite eruption in the p0745 period 2.78–2.63 Ga, in combination with the zircon evidence for a large volume of crust generated during his period and the petrological evidence for a hotter mantle, attests to an anomalous period of mantle activity (Condie, 1995, 1998; Davies, 1995; Arndt, 2004; Herzberg et al., 2010). Many suggestions have been made as to the cause of the large volume of crust formation, including: a superplume, or swarm of plumes; an avalanche of subducted continental lithosphere into the deep mantle, causing it to upwell and melt through decompression; or overturn of a two-layered mantle (Condie, 1995, 1998; Davies, 1995; Barley et al., 1998; Condie et al., 2001; Rey et al., 2003; O'Neill et al., 2007). Whatever the cause, the anomalous mantle activity resulted in prolonged, widespread, and extensive volcanism. This would have pumped enormous volumes of volcanic gases (CO_2 , H_2S , SO_2) into the atmosphere. Recent experience of the effects of even a single large volcanic eruption on the atmosphere (e.g., Robock et al., 2009) and on the composition of weathering products (Gislason et al., 2009), show that the widespread volcanism of the Late Archean Superevent would have had a very significant effect on the composition of the atmosphere and the oceans, causing them to become highly reducing. Such a highly reducing late Archean atmosphere is indicated by the widespread occurrence of massive sulfide deposits of this age (Barley et al., 1998; Condie et al., 2001), as well as by the largest $\Delta^{33}\text{S}$ anomalies in Earth history commencing at about 2.65 Ga (Figure 16.12; Farquhar et al., 2000; Farquhar and Wing, 2003).

Late Archean greenstone successions commonly contain p0750 BIFs, including silicate, carbonate, and sulfide facies types that may be up to several hundreds of meters thick and extend laterally for several hundred kilometers in folded greenstone belts (Peter, 2003; Klein, 2005). In most cases, these “Algoma-type” BIFs can be directly associated with volcanism, and thus represent local exhalatives. In contrast, younger, “Superior-type”, or cratonic basin-type BIFs were deposited on continental margins as a result of upwelling, reduced, deep seawater and its interaction with more oxygen-rich, near-surface waters (Cloud, 1973; Klein and Beukes, 1989; Trendall and Blockley, 2004; Beukes and Gutzmer, 2008). A recent study in the Yilgarn Craton has shown that

late Archean hematite-magnetite-pyrite BIF was precipitated abiogenically, first as low-Fe jaspilitic chert from reduced hydrothermal exhalations that interacted with a pool of free O₂, and subsequently through enrichment and reduction to magnetite and then pyrite through the actions of interbasinal fluid circulation (Czaja et al., 2010a).

s0195 **Explosion in Microbial Life (With a Contribution from C. Johnson)**

p0755 The period of late Archean crustal growth was accompanied by large excursions in many of the chemical proxies of microbial life, including $\delta^{13}\text{C}_{\text{kerogen}}$ (to -61‰), $\delta^{56}\text{Fe}$ (to -3.1‰), $\delta^{34}\text{S}$ (to -20‰), and, in the younger half of the period, $\Delta^{33}\text{S}$ (to $+8\text{‰}$; Figure 16.15). These proxies show that life was significantly out of equilibrium with geological processes during this period, that the atmosphere was highly reducing (Rye and Holland, 1998; Farquhar et al., 2000; Farquhar and Wing, 2003), and that equilibrium between the biosphere and geological processing was not re-established until sometime after ~ 2.45 Ga, when the Earth cooled and oxygen levels started to rise in the atmosphere (see Sections 16.3.3.3, 16.3.3.4).

p0760 One of the best preserved and most fossiliferous stratigraphic units deposited in this time period is the c. 2725 Ma Tumbiana Formation of the Fortescue Group, in the Pilbara region of Western Australia (age from Blake et al., 2004). This formation consists of widespread stromatolitic carbonates deposited under lacustrine, fluvial and very shallow, shelf to coastal marine conditions (Figure 16.19; Walter, 1983; Buick, 1992; Sakurai et al., 2005; Bolhar and Van Kranendonk, 2007; Awramik and Buchheim, 2009). Low seawater sulfate is indicated by the absence of sulfate evaporite minerals and presence of halite crystal moulds (Buick, 1992; Eriksson et al., 2005; Awramik and Buchheim, 2009), although minor amounts of evaporative sulfates have been found in contemporaneous carbonates elsewhere (Golding and Walter, 1979). The presence of giant aragonite botryoids and stratiform sheets of magnesian calcite in rocks of similar age have been used to infer a late Archean ocean significantly oversaturated in CaCO₃ (Grotzinger and Kasting, 1993).

p0765 Tumbiana stromatolites are diverse and display clear phototactic behavior, including palimpsest fabrics after erect filaments (Figure 16.19; Buick, 1992). They also contain local, poorly-preserved microfossils (Schopf and Walter, 1983), and organic globules and aragonite nanocrystals that are remarkably similar to the organo-mineral building blocks of modern stromatolites dominated by cyanobacteria (Lepot et al., 2008). Kerogens from these stromatolitic carbonates and other near-contemporaneous rocks yield $\delta^{13}\text{C}$ values of up to -61‰ , indicative of methanotrophy or anaerobic oxidation of methane coupled to bacterial sulfate reduction (Hayes, 1983, 1994; Schidlowski, 1988; Packer, 1990; Buick, 1992; Rye and Holland, 1998; Hinrichs, 2002). Modeling

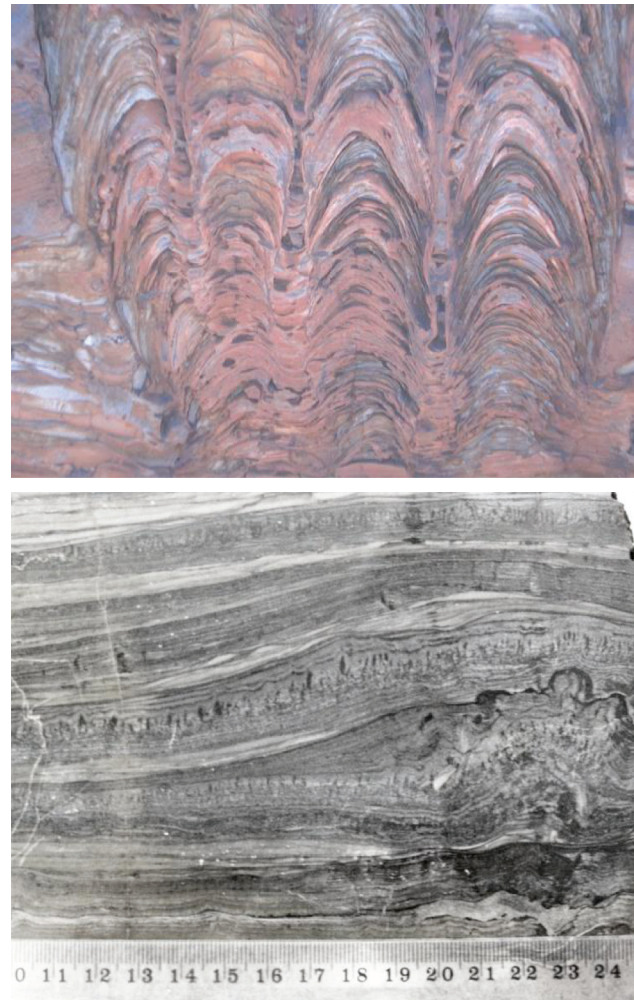


FIGURE 16.19 Branching, columnar stromatolite from the 2.72 Ga Tumbiana Formation, Fortescue Group (Australia). f0100

suggests that under conditions of low seawater sulfate ($<200\mu\text{M}$), 30–70% of carbon was processed through methanogenesis at this time, with methane escaping into, and accumulating in, the atmosphere (Habicht et al., 2002). Indeed, the global and highly negative $\delta^{13}\text{C}$ isotopic values characterizing this time period prompted Hayes (1994) to suggest that this period could be referred to as the “Age of Methanotrophs”.

Detailed analysis of Tumbiana Formation stromatolites p0770 has identified two sources of kerogen, including sulfur-rich globules interpreted as microbial cells selectively preserved through polymerization by early diagenetic sulfurization that was fuelled by bacterial sulfate reduction (Lepot et al., 2009). Buick (1992) argued that the lack of sulfate in the lacustrine deposystem, together with the textural evidence of phototactic behavior, could be used as evidence in favor of oxygenic photosynthesis and thus the presence of cyanobacteria at this time, forming part of a complex microbial ecosystem that also may have included sulfate reduction

(Kakegawa and Nanri, 2006), although this latter process is considered to have been minor prior to 2.5–2.4 Ga (Halevy et al., 2010). Evidence of a complex microbial ecosystem in Tumbiana Formation stromatolites was confirmed by Thomazo et al. (2011), who showed ^{15}N -enrichments that probably record the onset of nitrification and denitrification under the influence of oxygen. Production of oxygen by cyanobacteria has also been inferred by the presence of primary hematite formed from the flow of oxygenated groundwater at >2.76 Ga elsewhere in the Pilbara (Kato et al., 2009).

p0775 Cyanobacterial molecular fossils (steranes and related products of carbon maturation) were apparently discovered by Brocks et al. (1999) through analysis of ~2.7 Ga Jeerinah Formation shale of Western Australia. These molecular biomarkers, together with carbon isotopic values, were used as clear evidence of the existence of oxygenic photosynthetic processes at this time. Surprisingly, however, eukaryotic biomarkers from the same rocks were reported in the same publication, and this shed serious doubts on the validity of this discovery, as eukaryotic development is widely regarded as having arisen much later in Earth history.

p0780 Nevertheless, Eigenbrode et al. (2008) have independently confirmed the presence of methylhopane biomarker hydrocarbons in Neoproterozoic formations from the Mount Bruce Supergroup of Western Australia. Further support has been recently derived from c. 2.6–2.5 Ga rocks of the Kaapvaal Craton by Waldbauer et al. (2009), who reported on late Archean bitumens that contain hopanes attributable to bacteria, potentially including cyanobacteria and methanotrophs, but also steranes of eukaryotic origin. An early appearance of Eukaryotes is supported by phylogenies based on small subunit RNA genes and whole genomes (Pace, 1997; House and Fitz-Gibbon, 2002). Thus, together with arguments discussed above, as well as geochemical data (see Schopf, 2004 for an overview), the molecular fossil biomarker evidence strongly supports that cyanobacterial oxygenic photosynthesis was fully established and evolved well before (≥ 2.7 Ga) the atmosphere became more fully oxidized at c. 2.3 Ga (see Sections 16.3.3.3 through 16.3.3.5; Brocks et al., 2003; Kato et al., 2009).

p0785 A vital cyanobacteria-based biosphere is at least partly evidenced by the presence of thick black shale deposits at this time, a classic geologic biosignature of marine plankton (e.g., Sleep and Bird, 2007; Buick, 2008). However, low levels of biologically available nitrogen may have limited the growth of oxygen-producing plankton, and this, together with a highly reducing atmosphere and oceans, may have combined to delay the accumulation of oxygen in the atmosphere (e.g., Godfrey and Falkowski, 2009). Indeed, Pavlov et al. (2001a, b) and Kasting (2005) have suggested that the late Archean atmosphere was characterized by high methane concentrations and even a Titan-like organic haze produced at a rate comparable to the modern rate of organic carbon burial

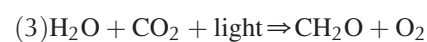
in marine sediments and accounting for the pronounced low- $\delta^{13}\text{C}$ kerogens in late Archean sediments (Hayes, 1994).

At ~2.75 Ga, several hundred million years before the initial increase in atmospheric O_2 , $\delta^{56}\text{Fe}$ values decrease to the lowest values yet measured in sedimentary rocks (Figure 16.15). This shift is seen in sedimentary sulfides, organic-carbon-rich bulk shales, and BIFs, suggesting a widespread shift in Fe cycling across many marine environments (Johnson and Beard, 2006). These isotopic variations contrast with the vast majority of Fe in the crust, as well as in the bulk of sedimentary detritus of Archean to modern age, which has a $\delta^{56}\text{Fe}$ value near zero, independent of atmospheric O_2 contents (Beard et al., 2003a, b; Yamaguchi et al., 2005).

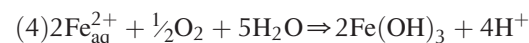
Two competing proposals have been put forth to explain the highly negative $\delta^{56}\text{Fe}$ excursions at this time. One interpretation favors abiological processes, whereby oxidation of marine hydrothermal $\text{Fe}^{2+}_{\text{aq}}$ during BIF genesis, or oxide precipitation on continental shelves, produced negative $\delta^{56}\text{Fe}$ values in seawater, which was directly incorporated into sulfide-rich marine sedimentary rocks (Rouxel et al., 2005; Dauphas and Rouxel, 2006; Anbar and Rouxel, 2007). These authors rejected microbial Fe cycling as an explanation for the Fe isotope excursions, arguing that insufficient quantities of low- $\delta^{56}\text{Fe}$ may be produced by microbial processes such as dissimilatory iron reduction (DIR).

In contrast, Johnson et al. (2008a, b) proposed that the large negative excursion in $\delta^{56}\text{Fe}$ values reflected an expansion in DIR prior to the rise in atmospheric O_2 , followed by a contraction in geographic extent <2.3 Ga, as BSR expanded in response to increasing seawater sulfate contents (Figure 16.15). Anaerobic metabolisms such as DIR would have thrived in the oceans prior to the rise in atmospheric O_2 , particularly if reactive Fe fluxes at 2.8–2.3 Ga had high $\text{Fe}^{3+}/\text{Fe}^{2+}$ ratios, as expected to occur as oxygen sinks were consumed prior to the rise in ambient O_2 .

Development of oxygenic photosynthesis marked a one to two order of magnitude increase in ocean primary productivity relative to anaerobic photosynthesis (e.g., Des Marais, 2000; Canfield et al., 2006; Rosing et al., 2006). Oxygenic photosynthesis is most simply written as:



Ambient O_2 , when combined with riverine or hydrothermally sourced $\text{Fe}^{2+}_{\text{aq}}$, would react at circum-neutral pH to produce ferric oxide precipitates:



Reactions 1–4 produce the essential components required to support heterotrophic respiration, including DIR, which may be written:



p0820 DIR is phylogenetically diverse, found throughout the Bacteria and Archaea, including hyperthermophiles, sulfate reducers, nitrate reducers, and methanogens, involving a wide variety of electron donors (e.g., Lovley et al., 2004), and is considered to be one of the earliest microbial metabolisms on Earth (Vargas et al., 1998; Lovley, 2004).

s0200 **16.3.3.2. Continental Maturation, Rusting of the Oceans and the Widespread Microbial Production of Oxygen (2.63–2.42 Ga)**

p0825 (with a contribution from C. Johnson and B. Beard)

p0830 The time period 2.63–2.42 Ga is characterized by waning crustal growth, and at the same time by stiffening and emergence of the continents (Arndt et al., 2001; Flament et al., 2008; Rey and Coltice, 2008). This led to the widespread development of shallow, stable continental shelves on which flourished widespread microbial communities fed by a release of nutrients from continents that were tied more deeply to the hydrological weathering cycle. This bloom of microbial life started pumping out significant amounts of oxygen, which filled reductant sinks in the oceans — especially dissolved reduced iron — and precipitated vast amounts of BIF on many continents (e.g., Catling et al., 2001). Indeed, the first chemical traces of oxygen are recognized during this time period, showing that the transformation to an oxygenated atmosphere had begun (Siebert et al., 2005; Anbar et al., 2007; Wille et al., 2007).

p0835 Continental growth slowed significantly after ~2.63 Ga, with only minor crustal growth recorded in a relatively few cratons to 2.5–2.42 Ga (e.g., Condie, 1998, 2000; Hartmann et al., 2006; Condie et al., 2009), such as the Slave and Rae provinces (Canada), Gawler Craton (Australia), North China Craton (China), and Dharwar Craton (India) (Jayananda et al., 2000; Davis, W. J. et al., 2003; Geng et al., 2006; Belousova et al., 2009; Berman et al., 2010). As with the earlier part of the Archean, tectonic styles of crust formation during this later stage of the Archean included plate tectonics (growth through subduction/accretion: Jayananda et al., 2000) and also the effects of partial convective overturn due to weak lithosphere (Chardon et al., 2002). However, most other pieces of crust had become stabilized by this time through the effects of widespread partial melting and depletion of the mid to lower crust, emplacement of post-tectonic granites, and maturation of the mantle root (e.g., Moser et al., 2008).

p0840 Widespread cratonization at c. 2.63 Ga was immediately followed by the deposition of thick, platformal successions from 2.63–2.42 Ga. An increased area of shallow continental shelves and highly reducing atmosphere promoted cyanobacterial activity and the production of oxygen at this time, leading to a gradual rise in oxygen — as reflected by various chemical proxies (Siebert et al., 2005; Anbar et al., 2007; Wille et al., 2007; Kaufman et al., 2008; Lindsay, 2008; Frei et al., 2009; Godfrey and Falkowski, 2009; Reinhard et al.,

2009; Kendall et al., 2010; Sethumadhav et al., 2010). Detailed studies show that microbial life was complex, highly advanced and diverse, including both sulfur and aerobic nitrogen cycling, in addition to cyanobacterial oxygenic photosynthesis (Ono et al., 2003, 2009; Kamber and Whitehouse, 2007; Kaufman et al., 2008; Partridge et al., 2008; Garvin et al., 2009; Czaja et al., 2010b). Despite the widespread production of oxygen at this time and evidence for a shallow surface oxidized layer in the oceans probably resulting from the activity of phototrophic plankton, sulfur isotopes indicate that the atmosphere and deep oceans were still highly reducing (Figure 16.15; Klein and Beukes, 1989; Farquhar et al., 2000; Pavlov et al., 2001a, b, 2003; Farquhar and Wing, 2003; Reinhard et al., 2009). Deep water environments were characterized by deposition of black shales and BIF, indicating continued reducing conditions in deep marine basins (Figure 16.20). Shallow water deposits include widespread stromatolitic carbonate platforms dominated by cyanobacteria (Altermann and Schopf, 1995; Kazmierczak and Altermann, 2002; Kazmierczak et al., 2009). Local evaporite deposits of calcium sulfates have also been described from rocks of this age, together with halite casts (Simonson et al., 1993; Sumner and Grotzinger, 2000; Hardie, 2003; Eriksson et al., 2005; Gandin et al., 2005; Gandin and Wright, 2007). Post-depositional alteration of evaporites to carbonates and chert is ascribed to the activity of bacterial sulfate reduction, whose effects are preserved as variable $\delta^{34}\text{S}$ values of pyrite (Gandin et al., 2005). Large and abundant crystal fans in the c. 2.5 Ga Campbellrand-Malmani carbonate platform of South Africa have been interpreted to represent pseudomorphs after aragonite that were precipitated as crusts directly onto the seafloor, and to reflect unusually high supersaturation of calcium carbonate and high HCO_3^- concentrations in the latest Archean oceans (Sumner and Grotzinger, 2000, 2004). However, many of the crystal fans

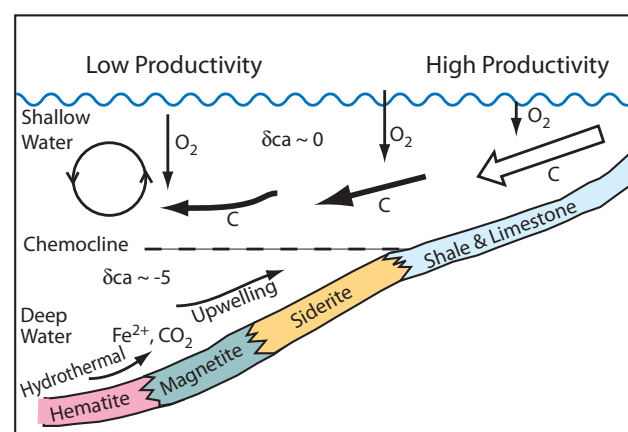


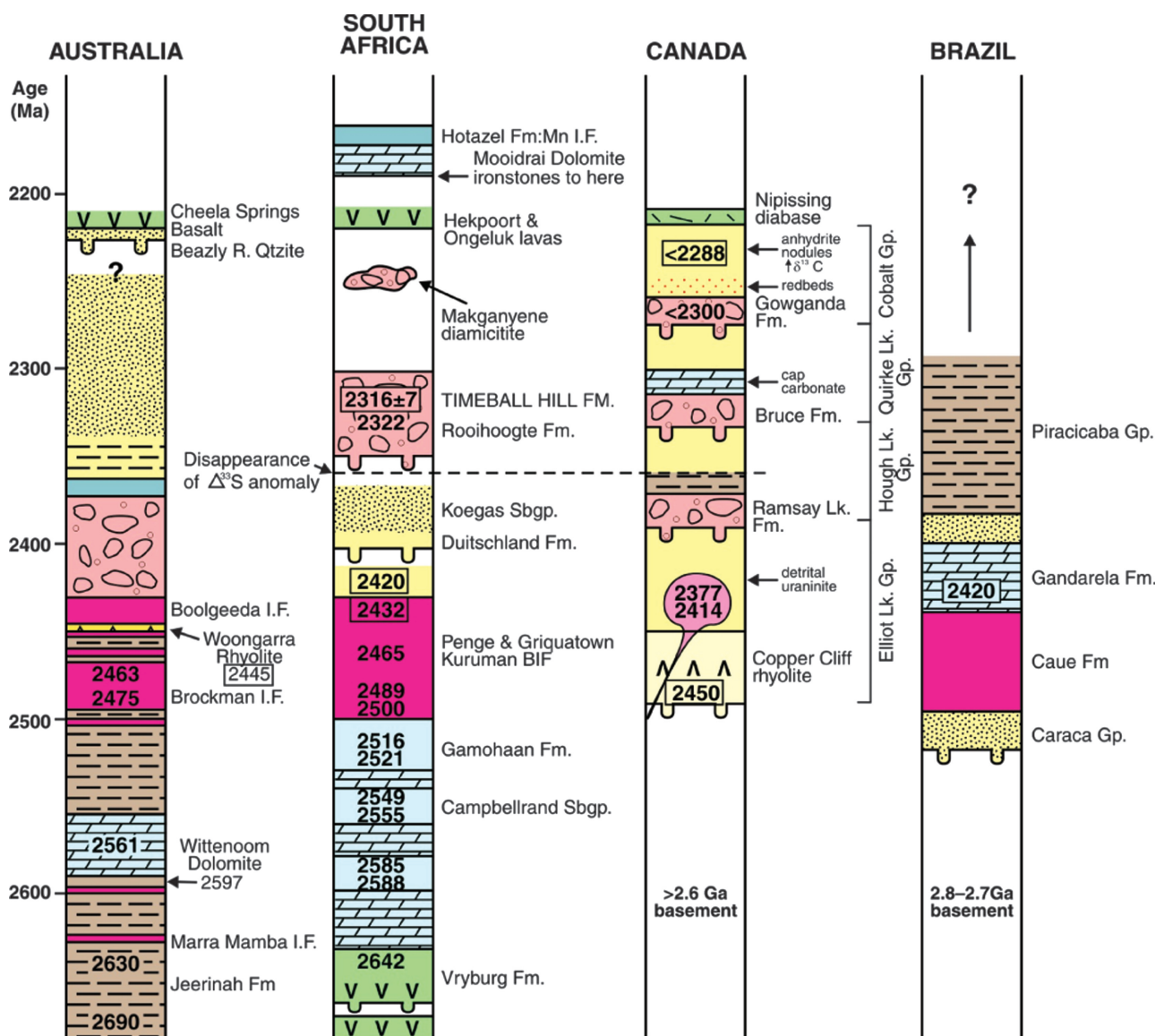
FIGURE 16.20 Facies model showing relationship between shale and limestone and three mineralogical varieties of iron formation (siderite, magnetite, and hematite) with depth, across a chemocline in a layered late Archean ocean. (from Beukes et al., 1990).

clearly cut through (i.e., have grown within) previous carbonate sediment, and occur only in shallow water environments; thus, the occurrence of such crystals most likely represent the effects of diagenesis, possibly as a result of evaporative conditions (W. Altermann, pers. comm., 2009).

p0845 The largest volume of BIF in Earth history was deposited over this period, as “Superior-type”, or cratonic basin-type iron formation (Figure 16.15). The best studied of these deposits include the coeval Hamersley (Australia) and Transvaal (South Africa) basins, with correlated impact spherule layers between the two basins (Simonson et al., 2009), despite a varied lithostratigraphy (Altermann and

Nelson, 1998; Pickard, 2002, 2003; Trendall et al., 2004; Eriksson et al., 2007). BIFs of this age also occur on many other continents, including South America, Russia, and North America (Figure 16.21; see Beukes and Gutzmer, 2008). The Hamersley Basin contains several units of BIF, totaling 900 m in thickness, with individual units up to 142 m thick (Trendall, 1972). These are interbedded with units of black shale, green “shale” (technically still iron-formation with 30–40 wt % Fe), and carbonate (Figure 16.2).

Three different scales of layering have been recognized in p0850 the BIF, including millimeter-scale couplets of iron and silica (Microbands), centimeter-scale bundles of laminated rocks



f0110 **FIGURE 16.21** Comparative stratigraphic columns across the Archean-Proterozoic transition, showing major accumulations of BIFs (red) and glacial deposits (light brown, with irregular ellipses overprint). Yellow = clastic sedimentary rocks; blue = carbonates; green = basaltic rocks and dolerite; pale yellow = felsic volcanic rocks; grey-blue = Mn-rich sedimentary rocks; light pink = granite. Numbers inside columns denote U-Pb zircon or Pb-Pb carbonate age dates (sources of information cited in text).

(Mesobands), and decimeter to meter-scale Macrobands, with at least some of the variation in layering controlled by orbital procession (Trendall and Blockley, 1970; Trendall, 1972). In Australia, BIFs were deposited on a continental platform, mostly below storm wave base, through upwelling of deep ocean Fe derived from (?mid-ocean) hydrothermal systems, which mixed with surficial O₂ in what was probably a layered ocean at this time (Figure 16.20; Cloud, 1973; Morris and Horwitz, 1983; Klein and Beukes, 1989; Beukes et al., 1990; Towe, 1990; Klein and Ladeira, 2000; Trendall and Blockley, 2004; Beukes and Gutzmer, 2008; Steinhofel et al., 2009). Many researchers now consider that bacteria – specifically iron-oxidizing bacteria – probably had a direct role in precipitating the iron formations (e.g., Konhauser et al., 2002; 2007a; Beukes and Gutzmer, 2008; Croal et al., 2008; Crowe et al., 2008). A variety of models to explain the variation between Fe and Si rich bands have been proposed, including a decoupled source of Fe (mid-ocean ridges) and Si (continental weathering: Hamade et al., 2003), the effects of temperature fluctuations in the oceans on iron-oxidizing bacteria (Posth et al., 2008), or positive feedbacks during chemical alteration of oceanic crust (Wang, Y. et al., 2009).

p0855 “Superior-type” BIFs at ~2.5 Ga, such as the Brockman and Kuruman iron formations, are interpreted by Johnson et al. (2008a, b) as reflecting extensive DIR activity, supported by exceptionally high Fe, but low S, fluxes. Johnson et al. (2008a, b) argued that the negative $\delta^{56}\text{Fe}$ values in Neoproterozoic and Paleoproterozoic marine sedimentary rocks cannot reflect those of the open oceans, as proposed by Rouxel et al. (2005) and Anbar and Rouxel (2007), because large ranges in $\delta^{56}\text{Fe}$ values are measured over centimeter distances in BIFs and black shales, which would require rapid changes in seawater $\delta^{56}\text{Fe}$ values and is inconsistent with the generally accepted long ocean residence times for Fe during this period. Moreover, Johnson et al. (2008a, b) noted that abiologic mechanisms for producing negative $\delta^{56}\text{Fe}$ values, such as extensive oxidation and precipitation that produces very low Fe contents in the remaining fluid, cannot explain the occurrence of negative $\delta^{56}\text{Fe}$ values in Fe-rich rocks such as BIFs. In a review of Fe isotope data from experimental systems and natural environments, Johnson et al. (2008a) noted that DIR produces several orders of magnitude larger quantities of low- $\delta^{56}\text{Fe}$ Fe than abiologic processes such as oxidation and precipitation, lending support to the interpretation that the negative $\delta^{56}\text{Fe}$ values in Neoproterozoic and Paleoproterozoic rocks may largely reflect biological Fe cycling.

p0860 The effects of thickening and strengthening of the continental lithosphere at the end of the late Archean growth cycle (e.g., Flament et al., 2008), when combined with the insulating effects resulting from the formation of one or more supercontinents (e.g., Coltice et al., 2007), led to the widespread emplacement of mafic-ultramafic sills and dykes from 2.57–2.42 Ga, although dykes were also emplaced into crust

outside of this range, at both older and younger ages (Figure 16.3; Heaman, 1997; Nemchin and Pidgeon, 1998; Vogel et al., 1998; Ernst and Buchan, 2001; Grant et al., 2009; Kulikov et al., 2010; Nilsson et al., 2010). This widespread mafic-ultramafic magmatism was tied to lithosphere extension and breakup of supercontinent(s) in the prelude to the next global supercycle that led to global tectonism and the formation of supercontinent Nuna (Columbia) in the interval 2.0–1.75 Ga (see Section 16.3.3.5).

16.3.3.3. Mantle Slowdown, Global Cooling and the Great Oxygenation Event (2.42–2.25 Ga) s0205

The period 2.42–2.25 Ga is perhaps the least represented p0865 time interval in the geological record after c. 4 Ga (Condie, 1998, 2000), and has recently been interpreted to reflect a global magmatic shutdown over 250 Ma (Condie et al., 2009). However, there is at least some evidence of geological activity, both in terms of basin sedimentation and in magmatism (e.g., Vuollo and Huhma, 2005; Feybesse et al., 2006; Dos Santos et al., 2009; Berman et al., 2010; French and Heaman, 2010) so that, although a complete shutdown of the mantle during this time period is unlikely, global geological activity certainly slowed significantly following on from the late Archean mantle-crust blowout (Figure 16.19). One possible reason for this magmatic slowdown is a significant cooling of the mantle (e.g., Davies, 1995), leading to an episode of stagnant-lid behavior (O’Neill et al., 2007; Ernst, 2009), similar to the apparently dominant tectonic style of Venus (Turcotte et al., 1999). Accompanying this period of severely limited geological activity was the global cooling of the atmosphere and concomitant rise in atmospheric oxygen, resulting in widespread glacial deposits (Figures 16.15 and 16.18; Kirschvink et al., 2000; Canfield, 2005). Atmospheric cooling itself likely had a feedback effect on the mantle, further slowing down mantle convection and limiting plate tectonics and crustal growth during this period (Lenardic et al., 2008; Landuyt and Bercovici, 2009).

Decreasing mantle temperatures led to thickening and p0870 strengthening of the continental lithosphere that, when coupled with cooling and thinning of the oceanic lithosphere, led to the emergence of continents and a change in the balance between volcanism and hydrothermal alteration prior to this time, and weathering and erosion of continents thereafter, with exposed rocks increasingly tied to hydrological rock weathering cycle (Vlaar, 2000; Flament et al., 2008; Rey and Coltice, 2008).

Recent studies of mass independent fractionation of sulfur p0875 isotopes have shown that the level of atmospheric oxygen rose to $>10^{-5}$ present atmospheric level (PAL) by 2.4–2.3 Ga during a period of widespread, or possibly global, glaciation (Figures 15, 21; Kirschvink, 1992; Kirschvink et al., 2000; but see also Young, 2002). Goldblatt et al. (2006) regard this change as a major switch between two stable

steady states for atmospheric oxygen, between an early, low-oxygen steady state, and a younger, high-oxygen steady state, with the change brought on by ultraviolet shielding of the troposphere. After the Paleoproterozoic glacial episode, oxygen levels in the atmosphere rose in a stepwise manner, leading to current levels only after the Neoproterozoic glaciations at c. 700 Ma (Des Marais et al., 1992; Kasting and Catling, 2003) (see Section 16.3.4.3).

p0880 The Paleoproterozoic glacial event is characterized by up to three intervals over the period 2450–2220 Ma, as gleaned primarily from the well-studied, rift-related Huronian Supergroup in North America (Figures 21, 22; Coleman, 1908; Roscoe, 1973; Nesbitt and Young, 1982; Krogh et al., 1984; Corfu and Andrews, 1986; Roscoe and Card, 1993; Fedo et al., 1997; Young and Nesbitt, 1999; Ojakangas et al., 2001). Glaciogenic rocks of this age have also been reported from South Africa (Visser, 1971; Bekker et al., 2001, 2004; Hannah et al., 2004; Polteau et al., 2006), Australia (Trendall, 1981; Martin, 1999), Finland (Marmo and Ojakangas, 1984), and India (Sinha-Roy et al., 1993; Mazumder et al., 2000). Originally considered to include low-latitude glaciations (Evans et al., 1997; Williams and Schmidt, 1997), this is now in some doubt (Hilburn et al., 2004), although the association of glacial rocks with deposits characteristic of tropical settings (carbonate rocks, redbeds and evaporates: Gay and Grandstaff, 1980; Nesbitt and Young, 1982; Ojakangas et al., 2001) supports a nearly global, at least partially low latitude, glaciation event, as do quite highly negative $\delta^{13}\text{C}_{\text{carbonate}}$ values (to -15%) from glacial diamictites and cap carbonates of this period (Lindsay and Brasier, 2002; Bekker et al., 2005; Polteau et al., 2006; Van Kranendonk, 2010b).

p0885 In South America, carbonates overlying BIFs in the Minas Supergroup are 2420 ± 19 Ma, but show no stratigraphic or carbon isotopic evidence of deposition during glaciation, which appears not to be recorded in this area (Babinsky et al., 1995; Bekker et al., 2003a). Rather, unconformably overlying carbonates contain the distinctive positive $\delta^{13}\text{C}$ values ($+5$ to $+8\%$) of the Lomagundi-Jatuli isotopic excursion (2.22–2.06 Ga: see Section 16.3.3.4) and are <2125 Ma (Bekker et al., 2003a). A post 2420 Ma age of glaciations is also inferred for glacial deposits in Australia, from detrital zircon data (Takehara et al., 2010), and from South Africa, based on an unpublished age of 2415 ± 6 Ma from the non-glaciogenic Koegas Formation underlying the glaciogenic Makganyene Formation (Figure 16.21; Kirschvink et al., 2000).

p0890 Dating of xenotime overgrowths from the Gordon Lake Formation, stratigraphically overlying the highest of three glacial units (Gowganda Formation) in the Huronian Supergroup suggests that glaciation may have occurred at, or after, 2376 ± 13 Ma (Ray et al., 2008). In the Lake Superior region, a population of 20 detrital zircons from the correlative glaciogenic Enchantment Lake Formation of the Chocloy Group indicates a maximum age of deposition of 2317

± 6 Ma (Ojakangas, 1988; Vallini et al., 2006). Diagenetic pyrites in C-rich shales from the Timeball Hill Formation in between glacial diamictites in South Africa, which are inferred to correlate with the second and third glacial events in the Huronian, have yielded a Re-Os age of 2316 ± 7 Ma (Hannah et al., 2004). The dated pyrites lack mass-independent sulfur isotope fractionation and have highly negative $\delta^{34}\text{S}$ values. When combined with the fact that they are interbedded with a thick ironstone layer consisting of hematitic pisolitic ferricretes and oolitic ironstone beds, these features strongly indicate a rise in atmospheric oxygen to $>10^{-5}$ PAL by this time (Prasad and Roscoe, 1996; Farquhar et al., 2000; Bekker et al., 2004; Hannah et al., 2004; Coetzee et al., 2006; see also Papineau et al., 2007). These data contrast with evidence of a reducing atmosphere at 2450 Ma, immediately before the glaciations (Utsunomiya et al., 2003).

A minimum age for the glaciations is given by the p0895 2219 ± 3 Ma to 2210 ± 3 Ma Nipissing diabase intrusions that cut through the Huronian Supergroup (Corfu and Andrews, 1986; Noble and Lightfoot, 1992), by the 2222 ± 12 Ma Hekpoort and Ongeluk lavas that overlie glacial units in South Africa, and by the $2209 \text{ Ma} \pm 15$ Ma Cheela Springs basalt that overlies glacial rocks in Australia (Figure 16.18; Cornell et al., 1996; Martin et al., 1998).

In Western Australia, glacial diamictites of the Turee p0900 Creek Group (Meteorite Bore Member: Trendall, 1981; Martin, 1999) lie conformably on BIF of the underlying Hamersley Group across a 15 cm thick transitional chert unit that grades from jaspilitic chert with mm-thick bands of iron-formation at the base, through jaspilitic chert in the middle, to grey chert at the top (Figure 16.23; Van Kranendonk, 2010b). The transitional chert unit is conformably overlain by a green, pyritic mudstone with sparse dropstones that marks the base of the Turee Creek Group and onset of clastic, glaciomarine deposition (Figure 16.24). This mudstone unit is overlain by



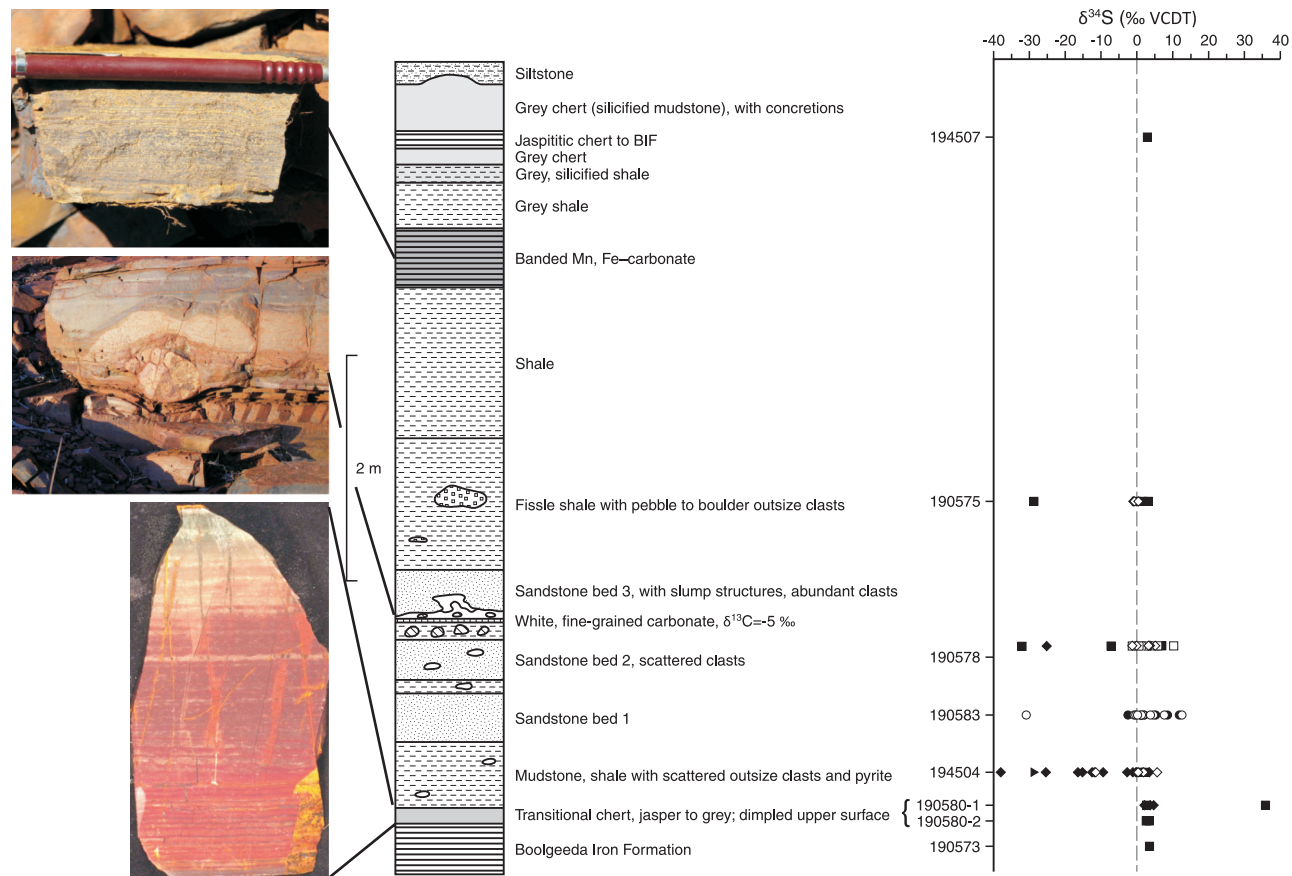
FIGURE 16.22 Paleoproterozoic tillite of the Gowganda Formation, Huronian Supergroup (Canada): note red, oxidized, granitic clasts. f0115



f0120 **FIGURE 16.23** Field photograph of the conformable depositional contact between BIF and the transitional chert unit (TC) of the Hamersley Group and overlying glacial mudstones and sandstones of the Turee Creek Group; author's finger points to the site of a possible GSSP for the Archean-Proterozoic boundary at the top of the transitional chert.

three beds of coarse sandstone containing angular to sub-angular quartz clasts, locally abundant detrital pyrite, and outsize clasts of porphyritic rhyolite, carbonate, and a variety of other lithology within a siltstone matrix. The uppermost of these sandstones contains a thin (1 cm), continuous carbonate bed near its base, which has $\delta^{13}\text{C}$ values of -5‰ . Shale overlying the glacial sandstones still contains dropstones, and contains a distinctive, Mn-rich BIF (up to 7.4 wt% MnO) (Figure 16.24; Van Kranendonk, 2010b).

Sulfur isotope data on pyrite from this section shows that it contains authigenic pyrite with small, but definite $\Delta^{33}\text{S}$ anomalies (-0.83 to 0.96‰ ; Williford et al., 2011) that are comparable to the range reported for the Pecors Fm (-0.07 to 0.88‰) deposited between the first two glacial episodes in the Huronian Supergroup (Papineau et al., 2007). A 90% range in $\delta^{34}\text{S}$ in Meteorite Bore Member pyrite (-45.5 to 46.4‰ ; Williford et al., 2011) is significantly larger than any observed prior to the Neoproterozoic and implies that seawater sulfate concentration had increased above $200 \mu\text{mol}$ by the time of deposition (Habicht et al., 2002). The Paleoproterozoic



f0125 **FIGURE 16.24** A) Stratigraphic section and S-isotope data from the proposed Archean-Proterozoic boundary at the contact of the Hamersley Group and Turee Creek Group, Western Australia (from Van Kranendonk, 2010a and Williford et al., 2011); B) closeup of transitional chert unit, showing gradation from iron formation at very base, through jaspitic chert, to grey chert at top, reflecting progressive scrubbing of iron from the oceans; C) large, well-rounded dropstone of porphyritic rhyolite in glacial mudstone and sandstone; D) banded Mn-rich (up to 7 wt%) iron-formation overlying the glacial deposits.

increase in seawater sulfate concentration is thought to have been driven by increased oxidative weathering of sulfides on the continents and has been constrained by 2322 ± 15 Ma rocks that do not exhibit S-MIF (Bekker et al., 2004).

p0910 Highly negative $\delta^{13}\text{C}$ values in the Timeball Hill Formation (South Africa) were used to infer the presence of seawater sulfate and its reduction by bacteria (Cameron, 1983). Moderately negative $\delta^{13}\text{C}$ values from Turee Creek Group carbonates (-5‰ ; Lindsay and Brasier, 2002; Van Kranendonk, 2010b), indicates support for global glaciation in the Paleoproterozoic (Kirschvink et al., 2000). Conversely, the presence of strongly positive $\delta^{13}\text{C}$ values from carbonate rocks of the Duitschland Formation, from units interbedded with glacial diamictites (Bekker et al., 2001; Guo et al., 2009), suggests a prelude to the younger (2.25–2.06 Ga), global, Lomagundi-Jatuli C-isotopic excursion and at least local imbalance between organic production and carbon burial via an organic carbon cycle operative during the Paleoproterozoic glaciations (see Section 16.3.3.4 and Coetzee et al., 2006).

p0915 Many models have been proposed to account for the rise in O_2 at this time. Some have suggested that it marks the advent of oxygenic photosynthesis (e.g., Hedges et al., 2001; Blank, 2004; Kopp et al., 2005), or that cyanobacteria were restricted to freshwater environments prior to 2.4 Ga before diversifying into marine environments (Blank and Sánchez-Baracaldo, 2010). However, the discovery of cyanobacterial microfossils and biomarkers in much older rocks (2.5 Ga: Altermann and Schopf, 1995; Kazmierczak and Altermann, 2002; Kazmierczak et al., 2009), together with chemical evidence of their existence even well back into the Archean (Cloud, 1972; Siebert et al., 2005; Ono et al., 2006; Anbar et al., 2007; Wille et al., 2007; Hoashi et al., 2009; Kato et al., 2009), demonstrate that photosynthetic production of O_2 commenced much earlier (e.g., Nisbet et al., 2007) and that the rise of O_2 in the atmosphere at ~ 2.4 Ga was due to filling up of reductant sinks (reduced Fe and S) in the world's oceans, combined with a reduction in the volume of reducing gasses being emitted into the atmosphere by a lesser degree of volcanism as a function of a cooling Earth system (see Section 4 and e.g., Barley et al., 2005).

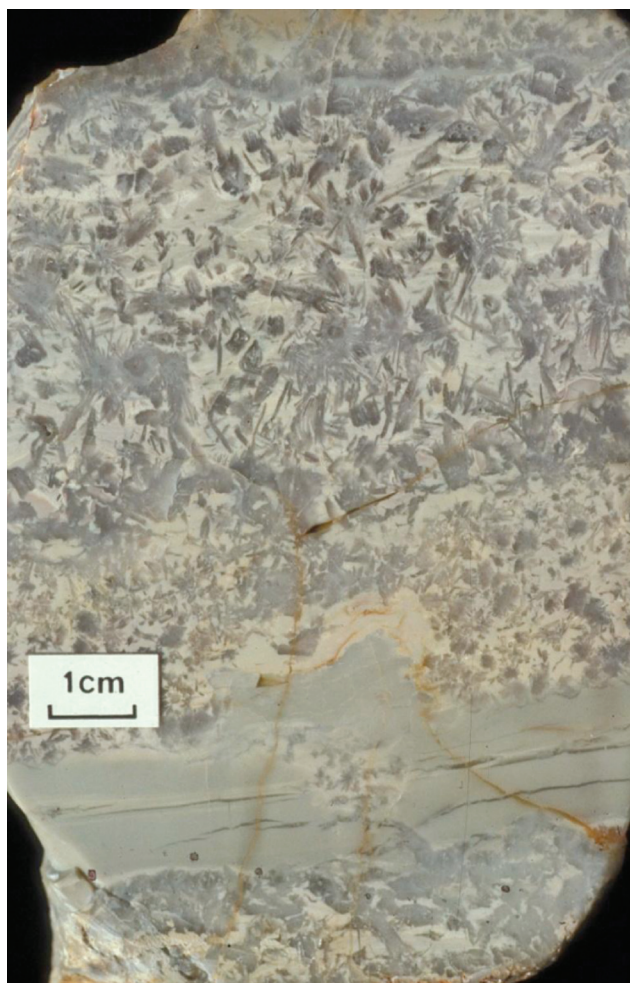
p0920 A number of authors have suggested that atmospheric O_2 rose in response to the collapse of a methane greenhouse atmosphere as a result of the irreversible loss of H_2 to space (Catling et al., 2001; Zahnle et al., 2006). Alternatively, Campbell and Allen (2008) suggested that the rise in atmospheric oxygen was associated with the formation of supercontinents, in which the development of supermountains provided nutrients (Fe, P) to the oceans, which provided the means for a bloom in cyanobacteria and a resultant marked increase in photosynthetic O_2 (see also Lindsay and Brasier, 2002). Kump and Barley (2007) suggested that an increase in subaerial volcanism and associated, more oxidized, volcanic gasses (*viz* SO_2) led to the rise in atmospheric O_2 , reflecting

the maturation of continents. This theme was followed up by Holland (2009), who suggested that the gradual increase in the oxidation state of the atmosphere resulted from an increase in the $\text{CO}_2/\text{H}_2\text{O}$ and/or $\text{SO}_2/\text{H}_2\text{O}$ ratios of volcanic gases. Konhauser et al. (2009) suggested that a depletion in oceanic Ni – as a function of reduced komatiitic volcanism and cooling mantle temperatures – stifled the activity of methanogens and led to a reduction in atmospheric methane, prior to, or contemporaneous with, a rise in O_2 . Thus, as suggested by Melezhik (2006), it appears there may have been many overlapping causes for the Paleoproterozoic glaciations and rise in oxygen.

The increase in $\delta^{56}\text{Fe}$ values between ~ 2.5 and 2.3 Ga p0925 (Figure 16.15) is interpreted by Johnson et al. (2008a) to reflect contraction of DIR in terms of its influence on Fe cycling in the open oceans as seawater sulfide contents increased through increased bacterial sulfate reduction (BSR) activity; increasing sulfide would have titrated reactive Fe, decreasing its availability to support DIR. The increase in range of $\delta^{34}\text{S}$ values after ~ 2.4 Ga records an increase in seawater sulfate contents, producing relatively large S isotope fractionations during BSR, when sulfate is in “excess” (Canfield, 2001). However, sulfate contents probably remained in the 1–2 mM range, significantly lower than the 28 mM concentrations in the modern oceans (Kah et al., 2004). Following the initial rise in atmospheric O_2 contents at ~ 2.3 Ga, Rouxel et al. (2005) and Anbar and Rouxel (2007) suggested that near-zero or positive $\delta^{56}\text{Fe}$ values are characteristic of seawater Fe under an O_2 -bearing atmosphere. Biogeochemical redox cycling of Fe and Mn has been recognized in c. 2.3 Ga rocks of the Hotazel sequence in South Africa (Tsikos et al., 2010), a feature which can be used to infer the presence of a redoxcline within basins (e.g., Dellwig et al., 2010).

16.3.3.4. Breakout Magmatism, the Lomagundi-Jatuli Carbon Isotopic Excursion, and the First Eukaryotes (2.25–2.06 Ga) s0210

The period from 2.25–2.06 Ga witnessed a dramatic rise in p0930 the level of atmospheric oxygen and was perhaps the most novel period in Earth history in terms of new rock types, with the deposition for the first time of: redbeds in continental and marine settings under conditions of oxidative continental weathering; widespread Ca-sulfates in shallow marine environments (Figure 16.25); and phosphorites, and Mn-rich sedimentary rocks in deeper-water environments (Manganese, like Fe, is soluble as Mn^{2+} and is deposited through oxidation reactions to Mn^{3+} or Mn^{4+}) (Perttunen, 1985; Holland, 1994, 2002, 2005; Martin et al., 1998; El Tabakh et al., 1999; Ojakangas et al., 2001; Pirajno and Grey, 2002; Lehtinen et al., 2005; Pollack et al., 2009; Maheshwari et al., 2010). In addition, this period is characterized by renewed magmatic activity on a global scale, but unlike its late



f0130 **FIGURE 16.25** Polished rock slab showing gypsum crystals in carbonate from the c. 2.2 Ga Yerrida Basin, Western Australia. (from Pirajno and Grey, 2002).

Archean predecessor, this event is accompanied by highly positive excursions in the $\delta^{13}\text{C}$ composition of carbonate rocks, known as the Lomagundi-Jatuli carbon isotopic excursion (LJE) (Figure 16.26; Karhu and Holland, 1996; Melezhik et al., 1999a, 2005a, 2007). Perhaps most significantly, this period of progressively increasing atmospheric O_2 is also the time of the first recorded eukaryotic fossils (2.1 Ga: Han and Runnegar, 1992), representing perhaps the first of several direct links between rising levels of atmospheric oxygen and the increasing evolutionary complexity of life (Margulis and Sagan, 1986; see Section 16.3.4.2).

p0935 Many other pieces of geological evidence support the Great Oxidation Event at this time, including the following:

- u0025 Hydrothermal uranium ores took the place of detrital uraninite placer deposits;
- u0030 Paleosols and surficial deposits became oxidized;
- u0035 The concentration of redox-sensitive elements (U, Mo, V) in carbonaceous shales began to increase;

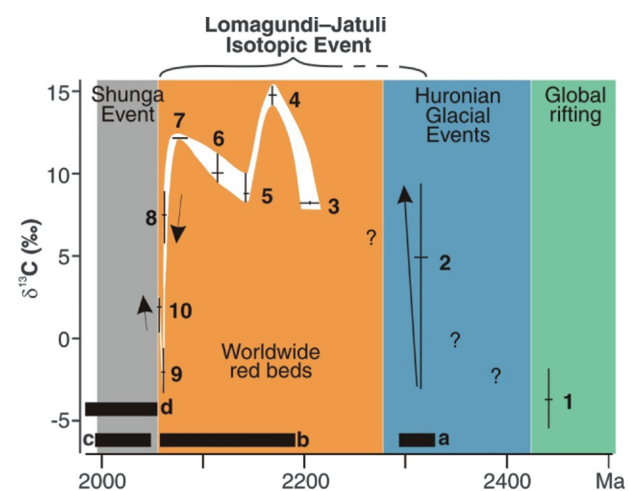


FIGURE 16.26 $\delta^{13}\text{C}$ variations in Early Palaeoproterozoic sedimentary carbonates based on high-precision U-Pb and Re-Os age data (for references see Melezhik et al., 2007). Vertical bars represent $\delta^{13}\text{C}$ variation, and horizontal bars indicate uncertainty in age. 1—Seidorechka Sedimentary Formation, Imandra/Varzuga Greenstone Belt, NW Russia; 2—Duitschland Formation, Transvaal Basin, S. Africa; 3—Sericite Schist Formation, Kuusamo Schist Belt, Finland; 4—Dunphy and Portage formations, Labrador Trough, Canada; 5—Pistolet Subgroup, Labrador Trough, Canada; 6—Lower Vistola Formation; 7—Siltstone Formation, Kuusamo Schist Belt, Finland; 8—Kuetsjärvi Sedimentary Formation, Pechenga Greenstone Belt, NW Russia; 9—Houtenbek Formation, Transvaal Basin, S. Africa; 10—Kolosjoki Sedimentary Formation, Pechenga Greenstone Belt, NW Russia. a—end of mass-independent fractionation of sulfur isotopes; b—abundant marine sulfates; c—first sedimentary phosphorites; d—break-up of Archaean supercontinent. Arrow-headed lines show stratigraphic $\delta^{13}\text{C}$ trend within the formation.

Phosphorites made their first appearance (Figure 16.17; u0040 Holland, 1994, 2005; Pollack et al., 2009).

In addition, manganiferous iron formations became significant p0960 and gave rise to giant ore bodies whose mineralization was formed during sediment deposition at 2.2–2.06 Ga from a layered, partly oxidized ocean affected by biogeochemical cycling of Fe and Mn and then concentrated during younger events (Evans et al., 2001; Roy, 2006; Schneiderhan et al., 2006; Dellwig et al., 2010; Tsikos et al., 2010). It is not surprising that there is a correlation between phosphorite and Mn-rich deposits, as P and Mn are in close association, formed through an excess of organic carbon deposited into seas by planktonic organisms (Kholodov and Nedumov, 2009).

Perhaps the best section where the change to a more p0965 oxidized atmosphere is recorded is in the Huronian Supergroup of North America, where rocks of the Lorrain Formation rest on an oxidized paleosol on the last of the three underlying glacial diamictites, contain ^{34}S -enriched ($\delta^{34}\text{S} = +15\text{‰}$), stratiform, nodular anhydrite, and include limestones with unusually high $\delta^{13}\text{C}_{\text{carbonate}}$ values of up to $+9.5\text{‰}$, characteristic of the worldwide Lomagundi-Jatuli isotopic excursion (Figure 16.26; Cameron, 1983; Prasad and

Roscoe, 1996; Bekker et al., 2006). These features indicate a significant rise in atmospheric oxygen (e.g., Martin et al., 1998), a related increase in marine sulfate concentration through the oxidative weathering of sulfides from exposed continental rocks (Cameron, 1983; Canfield et al., 2000; Schröder et al., 2008), and the onset of widespread bacterial sulfate reduction. This is well constrained as having occurred between the end of the global glaciations (<2316 Ma) and the emplacement of the c. 2220 Ma Nipissing Diabase that cuts through the Huronian Supergroup (Papineau et al., 2007).

p0970 Further evidence of a much more highly oxidized atmosphere thereafter comes from hematitic paleoweathering profiles on c. 2220 Ma basalts in South Africa (Holland and Beukes, 1990; Wiggering and Beukes, 1990; Rye et al., 1995; Holland and Rye, 1997; Rye and Holland, 1998; Yang et al., 2002; Yang and Holland, 2003) and from redbeds and hematitic rhyodacites of the c. 2060 Ma, subaerial, Rooiberg Group (Twist and Cheney, 1986; Eriksson and Cheney, 1992). In between these events, there is at least some evidence for at least local marine anoxia (Bau and Alexander, 2006).

s0215 Breakout Magmatism

p0975 The time period 2220–2200 Ma is marked by a global event of basaltic magmatism, representing a breakout event after the prolonged period of slowed mantle activity in the preceding 200–250 Ma (Figure 16.21; Condie et al., 2009). Thick flood basalt sequences of this age are recorded from Western Australia (2209 ± 15 Ma Cheela Springs Basalt: Martin et al., 1998) and South Africa (2222 ± 12 Ma Hekpoort and Ongeluk lavas: Cornell et al., 1996; Dorland, 2004). Equivalent intrusive rocks from North America include the extensive 2219 ± 3 Ma to 2210 ± 3 Ma Nipissing diabase intrusions (Corfu and Andrews, 1986; Noble and Lightfoot, 1992) and Seneterre dykes (2216+8/–4 Ma: Buchan et al., 1996), as also recorded in India (French and Heaman, 2010), and in China (2199 ± 11 Ma gneisses and 2193 ± 15 Ma gabbros: Zhao et al., 2008; Wang et al., 2010). Extensive granite-greenstone terrains were also formed at this time in West Africa (2229 ± 42 Ma Birimian: Abouchami et al., 1990; Feybesse et al., 2006) and central Brazil (2.23–2.20 Ga Mineiro belt: Ávila et al., 2010; 2209 ± 32 Ma Crixás greenstone belt: Jost et al., 2010). Geological and isotopic data have shown that the 2.25–2.0 Ga granite (dominantly TTG)-greenstone Man Craton of West Africa formed as dominantly juvenile crust ($\epsilon_{\text{Nd}(2100 \text{ Ma})} = +3.6$ to $+1.2$) in an oceanic plateau setting, through 5–15% melting of slightly depleted lherzolite in deep mantle plumes, which produced huge amounts of tholeiites in a short time (Abouchami et al., 1990; Boher et al., 1992; Lompo, 2009). Estimates of crustal growth rates in this craton are 60% higher than present. Sylvester and Attoh (1992) presented stratigraphic and geochemical data for Birimian greenstones and

showed that they consist of tholeiitic basalt and overlying calc-alkaline intermediate to felsic volcanic rocks that are similar to those in many Archean greenstone belts, concluding that:

“...hence, the Archean-Proterozoic boundary may not coincide with a worldwide, fundamental change in crust-mantle evolution.”

(Sylvester and Attoh, 1992: 377).

Lomagundi-Jatuli Isotopic Excursion

s0220

(contributed by V. A. Melezhik)

p0990

The discovery of ^{13}C -rich Paleoproterozoic sedimentary carbonates in the Jatuli complex, Russian Karelia (Galimov et al., 1968), and in the Lomagundi province in Zimbabwe (Schidlowski et al., 1976), presented geologists with a major puzzle concerning its significance. It took over a decade for the first realization (Baker and Fallick, 1989a, b), and a further decade for wide international acceptance, of the fact that these carbonates represent one of the major perturbations of the global carbon cycle (Karhu and Holland, 1996) and the largest magnitude known positive excursion of $\delta^{13}\text{C}$ in sedimentary carbonates at any time in Earth history (Figure 16.26; Melezhik et al., 1999a). The Lomagundi-Jatuli Event (LJE) appears to be an integral part of a series of other prominent Paleoproterozoic environmental events, whose interrelationship remains intriguing and only partially resolved (Melezhik et al., 2005a).

p0995

Considering the existing age constraints, it appears that the LJE developed after the “Huronian-age” glaciation (Bekker et al., 2005; Kopp et al., 2005; Melezhik, 2006). The mass-independent sulfur isotope data suggests that the LJE post-dates the initial accumulation of atmospheric O_2 (Bekker et al., 2004; Hannah et al., 2004; Anbar et al., 2007; Kaufman et al., 2008). It is also evident that the LJE coincides with worldwide terrestrial “red beds” and abundant Ca-sulfates (Melezhik et al., 2005b). An unprecedented accumulation of C_{org} -rich sediments, known as the Shunga Event, occurred in its aftermath (Melezhik et al., 1999b).

p1000

The currently available absolute chronology of the LJE (Bau et al., 1999; Lindsay and Brasier, 2002; Hannah et al., 2004) does not provide robust age constraints on its onset, its duration, nor its internal structure. The onset of the LJE has not been constrained. Buick et al. (1998) reported a positive isotopic shift at around 2330 Ma (Hannah et al., 2004) from the Transvaal Supergroup. However, Bekker et al. (2001) argued that this may represent an earlier, separate isotopic shift prior to the LJE *per se* (Figure 16.26). Data from Fennoscandia indicate that the accumulation of ^{13}C -rich carbonates was underway by ca. 2200 Ma, whereas the termination of the isotopic event was inferred at ca. 2060 Ma (Karhu, 1993). The global nature of the LJE has recently been verified by Maheshwari et al. (2010) and a recently obtained age of 2058 ± 2 Ma from Fennoscandia provides a direct time

p1005

constraint on the end of the LJE (Melezhik et al., 2007), thus suggesting a minimum ca. 140 Ma interval characterized by ^{13}C -rich carbonate accumulation.

p1010 The termination of the LJE coincides with a change in the tectonic regime from active rifting to passive margin thermal subsidence resulting in a global paleogeographic restructuring of major landmasses (e.g., Mazumder et al., 2000). It also corresponds exactly to the age of emplacement and extrusion of one of the world's largest magmatic provinces, the Bushveld Magmatic Province, comprising both the Rustenburg Layered Suite and the genetically related Rooiberg Group of subaerial volcanics (see Section 16.3.3.5; Buchanan et al., 2002; Armstrong et al., 2010). Large, shallow-water carbonate platforms and shallow-water carbonate shelves colonized by stromatolite-forming cyanobacteria drowned and disappeared in several continents at this time (Melezhik et al., 1997; Bekker and Eriksson, 2003; Bekker et al., 2003a, b; Wanke and Melezhik, 2005).

p1015 The LJE was followed by the onset of the ca. 2000 Ma Shunga Event, an unprecedented accumulation of C_{org} -rich sedimentary rocks and generation of giant petroleum deposits (Melezhik et al., 1999b; 2004; 2005a; Mossman et al., 2005), formation of the earliest phosphorites, and the emergence of an aerobic pathway in biogeochemical recycling of organic matter (Fallick et al., 2008) (see Section 16.3.3.5). The latter may explain an intriguing feature of the LJE, namely the lack of a subsequent compensating low $\delta^{13}\text{C}$ excursion (Karhu and Holland, 1996; Melezhik et al., 2007). A negative $\delta^{13}\text{C}$ might be anticipated to follow an episode of enhanced organic carbon burial as recycling and remineralization proceeded. This is also a characteristic feature of extinction events (Magaritz, 1989) and of ventilation, or turnover, of deep anoxic basins (e.g., Aharon and Liew, 1992), which have been considered to be one of the possible causes of the LJE. However, the creation of a new locus for organic carbon recycling, since the active biomass reservoir within the sediments and crust endures, might have resulted in no net return of oxidized organic carbon of low $\delta^{13}\text{C}$ to the ocean-atmosphere system to become recorded by sedimentary carbonate $\delta^{13}\text{C}$ (Fallick et al., 2008).

s0225 Phosphorites

p1020 (contributed by D. Papineau)

p1025 Worldwide occurrences of sedimentary phosphate deposits appear in the rock record after the Paleoproterozoic glaciations, suggesting that phosphogenesis was related to a global chemo-oceanographic change and probably not only to restricted, local, conditions (Papineau, 2010). A list of Paleoproterozoic phosphate deposits is shown in Table 16.2, which also includes details on the age constraints, associated sediments and minerals and estimated tonnage of P_2O_5 , when available.

One of the oldest and largest Paleoproterozoic phosphate p1030 deposit is the 2.2–2.0 Ga stromatolitic phosphorites that are embedded in a dolomite sequence in the Aravalli Supergroup in Rajasthan, India, composed mainly of carbonate fluorapatite (Banerjee, 1971; Chauhuan, 1979; Papineau et al., 2009). The Aravalli stromatolitic phosphorites were deposited in a semi-restricted environment and are hosted in dolomites with $\delta^{13}\text{C}_{\text{carb}}$ values near 0‰, but which have been regionally correlated to other dolomites with high $\delta^{13}\text{C}_{\text{carb}}$ values (Maheshwari et al., 1999; Sreenivas et al., 2001). Relatively high $\delta^{13}\text{C}_{\text{org}}$ values in these stromatolitic phosphorites have been attributed to high levels of primary productivity during deposition, which were likely stimulated by the abundance of phosphate in various Aravalli environments (Banerjee et al., 1986; Sreenivas et al., 2001) and may also relate to high $\delta^{13}\text{C}_{\text{carb}}$ values of contemporary carbonate. Another of the older phosphorite deposit includes uraniferous phosphorite bands in carbonates and graphitic gneisses in the c. 2.1 Ga Jatuli Group (Laajoki and Saikkonen, 1977; Äikäs, 1980, 1981).

Several large Paleoproterozoic phosphorites occur in the p1035 region of the Kursk Magnetic Anomaly (western Russia and Ukraine), on the Sino-Korean platform, and in the Aldan Shield (northeastern Russia) (Table 16.2; Yudin, 1996). Phosphorites in the Kursk Magnetic Anomaly typically occur in carbonaceous sedimentary rocks within intracratonic rift basins often associated with large BIFs (Nikitina and Shchipskiy, 1987). In the Susong Group in China, phosphorites have up to 26% P_2O_5 and occur in dolomites, cherts and graphitic schists stratigraphically above a conglomerate, as part of a transgressive sequence (Longkang and Zhendong, 1988). In the Chinpingshan area of China, Paleoproterozoic apatite-rich deposits are hosted in carbonates that are often manganiferous (Yudin, 1996). In Siberia and Yakutia of northeastern Russia, poorly dated Paleoproterozoic phosphorite deposits occur in highly metamorphosed skarn rocks and contain large reserves, estimated at 130 million tons (Guily, 1989; Yudin, 1996). Many of these deposits share similarities in depositional environments and mineralogical characteristics by preserving relatively high amounts of organic matter and/or sulfides, which are likely related to biological processes during deposition and diagenesis.

In North America, several Paleoproterozoic phosphorites p1040 occur along the southern shore of the Superior Craton. Uraniferous phosphatic sedimentary rocks in Minnesota contain up to 25% P_2O_5 in the form of nodular apatites (Ullmer, 1981, 1985; McSwiggen et al., 1986). Uranium (U^{4+}) likely substitutes for Ca^{2+} during the diagenetic formation of apatite and may have adsorbed onto organic matter in the depositional environment. Although relatively restricted in extent, phosphorites of Minnesota occur in graphitic and pyritiferous shales or mudstones that stratigraphically overlie a basal conglomerate. Nearby, in the Baraga Group in northern Michigan and its equivalent in western Ontario, phosphorites with up to 15% P_2O_5 occur in argillites and cherts, as pebbles,

TABLE 16.2 Paleoproterozoic Phosphate-Rich Sedimentary Rocks

Geographic and Geological Location	Age Constraints	Host Lithology and Associated Minerals	Phosphate Occurrences	Estimates P ₂ O ₅ Reserve	P ₂ O ₅ Range or Average	References
North America						
Michigamme Fm., Baraga Group, Michigan	1.80–1.87 Ga	Cherty dolomite with pyrite and argillite beds*	Carbonate fluorapatite nodules, thin beds and possibly stromatolites	—	15%	Manusco et al. (1975), Cannon and Klasner (1976), Hall (1985)
Thomson Fm., Minnesota	1.80–1.87 Ga	Carbonaceous shales with minor chert and pyrite*	Apatite-rich beds and fine-grained apatite in granular mosaic or nodule (uraniferous)	—	9–25%	Ullmer (1981, 1985), McSwiggen et al. (1986)
Menihok and Ferriman Fms., Knob Lake Group, Labrador and Québec	1.87–1.88 Ga	Cherty carbonaceous and pyritiferous turbidites	Phosphate beds and fragments and phosphate clasts (uraniferous)	—	—	Pufahl et al. (2006), Bell and Thorpe (1986)
Thelon Fm. and Hornby Group, N.W.T.	1.72–1.85 Ga	Saprolites, lithic quartz arenite and arkose with euhedral hematite cubes*	Fluorapatite, goyazite (Sr,Al) and baricite (Mg, Fe) cements, veins and crystals (uraniferous)	—	4–34%	Miller (1983), Miller et al. (1989), Gall and Donaldson (2006)
Fennoscandia						
Pilgularvi Fm., Pechenga Belt, NW Russia	1.90–2.06 Ga	Schist, gneisses and sandstones with graphite and sulfides*	Carbonate fluorapatite nodules, concretions, lenses, stromatolites, and oolites	—	2–11%	Yudin (1996); Bekasova and Dudkin (1982)
Ludikov Group, Omega Basin, NW Russia	1.98–2.06 Ga	Organic-rich greywacke with pyrite and stromatolitic dolomite with magnesite bands*	Phosphate nodules and clasts	—	—	Melezhik et al. (1999; 2005)
Jatuli-type formations (~16 occurrences), Finland	2.06–2.10 Ga	Carbonate marbles, graphitic gneisses, skarn rocks*	Uraniferous phosphorite bands, lenses and fine disseminations	>50 Mt	3–19%	Äikäs (1980, 1981), Laajoki and Saikkonen (1977)
Tuomivaara and Pahtavaara Fms., Kainuu Belt, Finland	1.90–2.08 Ga	Iron formations with sulfides, carbonate and graphite*	Fluorapatite bands	—	1–13%	Gehör (1994)
Vihanti, Nilsjö, and Nuottijärvi areas, Finland	1.88–1.92 Ga	Dolomites, gneisses and skarn rocks	Uraniferous phosphorite bands, lenses and fine disseminations	—	3–25%	Rehtijärvi et al. (1979), Vaasjoki et al. (1980)

t0015

Africa	
Upper Lomagundi, Zimbabwe	2.1–2.22 Ga Shales Phosphate beds Master (1991)
FB formation, Francevillian Supergroup, Gabon	ca. 2.0 Ga Black shales, cherts and Fe-Mn formation* Apatite nodules with silicified rims Mossman et al. (2005)
Asia	
Bish, Amursk, Tagnarar, Mustolaakh, Niryandzha, Seligdar and Dorozhnyy sectors, Aldan Shield, Yakutia	Paleoproterozoic Carbonate skarns and chlorite schists Apatite Yudin (1996); Gulyi (1989)
Chimpingshan area, China	Paleoproterozoic Carbonates, Mn-carbonates Apatite Yudin (1996)
Liuping Fm., Susong Group, China plus 3 other related major deposits	ca. 1.85 Ga Dolomite, graphitic schist, and chert* Phosphorite beds and lenses Longkang and Zhendong (1988)
Sinpkhup, Singpung and Yongby areas, North Korea	Paleoproterozoic Mica schist and carbonates* Apatite Yudin (1996), Bushinkii (1966), Notholt and Sheldon (1986)
Jharmarkotra Fm., Aravalli Supergroup, India	1.9–2.2 Ga Dolomite and ferruginous carbonate* Stromatolitic and amorphous carbonate fluorapatite Banerjee (1971), Chauhan (1979)
Slyudyanka, Siberia, Russia	Paleoproterozoic Carbonates, quartzites and skarn rocks* Fluoroapatite beds Yudin (1996), Bushinskii (1966)
Tim, Yastrebov and Ryl'sk suites, Kursk Magnetic Anomaly, Russia	Paleoproterozoic Carbonaceous schists and black shale Phosphorite beds, nodules, pebbles and breccia Borovskaya et al. (1985), Nikitina and Shchipanskiy (1987), Sozinov and Kazantsev (1978)
Krivoy Rog Basin, Ukrainian Shield	Paleoproterozoic Sandstones and metapelites* Phosphorite clasts, pebbles and beds Yatsenko et al. (1988)

*Occurs in a transgressive sequence stratigraphically above a conglomerate unit unconformably sitting on Archean basement.

thin beds, and as small rounded laminated structures that are possibly stromatolites (Manusco et al., 1975; Cannon and Klasner, 1976; Hall, 1985). Further east in Québec and Labrador, cherty carbonaceous and pyritiferous turbidites also host uraniferous phosphorite beds (Bell and Thorpe, 1986).

p1045 In Fennoscandia, uraniferous phosphorite beds are bound in metamorphosed sedimentary rocks and have similar ages as the North American phosphorites. For instance, dolomites and apatite-rich gneisses with up to 24% P₂O₅ host thin phosphorite beds in various schist belts in western and central Finland (Rehtijärvi et al., 1979; Vaasjoki et al., 1980). In the Pechenga area of northwestern Russia, 1.90 to 2.06 Ga phosphorites in organic-rich sediments occur as concretions, beds, oolites and stromatolites in carbonaceous gritstones, shales and other sedimentary rocks (Bekasova and Dudkin, 1982; Yudin, 1996). The Pechenga Belt has been geochronologically correlated with the Onega Basin, where phosphate concretions occur in organic-rich and sulfidic shales (Melezhik et al., 1999b; 2005b).

p1050 Similar to the Aravalli stromatolitic phosphorites in India, phosphorite occurrences in the organic-rich zone of the Ludikovi Group of Fennoscandia are noteworthy examples of the intimate relationship between phosphorites and microbial activity. In fact, these phosphorites are part of a transgressive suite and occur stratigraphically above stromatolitic dolomites with a $\delta^{13}\text{C}_{\text{carb}}$ excursion (Melezhik et al., 2007), possibly suggesting a connection between phosphorites and primary productivity. In central and northern Finland, fluorapatite bands a few centimeters thick occur in organic-rich Paleoproterozoic sulfide facies BIFs of the Kainuu Schist Belt (Gehör, 1994). Possibly co-eval phosphorites in BIFs in Lapland of northern Sweden contain up to 18% P₂O₅ (Parák, 1973).

s0230 Models of phosphogenesis

p1055 The origin of phosphorites is still not well understood and there are several hypotheses for their origin, including biological, chemical, and volcano sedimentary (see reviews in Kazakov, 1937; Bushinskii, 1966; Cook and Shergold, 1986; Konhauser et al., 2007b). Kazakov (1937) recognized a striking similarity between the various phosphorites of the Russian platform, where most occurrences are part of a transgressive sequence and lie stratigraphically above basal conglomerates followed by arenaceous and/or argillaceous sandstones (see also Table 16.2). It was then proposed that the source of phosphorus in phosphorites was mineralized organic matter in deep marine environments, and that nutrient-rich water masses then ascended to continental shelves to form phosphate deposits (Kazakov, 1937). Many phosphorite deposits in the ocean today occur in areas of upwelling where phosphate, regenerated from the recycling of organic matter in the deep ocean, is brought to coastal areas and triggers blooms of primary productivity, such as along the

coasts of south-western Africa (Namibia: Bremner and Rogers, 1990), Baja California (Jahnke et al., 1983), and south-western South America (Peru-Chile: Veeh et al., 1973).

A simplified illustration of the upwelling model is shown p1060 in Figure 16.27, where cyanobacterial blooms in upwelling areas produce large quantities of organic matter that concentrate phosphorus. During decomposition and sedimentation processes, phosphorus is liberated from organic matter and can either return to the water column by upwelling or become concentrated in deep sediments.

Non-upwelling areas such as estuaries and semi-restricted p1065 embayments can also be host to phosphate deposits and/or authigenic carbonate fluorapatite (Bremner and Rogers, 1990). For instance, diagenetic phosphate minerals have been observed in the Long Island Sound and Mississippi Delta in the United States (Ruttenberg and Berner, 1993), and phosphorites occur along the eastern and southern coast of Australia (O'Brien and Veeh, 1980).

Most organic matter burial in marine sediments occurs in p1070 non-upwelling areas where deltaic shelf-estuarine sediments are deposited. In these environments, pore waters solutions in sediments often become enriched in dissolved phosphate due to its release during organic decomposition by anaerobic heterotrophic microbial communities (Berner, 1990). During early diagenesis, phosphorus can be released from organic matter, but also from iron-oxides in anoxic sediments, which may also play a role in phosphogenesis (Ingall and Jahnke, 1994; Van Cappellen and Ingall, 1994). Oceanic islands and seamounts can also host sedimentary phosphorites because these sites expose sediments to oxygen minimum zones (see Glenn et al., 1994 and references therein). At the transition between anoxic and oxygenated waters in the water column, phosphogenesis can be promoted by microbial communities of primary producers in the euphotic zone, as well as those involved in the anoxic recycling of organic matter and the regeneration of phosphate. Another possible link in the model for phosphogenesis are major glaciations, where post-glacial oceanic overturn after thawing could drive a rise in sea level and upwelling of phosphorus-rich bottom waters (Arthur and Jenkyns, 1981; Cook and Shergold, 1984; Donnelly et al., 1990; Glenn et al., 1994).

The formation of sedimentary phosphorites ultimately p1075 depends on a significant enrichment of phosphorus from seawater by microbial activity and the recycling of this organic matter in sediments (Figure 16.27). Microbial influence on the formation of phosphorites is conspicuous, and different microorganisms probably have a range of involvement from heterotrophy and phosphorus regeneration to active apatite biomineralization. The detailed mechanisms involved in the precipitation of authigenic carbonate fluorapatite from seawater or during diagenesis are not well established, but carbon, oxygen and sulfur isotopic evidence of carbonate and sulfate in carbonate fluorapatite suggest that diagenetic processes, especially microbial sulfate reduction

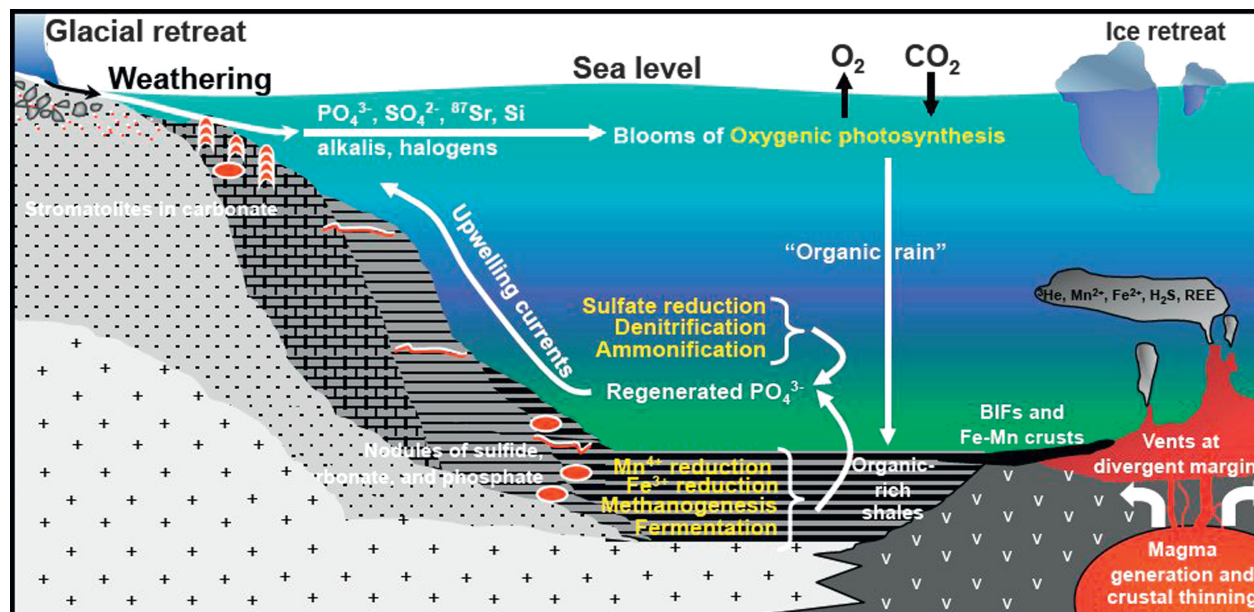


FIGURE 16.27 Simplified illustration of the flow of phosphate in an upwelling model for phosphogenesis. Sedimentary phosphate accumulations as seen in the Precambrian are shown as red ovals (for concretions or nodules), curved lines (for thin beds), stromatolite columns and small dots (for fine disseminations) in various lithotypes (shale – BIF, limestone, sandstone – chert and conglomerate from bottom up). The water column is color-coded to represent redox states as turquoise (oxic and photic zone), blue (redox transition zone) and green (deep anoxic zone). From Papineau (2010).

and fermentation, play important roles (Kolodny and Kaplan, 1970; McArthur et al., 1980, 1986; Benmore et al., 1983). The precipitation of carbonate fluorapatite ultimately occurs during early or late diagenesis from the decay of organic matter.

creating new opportunities for large aerobic organisms, specifically multicellular oxygen-respiring eukaryotic organisms (Figure 16.28). Eukaryotes, representing the most fundamental separation among known life forms (Margulis and Sagan, 1986), appear to have developed in this time period, or somewhat before. The oldest macroscopic eukaryotic fossil is *Grypania spiralis*, a coiled megascopic eukaryotic algae from the nearly 2 Ga Negaunee Iron-Formation of Michigan (Han and Runnegar, 1992). Large colonial organisms with coordinated growth in an oxygenated

s0235 **Eukaryotes**

p1080 The rise of atmospheric oxygenation in the Paleoproterozoic was followed by a significant leap in biological evolution,

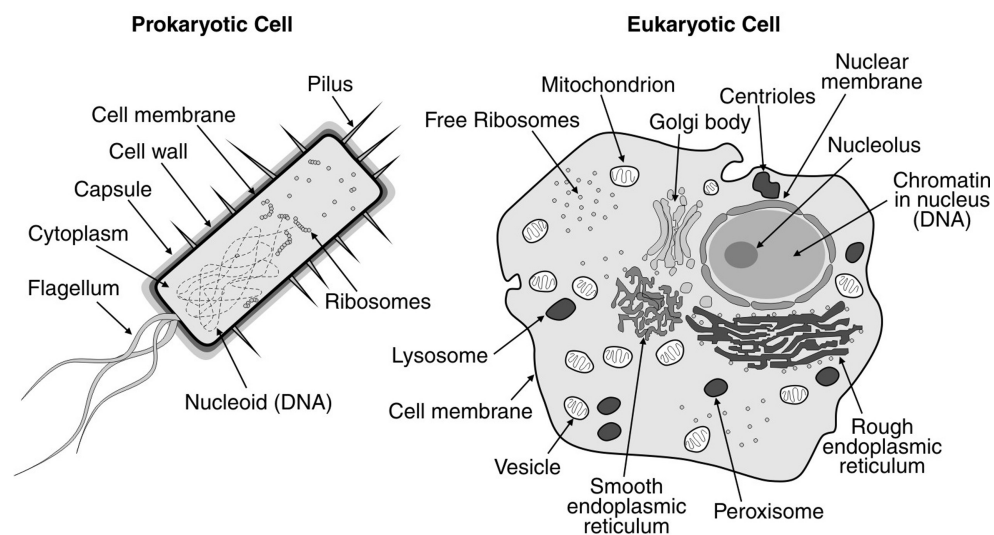


FIGURE 16.28 Diagrammatic sketch showing the differences between prokaryotic and eukaryote cells. (redrawn from Lane, 2009).

environment have been inferred for nearly contemporaneous, ~2.1 Ga, rocks from Gabon, West Africa, based on pyrite nodules in siltstones (Albani et al., 2010) and sterane biomarkers of eukaryotic origin (Dutkiewicz et al., 2007). Macroscopic eukaryote fossils and trace fossils have also been described from the 2.0–1.8 Ga Stirling Range biota of Western Australia (Rasmussen et al., 2002; 2004; Bengtson et al., 2007), in the ca. 1.9 Ga Belcher Group (northern Canada: Hofmann, 1976), and in the ca. 1.9 Ga Pechenga greenstone belt (northwest Russia: Akhmedov et al., 2000)). The rise of eukaryotes at this time matches evidence from whole genome sequence analysis (Hedges et al., 2001), although it must be emphasized that there is new biomarker evidence for eukaryotes at 2.6–2.5 Ga (Waldbauer et al., 2009; see Section 3.3.1), micropaleophytes have been described from c. 2.4 Ga rocks in China (Sun and Zhu, 1998), and the anaerobic metabolism of basal eukaryotes is consistent with an origin early in Earth history.

p1085 Eukaryote development is linked to the rise of oxygen, because these large (10^4 – 10^5 x the volume of bacteria), complex, heterotrophic cells satisfy their ATP (adenosine triphosphate) needs through the oxidative breakdown of reduced organic compounds (e.g., Margulis et al., 1976; Martin and Müller, 1998). They replicate through sexual division of DNA bound in chromosomes, and contain a complex suite of internal features, including a nucleus separated from the rest of the cell by a membrane, mitochondria (which use oxygen), and chloroplasts that have chlorophyll and are capable of photosynthesis (Figure 16.28). Significantly, chloroplasts and mitochondria are capable of direct division, despite being part of a larger protist cell. This evidence, combined with the fact that both mitochondria and chloroplasts have their own protein-synthesizing machinery that more closely resembles those of prokaryotes, led to the interpretation that the origin of the eukaryotic cell was through endosymbiosis between a prokaryotic host (an archaeobacterium, capable of withstanding high temperatures and acidic conditions) and photosynthetic cyanobacteria (forming the chloroplasts in eukaryotic cells) (Figure 16.29; Margulis, 1970, 1993; Margulis and Sagan, 1986; Joen, 1991). Two more detailed symbiosis hypotheses have since been developed. These include the “hydrogen hypothesis”, whereby symbiosis occurred between an anaerobic, autotrophic prokaryotic host (methanogenic archaeobacterium) that utilized the hydrogen and carbon dioxide waste products of anaerobic metabolism by a fermentative α -proteobacterium ancestor to the mitochondrion (Martin and Müller, 1998). The “syntrophy hypothesis” is quite similar, but involves the symbiosis between a methanogenic archaea and δ -proteobacteria (ancestral sulfate-reducing myxobacteria: Moreira and López-García, 1998; López-García and Moreira, 1999). In these models, mitochondria are thought to have derived from a later, independent symbiotic event. A key advance of the eukaryotes was that they were able to generate large

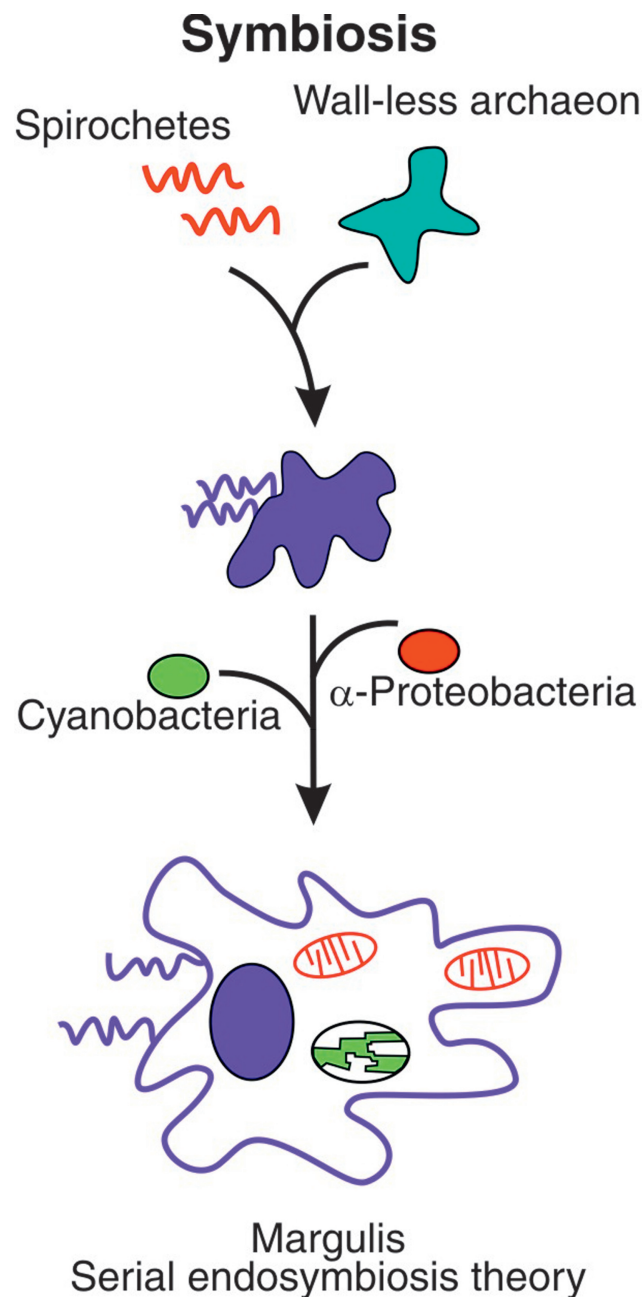


FIGURE 16.29 The Margulis endosymbiosis model of eukaryote development. (redrafted from López-García and Moreira, 1999). f0150

amounts of energy, relative to prokaryotes, by packing hundreds of mitochondria into a single cell and thereby dramatically increasing their size. Sexual reproduction led to mitosis and hence to more rapid and complex evolutionary change, enhanced by increasingly complex symbiosis. It appears that a major development in eukaryote evolution occurred at 2.1–1.8 Ga, possibly as a result of eukaryotes acquiring chloroplasts at the time when oxygen rose to levels of 1–2% PAL (Knoll, 1992).

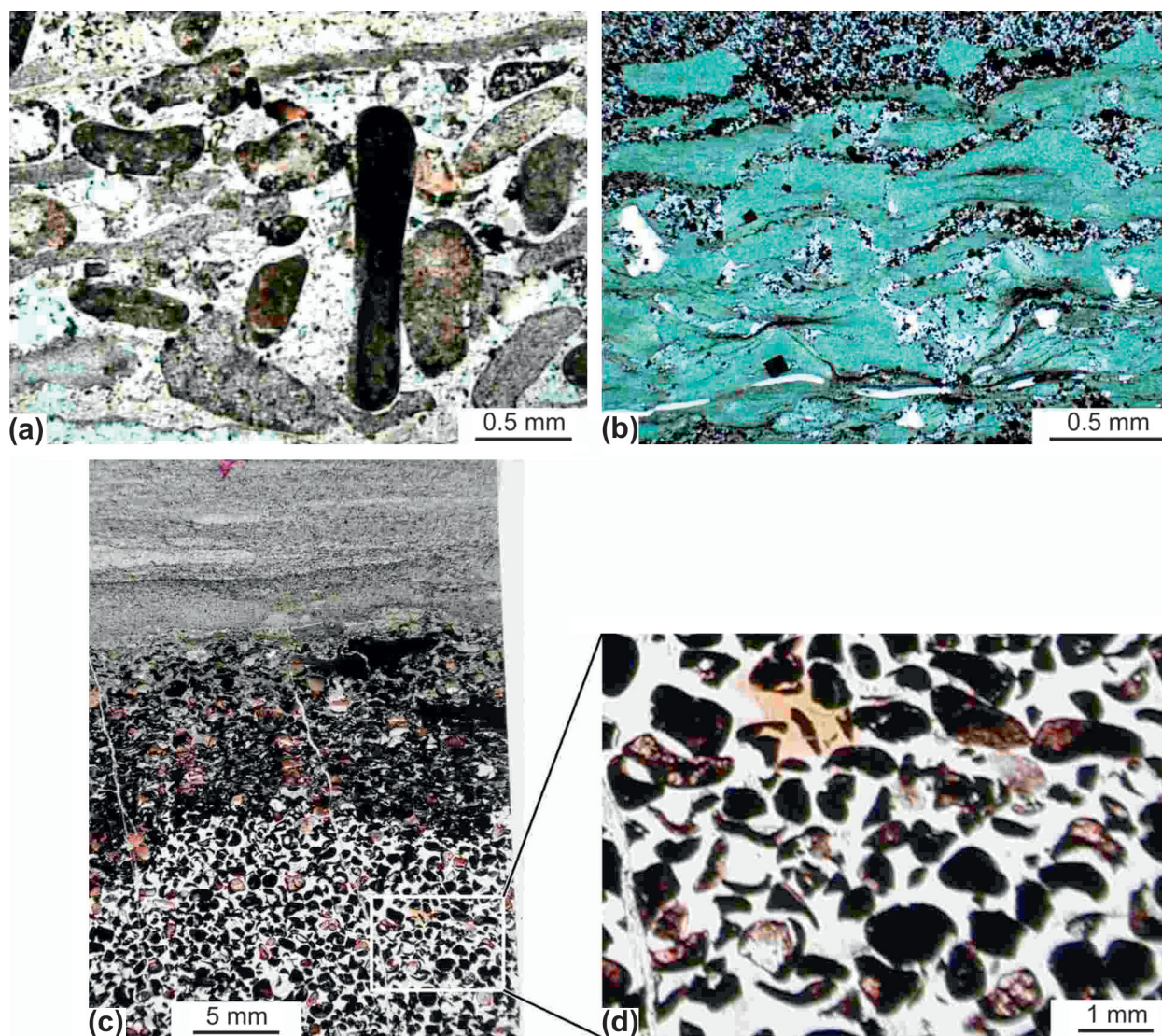


FIGURE 16.30 Photomicrographs of typical granular iron formation from the c. 1.8 Ga Earraheedy Basin, Western Australia. A) peloidal granular iron formation; B) green stilpnomelane shales and finely granular iron formation; C) cut section of drillcore showing granular iron formation and contact with fine-grained clastic sediment; D) closeup of iron formation in c), showing Fe-coated grains and broken-off Fe-coatings of grains. (From Pirajno et al., 2009)

s0240 16.3.3.5. *Global Orogenesis, Re-Appearance of BIF, Natural Uranium Reactors, and Shungite (c. 2.06–1.78 Ga)*

p1090 The period 2.06–1.78 Ga represents one of the most significant periods of crustal growth in Earth history (Figure 16.18; Condie, 1998, 2004), which initiated with the emplacement of the world's largest layered mafic-ultramafic igneous intrusion (Rustenberg Layered Suite) and associated volcanic and granitic rocks (Rooiberg Group) of the Bushveld Magmatic Province, at 2.06 Ga (Schweitzer et al., 1995; Buchanan, 2006; Cawthorne et al., 2006; Armstrong et al., 2010; Vantongeren et al., 2010). This global tectonism led to the formation of a new supercontinent, Columbia (Nuna) at ~1.8 Ga (Zhao et al., 2002; Reddy and Evans, 2009), and coincided with the

end of the L-J isotopic excursion (Melezhik et al., 2007). Komatiites re-appeared during this event in several places, including Fennoscandia at 2056 ± 25 Ma (Hanski et al., 2001), French Guiana at 2.11 ± 0.09 Ga (Capdevila et al., 1999), and in the Ottawa Islands of the Trans-Hudson Orogen of North America, at 1.9 Ga (Arndt et al., 1987). Iron-formations also make a re-appearance over this interval, indicating the presence of at least partly reducing ocean basins (see below). Two examples of the first true ophiolites also appear in the rock record during this time, including the c. 2.0 Ga Purtuniqu ophiolite of the Cape Smith Belt in the Trans-Hudson Orogen (Scott et al., 1991), and the contemporaneous Jormua ophiolite in Baltica (Kontinen, 1987). Oceanic crust was thicker than at present (Moores, 1993) and ophiolite formation was

associated with ocean closure following a long-lived rifting event in North America (Halls et al., 2008).

p1095 Global terrane accretion and orogenesis (including ultra-high-temperature metamorphism: Santosh et al., 2007) at 1.92–1.76 Ga led to the formation of the supercontinent Columbia (Nuna) (Hoffman, 1989; Myers et al., 1996; Rogers and Santosh, 2002; Wardle et al., 2002; Zhao et al., 2002; Cawood and Tyler, 2004; Ansdell et al., 2005; Reddy and Evans, 2009). This huge increase in magmatic and tectonic activity has been interpreted as relating to a mantle superswell (Hoffman, 1989) and/or mantle overturn event (Davies, 1995), and almost certainly led to an increase in atmospheric carbon dioxide as a result of increased volcanism, and thus the re-appearance of reducing oceans and iron-formations.

p1100 A number of distinct rock types were deposited over this interval, including phosphorites and unusually organic-rich black shales, called shungites (see below). Oxygen levels had risen to such a degree that natural fission reactors developed in some of the black shale deposits. The increase in atmospheric oxygen levels also led to the continued development of eukaryotes.

s0245 Re-Appearance of Iron-Formation

p1105 Thick deposits of iron-formation re-appear in the geological record at between c. 2.0–1.75 Ga. In contrast to their older, well banded counterparts, these deposits are characterized by granular iron-formation, consisting of peloids and oolites (Figure 16.31), and commonly with thin irregular bedding, cross-bedding, and local stromatolites, indicating deposition in shallow water conditions (e.g., Williams and Schmidt, 2004; Pirajno et al., 2009). Analysis of Fe-isotopes from iron-rich stromatolites suggests at least the local activity of iron-oxidizing microbes at this time (Planavsky et al., 2009). In some cases at least, precipitation of Fe is directly associated with volcanic activity (Williams and Schmidt, 2004) in foredeep settings (Hoffman, 1987; Schneider et al., 2002).

p1110 The oldest examples of iron formation during this interval are 2.02 Ga rocks along the margin of the Wyoming Craton (Frei et al., 2008), whereas the youngest deposits occur in two separate basins in Western Australia, and are <1.8 Ga (Rasmussen and Fletcher, 2002; Evans et al., 2003; Halilovic et al., 2004; Pirajno et al., 2009; Wilson et al., 2010). These young ages for iron formation in Western Australia contradict the hypothesis that the 1.85 Ga Sudbury Impact caused the global disappearance of BIF, through stirring of the world's oceans (Addison et al., 2005; Slack and Canon, 2009; Cannon et al., 2010). Rather, the young age of these deposits show that BIFs disappeared gradually from the world's oceans, at different times in different places.

p1115 Most consider that the Paleoproterozoic oceans were stratified, with reducing conditions and abundant dissolved iron in the deep oceans, and an oxidized upper layer (e.g., Planavsky et al., 2009; Poulton et al., 2010). This is

supported by the deposition of uranium-rich sedimentary rocks, phosphorites and manganese-rich deposits, all of which require both a reducing water body and an oxidized component for solution transfer and deposition, respectively. The dominant precipitation of iron-formation under shallow-water conditions over this time interval suggests that the oxidized ocean layer was relatively thin, and/or that the continental shelves were much wider than during Archean BIF deposition. Deposition of iron-formation at this time may have limited primary productivity by scavenging P from the oceans through adsorption (Bjerrum and Canfield, 2002).

Shungite

(Contributed by V. Melezhik)

The Lomagundi-Jatuli Event and the 2.2–2.1 Ga “redbed environments” on the Fennoscandian Shield were abruptly superseded by an unprecedented accumulation of organic carbon-rich formations, representing the worldwide Shunga Event (Melezhik et al., 2005b). Such formations, dated to 2.01 Ga (Hannah et al., 2006), were the source rocks for giant petroleum deposits (Melezhik et al., 2004), whose oil reservoirs were largely destroyed during the 1.92–1.79 Ga Svecofennian orogenesis, although the southeastern part of the shield preserves a spectacular petrified oil field and oil spills.

s0250

p1120

p1125

Natural Fission Reactors

Another result of the rise in oxygen is that uranium was mobilized from older continental rocks and sediments (where it was bound as uraninite, formed under anoxic conditions) into solution within oxidized water bodies. In restricted oxidized water bodies, this could lead to significant enrichment of uranium. Gauthier-Lafaye and Weber (2003) and Coogan and Cullen (2009) have suggested that redeposition of this uranium at the margins of such bodies (or at the chemocline with reducing bottom waters) resulted in the high concentrations that led to the formation of critical natural fission reactors at Oklo and Bangombé in the Franceville Basin, Gabon, at ca. 2.0 Ga (Gauthier-Lafaye et al., 1996). Associated manganese deposits also formed through a process of dissolution and re-precipitation in layered water bodies (Gauthier-Lafaye and Weber, 2003).

s0255

p1130

[AU2]

16.3.4. Adult Earth (~1.78–present)

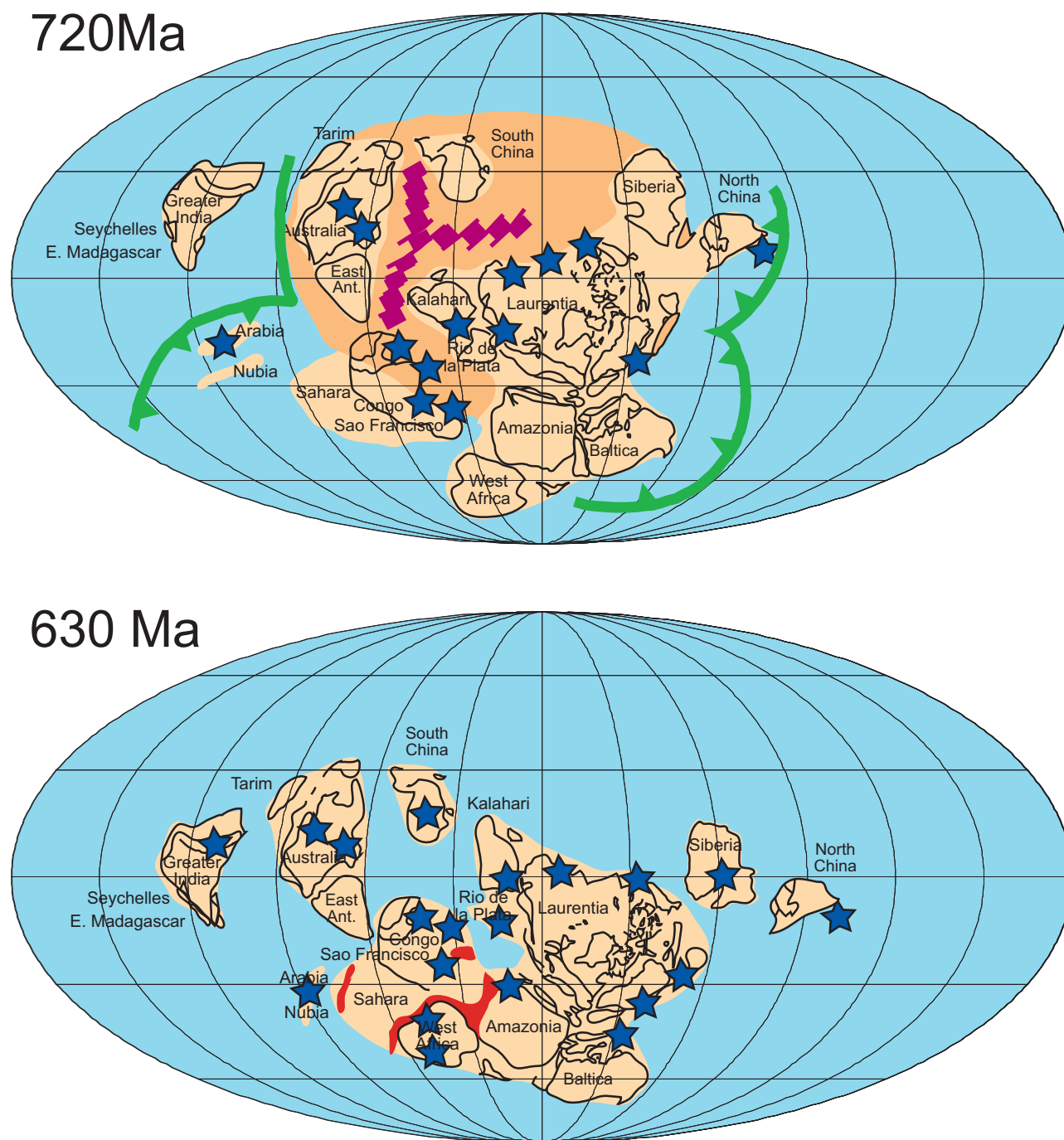
(with a contribution from F. Pirajno)

The billion-year-long period from the end of iron formation deposition at ~1.78 Ga until the onset of widespread glaciation and the rather restricted re-appearance of BIFs commencing at ~0.8 Ga is marked by relative stability of the major isotopic systems (Figure 16.15). This is despite the fact that a major supercontinent, Rodinia, formed at 1.3–0.9 Ga and lasted for ~150 Ma through this interval (Figure 16.32; Li et al., 2008). Supercontinent assembly was accompanied by

s0260

p1135

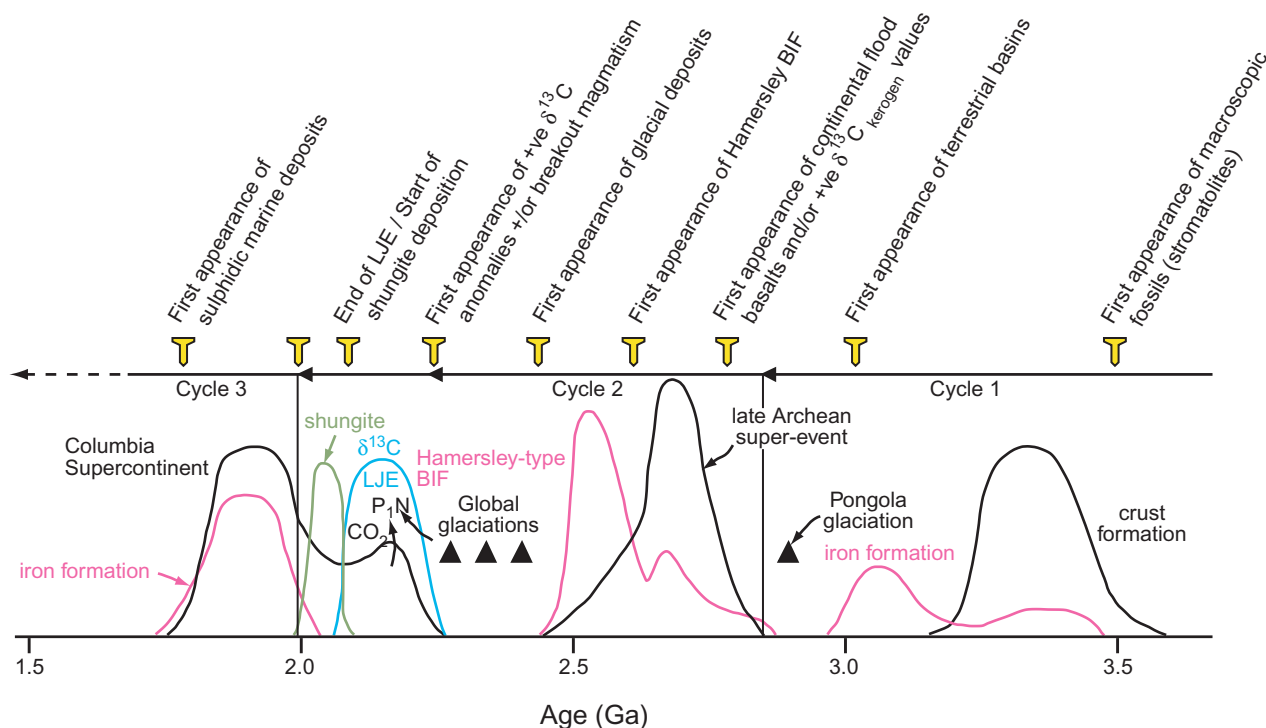
p1140



f0160 **FIGURE 16.31** Reconstructions of supercontinent Rodinia at 700 Ma and 635 Ma, showing the distribution of known glacial deposits. Sourced from Li et al. (2008) and Hoffman (2009).

a rise in the concentration of seawater sulfate and the commencement of variations in the $\delta^{13}\text{C}$ record for the first time since the Paleoproterozoic glaciations (Figure 16.15). Supercontinent formation followed on from a global period of extensional rifting of the 1.8 Ga supercontinent, Nuna (Columbia). However, accretionary tectonics continued locally after the formation of Nuna (Columbia), leading to the

assembly of the Mawson continent in Australia/Antarctica, to 1600 Ma (Payne et al., 2009), and accretion of the Yavapai (1.8–1.69 Ga) and Mazatzal (1.71–1.62 Ga) orogens onto the southwestern part of North America (Karlstrom and Bowring, 1988). Diachronous breakup of Rodinia through widespread rifting commenced at 825 Ma, at about the time of the onset of the first of the widespread Neoproterozoic



f0165 **FIGURE 16.32** Major cycles of crustal growth and biospheric response through the middle part of the Precambrian, showing relative peaks of activity, whose sharp boundaries may be used as GSSPs (spikes at top of diagram). Vertical dotted line represents the position of a potentially revised Archean-Proterozoic boundary.

(Cryogenian) glaciations (see Section 16.3.4.3), and continued through to 600 Ma, when the western part of the new supercontinent Gondwanaland had already begun to aggregate (Li et al., 2008).

p1145 A distinctive suite of anorogenic rocks known as the anorthosite-mangerite-charnockite-rapakivi granite (AMCG) suite was emplaced into Paleoproterozoic orogenic belts and their forelands through much of the middle Proterozoic, from 1.6–1.3 Ga (Emslie, 1991; Anderson and Morrison, 2005). This suite is characterized by high temperature granitic magmas that developed through extensive crystal-liquid fractionation from voluminous melts. In part, these magmas were derived from the partial melting of older crust, but they were also derived from remelting of underplated tholeiitic basalt (Emslie et al., 1994; Frost and Frost, 1997; Anderson and Morrison, 2005; Dall’Agnol et al., 2005) that derived from mantle melting episodes during continental breakup of previously thickened crust, associated with a mantle superwell (e.g. Hoffman, 1989; Windley, 1995). A mantle connection is confirmed by aluminous orthopyroxene megacrysts in anorthositic rocks, which indicate crystallization at pressures of 6.2–11 kbar, or lower crustal to upper mantle depths (Emslie et al., 1994). Similar conditions associated with extensional collapse of the Grenville Orogen led to the emplacement of AMCG suite rocks there at 1.1–1.0 Ga (Windley, 1993; Anderson and Morrison, 2005).

Oxygen levels continued to rise during this period (Des p1150 Marais et al., 1992; Canfield, 2005), and the absence of massive siderite beds in rocks younger than c. 1.8 Ga is testament to the falling partial pressure of atmospheric pCO₂ (Ohmoto et al., 2004). However, methane concentrations could have remained high during the Proterozoic, keeping the continents warm through a thin organic haze in the atmosphere (Pavlov et al., 2003; Kasting, 2005).

Two types of distinctive ore deposits characterize this p1155 period, both of which can be related to a rise in atmospheric oxygen (Holland, 2005). The first deposit type is unconformity-related U deposits, which formed at between c. 1.74 and 0.8 Ga, particularly in Canada and Australia (Marmont, 1987; Jefferson et al., 2007; Pirajno, 2009). These deposits are associated with major unconformities and occur above and below a paleosurface separating predominantly low-grade fluvial and lacustrine Proterozoic metasedimentary sequences from older, paleoweathered, metamorphosed basement (Kerrich et al., 2005). The unconformity acted as a redox front between oxidizing (above) and reducing (below) domains, with mineralization resulting from initial dissolution and transport of uranium under initially oxidizing, near-surface conditions (sedimentary brines: Polito et al., 2005) and subsequent precipitation under reducing conditions of diagenetic and/or meteoritic fluids (Hiatt et al., 2010).

p1160 The second ore deposit type is giant sediment-hosted exhalative, stratiform, massive sulfide (or SEDEX) deposits, which formed mostly between 1.8–1.0 Ga: these include the largest massive sulfide deposits in the world (e.g., the Broken Hill and Mt. Isa deposits in Australia, the Sullivan deposit in Canada: Barley and Groves, 1992; Pirajno, 2009). These deposits arose through the flow of hydrothermal fluids (heated basinal brines: Kyser, 2007) that rose up along graben-bounding faults to exhale at higher levels within the upper parts of thick sedimentary successions in reduced sedimentary units such as shale, siltstone or mudstone and intercalated carbonate rocks (Pirajno, 2009). Alteration envelopes bearing locally significant Mn indicate that the reduced, ore-bearing fluids mixed with oxidized fluids and that this caused precipitation of the ores. In higher levels parts of basins, the oxidized fluids may have derived from meteoric waters, whereas in deeper parts of basins they may have derived from stratigraphically low evaporites. The formation of some SEDEX may have been associated with high heat flow and the emplacement of high heat producing granites emplaced during the breakup of Nuna (Columbia), with the heat being produced by radiogenic decay of U, Th and K⁴⁰ (Groves et al., 2005).

s0265 16.3.4.1. Canfield Ocean (1.78 Ga–750 Ma)

p1165 Canfield (1998, 2004) has suggested that the middle Proterozoic oceans were stratified, with an oxygenated surface layer and euxinic deeper waters characterized by a vast, even global, reservoir of H₂S. This model is supported by observations of low seawater sulfate (5–15% of modern values) and anoxic, sulfidic deep waters (Lyons et al., 2000; Shen et al., 2002; 2003; Arnold et al., 2004; Kah et al., 2004), and by the presence of massive sulfide deposits. Atmospheric oxygen levels have been estimated to be in the range 8–15% PAL at this time (Figure 16.14). Canfield (2005) and Buick (2007) have suggested that N₂O may have become an important greenhouse gas. The transition from iron-rich, oxygen-deficient Paleoproterozoic oceans to sulfidic oceans is considered to reflect the result of one or both of the following effects associated with the rise in atmospheric oxygen:

- o0075 1) Filling up of the oceanic Fe oxygen sink;
- o0080 2) Enhanced sulfide weathering of exposed continental rocks led to an increased flux of sulfates to the oceans, where they underwent widespread microbial dissimilatory sulfate reduction to produce sulfides.

p1180 Although there is some significant support for the second model (e.g., Poulton et al., 2004), others have suggested that there may have been strong lateral and vertical gradients in seawater sulfate concentrations reflecting a more complex system for mid-Proterozoic oceans (Lyons et al., 2009; Pufahl et al., 2010). One significant difference compared with the earlier cessation of BIF deposition at 2.4 Ga is that the

cessation of iron-formation deposition at c. 1.78 Ga is not marked by the widespread occurrence of Mn-rich deposits: why this should be so remains to be investigated.

16.3.4.2. Eukaryote Diversification

Eukaryotic organisms commenced diversification during the middle Proterozoic. The oldest reported eukaryotic acritarchs are from the ~1800 Ma Changzhougou Formation in China (Lamb et al., 2009). Multicellular organisms have also been recognized in 1700 Ma rocks from China (Zhu and Chen, 1995) and Haines (1997) described tool marks made by algal filaments in ~1.75 Ga rocks from northern Australia. *Grypania spiralis*, the oldest eukaryote fossil (c. 2.1 Ga; see also Section 16.3.3.5), has also been found in ~1600–1450 Ma rocks in India (Sarangi et al., 2004; Sharma and Shukla, 2009), China (Du et al., 1986), and the USA (Walter et al., 1976). The long persistence of this fossil has been used to suggest a limited evolution of eukaryotes due to the persistence of deep-sea euxinia, which may have kept ocean Mo inventories low and depressed Fe, thereby limiting the supply of fixed N to, and rate of N₂ fixation by, eukaryotes (Knoll, 1992; Anbar and Knoll, 2002; Glass et al., 2009).

By the middle Proterozoic (1500–1400 Ma), however, it appears from macroscopic and microfossil evidence that eukaryotes had started to diversify, and by 1200 Ma, the fossil record shows significant eukaryote diversity, as well as microfossil evidence for putative fungal affiliations and terrestrial microbial communities in a more fully oxygenated environment (Knoll, 1992, 2003; Butterfield, 2000; Javaux et al., 2001, 2004; Knoll et al., 2004; Nagovitsin, 2009; Parnell et al., 2010). An example of older macroscopic fossils is the “string of beads”, which is found at a number of localities in ~1500–1400 Ma rocks, and is interpreted as primitive seaweed (metaphytes) with holdfasts (Grey and Williams, 1990; Fedonkin and Yochelson, 2002; Grey et al., 2002; Martin, 2004). Simple acritarchs appear in the fossil record at about middle Proterozoic time (~1500 Ma), followed by more complex acritarchs, together with evidence for terrestrial habitation from 1200–1000 Ma onwards (see also Chapters 17 and 18; Knoll, 1992, 2003; Heckman et al., 2001; Prave, 2002; Knauth and Kennedy, 2009). Other evidence for a pre-glacial expansion of eukaryotes includes the first definitive appearance of green algae and heterotrophic eukaryotes (Porter, 2004).

Despite the rise of eukaryotes during this time interval, a severe limit was placed on their development in the form of hydrogen sulfide in the deep “Canfield” oceans, which restricted oxygenated niches and bound up essential nutrients.

16.3.4.3. Late Proterozoic Environmental Instability (850–582 Ma)

(with a contribution from P.F. Hoffman)

Beginning at about 850–800 Ma, Earth entered a second major period of Proterozoic environmental instability after

a “hiatus” of almost 1 billion years. Although yet to be formally defined (see Chapters 17 and 18), the Cryogenian Period lasted for ~250 Ma and was characterized by at least two widespread, probably even global, glaciations that were accompanied by large positive and negative $\delta^{13}\text{C}$ excursions. The early part of this period was marked by unprecedented stromatolite proliferation and diversification (Grotzinger and Knoll, 1999), but then by a decline in stromatolite forms and disappearance of early marine microsparite crack fill (molar tooth structure).

p1210 Between c. 750–580 Ma, there is a growing consensus that three intercontinental – even possibly global – glaciation events occurred, evidence for which is preserved as glacially-derived diamictites deposited in passive rift basins formed during the breakup of Rodinia (Mawson, 1949; Harland, 1964; Harland and Rudwick, 1964; Hambrey and Harland, 1985; Kirschvink, 1992; Powell et al., 1993; Young, 1995; Hoffman et al., 1998; Hoffman and Schrag, 2002; Godd ris et al., 2007; Eyles, 2008). These events are represented by glacial or proximal proglacial deposits on many of the known paleocontinents and microcontinents; examples have now been found in western North America (Young, 1995), China (Wang and Li, 2003), Australia (Young and Gostin, 1991), West Africa (Deynoux et al., 2006), South America (Pecoits et al., 2007), and Oman (Allen, 2007) (Table 16.3).

p1215 According to U-Pb zircon chronometry of tuffs in bounding strata, the three glaciations include the 720–658 Ma Sturtian glaciation; 655–635 Ma Marinoan glaciation; and 584–582 Ma Gaskiers glaciation (Fanning and Link, 2004; Hoffmann et al., 2004; Condon et al., 2005; Halverson et al., 2005; Fanning, 2006; Kendall et al., 2006; Babinsky et al., 2007; Etienne et al., 2008; Zhang et al., 2008). There is less secure evidence in central and southern Africa, in China, and in Brazil, of a more limited glaciation around 750 Ma (e.g., Frimmel et al., 1996; Borg et al., 2003; Babinsky et al., 2007; see Chapters 17 and 18).

p1220 Neoproterozoic glacial deposits are characterized by abrupt onsets and terminations, are associated with “cap carbonates” that have unusual sedimentological, geochemical, and isotopic characteristics, and were deposited during post-glacial seawater rise (e.g., James et al., 2001). These rocks are also associated with the return of BIFs (and subsequently phosphorites and Mn deposits) to the rock record after an absence of almost one billion years (see Section 16.3.3.5). Glacial deposits of this age are characterized by rapid shifts to both highly positive and highly negative $\delta^{13}\text{C}_{\text{carb}}$ values (Hoffman et al., 1998; Kirschvink et al., 2000; Hoffman and Schrag, 2002; Macdonald et al., 2010), and this period was also a time of worldwide black shale deposition (Condie et al., 2001) and low oceanic sulfate (Hurtgen et al., 2002). Significantly, fossils of multicellular animals also appear in the rock record at this time (calcified fossils of sponge-grade metazoans: Maloof et al., 2010), and their

development has been linked to a rise in oxygen levels near the end of the major glaciations (see Section 16.3.4.4).

Combined sedimentological and paleomagnetic evidence p1225 reveals that tidewater glaciers existed close to the paleo-equator during parts of the middle and late Cryogenian (Embleton and Williams, 1986; Sumner et al., 1987; Evans, 2000; Hoffman and Schrag, 2002; Trindade and Macouin, 2007). The conformable occurrence of glacial deposits within thick successions of carbonate strata suggests that some glaciers flowed into the warmest parts of the ocean, and this can be used to imply that colder areas of the world were frozen, as well – a situation referred to as “snowball” Earth (Kirschvink, 1992; Hoffman and Schrag, 2002). Harland (1964) recognized that such pan-glacial episodes might provide a basis for global stratigraphic correlation. This was conceptually adopted in the selection of the GSSP for the base of the Ediacaran Period (Knoll et al., 2004).

In the “snowball” Earth model, marine geochemical p1230 anomalies (e.g., BIFs, global “cap” carbonates, and boron, sulfur and carbon isotope excursions) were used to suggest that the world’s oceans may have been ice-covered for long periods (Kirschvink, 1992; Hoffman et al., 1998; Hoffman, 1999; Hoffman and Schrag, 2002; Kasermann et al., 2010). In this model, the unusual aggregation of the Rodinia Supercontinent around the equator led to a substantial increase in albedo and in the silicate weathering rate, leading to a drawdown of atmospheric CO_2 and consequently, a significantly cooler planet (Kirschvink, 1992; Schrag et al., 2002). Planetary cooling led to one or more periods of global glaciation, each of which may have shut down biological activity and restricted the exchange of seawater with atmospheric oxygen, prompting a return of seawater to anoxic conditions and near-mantle $\delta^{13}\text{C}$ values of -6‰ (Hoffman and Schrag, 2002; Macdonald et al., 2010). Ocean anoxia resulted in the increased concentration of dissolved ferrous iron sourced from hydrothermal ridges that, when mixed with renewed oxygenated seawater as glacial episodes waned, precipitated onto the seafloor as BIF (see Canfield et al., 2008). Global glaciation events were terminated by the buildup of volcanic-derived CO_2 in the atmosphere, creating a runaway greenhouse that melted the glaciers (e.g., Pierrehumbert, 2004). Sea level rise following glacial events was accompanied by the rapid deposition of cap carbonates, whose origin is still controversial; some regard these rocks as evidence of rapid CO_2 drawdown immediately upon deglaciation (Hoffman and Schrag, 2002; Kasermann et al., 2010); others suggest deposition in response to carbonate weathering of exposed continental shelves (Higgins and Schrag, 2003), or to microbial activity (Elie et al., 2007); whereas Kennedy et al. (2001, 2008) suggest these features relate to rapid destabilization of vast gas hydrate/methane clathrate reserves that had been stored in permafrost during the “snowball” events, an idea that has at least partial support from carbon isotope evidence from China (Wang et al.,

t0020

TABLE 16.3 Neoproterozoic Glacigenic Formations by Paleocontinent

	Paleocontinent	mid-Cryogenian	end-Cryogenian	mid-Ediacaran
1.	Alaska-Chukotka	Hula Hula		
2.	Amazonia	Puga	Serra Azul	
3.	Arabia	Gubrah	Fiq	
4.		Ayn	Shareef	
5.	Arequipa	Chiquerío		
6.	Australia	Sturt	Elatina	
7.		Areyonga	Olympic	
8.		Walsh	Landrigan	Egan
9.	Avalonia			Gaskiers
10.				Squantum
11.	Baltica		Smalfjord	Mortensnes
12.				Moelv
13.				Glusk
14.				Churochnaya
15.	Cadomia			Granville
16.	Congo	Grand	Petite	
17.		Chuoss	Ghaub	
18.		Inférieure	Supérieure	
19.	Laurentia	Surprise	Wildrose	
20.		Toby	Vreeland	
21.		Rapitan	Stelfox (Ice Brook)	
22.		Ulvesø	Storeelv	
23.		Petrovbeen	Wilsonbeen	
24.		Port Askaig	Stralinchy-Reelan	Inishowen-Loch na Cille
25.		Konnarock		
26.	India		Blaini	
27.	Iran		Rizu	
28.	Kalahari	Kaigas	Numees	
29.	Kazakhstan	Baykonur?		
30.	North China			Fengtai
31.	Rio Plata			Sierra del Volcán
32.	Sao Francisco	Macaúbas		
33.	Siberia	Ballaganakh	Bol'shoy Patom	
34.	South China	Chang'an	Nantuo	
35.	Tarim	Bayisi	Tereeken	Hankalchoug
36.	Tuva-Mongolia	Maikhan UI	Tsagan Oloom	
37.	West Africa		Jbéliat	
38.		Bakoye		
39.		Kodjari		

(Continued)

TABLE 16.3 Neoproterozoic Glacigenic Formations by Paleocontinent—cont'd

1. northeastern Brooks Range, Arctic Alaska
2. Alto Paraguay, Mato Grosso, southwestern Brazil
3. Hajar Mountains, northeastern Oman
4. Mirbat coast, southwestern Oman
5. Chiquerío-Arequipa-Antofalla block, southern Peru and northern Chile
6. Adelaide geosyncline, South Australia
7. Centralian superbasin, central Australia
8. Kimberleys, Western Australia
9. Avalon Peninsula, southeastern Newfoundland, eastern Canada
10. Boston basin, Massachusetts, eastern United States
11. East Finnmark, northern Norway
12. Sparagmite basins, southern Norway
13. East European platform, Russia
14. Polyudov Ridge, northern Urals, northeastern Russia
15. Brittany, northwestern France
16. Zambian copper belt, Zambia and southern Congo
17. Otavi platform, northern Namibia
18. West Congo belt, Angola and Congo Republic
19. Death Valley, California, western United States
20. Rocky Mountains, British Columbia, western Canada
21. Mackenzie Mountains, Northwest Territories and Yukon Territory, Canada
22. Fjord region, central East Greenland
23. Ny Friesland and Nordaustlandet, northeastern Svalbard
24. Dalradian, southwestern Scotland and northwestern Ireland
25. Southern Appalachians, eastern United States
26. Lesser Himalaya, northern India
27. Lut block, central Iran
28. Gariiep belt, southwestern Namibia and northwestern South Africa
29. Kazakh block, Kazakhstan
30. Sino-Korean craton, North China
31. Tandilia, northern Argentina
32. Bambuí platform, eastern Brazil
33. Patom foredeep, south-central Siberia
34. Yangtze platform, South China
35. Quruqtagh, Xinjiang, northwestern China
36. Dzabkhan basin, southwestern Mongolia
37. Taoudeni basin, Adrar, Mauritania
38. Taoudeni basins, Tambaoura Plateau, Mali
39. Volta basin, Benin, Burkina Fasso and northern Ghana

2008). Increased weathering at the end of glaciations resulted in an increased supply of nutrients to the oceans and a biological bloom, leading to increased burial of organic material, widespread production of methane, and a resultant decrease in $\delta^{13}\text{C}$ values of seawater (e.g., Halverson et al., 2002).

p1235 Predictive tests of the “snowball” Earth hypothesis identified by Kirschvink (1992) that have been met include:

- o0085 1) Glacial units should be more or less synchronous (but see below);
- o0090 2) Lithological successions are similar in different continents, reflecting the global scale of climate fluctuations;
- o0095 3) An association of glacial units with BIFs, indicative of ocean anoxia.

p1255 Additional support for a series of global climatic changes over this period is evidenced by:

- o0100 4) The successful correlation of carbon isotopic excursions across the world (Halverson et al., 2005; Lindsay et al., 2005; Macdonald et al., 2010).

p1265 Despite the broad success of the “snowball” Earth model in explaining many of the features of Neoproterozoic geology, several problems exist with some of the details. For example, it has been found that BIFs *predate* Neoproterozoic glaciations in some places, which has been used to suggest that the BIFs relate to the increased rifting and basin development associated with Rodinia break-up, rather than the effects of prolonged sea ice cover and ocean anoxia (i.e. BIFs deposited after glaciations: Johnston et al., 2010). Also, it is now well documented that the Sturtian glaciation was markedly regional and/or diachronous over a fairly long duration (almost 80 Ma), much longer than was inferred from modeling climatic feedback effects in the Snowball Earth hypothesis (500,000 years: Hoffman and Schrag, 2002). Furthermore, detailed analysis of some successions indicate alternations between cold and temperate, non-glacial, conditions, or evidence for oscillatory glaciations, thus ruling out extreme “snowball” Earth events and a complete biological shutdown (Leather et al., 2002; Allen and Etienne, 2008; Passchier and Erukanure, 2010), and thus leading to models of a “slushball” Earth with an equatorial belt of open water (e.g., Hyde et al., 2000). Questions have also been raised as to how multicellular life could have developed in an ice-covered world. Finally, Le Hir et al. (2009) presented modeling data that showed continental weathering alone cannot account for the volume of cap carbonates.

p1270 These objections aside, most would agree that Neoproterozoic Earth experienced a period of deep cooling, although the cause(s) of the onset of these events are disputed (see Williams, 1975, 1993; Williams et al., 1998; Pais et al., 1999; Rautenbach, 2001; Schrag et al., 2002).

16.3.4.4. Increasing Oxygen, the Rise of Animals, and Post-Glacial Phosphorites s0280

(with a contribution from D. Papineau) p1275

Neoproterozoic glaciations were accompanied by the rise of atmospheric oxygen and of complex, multicellular animals (diapause eggs and embryos in South China and sponge biomarkers in Oman: Knoll and Carroll, 1999; Knoll, 2003; Love, 2006; Gaidos et al., 2007; Yin et al., 2007; Saul, 2009; Wang, X. et al., 2009). Deepwater, benthic, soft-bodied macrofossils (Ediacaran biota) appeared soon after the mid-Cryogenian glaciation (Narbonne, 2005; Yuan et al., 2011), and broadly coincided with a rise of atmospheric free oxygen above ~0.1 present atmospheric level after the end of the Marinoan glaciation event (655–635 Ma), a period also characterized by a significant release of methane from melting permafrost, and of ocean acidification (Fike et al., 2006; Canfield et al., 2007; McFadden et al., 2008; Shields-Zhou and Och, 2011).

Perhaps the oldest evidence for metazoans comes from ~850 Ma-old rocks from Canada, where Neuweiler et al. (2009) have discovered textural evidence of metazoan-grade tissue. Calcified fossils of sponge-grade metazoans have also been discovered in pre-Marinoan rocks from South Australia (Maloof et al., 2010). However, metazoans did not really develop until the ice ages had changed the environment through rising levels of oxygen after the Marinoan glaciation (e.g., Bao et al., 2008; Love et al., 2009; Shields-Zhou and Och, 2011; Yuan et al., 2011).

The late Proterozoic glaciations were followed by the widespread deposition of phosphorites (Table 16.2; Papineau, 2010), a red algal bloom (Elie et al., 2007), and development of fungi (Yuan et al., 2005). Increased weathering rates during this period of global rifting are likely to have perturbed the carbon-silicate cycle and led to a decrease in atmospheric CO_2 levels (Berner, 1993). Global Neoproterozoic glaciations also contributed to widespread weathering of continental crust, which is evidenced in part by an unprecedented global increase in $^{87}\text{Sr}/^{86}\text{Sr}$ (Veizer et al., 1983; Donnelly et al., 1990; Kaufman et al., 1993; Kennedy et al., 1998; Brasier et al., 2000; Shields and Veizer, 2002; Shields, 2008), high chemical index of alteration of shales (Condie et al., 2001), and the widespread deposition of detrital clay minerals, an event that has been referred to as the “clay mineral factory” (Kennedy et al., 2006). Because rivers are the dominant sources of sulfate for the ocean, the seawater sulfate concentration increased during this period of high weathering rates, and increased redox states.

Sedimentary sulfides and sulfates in Neoproterozoic interglacial and post-glacial marine sedimentary rocks record wide variations in $\delta^{34}\text{S}$ values, as well as ^{34}S -enriched compositions of sulfide and sulfate minerals immediately after glaciations (Gorjan et al., 2000; Hurtgen et al., 2005; Fike et al., 2006; Halverson and Hurtgen, 2007; Fike and

Grotzinger, 2008). This is consistent, in part, with microbial sulfate reduction in oceans with increased sulfate concentrations (e.g., Habicht et al., 2002). The expected consequence of high weathering rates in the Neoproterozoic is higher fluxes of phosphate delivery by rivers to seawater that should have stimulated photosynthetic oxygen production (Lenton and Watson, 2004). High nutrient delivery was also facilitated by the rise of the Transgondwanan supermountains during the late Early Cambrian period (Squire et al., 2006).

p1300 High nutrient supply at the Neoproterozoic-Cambrian boundary has been correlated with episodes of carbon isotope excursions that were contemporaneous with hydrocarbon burial and evaporite deposition (Brasier, 1991). Evidence for high rates of primary productivity between and after the Neoproterozoic glaciations is preserved as various geochemical and geological signatures. For instance, Neoproterozoic interglacial and post-glacial carbonates enriched in ^{13}C occur almost everywhere that sequences of this age are preserved (see Kaufman et al., 1997; Shields and Veizer, 2002; Halverson et al., 2005, and references therein). Organic biomarker evidence has also been used to infer high rates of primary productivity after a Neoproterozoic snowball Earth event, which has been proposed as due to high nutrient availability from weathering (Elie et al., 2007).

p1305 Large sedimentary phosphorite deposits are abundant in the late Neoproterozoic-Cambrian, which was a time interval when oceanic circulation experienced dramatic changes. Stagnation of the oceans during snowball Earth events was followed by periods of vigorous circulation during continental breakup, which could have been conducive to phosphorite formation (Donnelly et al., 1990). Major Neoproterozoic-Cambrian phosphorite deposits occur in North and South America, Africa, Europe, Asia and Australia (Notholt and Sheldon, 1986), and most of them stratigraphically overlie glacially-derived sedimentary rocks (Cook and Shergold, 1984). For instance, major phosphorites occur stratigraphically above glacial tillites in the Australian Adelaide Geosyncline (Howard, 1986), in the Chinese Doushantuo Formation (Yueyan, 1986), in the West African Volta and Taoudeni Basins (Slansky, 1986; Flicoteaux and Trompette, 1998), in the Brazilian Bambuí Group and correlative sequences (Dardenne et al., 1986; Misi et al., 2006), in the Khubsugul Basin and related deposits of the Mongolian-Siberian region (Ilyin et al., 1986; Yanshin, 1986), and many other places in Vietnam, Kazakhstan, Pakistan, India, Europe and North America. Many of these phosphorites formed during major transgressions (Brasier, 1980) and along newly rifted continental margins.

p1310 Biological involvement in the formation of Neoproterozoic-Cambrian phosphorites is preserved as various types of biological structures. Microorganisms were important in the formation of these phosphorites, as evidenced in part by several examples of stromatolitic phosphorites (with

columnar carbonate fluorapatite) of Cambrian age in Australia (Southgate, 1980; Schmidt and Southgate, 1982), Algeria (Bertrand-Sarfati et al., 1997), China (Yueyan, 1986), Russia (Yanshin, 1986), and elsewhere. Perhaps even more striking is the fact that many phosphorites of Late Neoproterozoic-Cambrian age preserve unique remains of multicellular organisms, including animal embryos (Xiao et al., 1998, 2007; Steiner et al., 2004), brachiopods (Cowan et al., 2005), and various other fossils of eukaryotic organisms (Cook and Shergold, 1984; Brasier, 1990).

Shortly after the end of the Neoproterozoic glaciations, p1315 exceptional fossils of early animal evolution are preserved in marine sedimentary rocks, and these include new macroscopic organisms shaped as spheres, disks, fronds, worms and other radial and bilateral body architectures (e.g., Runnegar, 1991; Grotzinger et al., 1995; Jensen et al., 1998; Narbonne, 1998, 2005; Canfield et al., 2007). The Neoproterozoic rise in atmospheric oxygen was also responsible for the most significant leap in biological diversity and complexity in Earth history; the Cambrian explosion. New organisms that emerged in the oceans of the Early Cambrian include sponges, brachiopods, conodonts and trilobites, and many of these metazoans had biomineralized skeletons, complex shapes, and undulated/articulated bodies.

16.4. A LINKED, CAUSATIVE SERIES OF EVENTS IN PRECAMBRIAN EARTH EVOLUTION

s0285

The events outlined in this chapter show that Precambrian p1320 Earth was characterized by a distinctly non-uniform, highly episodic development, marked by periods of intense geological activity interspersed with periods of relative quiescence – a sort of punctuated equilibrium of planetary evolution (Table 16.4, Figure 16.18; Condie, 1995, 1998, 2000, 2004; Davies, 1995; Campbell and Allen, 2008; Condie et al., 2009). Whereas some have suggested that such apparent non-uniformitarian activity reflects only the biased preservation of an incomplete geological record (Kemp et al., 2006; Hawkesworth et al., 2009, 2010), such notions are discounted by the fact that peaks of crustal growth – as defined by peaks in zircon ages – correlate with peaks in the rate and volume of komatiites, plume-derived magmas in LIPs, and BIF, and with changes in the biosphere (Isley and Abbott, 1999; Abbott and Isley, 2002; Lindsay and Brasier, 2002; Sleep and Bird, 2008), proving beyond reasonable doubt that crustal growth was indeed episodic through the Precambrian (McCulloch and Bennett, 1994; Stein and Hofmann, 1994; Parman, 2007; Pearson et al., 2007; Condie et al., 2009).

Furthermore, a number of features of the geological p1325 record show that the nature of continental crust changed uniquely at ca. 2.5 Ga, not only in terms of composition

TABLE 16.4 Causative Events in Precambrian Earth History

t0025

4568 Ma	gravitational collapse of an interstellar dust cloud → formation of the sun, planets, and meteorites
4404 Ma	Cooling → formation of first crust, atmosphere and oceans, and origin of life; but high internal heat and continued meteor bombardment → rapid and thorough crustal recycling
4030 Ma	Cooling, differentiation, and tapering of bombardment → preservation of first crust
3490 Ma	Cooling, differentiation, and tapering of bombardment → first stable protocontinents, with shallow-water stromatolites
3000 Ma	Cooling and differentiation → widespread crust extraction and first emerged continental platform successions with terrestrial microbial communities
2780 Ma	Widespread crust formation at the crossover point of heat generation and conductive heat loss → mantle warming and crust-forming superevent, high pCO ₂ , bloom of (?cyanobacterial) microbial life → rise in O ₂ and global methanogenesis
2630 Ma	Decreasing mantle activity → diminishing crust formation, but widespread hydrothermal activity and precipitation of BIF; microbial development limited by largely submerged continents
2420 Ma	Continued mantle cooling → continental emergence, increased silicate weathering, drawdown of CO ₂ , loss of methane and global cooling → decreased magmatism, global glaciations, rise in O ₂
2250 Ma	Mantle warming → global breakout magmatism, increase in atmospheric CO ₂ , bloom in microbial life → rise in O ₂ , positive δ ¹³ C excursions (LJE), deposition of phosphorites, Ca-sulfates, and Mn deposits, rise in eukaryotes
2068 Ma	Mantle superswell → global rifting and orogeny, reduced deep oceans with deposition of iron-formation and shungite, but oxidized upper oceans and formation of natural uranium fission reactors
1780 Ma	Nuna (Columbia) supercontinent assembly → increased weathering, higher seawater sulfate concentrations and sulfate reduction → sulphidic “Canfield” ocean, giant sulfide deposits
850 Ma	Breakup of Rodinia → increased volcanism, reducing oceans, low oceanic sulfate, deposition of BIF and global black shales
750 Ma	Equatorial concentration of continents, increased albedo, and rift-related uplift → widespread and/or global glaciations, slowdown of biological activity
635 Ma	Rise in volcanic-generated atmospheric pCO ₂ → Deglaciation, sealevel rise, global deposition of cap carbonates → rapid CO ₂ drawdown, rise in oxygen → Ediacaran fauna
542 Ma	Formation of Gondwana Supermountains → increased silicate weathering and supply of nutrients to oceans, CO ₂ drawdown, rise in atmospheric O ₂ → Cambrian explosion

(Condie and Wronkiewicz, 1990; Taylor and McLennan, 1985), but also in terms of crustal rigidity and exposure above sea level (Arndt, 1999; Eriksson et al., 1999; 2006; Flament et al., 2008; Rey and Coltice, 2008). The data therefore suggest that crustal growth developed progressively and episodically from ~4.03–2.5 Ga (McCulloch and Bennett, 1994), peaked at c. 2.5 Ga, and has been essentially recycled in an approximately steady state through the supercontinent cycle ever since (Taylor and McLennan, 1985; Bowring and Housh, 1995; Scholl and von Huene, 2007; Bennett et al., 2010).

p1330

The differences in crustal composition and behavior across the 2.5 Ga transition are due to a markedly hotter Archean mantle, estimated to be 3–4 times hotter than today. Such increased mantle temperatures resulted in raised isotherms within continental lithosphere, thereby creating softer lithosphere with a greater propensity to melt under any superimposed stress, such as lateral compression (e.g., Cruden et al., 2006; Rey and Houseman, 2006; O’Neill

et al., 2007; see also Hansen 2007). Numerical modeling has shown that these uniquely Archean conditions would have resulted in a tectonic mode termed stagnant lid behavior, whereby periods of rapid subduction relating to planetary-scale resurfacing events were interspersed with periods of relative quiescence (Abbott and Isley, 2002; O’Neill et al., 2007; Condie et al., 2009). The crustal record, combined with numerical modeling results, show that this style of tectonics affected Earth through to at least 1.78 Ga, with quiescent periods marked by low rates of volcanism, increased levels of atmospheric oxygen (low Δ³³S values), and cool climatic conditions. These contrast with resurfacing events that are characterized by high rates and volumes of magmatism, high atmospheric CO₂ (large Δ³³S anomalies), high degrees of continental weathering, and — once cyanobacteria had become established — high rates of microbial activity, leading to perturbations in the carbon cycle (Figure 16.15; Hayes and Waldbauer, 2006). Such periods of rapid crust formation are analogous with events caused by the Cretaceous superplume

event (e.g., rapid crust formation, high $p\text{CO}_2$, oceanic euxinia), which derived from episodic, anomalous heat flow from lower mantle domains (Leckie et al., 2002; Herzberg and Gazel, 2009).

p1335 Indeed, given our knowledge of thermodynamics, it is likely that all of the changes wrought throughout Precambrian Earth history were ultimately driven by, and relate to, secular changes in, and the episodic nature of, heat flow from the core-mantle boundary (e.g., Richter, 1988; Greff-Lefftz and Legros, 1999; Labrosse and Jaupart, 2007; O'Neill et al., 2007; Condie et al., 2009; Landuyt and Bercovici, 2009; Herzberg et al., 2010). These changes apply not only to changes in crustal development and composition through time, but also to the establishment of, and changes in, the biosphere, as shown in Figure 16.32 (Kirschvink, 1992; Lindsay and Brasier, 2002; Schrag et al., 2002; Squire et al., 2006; Campbell and Allen, 2008).

p1340 In general, the geological data show that changes in heat flow from the mantle resulted in periods of rapid crust formation that were accompanied by high volumes of magmatism and volcanic-derived CO_2 . This changed the composition of the atmosphere and oceans and led to increased microbial activity and the deposition of iron-formations (Figure 16.32). The huge release of mantle heat during these periods of rapid crust formation, accompanied by blanketing of the core-mantle boundary by newly subducted lithosphere (e.g., Santosh, 2010) – but possibly also reflecting geodynamical changes caused by core oscillations induced by lunar-solar tidal forces (Greff-Lefftz and Legros, 1999) – resulted in subsequent cooling of the mantle and associated slowdown of magmatic activity, a decrease in volcanic-derived CO_2 , slowing in the rate of microbial activity, cooling of the atmosphere, and deposition of glacial rocks.

p1345 Three of these major cycles can be recognized in the Precambrian geological record, each characterized by an initial, 200 Ma-long, burst of geological activity associated with the breakout of mantle-derived magmas, accompanied, and outlasted, by widespread deposition of iron-formation (Figure 16.32). This was followed in the first two cycles by cooling of the atmosphere, glaciation, and the rise in atmospheric oxygen. The events of cycle two were followed by a major perturbation in the carbon cycle (the Lomagundi-Jatuli Event), and subsequent deposition of highly carbonaceous shales (the worldwide Shunga Event: Melezhik et al., 2005a). Cycle three partially commenced at c. 2.22 Ga with breakout magmatism on many continents, but did not really take off until c. 2.06 Ga, with the emplacement and eruption of the Bushveld Igneous Province and aggregation of Supercontinent Nuna/(Columbia) (2.06–1.78 Ga). That the start of cycle 3 (2.25–2.06 Ga) partially overlapped with the follow-on effects of cycle two may explain the Lomagundi-Jatuli Excursion (2.25–2.06 Ga) and Shunga Event (c. 2.0 Ga), as increased atmospheric CO_2 associated with breakout magmatism, combined with

increased nutrients (P, N) resulting from high weathering rates associated with the decline of the immediately preceding glaciations, provided essentially perfect conditions for a prolonged microbial bloom.

Two of the major series of causative linked events remain p1350 controversial and are discussed in more detail below: 1) the origin and driving force behind the late Archean superevent; 2) the rise in oxygen levels.

16.4.1. The Late Archean Superevent s0290

Many researchers ascribe the deposition of late Archean BIF p1355 and rise in atmospheric oxygen to the evolutionary development of oxygenic photosynthetic cyanobacteria. It is thought that cyanobacteria flourished on widespread continental shelves, newly formed during a period of rapid crustal growth and supercontinent amalgamation at 2.8–2.5 Ga, through uniformitarian plate tectonic processes (the so-called “Late Archean Superevent”: Cloud, 1973; Barley et al., 1998; Rey et al., 2003; Guo et al., 2009). The newly created oxygen was first used to oxidize reduced chemical species – such as ferrous iron dissolved in seawater and sulfide minerals in weathering profiles – depositing huge volumes of BIF and sulfates as a result (Cloud, 1973; Cameron, 1982). It was only after these sinks were saturated with oxygen that it began to accumulate in the atmosphere, which occurred by ~2.3 Ga (Holland, 2002; Bekker et al., 2004). Cooling of the atmosphere followed the deposition of BIF accompanied the rise in oxygen, as shown by the widespread appearance of glacial deposits at this time (Evans et al., 1997; Kirschvink et al., 2000).

However, three major problems exist with this model. p1360

- 1) If the period of rapid crustal growth relates to uniformitarian plate tectonic processes, then why do late Archean o0105 terrains contain unusually high volumes of deep mantle-derived komatiite? Why are they so endowed in gold and base-metal deposits? And why do they immediately precede a unique, global change in crustal composition and continental freeboard (Taylor and McLennan, 1985; Arndt, 1999)?
- 2) Many recent studies support the rise of oxygenic cyano- o0110 bacteria well prior to the Great Oxidation Event, at 2.7 Ga (Buick, 1992; Wille et al., 2007; Kato et al., 2009), or even much earlier (2.9–3.46 Ga: Altermann et al., 2006; Ohmoto et al., 2006; Ono et al., 2006; Hoashi et al., 2009). If this was the case, then why was BIF deposited in such concentrations at 2.6–2.4 Ga and not earlier? What caused the widespread deposition of these unusual rocks? And what caused the environmental chaos at 2.8–2.4 Ga, if not the evolutionary development of oxygenic cyanobacteria? Was the atmosphere somewhat reducing, with oxidized oases? Or was it more extreme, with high concentrations of CO_2 and methane? Were oceans

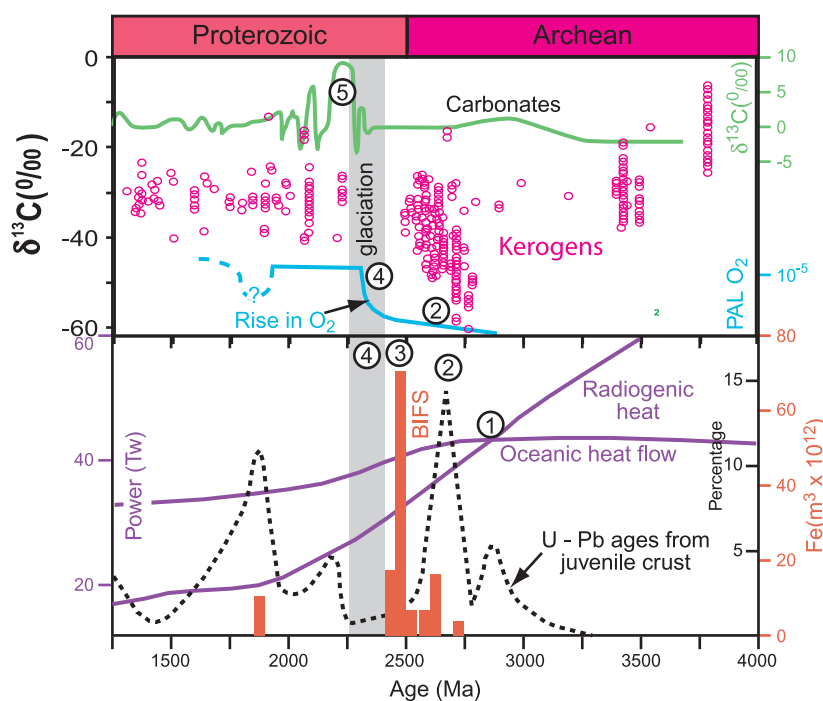


FIGURE 16.33 A causative, linked series of events across the Archean-Proterozoic boundary transition: 1) radiogenic heat flow decreases to below the rate of oceanic heat flow, meaning that oceanic crust starts to cool for the first time in Earth history; 2) major peak in juvenile crustal growth (planetary resurfacing event of O'Neill et al., 2007), releasing huge volumes of CO₂ into the atmosphere and causing a rise of methanogens; 3) increased hydrothermal flux and chemical weathering results in precipitation of huge volumes of BIF; 4) mantle cooling and a decrease in hydrothermal Fe and volcanic CO₂ following the late Archean Superevent (1–3), combined with an increase in oxygen production from cyanobacterial respiration results in atmospheric oxidation and global magmatic slowdown; 5) microbial bloom resulting from delivery of increased nutrients to the oceans following deglaciation, combined with increased atmospheric pCO₂ from renewed volcanism, results in disequilibrium in the biosphere – the Lomagundi-Jatuli isotopic excursion.

alkaline or acidic? What changes occurred in atmospheric composition over this period?

o0115 **3)** How did this period of change come to an end and why? What caused the deposition of BIF to cease and the atmosphere to cool? And when did this occur – was it globally synchronous, or are glacial deposits diachronous and deposited at different times on different continents?

p1380 A variety of models have been presented to explain some, or in a few cases all, of the changes associated with this transitional period, but they are insufficiently constrained in terms of real field evidence, absolute ages and causative relationships. For example, Barley et al. (1997) proposed that extreme environmental conditions and deposition of BIF during the latest Archean were caused by prolonged volcanism driven by rising mantle superplumes, but they lacked supporting geochronological and geochemical data. Campbell and Allen (2008) noted that peaks in global zircon ages preceded steps in the rise of oxygen (Des Marais et al., 1992; Canfield, 2005) and postulated that periods of supercontinent amalgamation formed supermountains that eroded quickly, thereby releasing nutrients (Fe, P) into the oceans and leading to an explosion of cyanobacteria and increased burial of organic carbon and pyrite. This in turn led to a rise in oxygen because its drawdown through reaction with these elements was decreased. However, this model is negated (at least for the earliest stage) by the fact that the bulk of late Archean crust was only eroded to shallow levels (5 ± 2 km: Galer and Mezger, 1998) and that this period was one of pronounced low continental freeboard (Eriksson et al.,

1999); thus, the postulated supermountains did not exist at this time.

Rather, it is suggested that the changes wrought on Earth p1385 across the Archean-Proterozoic transition are part of a series of causative, linked events and that the rise of oxygen was intimately related to interconnected geological and biological processes, as follows (Figure 16.33).

1. Secular decline in mantle heat to below the level of conductive heat loss through the crust at ~2.8 Ga o0120 (Labrosse and Jaupart, 2007), gave rise to cooling of oceanic lithosphere and the onset of widespread plate tectonics. Rapid sinking of these plates gave rise to anomalous heat loss through a series of deep mantle plumes (Herzberg et al., 2010), resulting in widespread crust formation (2.8–2.7 Ga) →
2. Widespread mantle melting, rapid crust production, and o0125 depletion of lower crust, leading to widespread generation of granites and formation of stable, buoyant lithosphere (2.7–2.63 Ga) →
3. Extreme global volcanism pumped huge volumes of o0130 gasses into the atmosphere and resulted in an extreme greenhouse atmosphere (~60–100°C?) with high pCO₂. Deep chemical weathering of newly erupted (and exposed) volcanic rocks resulted in the deposition of kilometers of chemical sedimentary rocks around the world, including vast resources of BIF (2.63–2.42 Ga) →
4. Emergence of continents and secular cooling of the o0135 mantle led to cooling of the geotherm, due to the partitioning of radiogenic elements into the top 5–10 km of the

continental crust. Increased oxygen production, coupled with drawdown of atmospheric CO₂ in crustal and oceanic sinks cooled the atmosphere, deposited glacial rocks, and gave rise to an oxidized atmosphere (2.42–2.22 Ga; e.g., Buggisch et al., 2010) →

o0140 **5.** Chemical weathering of continents following glaciation buffered atmospheric pCO₂, boosted primary productivity by flooding ecosystems with nutrients (P, N, Fe, etc), and increased oxygen production, leading to disequilibrium and chaos in the biosphere (2.22–2.06 Ga).

s0295 **16.4.2. The Rise in Atmospheric O₂ and the LJE**

p1415 (with a contribution from D. Papineau)

p1420 At present, there is no consensus on the causative mechanism(s) responsible for the LJE. Increased carbon burial was originally proposed (Baker and Fallick, 1989a, b) and is still considered by some (Karhu and Holland, 1996; Bekker et al., 2001, 2003a) as the most plausible driving force. However,

[AU4] Melezhik and Fallick (1996) recognized the LJE as a paradox because of the absence of geological evidence for buried carbon to compensate ¹³C-rich carbonates, although some minor “black shales” have been reported in association with ¹³C-rich carbonates (Bekker et al., 2001, 2003a, 2003b).

[AU5] Yudovich et al. (1991), and Hayes and Waldbauer (2006) linked the LJE to fermentative and methanogenic diagenesis in deeper levels of the sediment column as a response to increasing concentration of O₂. However, a large range in δ¹³C variations that is commonly associated with such

[AU6] diagenesis (Watson et al., 1995) is not seen in any ¹³C-rich Paleoproterozoic carbonate sections (Melezhik et al., 1999a).

[AU7] Aharon (2005) appealed to a redox-stratified ocean model that implies decoupling of the P and C cycles. However, long-term (i.e., >1 Ma) stagnation of the ocean circulation cannot be physically sustained (Sarmiento and Herbert, 1988).

[AU8] Despite the obvious problem in finding driving forces for the LJE, the latter has nevertheless been given global significance (Baker and Fallick, 1989a, b; Karhu and Holland, 1996; Melezhik et al., 1999a; Aharon, 2005).

p1425 The consequences of combined higher tectonic activity during global rifting (Heaman, 1997; Barley et al., 2005; Bekker et al., 2006; Halls et al., 2008) and the cessation of glaciations at 2.2 Ga resulted in increased weathering rates that perturbed the carbon-silicate cycle as more Ca and Mg became available in seawater for carbonate precipitation and thereby led to a decrease in atmospheric CO₂ levels (Berner, 1993). A natural effect of increased delivery to seawater of material from eroded continental crust is more phosphate, since rivers are the most important sources of phosphorus to the oceans (Föllmi, 1995, 1996; Papineau, 2010). The

[AU9] Sr-isotope record of Paleoproterozoic carbonates shows an increase in ⁸⁷Sr/⁸⁶Sr from 0.7022 to 0.7046 between 2.5 and

1.9 Ga (Veizer and Compston, 1976), which is consistent with higher weathering rates during Paleoproterozoic periods of elevated tectonic activity (e.g., Blum and Erel, 1995). A re- [AU10]

evaluation of this global shift based on the lowermost ⁸⁷Sr/⁸⁶Sr for Paleoproterozoic carbonates, which attempts to exclude possible Sr contribution from detrital clay minerals, showed a similar trend (Shields and Veizer 2002; Shields, 2007), but also some exceptions with low ⁸⁷Sr/⁸⁶Sr during the LJE in a few localities (Bekker et al., 2003b). Evidence for [AU11]

intense weathering after the Paleoproterozoic glaciations also comes from a substantial increase in the chemical index of alteration (CIA) in shales deposited after the glaciations (Nesbitt and Young, 1982; Condie et al., 2001) and the widespread distribution of mature quartz sandstones in almost all Paleoproterozoic post-glacial successions (Bekker et al., 2006). Oxidative weathering also leads to higher levels of cations (e.g., Ca²⁺, Mg²⁺, Na⁺ and K⁺) and anions (e.g., PO₄³⁻, SO₄²⁻ and Cl⁻) in seawater, and the widespread deposition of sulfate evaporites after the Paleoproterozoic glacial period (Cameron, 1983; El Tabakh et al., 1999; Bekker et al., 2006) is also consistent with high weathering rates under intense greenhouse conditions.

Because photosynthetic organisms quickly incorporated p1430 phosphorus, it is likely that the continuous riverine supply of phosphorus stimulated cyanobacterial blooms along coastlines, and that phosphogenesis occurred wherever environmental and paleoceanographic conditions were adequate. Sedimentation in newly formed intracontinental rift basins, along with subsequent flooding of these new continental margins, constitute ideal sites for microbial communities to thrive, possibly because of their proximity to elevated nutrient sources. Active Paleoproterozoic rift basins are sites where diverse and abundant stromatolites often developed, especially in shallow-marine environments along the newly formed continental margin where carbonates commonly preserve δ¹³Ccarb excursions (e.g. Wanke and Melezhik, 2005).

Possible connections between δ¹³Ccarb excursions and p1435 high rates of primary productivity have been suggested before (Aharon, 2005; Kump and Arthur, 1999; Melezhik et al., [AU12]

1999a). In fact, the common stratigraphic association of phosphorites with ¹³C-enriched carbonates suggests a connection with atmospheric oxygenation and possibly also with high productivity. Calculations have shown that increased weathering flux of phosphorus to the oceans after major glaciations can stimulate photosynthetic oxygen production (Lenton and Watson, 2004) and this is may be a reason for the occurrence of positive δ¹³Ccarb excursions in proximity to continents along newly rifted margins.

What is interesting to also consider is the possible p1440 connection between renewed volcanism at this time and the disequilibrium in the biosphere as reflected by the global LJE (Lindsay and Brasier, 2002; Melezhik et al., 2005a). Typically, global volcanism results in a warming of the atmosphere as a result of increased volumes of atmospheric CO₂,

which in turn leads to increased rates of chemical weathering, drawdown of CO₂ and eventual cooling of the atmosphere, commonly leading to glaciation (e.g. Buggisch et al., 2010). However, in the case of the Paleoproterozoic, there is no evidence for a post 2.0 Ga glaciation, but rather a recurrence of BIF, while at the same time there is also evidence for a dramatic increase in atmospheric oxygen with the appearance of widespread evaporitic sulfates and redbeds (e.g. Holland, 1994).

p1445 It is suggested that the increase of volcanism at 2.2 Ga, coinciding with increased marine nutrients derived from deglaciation and rift-related weathering of continents, led to a prolonged microbial bloom and burial of organic carbon during the LJE. As volcanism slowed towards the end of the LJE, a rise in oxygen levels promoted weathering of sulfides in continental crust, which delivered increased levels of sulfate to the oceans, where a resultant bloom of sulfate reducing organisms led eventually to highly reducing deep oceans and shungite, all of which ceased when a new biogeochemical balance in the carbon cycle between oxygenic photosynthesis and aerobic respiration was established by the end of the global shungite event.

s0300 16.4.3. Linked Events and GSSPs

p1450 What is especially exciting about the series of contingent events identified above for the period 2.78–1.78 Ga is that each of the events is global, and each commences almost immediately after the preceding event, with minimal overlap. As such, these events are eminently suitable for use as timescale divisions, and their rapid transitions are amenable for use as GSSPs, as shown diagrammatically in Figure 16.33.

s0305 16.5. A REVISED PRECAMBRIAN TIMESCALE

p1455 The overview of the geological data presented in the previous sections shows that Precambrian Earth evolved in a distinct series of over 20 linked events, each of which arose directly as a result of antecedent events, and thus they accord well with Gould's (1994) historical principles of directionality and contingency (see Section 16.1). Each event has global significance. This allows for the very real possibility of a fully revised Precambrian timescale, founded on the linked geological development of the planet and evolution of the biosphere, and based on the extant rock record, with real boundaries marked by GSSPs in type sections. Nine events may qualify for such (see below), with the base Ediacaran Period already formalized with a GSSP (Chapter 18), and the upper level of the Precambrian formalized with the GSSP for the base Cambrian Period (Chapter 19).

Specifically, the history outlined in Section 16.3 indicates p1460 the following main Precambrian *events* (in italics) and first appearances:

- formation of the first solid solar system materials at 4567 Ma u0045
- *accretion of the Earth-Moon system, to ~4500 Ma* u0050
- first appearance of crustal material in the rock record, in the form of individual zircon grains, dated to 4404 Ma u0055
- first appearance of a coherent rock, at 4030 Ma u0060
- first appearance of well-preserved supracrustal rocks, c. 3810 Ma (Isua supracrustal belt) u0065
- first appearance of macroscopic fossils (stromatolites) in well-preserved crustal rocks, at ≥3481 Ma u0070
- first appearance of terrestrial biological communities in stable continental platforms (e.g., the Pongola Super-group), at ca. 3 Ga u0075
- *crust-forming superevent, 2.78–2.63 Ga* u0080
- first appearance of highly negative δ¹³C_{kerogen} values from widespread stromatolitic carbonate platforms, at 2.74 Ga u0085
- *deposition of widespread BIF, 2.63–2.42 Ga* u0090
- first appearance of global glaciations and bedded carbonate rocks with δ¹³C_{carbonate} values of –6‰, after 2.42 Ga u0095
- *global magmatic shutdown, glaciations, and the Great Oxidation Event, 2.42–2.25 Ga* u0100
- global breakout magmatism, onset of the LJE, and first appearance of phosphorites, Ca-sulfates, and eukaryotes, ca. 2.25 Ga u0105
- *LJE event, 2.25–2.06 Ga* u0110
- Unprecedented accumulation of organic carbon (Shunga Event), and onset of reducing oceans with return of BIF, 2.06 Ga u0115
- *global orogeny and deposition of BIF, 2.06–1.78 Ga* u0120
- *isotopic stability of the biological tracers, sulfidic deep oceans, and the diversification of eukaryotes, 1.78–0.85 Ga* u0125
- first appearance of metazoans, 850 Ma u0130
- first appearance of global glaciations and negative δ¹³C_{carbonate} values, c. 750 Ma u0135
- *global glaciations, 750–582 Ma (Cryogenian)* u0140
- first appearance of Ediacaran fossils (Ediacaran) u0145

The question then arises as how best to group Precambrian p1570 events into Periods, Eras and Eons. For example, one could argue on a purely temporal basis that the series of events presented herein could be divided into a short accretionary event (4.56–4.03 Ga), then a set of long-duration events from 4.03–2.78 Ga, followed by a set of relatively rapid events from 2.78–1.78 Ga, a long period with fewer events from 1.78 Ga–850 Ma, and finally a series of shorter events from 850–542 Ma. Such a scheme is satisfying in that it identifies differences in the rate of change over the development of our planet, as with human development (e.g., nascent, juvenile, adolescent, and mature stages; see

Section 16.3). However, such a purely temporal scheme pays no attention to the nature of the events themselves or their lithostratigraphic characteristics. Importantly, such a division ignores the fact that we are laden with the historical precedent of existing timescale nomenclature, in particular the well established Archean and Proterozoic eons and their chronometric boundary at 2.5 Ga. This division is so firmly established that it severely limits the degree of flexibility in revising the timescale, as any radical departure would almost certainly be ignored by the vast majority of Earth scientists.

p1575 In order to provide a useful and illustrative scheme for the division of the nearly four billion years of Precambrian time that will be accepted by stratigraphic specialists, the broad geological community and general public, one must first recognize the *most* significant lithostratigraphic changes in Earth history and use these to define the first-order divisions – the eons.

p1580 I regard the events outlined above as indicating two fundamental changes over the course of Precambrian time. First is the development of stable crust, such that it was able to remain on the surface of the Earth and provide both a habitat for emerging life and a foundation for the preservation of a stratigraphic record from which we have been able to unravel the history of our planet. The second fundamental change is the transition from a warm, greenhouse, early Earth, with reducing oceans and atmosphere, widespread deposition of BIF, and only primitive life, to a cooler, more modern Earth with an oxidized atmosphere and more complex life (eukaryotes). Stratigraphically, this second major change is dramatically represented by the disappearance of BIF from the rock record and appearance of widespread, thick, glacial deposits at about 2.42 Ga, a well-constrained transition that could be used to represent the Archean-Proterozoic boundary (Figure 16.21).

s0310 16.5.1. A Hadean Eon

p1585 With these fundamental divisions in mind, a possible chronostratigraphic revision of the Precambrian timescale is presented in Figure 16.34. In this scheme, the Precambrian timescale is divided into three eons, formally recognizing for the first time a **Hadean Eon** for the earliest period of Earth history, extending from the age of formation of the solar system at $T_0=4567$ Ma, to the age of Earth's oldest dated rock from the Acasta Gneiss Complex, at 4030 Ma. An older subdivision of the Hadean relates to the early accretionary history of the Earth, from the age of formation of the solar system ($T_0=4567$ Ma) to the age of the oldest preserved crustal material on Earth, the 4404 ± 8 Ma detrital zircon from the Jack Hills greenstone belt of Western Australia (Wilde et al., 2001) – this could be named the Chaotian Era to represent a chaotic period of accretion (modified from Goldblatt et al., 2009a). A younger era within the Hadean Eon could be established for the time interval represented by the

age of the oldest detrital zircon (4404 Ma) to the age of the oldest preserved rock (4030 Ma Acasta Gneiss), and could be named the “Jack Hillsian Era”, or “Zirconian Era” (modified from Goldblatt et al., 2009a), after the Jack Hills greenstone belt that contains the best record of detrital zircons over this interval. Both the lower (4567 Ma) and upper (4030 Ma) age limits for the Hadean Eon would necessarily be defined as chronometric boundaries, as there is no preserved stratigraphy. The upper age limit of the Hadean Eon would also serve as the lower limit of the Archean Eon.

16.5.2. The Archean Eon

s0315

A revised **Archean Eon** can be defined as the time of p1590 Precambrian history from the first appearance of preserved rocks at the Earth's surface (4030 Ma Acasta Gneiss), to the first appearance of widespread glacial rocks, cooler Earth conditions, and the rise of atmospheric oxygen at ca. 2420 Ma. The Archean Eon may be divided into three eras and six periods (Figure 16.34).

16.5.2.1. Paleoarchean Era: 4030–3490 Ma

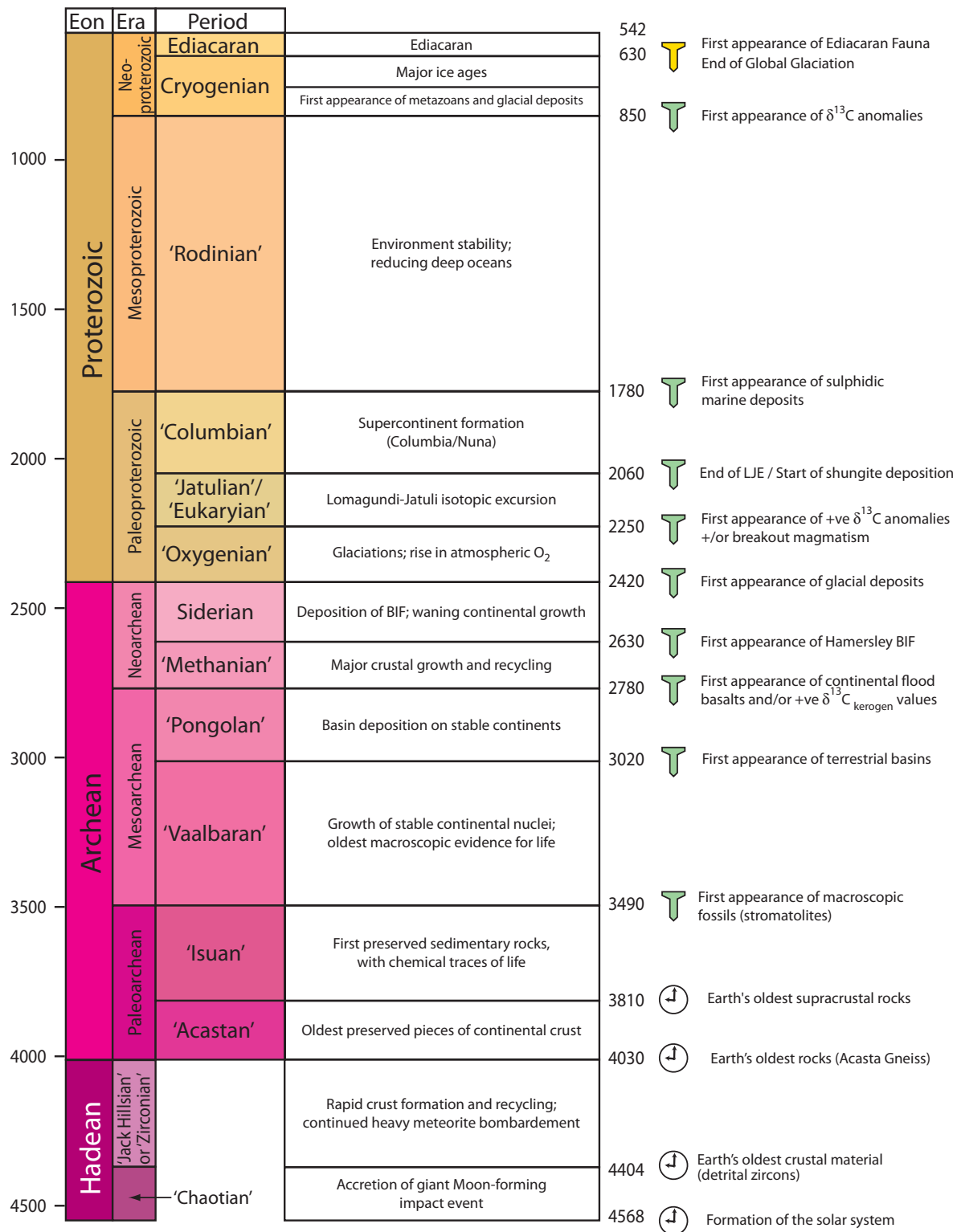
s0320

The Paleoarchean Era is proposed to extend from 4030–3490 p1595 Ma and to be defined as the time when continental crust was being progressively more widely preserved on the Earth's surface, but as gneissic terrains in a highly deformed state. Possible traces of life were preserved in supracrustal rocks, but definitive signs of life are restricted to the following era. This oldest Archean Era could be subdivided into two periods: an older *Acastan Period* (4030–3810 Ma), named after the Acasta Gneiss Complex of the Slave Craton, Canada, which is representative of the dominantly gneissic crust formed during this time; and a younger, *Isuan Period* (3810–3490 Ma), named after the Isua supracrustal belt of the North Atlantic Craton, Western Greenland, which contains the oldest well preserved supracrustal rocks with recognizable primary structures. The upper age limit for the Paleoarchean Era is defined as the first appearance of well-preserved signs of life, as defined for the Mesoarchean Era, below. The lower boundary and “Acastan-Isuan” boundary would necessarily be defined as chronometric boundaries, as there is no preserved stratigraphy, whereas the upper age limit for the Paleoarchean Era may be defined by a GSSP, as described below.

16.5.2.2. Mesoarchean Era: 3490–2780 Ma

s0325

A revised Mesoarchean Era would have a lower boundary p1600 with the Paleoarchean Era at a GSSP, which could be defined by the first appearance of definitive evidence of life in well-preserved rocks from the North Pole region of the Pilbara Craton, Australia. This evidence occurs in the form of fossil stromatolites within the Dresser Formation of the Warrawoona Group (Pilbara Supergroup), as first described by



f0175 **FIGURE 16.34** Proposed scheme for a fully revised Precambrian timescale: clock symbols = chronometric boundaries; green spikes = boundaries where possible GSSPs are recognized; yellow spike = formally recognized GSSP.

[AU13] Walter et al. (1980), but subsequently confirmed by a variety of others (Buick and Dunlop, 1990; Philippot et al., 2007; Van Kranendonk, 2007a, 2010b; Van Kranendonk et al., 2008b). The lower age limit of this era is constrained by a Pb-Pb age of 3490 Ma on syn-depositional barite from the lower part of the Dresser Formation, and a U-Pb SHRIMP zircon age from the unconformably overlying, upper (non-barite-bearing, non-stromatolitic) part of the Dresser Formation, at 3481 ± 2 Ma (Thorpe et al., 1992; Van Kranendonk et al., 2008b). The GSSP would be cited at the lower contact of the Dresser Formation, where it lies on pillow basalts of the older North Star Basalt. Based on these data, an age of 3490 Ma is recommended as the best estimate of the age for the base of the Mesoarchean Era. The Dresser Formation is well-exposed within a series of gently- to moderately-dipping rocks of the North Pole Dome, and has a conformable contact with underlying basalts, so that it is suitable to be used as a GSSP.

p1605 The Mesoarchean Era may be divided into two periods (Figure 16.34). An older period, from 3490–3020 Ma, represents the time of development of the first stable continental nuclei of the Pilbara and Kaapvaal cratons, including their buoyant, stable subcontinental mantle lithospheric keels. The lower boundary of this period would be the same as that which defines the base of the Mesoarchean, at the first appearance of definitive evidence for life within well-preserved supracrustal rocks of the Pilbara Craton. Abundant and diverse evidence for life exists throughout this period (see Van Kranendonk, 2007a, 2010b for a review). A suitable name could be the *Vaalbaran Period*, after the type areas of the Kaapvaal and Pilbara cratons, or a name that reflects the development of continental nuclei, or proto-cratonic kernels.

p1610 A younger Mesoarchean period relates to the first appearance of stable platform successions that contain evidence of microbial colonization of shallow sandy environments. A number of basins with well-preserved supergroups are preserved on the Pilbara and Kaapvaal cratons, including the famous Witwatersrand and Pongola supergroups in South Africa (3.0–2.9 Ga), and the De Grey Supergroup in Australia (3.02–2.94 Ga; Figure 16.13). Both of the supergroups in South Africa contain well-preserved evidence of terrestrial microbial communities, and candidate GSSPs could be considered near the base of these successions. Alternatively, the base of the De Grey Supergroup in Australia is well exposed and a GSSP could be erected at the conformable contact between a discontinuous basal conglomerate and overlying quartz-rich sandstone within the Gorge Creek Group, at the base of the De Grey Supergroup, dated at c. 3020 Ma (Van Kranendonk, 2004b; Van Kranendonk et al., 2007a). The advantage of a GSSP in the Gorge Creek Group is that it would include all of the stable continental successions (Dominion Group can be excluded, as it is moderately to steeply dipping, metamorphosed, and of limited extent). A candidate name for this

period could be the *Pongolan Period*, named after the >9 km thick Pongola Supergroup (Gold, 2006), in which evidence for terrestrial microbial communities is well preserved (Noffke et al., 2003, 2008). The upper boundary for this period would be a GSSP that marks the lower boundary of the Neoproterozoic Era (see below).

16.5.2.3. Neoproterozoic Era: 2780–2420 Ma s0330

A revised Neoproterozoic Era is proposed to encompass the p1615 period of abundant crustal growth and recycling, major ore-forming events (including the widespread deposition of BIF), and the widespread bloom of microbial life that occurred over the period from 2780–2420 Ma. This era is capped by the onset of major, worldwide glaciations and the change to a more oxygenated atmosphere.

The Neoproterozoic Era may be divided into two periods: p1620 a lower period (2780–2630 Ma) encompassing the time of rapid and voluminous crust formation, widespread flourishing of microbial life on newly created continental shelves, and highly negative $\delta^{13}\text{C}$ values; and a younger period that encompasses the global deposition of BIF, highly positive $\Delta^{33}\text{S}$ values, and the gradual emergence of continents. Suggested names are the *Methanian Period* for the older part of the era, to reflect the dominance of methanotrophs during this interval (Hayes' (1994) "Age of methanotrophs"), and the *Siderian Period* for the younger part of the Neoproterozoic Era, reflecting the enormous volumes of BIF deposited on many continents around the world at this time.

The lower boundary of the Neoproterozoic Era and Methanian Period should be cited at a point near the onset of p1625 widespread crust formation, which a global compilation of data indicates was at ~2780 Ma, and below the first appearance of highly negative $\delta^{13}\text{C}_{\text{kerogen}}$ values (Hayes and Waldbauer, 2006). The best preserved succession that includes both a fairly complete record of the onset of global magmatism at this time, as well as evidence of widespread microbial life and methanotrophy (e.g., Packer, 1990; Buick, 1992), is the Fortescue Group in Western Australia. Eruption of this succession of continental flood basalts commenced at 2775 ± 10 Ma (Arndt et al., 1991). A GSSP for the lower [AU14] boundary of the Neoproterozoic Era could be placed at the lower contact of the oldest flood basalt unit, the Mount Roe Basalt, which lies conformably on clastic sedimentary rocks of the Bellary Formation (Thorne and Trendall, 2001). This [AU15] locality is preferred over a site within the Ventersdorp Supergroup of South Africa, as this succession is significantly younger (c. 2700 Ma) and lies well within the middle of the period of rapid and voluminous crust formation, although protobasinal phases of the supergroup together with the Gabarone Granite Complex (2780.6 ± 1.8 Ma) and Kanye Volcanic Formation (2769.3 ± 2.3 Ma) are close in age to that of the Mount Roe Basalt (van der Westhuizen et al., 2006). [AU16]

p1630 The boundary separating the Methanian Period from the Siderian Period should correspond to the first appearance of widespread Hamersley-type BIF. The type area for this is in the
 [AU17] Hamersley Basin of Western Australia (Trendall and Blockley,
 [AU18] 1970, 2004), where the $\geq 2597 \pm 5$ Ma Marra Mamba Iron
 [AU19] Formation lies in transitional, conformable contact on the
 2629 \pm 5 Ma Jeerinah Formation of the Fortescue Group
 (Davy, 1985; Williams, 1989; Trendall et al., 1998, 2004), and
 it is possible that this contact be used as a GSSP.

s0335 16.5.3. The Archean-Proterozoic Boundary

p1635 The younger of the first-order divisions of Precambrian time
 is recognized as the boundary between the Archean and
 Proterozoic eons. In the revised, chronostratigraphic scheme
 developed herein, this boundary is placed at the major change
 between a reducing early Earth, characterized by granite-
 greenstone type crust, reducing atmosphere and oceans,
 abundant BIF, and primitive microbial life, to a cooler, more
 modern Earth characterized by the supercontinent cycle, an
 oxidized atmosphere, cooler climate, and development of
 [AU20] eukaryotic life (see also Young, 1973). This change occurred
 at ~ 2420 Ma, which is the current best estimate of the age of
 disappearance of Hamersley-type BIFs from the rock record
 and first appearance of widespread glacial deposits (see
 Sections 16.3.3.2 and 3.3.3). This boundary has the potential
 to be represented by a GSSP at a locality in Western Australia,
 where glaciogenic rocks of the lower Turee Creek Group lie
 conformably on the topmost BIF of the Hamersley Group
 (Figure 16.23). The Western Australian example appears to
 be the most suitable section, as it contains the disappearance
 of the $\Delta^{33}\text{S}$ isotopic signature characteristic of this interval
 (Williford et al., 2011), and because all other Paleoproter-
 ozoic sections are represented by an unconformable lower
 contact at the base of the first glacial deposits. The Turee
 Creek Group is also highly suitable, as it documents both the
 onset of, and coming out of, the glaciation event, based on the
 carbon isotope record and occurrence of overlying Mn-
 bearing units (Figure 16. 24; Van Kranendonk, 2010a). More
 detailed investigations of this potential GSSP boundary
 section are underway.

s0340 16.5.4. The Proterozoic Eon

p1640 A revised **Proterozoic Eon** is envisaged to extend from the
 Archean-Proterozoic boundary at ~ 2420 Ma, to the end of
 the Edicaran Period, which is marked by the GSSP at the base
 of the Phanerozoic Eon (Paleozoic Era, Cambrian Period). As
 with the current Proterozoic Eon, a revised Proterozoic Eon
 based on chronostratigraphy is envisaged to consist of three
 eras (Paleoproterozoic, Mesoproterozoic, and Neo-
 proterozoic), but the boundary ages for these divisions differs
 from their current ages and their subdivisions into periods
 would also differ from current practice (Figure 16.34).

16.5.4.1. Paleoproterozoic Era: 2420–1780 Ma s0345

A revised **Paleoproterozoic Era** would include the period of p1645
 worldwide glaciations, oxygenation of the atmosphere and
 rise of eukaryotes, the re-appearance of iron-formation in the
 rock record, and the formation of the supercontinent Nuna
 (Columbia). This era would extend from the first appearance
 of glacial deposits at ~ 2420 Ma, to the disappearance of BIF
 at ~ 1780 Ma, encompassing the breakup of late Archean
 supercontinent(s) and subsequent formation of the Nuna
 (Columbia) supercontinent.

The Paleoproterozoic Era could be divided into three p1650
 periods, based on distinct rock assemblages and isotopic
 signatures. The oldest period relates to the period of world-
 wide glaciations, global mantle slowdown, and oxygenation
 of the atmosphere, from 2420 Ma to about 2250 Ma
 (e.g. Holland, 1994, 2002; Kirschvink et al., 2000; Condie
 et al., 2009). This period could be named the *Oxygenian*
Period, as it is during this time that widespread evidence for
 an oxidizing atmosphere first appears (see Section 16.3.3.3).
 The lower boundary of this period would be marked by the
 Archean-Proterozoic GSSP, and the upper boundary by the
 defining GSSP of the subsequent period (Figure 16.34).

The next period within a revised Paleoproterozoic Era p1655
 should recognize the extraordinary Lomagundi-Jatuli $\delta^{13}\text{C}$
 isotopic excursion event, which occurred at a global scale over
 the time period from 2250–2060 Ma. This period is also
 characterized by the first Eukaryote fossils and thus two
 possible names could be the ‘*Jatulian*’ or ‘*Eukaryian*’ *Period*.
 Two immediately apparent possibilities for a basal GSSP are at
 the conformable base of the Lorrain Formation in the Huronian
 Supergroup (Canada) (Figure 16. 21), or the Ahmalahti/
 Neverskrukk formations in the Pechenga greenstone belt.

The final period of a revised Paleoproterozoic Era is p1660
 represented by the time of crustal aggregation to form
 supercontinent Columbia (Nuna), a period characterized by
 the deposition of thick, organic-rich sedimentary units to
 form shungite, and a return of iron-formations, from about
 2060–1780 Ma. A suggested name is the ‘*Columbian*
Period’. Possible GSSP localities include the base of the
 Rooiberg Group in South Africa, marking the onset of volu-
 minous magmatism associated with this period, or at the base
 of the Kolasjoki Formation in the Pechenga greenstone belt.

16.5.4.2. Mesoproterozoic Era: 1780–850 Ma s0350

A revised **Mesoproterozoic Era** would extend from ca. 1780 p1665
 Ma to ~ 850 Ma and encompass the period of environmental
 stability marked by sulfidic deep oceans, the slow diversifi-
 cation of eukaryotes, and the disassembly of supercontinent
 Nuna (Columbia) and subsequent aggregation of supercon-
 tinent Rodinia (1.3–0.9 Ga). No subdivisions of this era into
 periods have yet been recognized.

A number of possibilities exist for a basal GSSP for
 a revised Mesoproterozoic Era, including the first appearance p1670

of acritarchs, the first sulfidic ocean deposits, or perhaps at the base of successions with giant sulfide deposits. These attractive possibilities have yet to be investigated in detail.

s0355 **16.5.4.3. Neoproterozoic Era: 850–541 Ma**

p1675 A revised Neoproterozoic Era is considered to commence with the breakup of Rodinia and first appearance of evidence for environmental instability, at ca. 850 Ma. Currently, the Neoproterozoic Subcommittee of the ICS is investigating changes and possible GSSPs within the Neoproterozoic Era, and so far has established an *Ediacaran Period* (~630–541 Ma) (Figure 16.34; Knoll et al., 2004) for the youngest part of the era. This subcommittee is working towards the establishment of a *Cryogenian Period* for the time of the major Neoproterozoic glaciations (but note that the youngest, or Gaskiers glaciation, lies within the Ediacaran Period: see Chapter 18). At present, neither a type locality nor an age has been established for the base GSSP of a *Cryogenian Period*, but global correlations of $\delta^{13}\text{C}$ and Sr-isotope anomalies give hope that a GSSP may be defined in the foreseeable future (see Chapter 17).

s0360 **16.5.5. Summary of Proposed Changes and GSSPs**

p1680 In summary, the results of a global compilation of available knowledge suggest that changes in Earth history throughout the Precambrian relate to a causative, linked series of events that are recorded in the rock record and that can be used to erect a chronostratigraphic division of the Precambrian timescale (Figures 16.33 and 16.34).

p1685 Three Precambrian eons can be identified, relating to:

- o0145 **1)** the early development of the planet (Hadean Eon: 4567–4030 Ma);
- o0150 **2)** a major period of crust formation and establishment of a biosphere, characterized by a highly reducing atmosphere (Archean Eon: 4030–2420 Ma);
- o0155 **3)** a period marked by the progressive rise in atmospheric oxygen, supercontinent cyclicity, and the evolution of more complex (eukaryotic) life (Proterozoic Eon: 2420–542 Ma).

p1705 Each of these eons may be subdivided into a number of eras and periods that reflect lower-order changes in the geological record (Figure 16.34).

- u0150 \odot 4567 Ma: Start of Hadean Eon/ Chaotian Era; start of the solar system, formation of Earth; chronometric boundary, on Ca-Al-rich refractory inclusions in meteorites
- u0155 \odot 4404 Ma: end of Chaotian Era/start Jack Hillsian (Jacobian) Era; end of major accretion and Moon-forming giant impact, and first appearance of crustal material;

chronometric boundary, on oldest detrital zircon from Jack Hills greenstone belt (Yilgarn Craton, Australia)

- \odot 4030 Ma: end Hadean Eon (Jack Hillsian (Jacobian) Era)/start Archean Eon (Paleoarchean Era, Acastan Period); start of the stratigraphic record; chronometric boundary at world's oldest rock in the Acasta Gneiss (Slave Craton, Canada) u0160
- \odot ~3820 Ma: end Acastan Period/start Isuan Period; first appearance of supracrustal rocks; chronometric boundary in the Isua supracrustal belt (North Atlantic Craton, western Greenland) u0165
- 3490 Ma: end Paleoarchean Era (end Isuan Period)/start Mesoarchean Era (Vaalbaran Period); well-preserved crustal lithosphere with macroscopic evidence of fossil life; GSSP at base of stromatolitic Dresser Formation (Warrawoona Group, Pilbara Supergroup, Australia) u0170
- ~3020 Ma: end Vaalbaran Period/start Pongolan Period; first appearance of stable continental basins, containing evidence of microbial life in terrestrial environments; GSSP just above the base of the De Grey Supergroup (Pilbara Craton, Australia) u0175
- ~2780 Ma: end Mesoarchean Era (Pongolan Period)/start Neoarchean Era (Methanian Period); onset of global volcanism associated with late Archean superevent and of highly negative $\delta^{13}\text{C}_{\text{kerogen}}$ values; GSSP at base of Mount Roe Basalt (Fortescue Group, Mount Bruce Supergroup, Australia) u0180
- ~2630 Ma: end Methanian Period/start Siderian Period; first appearance of global BIFs; GSSP at base of Marra Mamba Iron Formation (Hamersley Group, Mount Bruce Supergroup, Australia) u0185
- ~2420 Ma: End Archean Eon (Neoarchean Era, Siderian Period)/start Proterozoic Eon (Paleoproterozoic Era, Oxygenian Period); first appearance of glacial deposits, rise in atmospheric oxygen, and disappearance of BIF; GSSP at base of Kazput Formation (Turee Creek Group, Mount Bruce Supergroup, Australia) u0190
- ~2250 Ma: End *Oxygenian Period*/start *Jatulian (or Eukaryian) Period*; end of glaciations and first appearance of cap carbonates with high $\delta^{13}\text{C}$ values (start of Lomagundi-Jatuli isotopic excursion), and of oxidized paleosols and redbeds; GSSP at base of Lorrain Formation (Cobalt Group, Huronian Supergroup, Canada) u0195
- 2060 Ma: End *Jatulian (or Eukaryian) Period*/start *Columbian Period*; end of Lomagundi-Jatuli isotopic excursion and first appearance of widespread global volcanism and iron-formations; GSSP at conformable base of Rooiberg Group (Bushveld Magmatic Province, Kaapvaal Craton, South Africa), or at base of the Kuetsjärvi Volcanic Formation (Pechenga greenstone belt, Fennoscandia) u0200
- ~1780 Ma: End Paleoproterozoic Era (*Columbian Period*)/start Mesoproterozoic Era; first appearance of sulfidic reducing oceanic deposits, first acritarchs, and

- u0210 successions with giant sulfide ore deposits; GSSP, unassigned
 ~850 Ma: End Mesoproterozoic Era/start Neoproterozoic Era (*Cryogenian Period*); onset of $\delta^{13}\text{C}$ anomalies?; GSSP, unassigned
- u0215 ~630 Ma: End Cryogenian Period/start Ediacaran Period; GSSP at conformable contact at base of cap carbonate overlying Marinoan glaciation
- u0220 542 Ma: End Proterozoic Eon (Neoproterozoic Era, Ediacaran Period)/start Phanerozoic Eon (Paleozoic Era, Cambrian Period).

p1785 The suggested changes proposed herein, including the four chronometric and ten chronostratigraphic (GSSP) boundaries listed above, are intended as a guide for future discussions and refinements of the Precambrian timescale, and will need to be ratified by the members of the Precambrian sub-commission and formally accepted by the ICS before they can be accepted for use by the geological community. The goal over the next few years is to develop proposals for the major eons and their boundaries and then work down through the era and period boundaries, forming working groups to decide on the best sections for GSSPs and the most suitable names to use.

p1790 It is recognized that change is never easy and consensus often difficult, but I believe that changing the Precambrian timescale will be of significant benefit to the community as a whole and will help to drive new research that will unveil new truths about the history of our planet.

s0365 ACKNOWLEDGMENTS

p1795 W. Bleeker was invited by F. Gradstein to start the project of a revised, more naturalistic Precambrian timescale for GTS2004, and I am indebted to him for instigating this process that I have inherited. Discussions with W. Bleeker and with D. Evans, A. Lepland, C. Hatton, C. O'Neill, F. Pirajno, and P. Pufahl are gratefully acknowledged. Brian Windley and Alfred Kröner provided inspiration, by example. Felix Gradstein and Gabi Ogg are thanked for their patience and support. J-F. Moyen, F. Pirajno, W. Altermann, and S.A. Wilde contributed to the making of Figure 3. C. Schroder, S. Dowsett and Gabi Ogg drafted the figures. This chapter is published with permission of the Executive Director, Geological Survey of Western Australia.

ectitle0370. REFERENCES

Abbott, D.H., Isley, A.E., 2002. The intensity, occurrence, and duration of superplume events and eras over time. *Journal of Geodynamics* 34, 265–307.

Abouchami, W., Boher, M., Michard, A., Albarede, F., 1990. A major 2.1 Ga event of mafic magmatism in West Africa: an early stage of crustal accretion. *Journal of Geophysical Research* 95, 17605–17629.

Addison, W.D., Brumpton, G.R., Vallini, D.A., McNaughton, N.J., Davis, D.W., Kissin, S.A., Fralick, P.W., Hammond, A.L., 2005. Discovery of distal ejecta from the 1850 Ma Sudbury impact event. *Geology* 33, 193–196.

Aharon, P., Liew, T.C., 1992. An assessment of the Precambrian/Cambrian transition events on the basis of carbon isotope records. In: Schidlowski, M., Golubic, S., Kimberley, M.M., McKirdy, D.M., Trudinger, P.A. (Eds.), *Early Organic Evolution: Implications for Mineral and Energy Resources*. Springer, Berlin, pp. 212–223.

Äikäs, O., 1980. Uraniferous phosphorite and apatite-bearing gneisses in the Proterozoic of Finland. *Proceedings of the International Uranium Symposium on the Pine Creek Geosyncline*, 675–681.

Äikäs, O., 1981. Proterozoic phosphorites in Finland. *IGCP 156 Newsletter* 9, 21–27.

Akhmedov, A.M., Belova, M.Y., Krupenik, V.A., Sidorova, I.N., 2000. Fungous microfossils from Paleoproterozoic black shales of the Pechenga Complex in the Kola Peninsula. *Doklady Earth Science* 373, 782–785.

Albani, A.E., Bengtson, S., Canfield, D.E., Bekker, A., Macchiarelli, R., Mazurier, A., Hammarlund, E.U., Boulvais, P., Dupuy, J.-J., Fontaine, C., Fürsich, F.T., Gauthier-Lafaye, F., Janvier, P., Javaux, E., Ossa, F.O., Pierson-Wickmann, A.-C., Riboulleau, A., Sardini, P., Vachard, D., Whitehouse, M., Meunier, A., 2010. Large colonial organisms with coordinated growth in oxygenated environments 2.1 Gyr ago. *Nature* 466, 100–104.

Albarède, F., Blichert-Toft, J., 2007. The split fate of the early Earth, Mars, Venus, and Moon. *Comptes rendus: Geoscience* 339, 917–927.

Allaart, J.H., 1976. The pre-3760 m.y. old supracrustal rocks of the Isua area, Central West Greenland, and the associated occurrence of quartz-banded ironstone. In: Windley, B.F. (Ed.), *The Early History of the Earth*. Wiley, London, pp. 177–189.

Allègre, C.J., Manhès, G., Göpel, C., 1995. The age of the Earth. *Geochimica et Cosmochimica Acta* 59, 1445–1456.

Allen, P.A., 2007. The Huqf Supergroup of Oman: basin development and context for Neoproterozoic glaciation. *Earth Science Reviews* 84, 139–185.

Allen, P.A., Etienne, J.L., 2008. Sedimentary challenge to Snowball Earth. *Nature Geoscience* 1, 817–825.

Allwood, A.C., Walter, M.R., Kamber, B.S., Marshall, C.P., Burch, I.W., 2006. Stromatolite reef from the Early Archaean era of Australia. *Nature* 441, pp. 717–717.

Allwood, A.C., Walter, M.R., Burch, I.W., Kamber, B.S., 2007. 3.43 billion-year-old stromatolite reef from the Pilbara Craton of Western Australia: Ecosystem-scale insights to early life on Earth. *Precambrian Research* 158, 198–227.

Altermann, W., Schopf, J.W., 1995. Microfossils from the Neoproterozoic Campbell Group, Griqualand West Sequence of the Transvaal Supergroup, and their paleoenvironmental and evolutionary implications. *Precambrian Research* 75, 65–90.

Altermann, W., Nelson, D.R., 1998. Sedimentation rates, basin analysis and regional correlations of three Neoproterozoic sub-basins of the Kaapvaal craton as inferred from precise U-Pb zircons ages from volcanoclastic sediments. *Sedimentary Geology* 120, 225–256.

Altermann, W., 2005. The 3.5 Ga Apex fossil assemblage – consequences of an enduring discussion. In: 14th International Conference on the Origin of Life, ISSOL'05, abstract volume, Beijing, China, pp. 136–137.

Altermann, W., Kazmierczak, J., Oren, A., Wright, D.T., 2006. Cyanobacterial calcification and its rock-building potential during 3.5 billion years of Earth history. *Geobiology* 4, 147–166.

Altermann, W., 2007a. Accretion, trapping and binding of sediment in Archean stromatolites – morphological expression of the antiquity of life. *Space Science Reviews* 135, 55–79.

- Altermann, W., 2007b. The early Earth's record of enigmatic cyanobacteria and supposed extremophilic bacteria at 3.8 to 2.5 Ga. In: Seckbach, J. (Ed.), *Algae and Cyanobacteria in Extreme Environments, Cellular Origin, Life in Extreme Habitats and Astrobiology (COLE)* 11. Springer, Berlin, pp. 759–778.
- Amelin, Y., Krot, A., Hutcheon, I.D., Ulyanov, A.A., 2002. Lead isotopic ages of chondrules and calcium-aluminium-rich inclusions. *Science* 297, 1678–1683.
- Amelin, Y., Connelly, J., Zartman, R.E., Chen, J.H., Gopel, C., Neymark, L.A., 2009. Modern U-Pb chronometry of meteorites: Advancing to higher time resolution reveals new problems. *Geochimica et Cosmochimica Acta* 73, 5212–5223.
- Amthor, J.E., Grotzinger, J.P., Schroder, S., Bowring, S.A., Ramezani, J., Martin, M.W., Matter, A., 2003. Extinction of Cloudina and Nanacalathus at the Precambrian-Cambrian boundary in Oman. *Geology* 31, 431–434.
- Anbar, A.D., Knoll, A.H., 2002. Proterozoic ocean chemistry and evolution: a bioinorganic bridge. *Science* 297, 1137–1142.
- Anbar, A.D., Duan, Y., Lyons, T.W., Arnold, G.L., Kendall, B., Creaser, R.A., Kaufman, A.J., Gordon, G.W., Scott, C., Garvin, J., Buick, R., 2007. A whiff of oxygen before the Great Oxidation Event? *Science* 317, 1903–1906.
- Anbar, A.D., Rouxel, O., 2007. Metal stable isotopes in paleoceanography. *Annual Review of Earth and Planetary Sciences* 35, 717–746.
- Anderson, J.L., Morrison, J., 2005. Ilmenite, magnetite, and peraluminous Mesoproterozoic anorogenic granites of Laurentia and Baltic. *Lithos* 80, 45–60.
- Ansdell, K.M., Heaman, L.M., Machado, N., Stern, R.A., Corrigan, D., Bickford, P., Annesley, I.R., Böhm, O., Zwanzig, H.V., Bailes, A.H., Syme, R., Corkery, T., Ashton, K.E., Maxeiner, R.O., Yeo, G.M., Delaney, G.D., 2005. Correlation chart of the evolution of the Trans-Hudson Orogen – Manitoba-Saskatchewan segment. *Canadian Journal of Earth Sciences* 42, 761.
- Appel, P.W.U., Fedo, C.M., Moorbath, S., Myers, J.S., 1998. Recognisable primary volcanic and sedimentary features in a low-strain domain of the highly deformed, oldest-known (ca. 3.7–3.8 Gyr) greenstone belt, Isua, Greenland. *Terra Nova* 10, 57–62.
- Arculus, R.J., Delano, J.W., 1980. Implications for the primitive atmosphere of the oxidation state of Earth's upper mantle. *Nature* 288, 72–74.
- Armstrong, R.A., Kamo, S., Harmer, R.E.J., 2010. Rapid emplacement of one of the world's greatest continental magmatic provinces—precise age constraints on the Bushveld Complex. *Australian Earth Sciences Convention 2010, Abstracts*, 107–108.
- Armstrong, R.L., 1981. Radiogenic isotopes: the case for crustal recycling on a near steady-state no-continental-growth Earth. *Philosophical Transactions of the Royal Society, Series A* 301, 443–472.
- Armstrong, R.L., 1991. The persistent myth of crustal growth. *Australian Journal of Earth Sciences* 38, 613–630.
- Arndt, N., Brüggmann, G.E., Lehnert, K., Chauvel, C., Chappell, B.W., 1987. Geochemistry, petrogenesis and tectonic environment of circum-Superior Belt basalts, Canada. In: Pharaoh, T.C., Beckinsale, R.D., Rickard, D. (Eds.), *Geochemistry and Mineralization of Proterozoic volcanic suites*. Geological Society of London, Special Publication, 33, pp. 133–145.
- Arndt, N., 1999. Why was flood volcanism on submerged continental platforms so common in the Precambrian? *Precambrian Research* 97, 155–164.
- Arndt, N., Bruzack, G., Reischmann, T., 2001. The oldest continental and oceanic plateaus: Geochemistry of basalts and komatiites of the Pilbara Craton, Australia. In: Ernst, R.E., Buchan, K.L. (Eds.), *Mantle Plumes: Their identification through time*. Geological Society of America, Special Paper, 352, pp. 359–387.
- Arndt, N., 2003. Komatiites, kimberlites, and boninites. *Journal of Geophysical Research* 108, ECV5, p. 11.
- Arndt, N., 2004. Crustal growth rates. In: Eriksson, P.G., Altermann, W., Nelson, D.R., Mueller, W.U., Catuneanu, O. (Eds.), *The Precambrian Earth: tempos and Events, Developments in Precambrian Geology* 12. Elsevier, Amsterdam, pp. 155–158.
- Arndt, N.T., Jenner, G.A., 1986. Crustally contaminated komatiites and basalts from Kambalda, Western Australia. *Chemical Geology* 56, 229–255.
- Arndt, N.T., Leshner, C.M., Barnes, S.J., 2008. Komatiite. Cambridge University Press, New York, p. 467.
- Arnold, G.L., Anbar, A.D., Barling, J., Lyons, T.W., 2004. Molybdenum isotope evidence for widespread anoxia in Mid-Proterozoic oceans. *Science* 304, 87–90.
- Arthur, M.A., Jenkyns, H.C., 1981. Phosphorites and Paleocyanography. *Oceanologica Acta*, SP 4, 83–96.
- Aspler, L.B., Chiarenzelli, J.R., 1998. Two Neoproterozoic supercontinents? Evidence from the Paleoproterozoic. *Sedimentary Geology* 120, 75–104.
- Ávila, C.A., Teixeira, W., Cordani, U.G., Moura, C.A.V., Pereira, M., 2010. Rhyacian (2.23–2.20 Ga) juvenile accretion in the southern Sao Francisco craton, Brazil: Geochemical and isotopic evidence from the Serinha magmatic suite, Mineiro belt. *Journal of South American Earth Sciences* 29, 464–482.
- Awramik, S.M., Buchheim, H.P., 2009. A giant, Late Archaean lake system: the Meentheena Member (Tumbiana Formation; Fortescue Group), Western Australia. *Precambrian Research* 174, 215–240.
- Babinsky, M., Chemale Jr., F., Van Schmus, W.R., 1995. The Pb/Pb age of the Minas Supergroup carbonate rocks, Quadrilátero Ferrífero, Brazil. *Precambrian Research* 72, 235–245.
- Babinsky, M., Vierra, L.C., Trindale, R.I.F., 2007. Direct dating of the Sete Lagoas cap carbonate (Bambuí Group, Brazil) and implications for the Neoproterozoic glacial events. *Terra Nova* 19, 401–406.
- Baker, A.J., Fallick, A.E., 1989a. Evidence from Lewisian limestones for isotopically heavy carbon in two thousand million year old sea water. *Nature* 337, 352–354.
- Baker, A.J., Fallick, A.E., 1989b. Heavy carbon in two-billion-year-old marbles from Lofoten-Vesterålen, Norway: Implications for the Precambrian carbon cycle. *Geochimica et Cosmochimica Acta* 53, 1111–1115.
- Baker, J., Bizzarro, M., Wittig, N., Connelly, J., Haack, H., 2005. Early planetesimal melting from an age of 4.5662 Gyr for differentiated meteorites. *Nature* 436, 1127–1131.
- Banerjee, D.M., 1971. Precambrian stromatolitic phosphorites of Udaipur, Rajasthan, India. *Geological Society of America Bulletin* 82, 2319–2329.
- Banerjee, D.M., Schidlowski, M., Arndt, J.D., 1986. Genesis of Upper Proterozoic–Cambrian phosphorite deposits of India: Isotopic inferences from carbonate fluorapatite, carbonate and organic carbon. *Precambrian Research* 33, 239–253.
- Banerjee, N.R., Simonetti, A., Furnes, H., Staudigel, H., Muehlenbachs, K., Heaman, L., Van Kranendonk, M.J., 2007. Direct dating of Archean microbial ichnofossils. *Geology* 35, 487–490.
- Bao, H., Lyons, J.R., Zhou, C., 2008. Triple oxygen isotope evidence for elevated CO₂ levels after a Neoproterozoic glaciation. *Nature* 453, 504–506.

- Barley, M.E., Groves, D.I., 1992. Supercontinent cycles and the distribution of metal deposits through time. *Geology* 20, 291–294.
- Barley, M.E., Pickard, A.L., Sylvester, P.J., 1997. Emplacement of a large igneous province as a possible cause of banded iron formation 2.45 billion years ago. *Nature* 385, 55–58.
- Barley, M.E., Krapez, B., Groves, D.I., Kerrich, R., 1998. The Late Archean bonanza: metallogenic and environmental consequences of the interaction between mantle plumes, lithospheric tectonics and global cyclicity. *Precambrian Research* 91, 65–90.
- Barley, M.E., Bekker, A., Krapez, B., 2005. Late Archean to early Paleoproterozoic global tectonics, environmental change and the rise of atmospheric oxygen. *Earth and Planetary Science Letters* 238, 156–171.
- Battistuzzi, F.U., Feijao, A., Hedges, S.B., 2004. A genomic timescale of prokaryote evolution: insights into the origin of methanogenesis, phototrophy, and the colonization of land. *BMC Evolutionary Biology* 4, 44. doi: 10.1186/14712148444.
- Bau, M., Romer, R.L., Lüders, V., Beukes, N.J., 1999. Pb, O, and C isotopes in silicified Moodraai dolomite (Transvaal Supergroup South Africa): Implications for the composition of Paleoproterozoic seawater and ‘dating’ the increase of oxygen in the Precambrian atmosphere. *Earth and Planetary Science Letters* 174, 43–57.
- Bau, M., Alexander, B., 2006. Preservation of primary REE patterns without Ce anomaly during dolomitization of Mid-Paleoproterozoic limestone and the potential re-establishment of marine anoxia immediately after the ‘Great Oxidation Event’. *South African Journal of Geology* 109, 81–86.
- Beard, B.L., Johnson, C.M., Skulan, J.L., Neelson, K.H., Cox, L., Sun, H., 2003a. Application of Fe isotopes to tracing the geochemical and biological cycling of Fe. *Chemical Geology* 195, 87–117.
- Beard, B.L., Johnson, C.M., Von Damm, K.L., Poulson, R.L., 2003b. Iron isotope constraints on Fe cycling and mass balance in oxygenated Earth oceans. *Geology* 31, 629–632.
- Bédard, J., 2006. A catalytic delamination-driven model for coupled genesis of Archaean crust and sub-continental lithospheric mantle. *Geochimica et Cosmochimica Acta* 70, 1188–1214.
- Bekasova, N.B., Dudkin, O.B., 1982. Composition and nature of concretionary phosphorites from the early Precambrian of Pechenga (Kola Peninsula). *Lithology and Mineral Resources* 16, 625–630.
- Bekker, A., Kaufman, A.J., Karhu, J.A., Beukes, N.J., Swart, Q.D., Coetzee, L.L., Eriksson, K.A., 2001. Chemostratigraphy of the Paleoproterozoic Duitschland Formation, South Africa: implications for coupled climate change and carbon cycling. *American Journal of Science* 301, 261–285.
- Bekker, A., Eriksson, K.A., 2003. A Paleoproterozoic drowned carbonate platform on the southeastern margin of the Wyoming Craton: a record of the Kenorland breakup. *Precambrian Research* 120, 327–364.
- Bekker, A., Sial, A.N., Karhu, J.A., Ferreira, V.P., Noce, C.M., Kaufman, A.J., Romano, A.W., Pimentel, M.M., 2003a. Chemostratigraphy of carbonates from the Minas Supergroup, Quadrilátero Ferrífero (Iron Quadrangle), Brazil: a stratigraphic record of Early Proterozoic atmospheric, biogeochemical and climatic change. *American Journal of Science* 303, 865–904.
- Bekker, A., Karhu, J.A., Eriksson, K.A., Kaufman, A.J., 2003b. Chemostratigraphy of Paleoproterozoic carbonate successions of the Wyoming Craton: Tectonic forcing of biogeochemical change? *Precambrian Research* 120, 279–325.
- Bekker, A., Holland, H.D., Wang, P.L., Rumble III, D., Stein, H.J., Hannah, J.L., Coetzee, L.L., Beukes, N.J., 2004. Dating the rise of atmospheric oxygen. *Nature* 427, 117–120.
- Bekker, A., Kaufman, A.J., Karhu, J.A., Eriksson, K.A., 2005. Evidence for Paleoproterozoic cap carbonates in North America. *Precambrian Research* 137, 167–206.
- Bekker, A., Karhu, J.A., Kaufman, A.J., 2006. Carbon isotope record for the onset of the Lomagundi carbon isotope excursion in the Great Lakes area, North America. *Precambrian Research* 148, 145–180.
- Bell, R.T., Thorpe, R.I., 1986. Pb-Pb isochron age of uriferous phosphorite at the base of the Menihok Formation, Labrador Trough. *Geological Survey of Canada, Paper* 86–1B, 585–589.
- Belousova, E.A., Reid, A.J., Griffin, W.L., O’Reilly, S.Y., 2009. Rejuvenation vs. Recycling of Archaean crust in the Gawler Craton, South Australia: Evidence from UPb and Hf isotopes in detrital zircon. *Lithos* 113, 570–582.
- Bengston, S., Rasmussen, B., Krapez, B., 2007. The Paleoproterozoic megascopic Stirling biota. *Paleobiology* 33, 351–381.
- Benmore, R.A., Coleman, M.L., McArthur, J.M., 1983. Origin of sedimentary francolite from its S and C isotope composition. *Nature* 302, 516–518.
- Bennett, V.C., Nutman, A.P., McCulloch, M.T., 1993. Nd isotopic evidence for transient, highly depleted mantle reservoirs in the early history of the Earth. *Earth and Planetary Science Letters* 119, 299–317.
- Bennett, V.C., Hiess, J.M., Nutman, A.P., Brandon, A.D., Wan, Y., 2010. 4.5 billion years of crust-mantle evolution from a modern isotopic perspective. *Australian Earth Sciences Convention, Program with Abstracts*, 173.
- Berman, R.G., Sanborne-Barrie, M., Rayner, N., Carson, C., Sandeman, H.A., Skulski, T., 2010. Petrological and in situ SHRIMP geochronological constraints on the tectonometamorphic evolution of the Committee Bay belt, Rae Province, Nunavut. *Precambrian Research* 181, 1–20.
- Berner, R.A., 1990. Diagenesis of phosphorus in sediments from non-upwelling areas. In: Burnett, W.C., Riggs, S.R. (Eds.), *Phosphate deposits of the world. Neogene to modern phosphorites*, vol. 3. Cambridge University Press, Cambridge, pp. 27–32.
- Berner, R.A., 1993. Weathering and its effect on atmospheric CO₂ over Phanerozoic time. *Chemical Geology* 107, 373–374.
- Berry, A.J., Danyushevsky, L.V., O’Neill, H.S.C., Newville, M., Sutton, S.R., 2008. Oxidation state of iron in komatiitic melt inclusions indicates hot Archaean mantle. *Nature* 455, 960–964.
- Bertrand-Sarfati, J., Flicoteaux, R., Moussine-Pouchkine, A., Ahmed, A.A.K., 1997. Lower Cambrian apatitic stromatolites and phosphoarenites related to the glacio-eustatic cratonic rebound (Sahara, Algeria). *Journal of Sedimentary Research* 67, 957–974.
- Beukes, N.J., Klein, C., Kaufman, A.J., Hayes, J.M., 1990. Carbonate petrography, kerogen distribution, and carbon and oxygen isotope variations in an Early Proterozoic transition from limestone to iron-formation deposition, Transvaal Supergroup, South Africa. *Economic Geology and the Bulletin of the Society of Economic Geologists* 85, 663–690.
- Beukes, N.J., Gutzmer, J., 2008. Origin and paleoenvironmental significance of major iron formations at the Archaean-Paleoproterozoic boundary. *Society of Economic Geologists Reviews* 15, 5–47.
- Bevan, A.W.R., 2007. Early solar system material, processes and chronology. In: Van Kranendonk, M.J., Smithies, R.H., Bennett, V. (Eds.), *Earth’s Oldest Rocks. Developments in Precambrian Geology*, 15. Elsevier, Amsterdam, pp. 31–59.

- Bickford, M.E., Wooden, J.J., Bauer, R.L., Schmitz, M.D., 2007. Paleoproterozoic gneisses in the Minnesota River Valley and northern Michigan, USA. In: Van Kranendonk, M.J., Smithies, R.H., Bennet, V. (Eds.), *Earth's Oldest Rocks. Developments in Precambrian Geology, 15*. Elsevier, Amsterdam, pp. 731–750.
- Bizzarro, E.A., Baker, J.A., Haack, H., Ulfbeck, D., Rosing, M., 2003. Early history of the Earth's crust-mantle system inferred from hafnium isotopes in chondrites. *Nature* 421, 931–933.
- Bjerrum, C.J., Canfield, D.E., 2002. Ocean productivity before about 1.9 Gyr ago limited by phosphorus adsorption onto iron oxides. *Nature* 417, 159–162.
- Blake, R.E., Chang, S.J., Lepland, A., 2010. Phosphate oxygen isotopic evidence for a temperate and biologically active Archean ocean. *Nature* 464, 1029–1032.
- Blake, T.S., Buick, R., Brown, S.J., Barley, M.E., 2004. Geochronology of a Late Archean flood basalt province in the Pilbara Craton, Australia: constraints on basin evolution, volcanic and sedimentary accumulation, and continental drift rates. *Precambrian Research* 133, 143–173.
- Blank, C.E., 2004. Evolutionary timing of the origins of mesophilic sulphate reduction and oxygenic photosynthesis: a phylogenomic dating approach. *Geobiology* 2, 1–20.
- Blank, C.E., Sánchez-Baracaldo, P., 2010. Timing of morphological and ecological innovations in the Cyanobacteria – a key to understanding the rise in atmospheric oxygen. *Geobiology* 8, 1–23.
- Bleeker, W., Ketchum, J.W.F., Jackson, V.A., Villeneuve, M.E., 1999. The Central Slave Basement Complex; Part I, Its structural topology and autochthonous cover. *Canadian Journal of Earth Sciences* 36, 1083–1109.
- Bleeker, W., 2003. The Late Archean record: a puzzle in ca. 35 pieces. *Lithos* 71, 99–134.
- Bleeker, W., 2004a. Towards a “natural” Precambrian time scale. In: Gradstein, F.M., Ogg, J.G., Smith, A.G. (Eds.), *A Geologic Time Scale 2004*. Cambridge University Press, Cambridge, pp. 141–146.
- Bleeker, W., 2004b. Towards a “natural” time scale for the Precambrian – A proposal. *Lethaia* 37, 1–4.
- Bleeker, W., Ernst, R., 2006. Short-lived mantle generated magmatic events and their dyke swarms: The key unlocking Earth's palaeogeographic record back to 2.6 Ga. In: Hanski, E., Mertanen, S., Rämö, T., Vuollo, J. (Eds.), *Dyke Swarms: Time Markers of Crustal Evolution*. Taylor & Francis, London, pp. 3–26.
- Blichert-Toft, J., Arndt, N.T., 1999. Hf isotope compositions of komatiites. *Earth and Planetary Science Letters* 171, 439–451.
- Blichert-Toft, J., Puchel, I.S., 2010. Depleted mantle sources through time: Evidence from Lu-Hf and Sm-Nd isotope systematic of Archean komatiites. *Earth and Planetary Science Letters* 297, 598–606.
- Blichert-Toft, J., Albarede, F., Rosing, M., Frei, R., Bridgwater, D., 1999. The Nd and Hf isotope evolution of the mantle through the Archean; results from the Isua supracrustals, West Greenland, and from the Birimian terranes of West Africa. *Geochimica et Cosmochimica Acta* 63, 3901–3914.
- Boher, M., Abouchami, W., Michard, A., Albarede, F., Arndt, N.T., 1992. Crustal growth in West Africa at 2.1 Ga. *Journal of Geophysical Research* 97, 345–369.
- Bolhar, R., Van Kranendonk, M.J., 2007. A non-marine depositional setting for the northern Fortescue Group, Pilbara Craton, inferred from trace element geochemistry of stromatolitic carbonates. *Precambrian Research* 155, 229–250.
- Borg, G., Kärner, K., Buxton, M., Armstrong, R., van der Merwe, S.W., 2003. Geology of the Skorpion Supergene Zinc deposit, southern Namibia. *Economic Geology* 98, 749–771.
- Bosak, T., Greene, S.E., Newman, D.K., 2007. A likely role for anoxygenic photosynthetic microbes in the formation of ancient stromatolites. *Geobiology* 5, 119–126.
- Bouvier, A., Wadhwa, M., 2010. The age of the Solar System redefined by the oldest Pb-Pb age of a meteoritic inclusion. *Nature Geoscience* 3, 637–641.
- Bowring, S.A., King, J.E., Housh, T.B., Isachsen, C.E., Podsek, F.A., 1989. Neodymium and lead isotope evidence for enriched early Archean crust in North America. *Nature* 340, 222–225.
- Bowring, S.A., Housh, T.B., Isachsen, C.E., 1990. The Acasta Gneisses: remnant of earth's early crust. In: Newsom, H.E., Jones, J.H. (Eds.), *Origin of the Earth*. Oxford University Press, New York, pp. 319–343.
- Bowring, S.A., Housh, T., 1995. The Earth's early evolution. *Science* 269, 1535–1540.
- Bowring, S.A., Williams, I.S., 1999. Priscoan (4.00–4.03 Ga) orthogneisses from northwestern Canada. *Contributions to Mineralogy and Petrology* 134, 3–16.
- Bowring, S.A., Grotzinger, J.P., Condon, D.J., Ramezani, J., Newall, M.J., Allen, P.A., 2007. Geochronologic constraints on the chronostratigraphic framework of the Neoproterozoic Huqf Supergroup, Sultanate of Oman. *American Journal of Science* 307, 1097–1145.
- Boyett, M., Blichert-Toft, J., Rosing, M., Storey, M., Télouk, P., Albarède, F., 2003. ¹⁴²Nd evidence for early Earth differentiation. *Earth and Planetary Science Letters* 214, 427–442.
- Brake, S.S., Hasiotis, S.T., Dannelly, H.K., Connors, K.A., 2002. Eukaryotic stromatolite builders in acid mine drainage: Implications for Precambrian iron formations and oxygenation of the atmosphere. *Geology* 30, 599–602.
- Brasier, M.D., 1980. The Lower Cambrian transgression and glauconite-phosphate facies in western Europe. *Journal of the Geological Society of London* 137, 695–703.
- Brasier, M.D., 1990. Phosphogenic events and skeletal preservation across the Precambrian-Cambrian boundary interval. In: Notholt, A.J.G., Jarvis, I. (Eds.), *Phosphorite Research and Development*. Geological Society, Special Publication, 52, pp. 289–303.
- Brasier, M.D., 1991. Nutrient flux and the evolutionary explosion across the Precambrian-Cambrian boundary interval. *Historical Biology* 5, 85–93.
- Brasier, M.D., McCarron, G., Tucker, R., Leather, J., Allen, P., Shields, G., 2000. New U-Pb zircon dates for the Neoproterozoic Ghubrah glaciation and for the top of the Huqf Supergroup, Oman. *Geology* 28, 175–178.
- Brasier, M.D., Green, O.R., Jephcoat, A.P., Kleppe, A.K., Van Kranendonk, M.J., Lindsay, J.F., Steele, A., Grassineau, N.V., 2002. Questioning the evidence for earth's oldest fossils. *Nature* 416, 76–81.
- Brasier, M.D., Green, O.R., Lindsay, J.F., McLaughlin, N., Steele, A., Stoakes, C., 2005. Critical testing for the Earth's oldest putative fossil assemblage from the ~3.5Ga Apex chert, Chinaman Creek, Western Australia. *Precambrian Research* 140, 55–102.
- Bremner, J.M., Rogers, J., 1990. Phosphorite deposits on the Namibian continental shelf. In: Burnett, W.C., Riggs, S.R. (Eds.), *Phosphate deposits of the world. Neogene to modern phosphorites*, vol. 3. Cambridge University Press, Cambridge, pp. 143–152.
- Brennecka, G.A., Weyer, S., Wadhwa, M., Janney, P.E., Zipfel, J., Anbar, A.D., 2010. ²³⁸U/²³⁵U variations in meteorites: Extant 247Cm and implications for Pb-Pb dating. *Science* 327, 449–451.

- Breuer, D., Spohn, T., 1995. Possible flush instability in mantle convection at the Archean-Proterozoic boundary. *Nature* 378, 606–610.
- Bridgwater, D., McGregor, V.R., Myers, J.S., 1974. A horizontal tectonic regime in the Archaean of Greenland and its implications for early crustal thickening. *Precambrian Research* 1, 179–197.
- Bridgwater, D., McGregor, V.R., 1974. Field work on the very early Precambrian rocks of the Isua area, southern West Greenland. *Rapport Grønlands Geologiske Undersøgelse* 65, 49–54.
- Brocks, J.J., Logan, G.A., Buick, R., Summons, R.E., 1999. Archean molecular fossils and the early rise of eukaryotes. *Science* 285, 1033–1036.
- Brocks, J.J., Buick, R., Summons, R.E., Logan, G.A., 2003. A reconstruction of Archean biological diversity based on molecular fossils from the 2.78 to 2.45 billion-year-old Mount Bruce Supergroup, Hamersley Basin, Western Australia. *Geochimica et Cosmochimica Acta* 22, 4321–4335.
- Broecker, W.S., Peng, T.H., 1982. *Tracers in the Sea*. Eldigio Press, New York, p. 690.
- Buchan, K.L., Halls, H.C., Mortensen, J.K., 1996. Paleomagnetism, U-Pb geochronology, and geochemistry of Marathon dykes, Superior Province, and comparison with the Fort Frances swarm. *Canadian Journal of Earth Sciences* 33, 1583–1595.
- Buchanan, P.C., Reimold, W.U., Koeberl, C., Kruger, F.J., 2002. Geochemistry of intermediate to siliceous rocks of the Rooiberg Group, Bushveld Magmatic Province, South Africa. *Contributions to Mineralogy and Petrology* 144, 131–143.
- Buchanan, P.C., 2006. The Rooiberg Group. In: Johnson, M.R., Anhaeusser, C.R., Thomas, R.J. (Eds.), *The Geology of South Africa*. Geological Society of South Africa/Council for Geoscience, Johannesburg/Pretoria, pp. 283–289.
- Buggisch, W., Joachimski, M.M., Lehnert, O., Bergstrom, S.M., Repetski, J.E., Webers, G.F., 2010. Did intense volcanism trigger the Ordovician icehouse? *Geology* 38, 327–330.
- Buick, I.S., Uken, R., Gibson, R.L., Wallmach, T., 1998. High- $\delta^{13}\text{C}$ Paleoproterozoic carbonates from the Transvaal Supergroup, South Africa. *Geology* 26, 875–878.
- Buick, R., Dunlop, J.S.R., 1990. Evaporitic sediments of Early Archaean age from the Warrawoona Group, North Pole, Western Australia. *Sedimentology* 37, 247–277.
- Buick, R., 1992. The antiquity of oxygenic photosynthesis: evidence from stromatolites in sulfate deficient lakes. *Nature* 255, 74–77.
- Buick, R., 2007. Did the Proterozoic ‘Canfield Ocean’ cause a laughing gas greenhouse? *Geobiology* 5, 97–100.
- Buick, R., 2008. When did oxygenic photosynthesis evolve? *Philosophical Transactions of the Royal Society B* 363, 2731–2743.
- Burkhardt, C., Kleine, T., Bourdon, B., Palme, H., Zipfel, J., Freidich, J.M., Ebel, D.S., 2008. Hf-W mineral isochron for Ca, Al-rich inclusions: Age of the solar system and the timing of core formation in planetesimals. *Geochimica et Cosmochimica Acta* 72, 6177–6197.
- Bushinskii, G.I., 1966. The origin of marine phosphorites. *Lithology and Mineral Resources* 31, 292–311.
- Butterfield, N.J., 2000. *Bangiomorpha pubescens* n. gen., n. sp. implications for the evolution of sex, multicellularity and the Mesoproterozoic/Neoproterozoic radiation of eukaryotes. *Paleobiology* 26, 386–404.
- Byerly, G.R., Kröner, A., Lowe, D.R., Todt, W., Walsh, M.M., 1996. Prolonged magmatism and time constraints for sediments deposition in the early Archaean Barberton greenstone belt: evidence from the Upper Onverwacht and Fig Tree Groups. *Precambrian Research* 78, 125–138.
- Calvert, A.J., Sawyer, E.W., Davis, W.J., Ludden, J.N., 1995. Archaean subduction inferred from seismic images of a mantle suture in the Superior Province. *Nature* 375, 670–674.
- Cameron, E.M., 1982. Sulfate and sulfate reduction in early Precambrian oceans. *Nature* 296, 145–148.
- Cameron, E.M., 1983. Evidence from early Proterozoic anhydrite for sulphur isotopic partitioning in Precambrian oceans. *Nature* 304, 54–56.
- Campbell, I.H., Allen, C., 2008. Formation of supercontinents linked to increases in atmospheric oxygen. *Nature Geoscience* 1, 554–558.
- Canfield, D., Rosing, M.T., Bjerrum, C., 2006. Early anaerobic metabolisms. *Philosophical Transactions of the Royal Society, Series B* 361, 1819–1836.
- Canfield, D.E., 1998. A new model for Proterozoic ocean chemistry. *Nature* 396, 450–453.
- Canfield, D.E., Habicht, K.S., Thamdrup, B., 2000. The Archean sulfur cycle and the early history of atmospheric oxygen. *Science* 288, 658–661.
- Canfield, D.E., 2001. Biogeochemistry of sulfur isotopes. *Reviews of Mineralogy and Geochemistry* 43, 607–636.
- Canfield, D.E., 2004. The evolution of the Earth surface sulphur reservoir. *American Journal of Science* 304, 839–861.
- Canfield, D.E., 2005. The early history of atmospheric oxygen: homage to Robert M. Garrels. *Annual Review of Earth and Planetary Science* 33, 1–36.
- Canfield, D.E., Poulton, S.W., Narbonne, G.M., 2007. Late-Neoproterozoic Deep-Ocean oxygenation and the rise of animal life. *Science* 315, 92–95.
- Canfield, D.E., Poulton, S.W., Knoll, A.H., Narbonne, G.M., Ross, G., Goldberg, T., Strauss, H., 2008. Ferruginous conditions dominated later Neoproterozoic deep-water chemistry. *Science* 321, 949–952.
- Cannon, W.F., Klasner, J.S., 1976. Phosphorite and other apatite-bearing sedimentary rocks in the Precambrian of northern Michigan. *United States Geological Survey, Circular* 476, 1–6.
- Cannon, W.F., Schulz, K.J., Horton Jr., J.W., Kring, D.A., 2010. The Sudbury impact layer in the Paleoproterozoic iron ranges of northern Michigan, USA. *GSA Bulletin* 122, 50–75.
- Canup, R.M., 2004. Simulations of a late lunar-forming impact. *Icarus* 168, 433–456.
- Canup, R.M., 2008. Accretion of the Earth. *Philosophical Transactions of the Royal Society, Series A* 366, 4061–4075.
- Capdevila, R., Arndt, N.T., Letendre, J., Sauvage, J.-F., 1999. Diamonds in volcaniclastic komatiite from French Guiana. *Nature* 399, 456–458.
- Card, K.D., 1990. A review of the Superior Province of the Canadian Shield, a product of Archean accretion. *Precambrian Research* 48, 99–156.
- Carlson, R.W., Lugmair, G.W., 2000. Timescales of planetesimal formation and differentiation based on extinct and extant radioisotopes. In: Canup, R., Righter, K. (Eds.), *Origin of the Earth and Moon*. Arizona University Press, Tucson, pp. 25–44.
- Caro, G., Bourdon, B., Birk, J.-L., Moorbath, S., 2006. High-precision $^{142}\text{Nd}/^{144}\text{Nd}$ measurements in terrestrial rocks: Constraints on the early differentiation of the Earth’s mantle. *Geochimica et Cosmochimica Acta* 70, 164–191.
- Caro, G., Bourdon, B., Haliday, A.N., Quitté, G., 2008. Super-chondritic Sm/Nd ratios in Mars, the Earth and the Moon. *Nature* 452, 336–339.
- Catling, D.C., Zahnle, K.J., McKay, C.P., 2001. Biogenic Methane, Hydrogen Escape, and the Irreversible Oxidation of Early Earth. *Science* 293, 839–843.

- Cavosie, A.J., Wilde, S.A., Valley, J.W., 2005. A lower age limit for the Archean based on $\delta^{18}\text{O}$ of detrital zircons. *Geochimica et Cosmochimica Acta* 69, A391.
- Cavosie, A.J., Valley, J.W., Wilde, S.A., 2007. The oldest terrestrial mineral record: a review of 4400 to 4000 Ma detrital zircons from Jack Hills, Western Australia. In: Van Kranendonk, M.J., Smithies, R.H., Bennet, V. (Eds.), *Earth's Oldest Rocks. Developments in Precambrian Geology, 15*. Elsevier, Amsterdam, pp. 91–112.
- Cawood, P.A., Tyler, I.M., 2004. Assembling and reactivating the Proterozoic Capricorn Orogen: Lithotectonic elements, orogenies, and significance. *Precambrian Research* 128, 201–218.
- Cawthorne, R.G., Eales, H.V., Walraven, F., Uken, R., Watkeys, M.K., 2006. The Bushveld Complex. In: Johnson, M.R., Anhaeusser, C.R., Thomas, R.J. (Eds.), *The Geology of South Africa. Geological Society of South Africa/Council for Geoscience, Johannesburg/Pretoria*, pp. 261–281.
- Champion, D.C., Smithies, R.H., 2007. Geochemistry of Paleoproterozoic granites of the East Pilbara Terrane, Pilbara Craton, Western Australia: implications for the growth of a Paleoproterozoic protocontinent. In: Van Kranendonk, M.J., Smithies, R.H., Bennet, V. (Eds.), *Earth's Oldest Rocks. Developments in Precambrian Geology, 15*. Elsevier, Amsterdam, pp. 369–410.
- Chardon, D., Peucat, J.-J., Jayananda, M., Choukroune, P., Fanning, M., 2002. Archean granite-greenstone tectonics at Kolar (South India): Interplay of diapirism and bulk inhomogeneous contraction during juvenile magmatic accretion. *Tectonics* 21 (1016), 17.
- Chardon, D.H., Choukroune, P., Jayananda, M., 1996. Strain patterns, decollement and incipient sagducted greenstone terrains in the Archean Dharwar craton (South India). *Journal of Structural Geology* 18, 991–1004.
- Chardon, D.H., Choukroune, P., Jayananda, M., 1998. Sinking of the Dharwar Basin (South India); implications for Archean tectonics. *Precambrian Research* 91, 15–39.
- Chauhan, D.S., 1979. Phosphate-bearing stromatolites of the Precambrian Aravalli phosphorite deposits of the Udaipur region, their environmental significance and genesis of phosphorite. *Precambrian Research* 8, 95–126.
- Chavagnac, V., 2004. A geochemical and Nd isotopic study of Barberton komatiites (South Africa): implication for the Archean mantle. *Lithos* 75, 253–281.
- Claoué-Long, J.C., Compston, W., Cowden, A., 1988. The age of Kambalda greenstones resolved by ion-microprobe: implications for Archean dating methods. *Earth and Planetary Science Letters* 89, 239–259.
- Cloud, P., 1972. A working model of the primitive earth. *American Journal of Science* 272, 537–548.
- Cloud, P., 1973. Paleogeological significance of iron formation. *Economic Geology* 68, 1135–1143.
- Cloud, P., 1987. Trends, transitions, and events in cryptozoic history and their calibration: apropos recommendations by the submission on Precambrian stratigraphy. *Precambrian Research* 37, 257–264.
- Coetsee, L.L., Beukes, N.J., Gutzmer, J., 2006. Links of organic carbon cycling and burial to depositional depth gradients and establishment of a snowball Earth at 2.3 Ga: Evidence from the Timeball Hill Formation, Transvaal Supergroup, South Africa. *South African Journal of Geology* 109, 109–122.
- Cohen, B.A., Swindle, T.D., King, D.A., 2000. Support for the lunar cataclysm hypothesis from lunar meteorite impact melt ages. *Science* 290, 1754–1756.
- Coleman, A.P., 1908. The lower Huronian ice age. *Journal of Geology* 16, 149–158.
- Collerson, K.D., Kamber, B.S., 1999. Evolution of the continents and atmosphere inferred from Th-U-Nb systematics of the depleted mantle. *Science* 283, 1519–1522.
- Coltice, N., Phillips, B.R., Bertrand, H., Ricard, Y., Rey, P., 2007. Global warming of the mantle at the origin of flood basalts over supercontinents. *Geology* 35, 391–394.
- Coltice, N., Marty, B., Yokochi, R., 2009. Xenon isotope constraints on the thermal evolution of the early Earth. *Chemical Geology* 266, 4–9.
- Compston, W., Williams, I.S., Meyer, C., 1984. U-Pb geochronology of zircons from Lunar breccia 73217 using a sensitive high mass-resolution ion microprobe. *Journal of Geophysical Research* 89, B525–B534.
- Compston, W., Pidgeon, R.T., 1986. Jack Hills, evidence of more very old detrital zircons in Western Australia. *Nature* 321, 766–769.
- Condie, K.C., Wronkiewicz, D.J., 1990. The Cr/Th ratio in Precambrian pelites from the Kaapvaal Craton as an index of craton evolution. *Earth and Planetary Science Letters* 97, 256–267.
- Condie, K.C., 1993. Chemical composition and evolution of the upper continental crust: contrasting results from surface samples and shales. *Chemical Geology* 104, 1–37.
- Condie, K.C., 1995. Episodic ages of greenstones: a key to mantle dynamics. *Geophysical Research Letters* 22, 2215–2218.
- Condie, K.C., 1998. Episodic continental growth and supercontinents: a mantle avalanche connection? *Earth and Planetary Science Letters* 163, 97–108.
- Condie, K.C., 2000. Episodic growth models: Afterthoughts and extensions. *Tectonophysics* 332, 153–162.
- Condie, K.C., DesMarais, D.J., Abbott, D., 2001. Precambrian superplumes and supercontinents: a record in black shales, carbon isotopes, and paleoclimates? *Precambrian Research* 106, 239–260.
- Condie, K.C., 2004. Supercontinents and superplume events: distinguishing signals in the geologic record. *Physics of the Earth and Planetary Interiors* 146, 319.
- Condie, K.C., 2008. Did the character of subduction change at the end of the Archean? Constraints from convergent-margin granitoids. *Geology* 36, 611–614.
- Condie, K.C., O'Neill, C., Aster, R.C., 2009. Evidence and implications for a widespread magmatic shutdown for 250 My on Earth. *Earth and Planetary Science Letters* 282, 294–298.
- Condon, D., Zhu, M., Bowring, S., Jin, Y., Wang, W., Yang, A., 2005. U-Pb ages from the Doushantou Formation, China. *Science* 308, 95–98.
- Coogan, L.A., Cullen, J.T., 2009. Did natural reactors form as a consequence of the emergence of oxygenic photosynthesis during the Archean? *GSA Today* 19, 4–10.
- Cook, P.J., Shergold, J.H., 1984. Phosphorus, phosphorites and skeletal evolution at the Precambrian-Cambrian boundary. *Nature* 308, 231–236.
- Cook, P.J., Shergold, J.H., 1986. Proterozoic and Cambrian phosphorites – an introduction. In: Cook, P.J., Shergold, J.H. (Eds.), *Phosphate Deposits of the World. vol. 1, Proterozoic and Cambrian Phosphorites*. Cambridge University Press, Cambridge, pp. 1–8.
- Corfu, F., Andrews, A.J., 1986. A U-Pb age for mineralized Nipissing diabase, Gowanda, Ontario. *Canadian Journal of Earth Sciences* 23, 107–109.
- Cornell, D.H., Schutte, S.S., Eglinton, B.L., 1996. The Ongeluk basaltic andesite formation in Griqualand West, South Africa: submarine alteration in a 2222 Ma Proterozoic sea. *Precambrian Research* 79, 101–123.

- Cowan, C.A., Fox, D.L., Runkel, A.C., Saltzman, M.R., 2005. Terrestrial-marine carbon coupling in ~500 m.y. old phosphatic brachiopods. *Geology* 33, 661–664.
- Croal, L.R., Johnson, C.M., Beard, B.L., Newman, D.K., 2004. Iron isotope fractionation by Fe(II)-oxidizing photoautotrophic bacteria. *Geochimica et Cosmochimica Acta* 68, 1227–1242.
- Croal, L.R., Jiao, Y., Kappler, A., Newman, D.K., 2008. Phototrophic Fe(II) oxidation in an atmosphere of H₂: implications for Archean banded iron formations. *Geobiology* 7, 21–24.
- Crowe, S.A., Jones, C., Katsev, S., Magen, C., O'Neill, A.H., Sturm, A., Canfield, D.E., Haffner, G.D., Mucci, A., Sundby, B., Fowle, D.A., 2008. Photoferrotrophs thrive in an Archean Ocean analogue. *Proceedings of the National Academy of Science* 105, 15938–15943.
- Crowley, J.L., 2003. U-Pb geochronology of 3810–3630 Ma granitoid rocks south of the Isua greenstone belt, southern West Greenland. *Precambrian Research* 126, 235–257.
- Crowley, J.L., Myers, J.S., Sylvester, P.J., Cox, R.A., 2005. Detrital zircons from the Jack Hills and Mount Narryer, Western Australia: Evidence for diverse >4.0 Ga source rocks. *Journal of Geology* 113, 239–263.
- Cruden, A.R., Nasser, M.H.B., Pysklywec, R., 2006. Surface topography and internal strain variation in wide hot orogens from three-dimensional analogue and two-dimensional numerical vice models. In: Butter, S.J.H., Schreurs, G. (Eds.), *Analogue and numerical modelling of crustal-scale processes*. Geological Society of London, Special Publications, 253, pp. 79–104.
- Czaja, A.D., Johnson, C.M., Beard, B.L., Van Kranendonk, M.J., 2010a. Iron isotope evidence for an abiological origin of a BIF from the Yilgarn craton. In: Tyler, I.M., Knox-Robinson, C.M. (Eds.), *Fifth International Archean Symposium Abstracts*. Geological Survey of Western Australia, Record, 2010/8, pp. 349–351.
- Czaja, A.D., Johnson, C.M., Beard, B.L., Eigenbrode, J.L., Freeman, K.H., Yamaguchi, K.E., 2010b. Iron and carbon isotope evidence for ecosystem and environmental diversity in the ~2.7 to 2.5 Ga Hamersley Province, Western Australia. *Earth and Planetary Science Letters* 292, 170–180.
- Dall'Agnol, R., Teixeira, N.P., Rämö, O.T., Moura, C.A.V., Macambira, M.J.B., de Oliveira, D.C., 2005. Petrogenesis of the Paleoproterozoic rapakivi A-type granites of the Archean Carajás metallogenic province, Brazil. *Lithos* 80, 101–129.
- Dardenne, M.A., Trompette, R., Magalhaes, L.F., Soares, L.A., 1986. Proterozoic and Cambrian phosphorites – regional review: Brazil. In: Cook, P.J., Shergold, J.H. (Eds.), *Phosphate Deposits of the World*. vol. 1, Proterozoic and Cambrian Phosphorites. Cambridge University Press, Cambridge, pp. 116–131.
- Dauphas, N., van Zuilen, M., Wadhwa, M., Davis, A.M., Marty, B., Janney, P.E., 2004. Clues from Fe isotope variations on the origin of Early Archean BIFs from Greenland. *Science* 306, 2077–2080.
- Dauphas, N., Rouxel, O., 2006. Mass spectrometry and natural variations in iron isotopes. *Mass Spectrometry Reviews* 25, 515–550.
- Dauphas, N., Cates, N.L., Mojzsis, S.J., Busigny, V., 2007. Identification of chemical sedimentary protoliths using iron isotopes in the N3750 Ma Nuvvuagittuq supracrustal belt, Canada. *Earth and Planetary Science Letters* 254, 358–376.
- David, J., Godin, L., Stevenson, R., O'Neil, J., Francis, D., 2009. U-Pb ages (3.8–2.7 Ga) and Nd isotope data from the newly identified Eoarchean Nuvvuagittuq supracrustal belt, Superior Craton, Canada. *GSA Bulletin* 121, 150–163.
- David, L.A., Alm, E.J., 2011. Rapid evolutionary innovation during an Archean genetic expansion. *Nature* 469, 93–96.
- Davies, G.F., 1995. Punctuated tectonic evolution of the Earth. *Earth and Planetary Science Letters* 36, 363–380.
- Davis, D.W., 1998. Speculations on the formation and crustal structure of the Superior province from U-Pb geochronology. In: Harrap, R.M., Helmstaedt, H. (Eds.), *Western Superior Transect Fourth Annual Workshop*. Lithoprobe Report, 65, pp. 21–28.
- Davis, D.W., Williams, I.S., Krogh, T.E., 2003. Historical development of zircon geochronology. *Reviews in Mineralogy and Geochemistry* 53, 143–181.
- Davis, W.J., Jones, A.G., Bleeker, W., Grütter, H., 2003. Lithosphere development in the Slave craton: a linked crustal and mantle perspective. *Lithos* 71, 575–589.
- Delano, J.W., 2001. Redox history of the Earth's interior since ~3900 Ma: Implications for prebiotic molecules. *Origins of Life and Evolution of Biospheres* 31, 311–341.
- Dellwig, O., Leipe, T., März, C., Glockzin, M., Pollehne, F., Schnetger, B., Yakushev, E.V., Böttcher, M., Brumsack, H.-J., 2010. A new particulate Mn-Fe-P-shuttle at the redoxcline of anoxic basins. *Geochimica et Cosmochimica Acta* 74, 7100–7115.
- Des Marais, D.J., Strauss, H., Summons, R.E., Hayes, J.M., 1992. Carbon isotope evidence for the stepwise oxidation of the Proterozoic environment. *Nature* 359, 605–609.
- Des Marais, D.J., 2000. When did photosynthesis emerge on Earth? *Science* 289, 1703–1705.
- Deynoux, M., Affaton, P., Trompette, R., Villeneuve, M., 2006. Pan-African tectonic evolution and glacial events registered in Neoproterozoic to Cambrian cratonic and foreland basins of West Africa. *Journal of African Earth Science* 46, 397–426.
- Domagal-Goldman, S.D., Kasting, J.F., Johnston, D.T., Farquhar, J., 2008. Organic haze, glaciations and multiple sulphur isotopes in the Mid-Archean Era. *Earth and Planetary Science Letters* 269, 29–40.
- Donnelly, T.H., Shergold, J.H., Southgate, P.N., Barnes, C.J., 1990. Events leading to global phosphogenesis around the Proterozoic/Cambrian boundary. *Phosphorite Research and Development*. Geological Society Special Publication 52, 273–287.
- Dorland, H.C., 2004. Provenance ages and timing of sedimentation of selected Neoarchean and Paleoproterozoic successions of the Kaapvaal craton. Unpublished PhD thesis. Rand Afrikaans University, Johannesburg, p. 326.
- Dos Santos, T.J.S., Fetter, A.H., Randall van Schmus, W., Hackspacher, P.C., 2009. Evidence for 2.35–2.30 Ga juvenile crustal growth in the northwest Borborema Province, NE Brazil. In: Reddy, S.M., Mazumder, R., Evans, D.A.D., Collins, A.S. (Eds.), *Paleoproterozoic supercontinents and Global Evolution*. Geological Society, London, Special Publications, 323, pp. 271–282.
- Du, R., Tian, L., Li, H., 1986. Discovery of megafossils in the Gaoyushang Formation of the Changchenian System, Jixian. *Acta Geological Sinica* 2, 115–120.
- Duck, L.J., Glikson, M., Golding, S.D., Webb, R.E., 2007. Microbial remains and other carbonaceous forms from the 3.24 Ga Sulphur Springs black smoker deposit, Western Australia. *Precambrian Research* 154, 205–220.
- Dutkiewicz, A., George, S.C., Mossman, D., Ridley, J., Volk, H., 2007. Oil and its biomarkers associated with the Paleoproterozoic Oklo natural fission reactors, Gabon. *Chemical Geology* 244, 130–154.

- Eigenbrode, J.L., Freeman, K.H., Summons, R.E., 2008. Methylhopane biomarker hydrocarbons in Hamersley Province sediments provide evidence for Neoproterozoic aerobicity. *Earth and Planetary Science Letters* 273, 323–331.
- El Tabakh, M., Grey, K., Pirajno, F., Schreiber, B.C., 1999. Pseudomorphs after evaporitic minerals interbedded with 2.2 Ga stromatolites of the Yerrida basin, Western Australia: origin and significance. *Geology* 27, 871–874.
- Elie, M., Nogueira, A.C.R., Nédélec, A., Trindade, R.I.F., Kenig, F., 2007. A red algal bloom in the aftermath of the Marinoan Snowball Earth. *Terra Nova* 19, 303–308.
- Embleton, B.J., Williams, G.E., 1986. Low paleolatitude of deposition for late Precambrian periglacial varvites in South Australia: implications for palaeoclimatology. *Earth and Planetary Science Letters* 79, 419–430.
- Emslie, R.F., 1991. Granitoids of rapakivi granite-anorthosite and related associations. *Precambrian Research* 51, 173–192.
- Emslie, R.F., Hamilton, M.A., Thériault, R.J., 1994. Petrogenesis of a Mid-Proterozoic anorthosite-mangerite-charnockite-granite (AMCG) complex: Isotopic and chemical evidence from the Nain Plutonic Suite. *The Journal of Geology* 102, 539–558.
- Eriksson, K.A., Simpson, E.L., Master, S., Henry, G., 2005. Neoproterozoic (c. 2.58 Ga) halite casts: implications for palaeoceanic chemistry. *Journal of the Geological Society of London* 162, 789–799.
- Eriksson, P.G., Cheney, E.S., 1992. Evidence for the transition to an oxygen-rich atmosphere during the evolution of red beds in the Lower Proterozoic sequences of southern Africa. *Precambrian Research* 52, 257–269.
- Eriksson, P.G., Mazumder, R., Sarkar, S., Bose, P.K., Altermann, W., van der Merwe, R., 1999. The 2.7–2.0 Ga volcano-sedimentary record of Africa, India and Australia: evidence for global and local changes in sea level and continental freeboard. *Precambrian Research* 97, 269–302.
- Eriksson, P.G., Mazumder, R., Catuneanu, O., Bumby, A.J., Ilondo, B.O., 2006. Precambrian continental freeboard and geological evolution: a time perspective. *Earth-Science Reviews* 79, 165–204.
- Eriksson, P.G., Altermann, W., Hartzer, F.J., 2007. The Transvaal Supergroup and its precursors. In: Johnson, M.R., Annhaeusser, C.R., Thomas, R.J. (Eds.), *The Geology of South Africa*. Geological Society of South Africa & Council of Geoscience, Johannesburg & Pretoria, pp. 237–260.
- Ernst, R.E., Buchan, K.L., 2001. Large mafic magmatic events through time and links to mantle plume heads. In: Ernst, R.E., Buchan, K.L. (Eds.), *Mantle plumes: Their identification through time*. Geological Society of America, Special Paper, 352, pp. 483–575.
- Ernst, W.G., 2009. Archean plate tectonics, rise of Proterozoic supercontinentality and onset of regional episodic stagnant-lid behaviour. *Gondwana Research* 15, 243–253.
- Etienne, J.L., Allen, P.A., Rieu, R., LeGuerroue, E., 2008. Neoproterozoic glaciated basins: a critical review of the Snowball Earth hypothesis by comparison with Phanerozoic glaciations. In: Hambrey, M.J., Christofferson, P., Glasser, N.F., Hubbard, B. (Eds.), *Glacial sedimentary processes and products*. International Association of Sedimentologists, Special Publication, 39, pp. 343–399.
- Evans, D.A.D., Beukes, N.J., Kirschvink, J.L., 1997. Low-latitude glaciation in the Paleoproterozoic era. *Nature* 386, 262–266.
- Evans, D.A.D., 2000. Stratigraphic, geochronological, and paleomagnetic constraints upon the Neoproterozoic climatic paradox. *American Journal of Science* 300, 347–433.
- Evans, D.A.D., Gutzmer, J., Beukes, N.J., Kirschvink, J.L., 2001. Paleomagnetic constraints on ages of mineralization in the Kalahari Manganese Field, South Africa. *Economic Geology* 96, 621–631.
- Evans, D.A.D., Sircombe, K., Wingate, M.T.D., Doyle, M., McCarthy, M., Pidgeon, R.T., van Niekerk, H.S., 2003. Revised geochronology of magmatism in the western Capricorn Orogen at 1805–1785 Ma: Diachroneity of the Pilbara-Yilgarn collision. *Australian Journal of Earth Sciences* 50, 853–864.
- Eyles, N., 2008. Glacio-epochs and the supercontinent cycle after ~3.0 Ga: tectonic boundary conditions for glaciation. *Palaeogeography, Palaeoclimatology, Palaeoecology* 285, 89–129.
- Fallick, A.E., Melezhik, V.A., Simonson, B., 2008. The ancient anoxic biosphere was not as we know it. In: Dobretsov, N., Kolchanov, N., Rozanov, A., Zavarzin, G. (Eds.), *Biosphere Origin and Evolution*. Springer Science+Business Media, pp. 169–188.
- Fanning, C.M., Link, P.K., 2004. U-Pb SHRIMP ages of Neoproterozoic (Sturtian) glaciogenic Pocatello Formation, southeastern Idaho. *Geology* 32, 881–884.
- Fanning, C.M., 2006. Constraints on the timing of the Sturtian Glaciation from southern Australia; ie for the true Sturtian. *Geological Society of America Annual Meeting Paper* 42–46.
- Farquhar, J., Bao, H.M., Thieme, M., 2000. Atmospheric influence of Earth's earliest sulfur cycle. *Science* 289, 756–758.
- Farquhar, J., Wing, B.A., 2003. Multiple sulphur isotopes and the evolution of the atmosphere. *Earth and Planetary Science Letters* 213, 1–13.
- Farquhar, J., Peters, M., Johnston, D.T., Strauss, H., Masterson, A., Wiechert, U., Kaufman, A.J., 2007. Isotopic evidence for Mesoarchean anoxia and changing sulfur chemistry. *Nature* 449, 706–709.
- Fedo, C.M., Young, G.M., Nesbitt, H.W., 1997. Paleoclimatic control on the composition of the Paleoproterozoic Serpent Formation, Huronian Supergroup, Canada: a greenhouse to icehouse transition. *Precambrian Research* 86, 201–223.
- Fedonkin, M.A., 1996. Geobiological trends and events in the Precambrian biosphere. In: Walliser, O.H. (Ed.), *Global events and event stratigraphy*. Springer, Berlin, pp. 89–112.
- Fedonkin, M.A., Yochelson, E.L., 2002. Middle Proterozoic (1.5 Ga) *Horodyskia moniliformis* Yochelson and Fedonkin, the oldest known tissue-grade colonial eukaryote. *Smithsonian Contributions to Paleobiology* 94, 1–29.
- Feybesse, J.-L., Billa, M., Guerrot, C., Duguey, E., Lescuyer, J.-L., Milesi, J.-P., Bouchot, V., 2006. The Paleoproterozoic Ghanian province: Geodynamic model and ore controls, including regional stress modelling. *Precambrian Research* 149, 149–196.
- Fike, D.A., Grotzinger, J.P., Pratt, L.M., Summons, R.E., 2006. Oxidation of the Ediacaran Ocean. *Nature* 444, 744–747.
- Fike, D.A., Grotzinger, J.P., 2008. A paired sulfate-pyrite $\delta^{34}\text{S}$ approach to understanding the evolution of the Ediacaran-Cambrian sulfur cycle. *Geochimica et Cosmochimica Acta* 72, 2636–2648.
- Flament, N., Coltice, N., Rey, P.F., 2008. A case for late-Archaean continental emergence from thermal evolution models and hypsometry. *Earth and Planetary Science Letters* 275, 326–336.
- Flicoteaux, R., Trompette, R., 1998. Cratonic and foreland Early Cambrian phosphorites of West Africa: palaeoceanographical and climatic contexts. *Palaeogeography, Palaeoclimatology, Palaeoecology* 139, 107–120.
- Föllmi, K.B., 1995. 160 m.y. record of marine sedimentary phosphorus burial: coupling of climate and continental weathering under greenhouse and icehouse conditions. *Geology* 23, 859–862.

- Foriel, J., Philippot, P., Rey, P., Somogyi, A., Banks, D., Menez, B., 2004. Biological control of Cl/Br and low sulfate concentration in a 3.5 Gyr-old seawater from North Pole, Western Australia. *Earth and Planetary Science Letters* 228, 451–463.
- Frei, R., Dahl, P.S., Duke, E.F., Frei, K.M., Hansen, T.R., Frandsson, M.M., Jensen, L.A., 2008. Trace element and isotopic characterization of Neoproterozoic iron formations in the Black Hills (South Dakota, USA): Assessment of chemical change during 2.9–1.9 Ga deposition bracketing the 2.4–2.2 Ga first rise of atmospheric oxygen. *Precambrian Research* 162, 441–474.
- Frei, R., Gaucher, C., Poulton, S.W., Canfield, D.E., 2009. Fluctuations in Precambrian atmospheric oxygenation recorded by chromium isotopes. *Nature* 461, 250–253.
- French, J.E., Heaman, L.M., 2010. Precise U-Pb dating of Paleoproterozoic mafic dyke swarms of the Dharwar craton, India: Implications for the existence of the Neoproterozoic supercraton Sclavia. *Precambrian Research* 183, 416–441.
- Frimmel, H.E., Klötzli, U.S., Siegfried, P.R., 1996. New Pb-Pb single zircon age constraints on the timing of Neoproterozoic glaciation and continental breakup in Namibia. *Journal of Geology* 104, 459–469.
- Frimmel, H.E., 2008. Earth's continental crustal gold endowment. *Earth and Planetary Science Letters* 267, 45–55.
- Frost, C.D., Frost, B.R., 1997. Reduced rapakivi-type granites: The tholeiitic connection. *Geology* 25, 647–650.
- Frost, D.J., McCammon, C.A., 2008. The redox state of Earth's mantle. *Annual Review of Earth and Planetary Sciences* 36, 389–420.
- Froude, C.F., Ireland, T.R., Kinny, P.D., Williams, I.S., Compston, W., Williams, I.R., Myers, J.S., 1983. Ion-microprobe identification of 4100–4200 Myr old terrestrial zircons. *Nature* 304, 616–618.
- Furnes, H., Banerjee, N.R., Staudigel, H., Muehlenbachs, K., McLoughlin, N., de Wit, M., Van Kranendonk, M.J., 2007. Comparing petrographic signatures of bioalteration in recent to Mesoproterozoic pillow lavas: Tracing subsurface life in oceanic igneous rocks. *Precambrian Research* 158, 156–176.
- Gaidos, E., Dubuc, T., Dunford, M., McAndrew, P., Padilla-Gamiño, J., Studer, B., Weersing, K., Stanley, S., 2007. The Precambrian emergence of animal life: a geobiological perspective. *Geobiology* 5, 351–373.
- Galer, S.J.G., Mezger, K., 1998. Metamorphism, denudation and sea level in the Archean and cooling of the Earth. *Precambrian Research* 92, 389–412.
- Galimov, E.M., Kuznetsova, N.G., Prokhorov, V.S., 1968. On the problem of the Earth's ancient atmosphere composition in connection with results of isotope analysis of carbon from the Precambrian carbonates. *Geochemistry* 11, 1376–1381.
- [AU21] Gall, Q., Donaldson, J.A., 2006. Diagenetic fluorapatite and aluminum phosphate-sulfate in Paleoproterozoic Thelon Formation and Horny Bay Group, northwestern Canadian Shield. *Canadian Journal of Earth Sciences* 43, 617–629.
- Gandin, A., Wright, D.T., Melezhik, V., 2005. Vanished evaporites and carbonate formation in the Neoproterozoic Kogelbeen and Gamohaana formations of the Campbellrand Subgroup, South Africa. *Journal of African Earth Sciences* 41, 1–23.
- Gandin, A., Wright, D.T., 2007. Evidence of vanished evaporites in Neoproterozoic carbonates of South Africa. In: Lugli, B.C., Babel, M. (Eds.), *Evaporites through space and time*. Geological Society of London, Special Publication, 285, pp. 285–308.
- Garvin, J., Buick, R., Anbar, A.D., Arnold, G.L., Kaufman, A.J., 2009. Isotopic evidence for an aerobic Nitrogen cycle in the latest Archean. *Science* 323, 1045–1048.
- Gaucher, E.A., Govindarajan, S., Ganesh, O.K., 2008. Paleotemperature trend for Precambrian life inferred from resurrected proteins. *Nature* 451, 704–708.
- Gauthier-Lafaye, F., Holliger, P., Blanc, P.L., 1996. Natural fission reactors in the Franceville basin, Gabon: A review of the conditions and results of a “critical event” in a geological system. *Geochimica et Cosmochimica Acta* 60, 4831–4852.
- Gauthier-Lafaye, F., Weber, F., 2003. Natural fission reactors: Time constraints for occurrence, and their relation to uranium and manganese deposits and to the evolution of the atmosphere. *Precambrian Research* 120, 81–100.
- Gay, A.L., Grandstaff, D.E., 1980. Chemistry and mineralogy of Precambrian paleosols at Elliot Lake, Ontario, Canada. *Precambrian Research* 12, 349–373.
- Gehör, S., 1994. REE distribution in the phosphorite bands within the Paleoproterozoic Tuomivaara and Pahtavaara iron-formations, central and northern Finland. In: Nironen, M., Kahkonen, Y. (Eds.), *Geochemistry of Proterozoic supracrustal rocks in Finland*, IGCP Project 179 Stratigraphic methods as applied to the Proterozoic record and IGCP Project 217 Proterozoic geochemistry. Geological Survey of Finland, Special Paper, 19, pp. 71–83.
- Geng, Y., Liu, F., Yang, C., 2006. Magmatic event at the end of the Archean in Eastern Hebei Province and its geological implication. *Acta Geologica Sinica* 80, 5–59.
- Gislason, S.R., Oelkers, E.H., Eiriksdottir, E.S., Kardjilov, M.I., Gisladdottir, G., Sigfusson, B., Snorrason, A., Elefsen, S., Hardardottir, J., Torssander, P., Oskarsson, N., 2009. Direct evidence of the feedback between climate and weathering. *Earth and Planetary Science Letters* 277, 213–222.
- Glass, J.B., Wolfe-Simon, F., Anbar, A., 2009. Coevolution of metal availability and nitrogen assimilation in Cyanobacteria and algae. *Geobiology* 7, 100–123.
- Glenn, C.R., Föllmi, K.B., Riggs, S.R., Baturin, G.N., Grimm, K.A., Trappe, J., Abed, A.M., Galli-Olivier, C., Garrison, R.E., Ilyin, A., Jehl, C., Rohrhch, V., Sadaqah, R., Schidlowski, M., Sheldon, R.E., Siegmund, H., 1994. Phosphorus and phosphorites: Sedimentology and environments of formation. In: Föllmi, K.B. (Ed.), *Concepts and Controversies in Phosphogenesis*. *Eclogae Geologicae Helveticae*, 87, pp. 747–788.
- Glikson, M., Duck, L.J., Golding, S.D., Hofmann, A., Bolhar, R., Webb, R., Baiano, J.C.F., Sly, L.I., 2008. Microbial remains in some earliest Earth rocks: Comparison with a potential modern analogue. *Precambrian Research* 164, 187–200.
- Godderis, Y., Veizer, J., 2000. Tectonic control of chemical and isotopic composition of ancient oceans: the impact of continental growth. *American Journal of Science* 300, 434–461.
- Goddéris, Y., Donnadieu, Y., Dessert, C., Dupré, B., Fluteau, F., François, L.M., Nédélec, A., Ramstein, G., 2007. Coupled modeling of global carbon cycle and climate in the Neoproterozoic: links between Rodinia breakup and major glaciations. *Comptes Rendus Geoscience* 339, 212–222.
- Godfrey, L.V., Falkowski, P.G., 2009. The cycling and redox state of nitrogen in the Archean ocean. *Nature Geoscience* 2, 725–729.
- Gold, D.J.C., 2006. The Pongola Supergroup. In: Johnson, M.R., Anhaeusser, C.R., Thomas, R.J. (Eds.), *The Geology of South Africa*.

- Geological Society of South Africa & Council for Geoscience, Johannesburg & Pretoria, pp. 135–148.
- Goldblatt, C., Lenton, T.M., Watson, A.J., 2006. Bistability of atmospheric oxygen and the Great Oxidation. *Nature* 443, 683–686.
- Goldblatt, C., Zahnle, K.J., Sleep, N.H., Nisbet, E.G., 2009a. The Eons of Chaos and Hades. *Solid Earth Discussion* 1, 47–53.
- Goldblatt, C., Claire, M.W., Lenton, T.M., Matthews, A.J., Watson, A.J., Zahnle, K.J., 2009b. Nitrogen-enhanced greenhouse warming on early Earth. *Nature Geoscience* 2, 891–896.
- Golding, L.Y., Walter, M.R., 1979. Evidence of evaporite minerals in the Archaean Black Flag Beds, Kalgoorlie, Western Australia. *BMR Journal of Australian Geology and Geophysics* 4, 67–71.
- Gomes, R., Levison, H.F., Tsiganis, K., Morbidelli, A., 2005. Origin of the cataclysmic Late Heavy Bombardment period of the terrestrial planets. *Nature* 435, 466–469.
- Gorjan, P., Veevers, J.J., Walter, M.R., 2000. Neoproterozoic sulfur-isotope variation in Australia and global implications. *Precambrian Research* 100, 151–179.
- Gough, D.O., 1981. Solar interior structure and luminosity variations. *Solar Physics* 74, 21–34.
- Gould, S.J., 1994. Introduction: The coherence of history. In: Bengtson, S. (Ed.), *Early Life on Earth, Nobel Symposium 84*. Columbia University Press, New York, pp. 1–8.
- Gradstein, F.M., Ogg, J.G., Smith, A.G., 2004. *A Geologic Time Scale 2004*. Cambridge University Press.
- Grant, M.L., Wilde, S.A., Wu, F., Yang, J., 2009. The application of zircon cathodoluminescence imaging, ThUPb chemistry and UPb ages in interpreting discrete magmatic and high-grade metamorphic events in the North China Craton at the Archean/Proterozoic boundary. *Chemical Geology* 261, 154–170.
- Grant, P.R., Grant, B.R., 2008. How and why species multiply: The radiation of Darwin's finches. Princeton University Press, Princeton. p. 218.
- Grassineau, N.V., Abell, P., Appel, P.W.U., Lowry, D., Nisbet, E.G., 2006. Early life signatures in sulphur and carbon isotopes from Isua, Barberton, Wabigoon (Steep Rock), and Belingwe greenstone belts (3.8 to 2.7 Ga). In: Kesler, S.E., Ohmoto, H. (Eds.), *Evolution of Earth's Atmosphere, Hydrosphere, and Biosphere – Constraints from Ore Deposits*. Geological Society of America, Memoir, 198, pp. 33–52.
- Greff-Lefftz, M., Legros, H., 1999. Core rotational dynamics and geological events. *Science* 286, 1707–1709.
- Grey, K., Williams, I.R., 1990. Problematic bedding-plane markings from the Middle Proterozoic Manganese Subgroup, Bangemall Basin, Western Australia. *Precambrian Research* 46, 307–328.
- Grey, K., Williams, I.R., Martin, D.M., Fedonkin, M.A., Gehling, J.G., Runnegar, B.N., Yochelson, E.L., 2002. New occurrences of 'strings of beads' in the Bangemall Supergroup: a potential biostratigraphic marker horizon. *Geological Survey of Western Australia, Annual Review 2000–2001*, 69–73.
- Griffin, W.L., Graham, S., O'Reilly, S.Y., Pearson, N.J., 2004. Lithosphere evolution beneath the Kaapvaal Craton: Re–Os systematics of sulfides in mantle-derived peridotites. *Chemical Geology* 208, 89–118.
- Griffin, W.L., O'Reilly, S.Y., 2007a. The earliest subcontinental lithospheric mantle. In: Van Kranendonk, M.J., Smithies, R.H., Bennett, V. (Eds.), *Earth's Oldest Rocks. Developments in Precambrian Geology*, 15. Elsevier, Amsterdam, pp. 1013–1035.
- Griffin, W.L., O'Reilly, S.Y., 2007b. Cratonic lithospheric mantle: is anything subducted? *Episodes* 30, 43–53.
- Grotzinger, J.P., Kasting, J.F., 1993. New constraints on Precambrian ocean composition. *Journal of Geology* 101, 235–243.
- Grotzinger, J.P., Bowring, S.A., Saylor, B.Z., Kaufman, A.J., 1995. Biostratigraphic and geochronologic constraints on early animal evolution. *Science* 270, 598–604.
- Grotzinger, J.P., Knoll, A.H., 1999. Stromatolites in Precambrian carbonates: evolutionary mileposts or environmental dipsticks? *Annual Reviews of Earth and Planetary Sciences* 27, 313–358.
- Groves, D.I., Vielreicher, R.M., Goldfarb, R.J., Condie, K.C., 2005. Controls on the heterogeneous distribution of mineral deposits through time. Geological Society of London, Special Publication 248, 71–101.
- Güly, V.N., 1989. Principal features of the mineralogy and genesis of apatite deposits on the Aldan crystalline shield. *International Geology Reviews* 31, 1025–1038.
- Guo, Q., Strauss, H., Kaufman, A.J., Schröder, S., Gutzmer, J., Wing, B., Baker, M.A., Bekker, A., Jin, Q., Kim, S.-T., Farquhar, J., 2009. Reconstructing Earth's surface oxidation across the Archean-Proterozoic transition. *Geology* 37, 399–402.
- Habicht, K.S., Gade, M., Thamdrup, B., Berg, P., Canfield, D.E., 2002. Calibration of sulfate levels in the Archean Ocean. *Science* 298, 2372–2374.
- Haines, P.W., 1997. Tool marks from ca 1750 Ma, northern Australia: evidence for large drifting algal filaments? *Geology* 25, 235–238.
- Halevy, I., Johnston, D.T., Schrag, D.P., 2010. Explaining the structure of the Archean mass-independent sulfur isotope record. *Science* 329, 204–207.
- Halilovic, J., Cawood, P.A., Jones, J.A., Pirajno, F., Nemchin, A.A., 2004. Provenance of the Earraheedy Basin: Implications for assembly of the Western Australian Craton. *Precambrian Research* 128, 343–366.
- Hall, C.R., 1985. Precambrian phosphorites of northern Michigan: Mode and environment of deposition. M.Sc. thesis, Michigan Technological University, p. 147.
- Hallbauer, D.K., 1986. The mineralogy and geochemistry of Witwatersrand pyrite, gold, uranium and carbonaceous matter. In: Annhaeuser, C.R., Maske, S. (Eds.), *Mineral Deposits of Southern Africa*. vol. 1. Geological Society of South Africa, pp. 731–752.
- Halliday, A.N., 2008. A young Moon-forming giant impact at 70–110 million years accompanied by late-stage mixing, core formation and degassing of the Earth. *Philosophical Transactions of the Royal Society A* 366, 4163–4181.
- Halliday, A.N., Wood, B.J., 2009. How did Earth accrete? *Science* 325, 44–45.
- Halls, H.C., Davis, D.W., Stott, G.M., Ernst, R.E., Hamilton, M.A., 2008. The Paleoproterozoic Marathon Large Igneous Province: New evidence for a 2.1 Ga long-lived mantle plume event along the southern margin of the North American Superior Province. *Precambrian Research* 162, 327–353.
- Halverson, G.P., Hoffman, P.F., Schrag, D.P., Kaufman, A.J., 2002. A major perturbation of the carbon cycle before the Ghaub glaciation (Neoproterozoic) in Namibia: prelude to snowball Earth? *Geochemistry, Geophysics, Geosystems* 3, 1035. doi:10.1029/2001GC000244.
- Halverson, G.P., Hoffman, P.F., Schrag, D.P., Maloof, A.C., Rice, A.H.N., 2005. Toward a Neoproterozoic composite carbon-isotope record. *Geological Society of America Bulletin* 117, 1181–1207.
- Halverson, G.P., Hurtgen, M.T., 2007. Ediacaran growth of the marine sulfate reservoir. *Earth and Planetary Science Letters* 263, 32–44.
- Hamade, T., Konhäuser, K.O., Raiswell, R., Goldsmith, S., Morris, R.C., 2003. Using Ge/Si ratios to decouple iron and silica fluxes in Precambrian banded iron formations. *Geology* 31, 35–38.

- Hambrey, M.J., Harland, W.B., 1985. The late Proterozoic glacial era. *Palaeogeography, Palaeoclimatology, Palaeoecology* 51, 255–272.
- Hamilton, W.B., 1998. Archean magmatism and deformation were not the products of plate tectonics. *Precambrian Research* 91, 143–180.
- Hamilton, W.B., 2003. An alternative Earth. *GSA Today* 13, 4–12.
- Hamilton, W.B., 2007. Earth's first two billion years—The era of internally mobile crust. In: Hatcher, J.R., Jr., R.D., Carlson, M.P., McBride, J.H., Martínez Catalán, J.R. (Eds.), *4-D Framework of Continental Crust*. Geological Society of America, Memoir, 200, pp. 233–296.
- Han, T.-M., Runnegar, B., 1992. Megascopic eukaryotic algae from the 2.1-billion-year-old Negaunee Iron-Formation, Michigan. *Science* 257, 232–235.
- Hanmer, S., Greene, D.C., 2002. A modern structural regime in the Paleoarchean (~3.64 Ga); Isua Greenstone Belt, southern West Greenland. *Tectonophysics* 346, 201–222.
- Hannah, J.L., Bekker, A., Stein, H.J., Markey, R.J., Holland, H.D., 2004. Primitive Os and 2316 Ma age for marine shale: implications for Paleoproterozoic glacial events and the rise of atmospheric oxygen. *Earth and Planetary Science Letters* 225, 43–52.
- Hannah, J.L., Stein, H.J., Zimmermann, A., Yang, G., Markey, R.J., Melezhik, V.A., 2006. Precise 2004 ± 9 Ma Re-Os age for Pechenga black shale: comparison of sulfides and organic material. 16th Annual V.M. Goldschmidt Conference, Melbourne. *Geochimica et Cosmochimica Acta* 70 (18) A228–A228.
- Hansen, V.L., 2007. Venus: a thin lithosphere analogue for early Earth? In: Van Kranendonk, M.J., Smithies, R.H., Bennett, V. (Eds.), *Earth's Oldest Rocks. Developments in Precambrian Geology, 15*. Elsevier, Amsterdam, pp. 987–1012.
- Hanski, E., Huhma, H., Rastas, P., Kamenetsky, V.S., 2001. The Palaeoproterozoic komatiite-picrite association of Finnish Lapland. *Journal of Petrology* 42, 855–876.
- Haqq-Misra, J.D., Domagal-Goldman, S.D., Kasting, P.J., Kasting, J.F., 2008. A revised, hazy methane greenhouse for the Archean Earth. *Astrobiology* 8, 1127–1137.
- Hardie, L.A., 2003. Secular variations in Precambrian seawater chemistry and the timing of Precambrian aragonite seas and calcite seas. *Geology* 31, 785–788.
- Harland, W.B., Rudwick, M.J.S., 1964. The great infra-Cambrian ice age. *Scientific American* 211, 28–36.
- Harland, W.B., 1964. Evidence of late Precambrian glaciation and its significance. In: Nairn, A.E.M. (Ed.), *Problems in Palaeoclimatology*. Interscience, London, pp. 119–149.
- Harley, S.L., Kelly, N.M., 2007. Ancient Antarctica: the Archean of the East Antarctic Shield. In: Van Kranendonk, M.J., Smithies, R.H., Bennett, V. (Eds.), *Earth's Oldest Rocks. Developments in Precambrian Geology, 15*. Elsevier, Amsterdam, pp. 149–186.
- Harper, C.L., Jacobsen, S.B., 1992. Evidence from coupled ¹⁴⁷Sm-¹⁴³Nd and ¹⁴⁶Sm-¹⁴²Nd systematics for very early (4.5 Ga) differentiation of the Earth's mantle. *Nature* 360, 728–732.
- Harrison, T.M., Blichert-Toft, J., Müller, W., Albarede, F., Holden, P., Mojzsis, S.J., 2005. Heterogeneous Hadean Hafnium: Evidence of continental crust at 4.4 to 4.5 Ga. *Science* 310, 1947–1950.
- Harrison, T.M., Schmitt, A.K., McCulloch, M.T., Lovera, O.M., 2008. Early (>4.5 Ga) formation of terrestrial crust: Lu-Hf, δ¹⁸O, and Ti thermometry results for Hadean zircons. *Earth and Planetary Science Letters* 268, 476–486.
- Harrison, T.M., 2009. The Hadean crust: Evidence from >4 Ga zircons. *Annual Review of Earth and Planetary Sciences* 37, 479–505.
- Hartmann, L.A., Endo, I., Suita, M.T.F., Santos, J.O.S., Frantz, J.C., Carneiro, M.A., McNaughton, N.J., Barley, M.E., 2006. Provenance and age delimitation of Quadrilátero Ferrífero sandstones based on zircon U-Pb isotopes. *Journal of South American Earth Sciences* 20, 273–285.
- Hartmann, W.K., 2003. Megaregolith evolution and cratering cataclysmic models – Lunar cataclysm as a misconception (28 years later). *Meteoritics and Planetary Sciences* 38, 579–593.
- Hashimoto, G.L., Abe, Y., Sugita, S., 2007. The chemical composition of the early terrestrial atmosphere: Formation of a reducing atmosphere from CI-like material. *Journal of Geophysical Research-Planets* 112, E05010. doi:10.1029/2006JE002844.
- Hawkesworth, C.J., Cawood, P., Kemp, T., Storey, C., Dhuime, B., 2009. A matter of preservation. *Science* 323, 49–50.
- Hawkesworth, C.J., Dhuime, B., Pietranik, A.B., Cawood, P.A., Kemp, A.I.S., Storey, C.D., 2010. The generation and evolution of continental crust. *Journal of the Geological Society, London* 167, 229–248.
- Hayes, J.M., 1983. Geochemical evidence bearing on the origin of aerobic life: a speculative hypothesis. In: Schopf, J.W. (Ed.), *Earth's Earliest Biosphere: Its Origin and Evolution*. Princeton University Press, pp. 291–301.
- Hayes, J.M., Lambert, I.B., Strauss, H., 1992. The sulphur isotopic record. In: Schopf, J.W., Klein, C. (Eds.), *The Proterozoic Biosphere: A Multidisciplinary Study*. Cambridge University Press, Cambridge, pp. 129–132.
- Hayes, J.M., 1994. Global methanotrophy at the Archean-Proterozoic transition. In: Bengtson, S. (Ed.), *Early Life on Earth, Nobel Symposium*. Columbia University Press, New York, 84, pp. 220–236.
- Hayes, J.M., Waldbauer, J.R., 2006. The carbon cycle and associated redox processes through time. *Philosophical Transactions of the Royal Society, Series B, Biological Sciences* 361, 931–950.
- Heaman, L.M., 1997. Global mafic magmatism at 2.45 Ga: Remnants of an ancient large igneous province? *Geology* 25, 299–302.
- Heather, K.B., Shore, G.T., 1999. *Geology, Swayze greenstone belt, Ontario*. Geological Survey of Canada Map. scale 1:50 000.
- Heckman, D.S., Geiser, D.M., Eidell, B.R., Stauffer, R.L., Kardos, N.L., Hedges, S.B., 2001. Molecular evidence for the early colonization of land by fungi and plants. *Science* 293, 1129–1133.
- Hedges, B.S., Chen, H., Kumar, S., Wang, D.Y.C., Thompson, A.S., Watanabi, H., 2001. A genomic timescale for the origin of eukaryotes. *BMC Evolutionary Biology* 1, 4. doi:10.1186/1471-2148-1-4.
- Hegner, E., Kröner, A., Hofmann, A.W., 1984. Age and isotope geochemistry of the Archean Pongola and Usushwana suites in Swaziland, southern Africa: a case for crustal contamination of mantle-derived magma. *Earth and Planetary Science Letters* 70, 267–279.
- Herzberg, C., Asimow, P.D., Arndt, N.T., Niu, Y., Leshner, C.M., G.F.J., Cheadle, M.J., Saunders, A.D., 2007. Temperatures in ambient mantle and plumes: constraints from basalts, picrites, and komatiites. *Geochemistry, Geophysics, Geosystems* 8, Q02006. doi: 10.1029/2006GC001390.
- Herzberg, C., Gazel, E., 2009. Petrological evidence for secular cooling in mantle plumes. *Nature* 458, 619–622.
- Herzberg, C., Condie, K., Korenaga, J., 2010. Thermal history of the Earth and its petrological expression. *Earth and Planetary Science Letters* 292, 79–88.
- Hiatt, E.E., Palmer, S.E., Kyser, K.T., O'Connor, T.K., 2010. Basin evolution, diagenesis and uranium mineralization in the Paleoproterozoic Thelon Basin, Nunavut, Canada. *Basin Research* 22, 302–323.

- Higgins, J.A., Schrag, D.P., 2003. Aftermath of a snowball Earth. *Geochemistry, Geophysics, Geosystems* 4, 1028. doi:10.1029/2002GC000403.
- Hilburn, I.A., Kirschvink, J.L., Tajika, E., Tada, R., Hamano, Y., Yamamoto, S., 2004. A negative fold test on the Lorrain Formation of the Huronian Supergroup: Uncertainty on the paleolatitude of the Paleoproterozoic Gowganda glaciation and implications for the great oxygenation event. *Earth and Planetary Science Letters* 232, 315–332.
- Hinrichs, K.-U., 2002. Microbial fixation of methane carbon at 2.7 Ga: was an anaerobic mechanism possible? *Geochemistry, Geophysics, Geosystems* 3, 1042. doi:10.1029/2001GC000286.
- Hirth, G., Kohlstedt, D.L., 1996. Water in the oceanic upper mantle: implications for rheology, melt extraction and the evolution of the lithosphere. *Earth and Planetary Sciences* 144, 93–108.
- Hoashi, M., Bevacqua, D.C., Otake, T., Watanabe, Y., Hickman, A.H., Utsunomiya, S., Ohmoto, H., 2009. Primary hematite formation in an oxygenated sea 3.46 billion years ago. *Nature Geoscience* 2, 301–306.
- Hoffman, P.F., 1987. Proterozoic foredeeps, foredeep magmatism and giant iron-formations. In: Kroner, A. (Ed.), *Proterozoic Lithospheric Evolution*. American Geophysical Union, Geodynamic Series, 17, pp. 85–98.
- Hoffman, P.F., 1989. Speculations on Laurentia's fist gigayear (2.0–1.0 Ga). *Geology* 17, 135–138.
- Hoffman, P.F., Kaufman, A.J., Halverson, G.P., Schrag, D.P., 1998. A Neoproterozoic Snowball Earth. *Science* 281, 1342–1346.
- Hoffman, P.F., 1999. The break-up of Rodinia, birth of Gondwana, true polar wander and the snowball Earth. *Journal of African Earth Sciences* 28, 17–33.
- Hoffman, P.F., Schrag, D.P., 2002. The snowball Earth hypothesis: testing the limits of global change. *Terra Nova* 14, 129–155.
- Hoffmann, K.-H., Condon, D.J., Bowring, S.A., Crowley, J.L., 2004. U-Pb zircon date from the Neoproterozoic Ghaub Formation, Namibia: constraints on Marinoan glaciation. *Geology* 32, 817–820.
- Hofmann, H.J., 1976. Precambrian microflora, Belcher Islands, Canada: Significance and systematics. *Journal of Paleontology* 50, 1040–1073.
- Hofmann, H.J., 1990. Precambrian time units and nomenclature – The geon concept. *Geology* 18, 340–341.
- Hofmann, H.J., Grey, K., Hickman, A., Thorpe, R., 1999. Origin of 3.45 Ga coniform stromatolites in Warrawoona Group, Western Australia. *Geological Society of America Bulletin* 111, 1256–1262.
- Holland, H.D., 1984. *The Chemical Evolution of the Atmosphere and Oceans*. Princeton University Press, Princeton, p. 582.
- Holland, H.D., 1994. Early Proterozoic atmospheric change. In: Bengtson, S. (Ed.), *Early Life on Earth*. Nobel symposium, 84. Columbia University Press, New York, pp. 237–344.
- Holland, H.D., 2002. Volcanic gases, black smokers, and the Great Oxidation Event. *Geochimica et Cosmochimica Acta* 66, 3811–3826.
- Holland, H.D., 2005. Sedimentary mineral deposits and the evolution of Earth's near-surface environments. *Economic Geology* 100, 1489–1509.
- Holland, H.D., 2009. Why the atmosphere became oxygenated: A proposal. *Geochimica et Cosmochimica Acta* 73, 5241–5255.
- Holland, H.D., Beukes, N.J., 1990. A paleoweathering profile from Griqualand West, South Africa: evidence for a dramatic rise in atmospheric oxygen between 2.2 and 1.9BYBP. *American Journal of Science* 290-A, 1–34.
- Holland, H.D., Rye, R., 1997. Evidence in pre-2.2 Ga paleosols for the early evolution of atmospheric oxygen and terrestrial biota: Comment. *Geology* 25, 857–858.
- Holm, N.G., Dumont, M., Ivarsson, M., Konn, C., 2006. Alkaline fluid circulation in ultramafic rocks and formation of nucleotide constituents: a hypothesis. *Geochemical Transactions* 7, 7.
- Holm, N.G., Neubeck, A., 2009. Reduction of nitrogen compounds in oceanic basement and its implications for HCN formation and abiotic organic synthesis. *Geochemical Transactions* 10, 9.
- Hopkins, M., Harrison, T.M., Manning, C.E., 2008. Low heat flow inferred from >4 Gyr zircons suggests Hadean plate boundary interactions. *Nature* 456, 493–496.
- House, C.H., Fitz-Gibbon, S.T., 2002. Using homolog groups to create a whole-genomic tree of free-living organisms: An update. *Journal of Molecular Evolution* 54, 539–547.
- Howard, P.F., 1986. Proterozoic and Cambrian phosphorites – regional review: Australia. In: Cook, P.J., Shergold, J.H. (Eds.), *Phosphate Deposits of the World*. vol. 1, Proterozoic and Cambrian Phosphorites. Cambridge University Press, Cambridge, pp. 20–41.
- Hren, M.T., Tice, M.M., Chamberlain, C.P., 2009. Oxygen and hydrogen isotope evidence for a temperate climate 3.42 billion years ago. *Nature* 462, 205–208.
- Hurtgen, M.T., Arthur, M.A., Suits, N.S., Kaufman, A.J., 2002. The sulfur isotopic composition of Neoproterozoic seawater sulfate: implications for a snowball Earth? *Earth and Planetary Science Letters* 203, 413–429.
- Hurtgen, M.T., Arthur, M.A., Halverson, G.P., 2005. Neoproterozoic sulfur isotopes, the evolution of microbial sulfur species, and the burial efficiency of sulfide as sedimentary pyrite. *Geology* 33, 41–44.
- Huston, D.L., Logan, G.A., 2004. Barite, BIFs and bugs: evidence for the evolution of the Earth's early hydrosphere. *Earth and Planetary Science Letters* 220, 41–55.
- Hutcheon, I.D., Marhas, K.K., Krot, A.N., Goswami, J.N., Jones, R.H., 2009. ²⁶Al in plagioclase-rich chondrules in carbonaceous chondrites: Evidence for an extended duration of chondrule formation. *Geochimica et Cosmochimica Acta* 73, 5080–5099.
- Hyde, W.T., Crowley, T.J., Baum, S.K., Peltier, W.R., 2000. Neoproterozoic 'snowball Earth' simulations with a coupled climate/ice-sheet model. *Nature* 405, 425–429.
- Iizuka, T., Horie, K., Komiya, T., Maruyama, S., Hirata, T., Hidaka, H., Windley, B.F., 2006. 4.2 Ga zircon xenocryst in an Acasta gneiss from northwestern Canada: evidence for early continental crust. *Geology* 34, 245–248.
- Iizuka, T., Komiya, T., Maruyama, S., 2007a. The early Archean Acasta Gneiss Complex: geochronological and isotopic studies and implications for early crustal evolution. In: Van Kranendonk, M.J., Smithies, R.H., Bennet, V. (Eds.), *Earth's Oldest Rocks. Developments in Precambrian Geology*, 15. Elsevier, Amsterdam, pp. 127–148.
- Iizuka, T., Komiya, T., Ueno, Y., Katayama, I., Uehara, Y., Maruyama, S., Hirata, T., Johnson, S.P., Dunkley, D.J., 2007b. Geology and geochronology of the Acasta Gneiss Complex, northwest Canada: new constraints on its tectonothermal history. *Precambrian Research* 153, 179–208.
- Iizuka, T., Komiya, T., Johnson, S.P., Kon, Y., Maruyama, S., Hirata, T., 2008. Reworking of Hadean crust in the Acasta gneisses, northwestern Canada: Evidence from in situ Lu-Hf isotope analysis of zircon. *Chemical Geology* 259, 230–239.
- Ilyin, A.V., Zaitsev, N.S., Bjamba, Z., 1986. Proterozoic and Cambrian phosphorites – deposits: Khubsugul, Mongolian People's Republic. In: Cook, P.J., Shergold, J.H. (Eds.), *Phosphate Deposits of the World*. vol. 1, Proterozoic and Cambrian Phosphorites. Cambridge University Press, Cambridge, pp. 162–174.

- Ingall, E.D., Jahnke, R., 1994. Evidence for enhanced phosphorus regeneration from marine sediments overlain by oxygen depleted waters. *Geochimica et Cosmochimica Acta* 58, 2571–2575.
- Ireland, T.R., Clement, S., Compston, W., Foster, J.J., Holden, P., Jenkins, B., Lanc, P., Schram, N., Williams, I.S., 2008. Development of SHRIMP. *Australian Journal of Earth Sciences* 55, 937–954.
- Isley, A.E., Abbott, D.H., 1999. Plume-related mafic volcanism and the deposition of banded iron-formation. *Journal of Geophysical Research* 104, 15461–15477.
- Isley, A.E., Abbott, D.H., 2002. Implications of the temporal distribution of high-Mg magmas for mantle plume volcanism through time. *Journal of Geology* 110, 141–158.
- Jacobsen, S.B., 2005. The Hf-W isotopic system and the origin of the Earth and Moon. *Annual Review of Earth and Planetary Sciences* 33, 531–570.
- Jahnke, R.A., Emerson, S.R., Roe, K.K., Burnett, W.C., 1983. The present day formation of apatite in Mexican continental margin sediments. *Geochimica et Cosmochimica Acta* 47, 259–266.
- James, N.P., Narbonne, G.M., Kyser, T.K., 2001. Later Neoproterozoic cap carbonates: Mackenzie Mountains, northwestern Canada: precipitation and global glacial meltdown. *Canadian Journal of Earth Sciences* 38, 1229–1262.
- Javaux, E.J., Knoll, A.H., Walter, M.R., 2001. Morphological and ecological complexity in early eukaryotic ecosystems. *Nature* 412, 66–69.
- Javaux, E.J., Knoll, A.H., Walter, M.R., 2004. TEM evidence for eukaryotic diversity in mid-Proterozoic oceans. *Geobiology* 2, 121–132.
- Javaux, E.J., Marshall, C.P., Bekker, A., 2010. Organic-walled microfossils in 3.2-billion-year-old shallow-marine siliciclastic deposits. *Nature* 463, 934–938.
- Jayananda, M., Moyen, J.-F., Martin, H., Peucat, J.-J., Auvray, B., Mahabaleswar, B., 2000. Late Archean (2550–2520 Ma) juvenile magmatism in the Eastern Dharwar craton, southern India: constraints from geochronology, Nd–Sr isotopes and whole rock geochemistry. *Precambrian Research* 99, 225–254.
- Jefferson, C.W., Thomas, D.J., Gandhi, S.S., Ramaekers, R., Delaney, G., Brisbin, D., Cutts, C., Quirt, D., Portella, P., Olseo, R.A., 2007. Unconformity-associated uranium deposits of the Athabasca Basin, Saskatchewan and Alberta. *Geological Association of Canada, Special Publication* 5, 273–305.
- Jenner, F.E., Bennet, V.C., Nutman, A.P., Friend, C.R.L., Norman, M.D., Yaxley, G., 2009. Evidence for subduction at 3.8 Ga: Geochemistry of arc-like metabasalts from the southern edge of the Isua Supracrustal Belt. *Chemical Geology* 261, 82–97.
- Jensen, S., Gehling, J.G., Droser, M.L., 1998. Ediacaran-type fossils in Cambrian sediments. *Nature* 393, 597–569.
- Joen, K.W., 1991. Amoeba and x-bacteria: Symbiont acquisition and possible species change. In: Margulis, L., Fester, R. (Eds.), *Symbiosis as a source of evolutionary innovation*. The MIT Press, Cambridge, pp. 118–131.
- Johnson, C.M., Beard, B.L., 2006. Fe isotopes: an emerging technique in understanding modern and ancient biogeochemical cycles. *GSA Today* 16, 4–10.
- Johnson, C.M., Beard, B.L., Roden, E.E., 2008a. The iron isotope fingerprints of redox and biogeochemical cycling in modern and ancient Earth. *Annual Reviews of Earth and Planetary Sciences* 56, 457–493.
- Johnson, C.M., Beard, B.L., Klein, C., Beukes, N.J., Roden, E.E., 2008b. Iron isotope constrain biologic and abiologic processes in Banded Iron Formation genesis. *Geochimica et Cosmochimica Acta* 72, 151–169.
- Johnston, D.T., Poulton, S.W., Dehler, C., Porter, S., Husson, J., Canfield, D.E., Knoll, A.H., 2010. An emerging picture of Neoproterozoic ocean chemistry: insights from the Chuar Group, Grand Canyon, USA. *Earth and Planetary Science Letters* 290, 64–73.
- Jost, H., Chemale Jr., F., Dussin, I.A., Tassinari, C.C.G., Martins, R., 2010. A U-Pb zircon Paleoproterozoic age for the metasedimentary host rocks and gold mineralization of the Crixás greenstone belt, Goiás, Central Brazil. *Ore Geology Reviews* 37, 127–139.
- Kah, L.C., Lyons, T.W., Frank, T.D., 2004. Low marine sulfate and protracted oxygenation of the Proterozoic biosphere. *Nature* 431, 834–838.
- Kakegawa, T., Nanri, H., 2006. Sulfur and carbon isotope analyses of 2.7 Ga stromatolites, cherts and sandstones in the Jeerinah Formation, Western Australia. *Precambrian Research* 148, 115–124.
- Kamber, B.S., Moorbath, S., Whitehouse, M.J., 2002. The oldest rocks on Earth: time constraints and geological controversies. *Geological Society of London, Special Publication* 190, 177–203.
- Kamber, B.S., Collerson, K.D., Moorbath, S., Whitehouse, M.J., 2003. Inheritance of early Archean Pb-isotope variability from long-lived Hadean protocrust. *Contributions to Mineralogy and Petrology* 145, 25–46.
- Kamber, B.S., Whitehouse, M.J., 2007. Micro-scale sulphur isotope evidence for sulphur cycling in the late Archean shallow ocean. *Geobiology* 5, 5–17.
- Kamber, B.S., 2007. The enigma of the terrestrial protocrust: evidence for its former existence and the importance of its complete disappearance. In: Van Kranendonk, M.J., Smithies, R.H., Bennet, V. (Eds.), *Earth's Oldest Rocks. Developments in Precambrian Geology*, 15. Elsevier, Amsterdam, pp. 75–89.
- Kappler, A., Pasquero, C., Konhauser, K.O., Newman, D.K., 2005. Deposition of banded iron formations by anoxygenic phototrophic Fe(II)-oxidizing bacteria. *Geology* 33, 865–868.
- Karhu, J.A., 1993. Palaeoproterozoic evolution of the carbon isotope ratios of sedimentary carbonates in the Fennoscandian Shield. *Geological Survey of Finland Bulletin* 371, 1–87.
- Karhu, J.A., Holland, H.D., 1996. Carbon isotopes and the rise of atmospheric oxygen. *Geology* 24, 867–870.
- Karlstrom, K., Bowring, S.A., 1988. Early Proterozoic assembly of tectonostratigraphic terranes in southwestern North America. *Journal of Geology* 96, 561–576.
- Kasermann, S.A., Prave, A.R., Fallick, A.E., Hawkesworth, C.J., Hoffmann, K.-H., 2010. Neoproterozoic ice ages, boron isotopes, and ocean acidification: implications for a snowball Earth. *Geology* 38, 775–778.
- Kasting, J.F., 1987. Theoretical constraints on oxygen and carbon dioxide concentrations in the Precambrian atmosphere. *Precambrian Research* 34, 205–229.
- Kasting, J.F., 1990. Bolide impacts and the oxidation state of carbon in the Earth's early atmosphere. *Origins of Life* 20, 199–231.
- Kasting, J.F., 1993. Earth's Early Atmosphere. *Science* 259, 920–926.
- Kasting, J.F., Catling, D., 2003. Evolution of a Habitable Planet. *Annual Review of Astronomy and Astrophysics* 41, 429–463.
- Kasting, J.F., 2005. Methane and climate during the Precambrian era. *Precambrian Research* 137, 119–129.
- Kasting, J.F., Wallmann, K., Veizer, J., Shields, G., Jaffres, J., 2006. Paleoclimates, ocean depth, and the oxygen isotopic composition of seawater. *Earth and Planetary Science Letters* 252, 82–93.

- Kato, Y., Suzuki, K., Nakamura, K., Hickman, A.H., Nedachi, M., Kusakabe, M., Bevacqua, D.C., Ohmoto, H., 2009. Hematite formation by oxygenated groundwater more than 2.76 billion years ago. *Earth and Planetary Science Letters* 278, 40–49.
- Kaufman, A.J., Jacobsen, S.B., Knoll, A.H., 1993. The Vendian record of Sr and C isotopic variations in seawater: implications for tectonics and paleoclimate. *Earth and Planetary Science Letters* 120, 409–430.
- Kaufman, A.J., Knoll, A.H., Narbonne, G.M., 1997. Isotopes, ice ages and terminal Proterozoic Earth history. *Proceedings of the National Academy of Science* 94, 6600–6605.
- Kaufman, A.J., Johnston, D.T., Farquhar, J., Masterson, A.L., Lyons, T.W., Bates, S., Anbar, A.D., Arnold, G.L., Garvin, J., Buick, R., 2008. Late Archean biospheric oxygenation and atmospheric evolution. *Science* 317, 1900–1903.
- Kazakov, A.V., 1937. The phosphorite facies and the genesis of phosphorites. *Geological investigations of agricultural ores. Scientific Institute of Fertilizers and Insecto-Fungicides, Transactions* 142, 95–113.
- Kazmierczak, J., Altermann, W., 2002. Neoproterozoic biomineralisation by benthic cyanobacteria. *Science* 298, 2351.
- Kazmierczak, J., Kremer, B., 2002. Thermal alteration of the Earth's oldest fossils. *Nature* 420, 477–478.
- Kazmierczak, J., Altermann, W., Kremer, B., Kempe, S., Eriksson, P.G., 2009. Mass occurrence of benthic coccoid cyanobacteria and their role in the production of Neoproterozoic carbonates of South Africa. *Precambrian Research* 173, 79–92.
- Kelley, D.S., Karson, J.A., Früh-Green, G.L., Yoerger, D.R., Shank, T.M., Butterfield, D.A., Hayes, J.M., Schrenk, M.O., Olson, E.J., Proskurowski, G., Jakuba, M., Bradley, A., Larson, B., Ludwig, K., Glickson, D., Buckman, K., Bradley, A.S., Brazelton, W.J., Roe, K., Elend, M.J., Delacour, A., Bernasconi, S.M., Lilley, M.D., Baross, J.A., Summons, R.E., Sylva, S.P., 2005. A Serpentinite-Hosted Ecosystem: The Lost City Hydrothermal Field. *Science* 307, 1428–1434.
- Kemp, A.I.S., Hawkesworth, C.J., Paterson, B.A., Kinny, P.D., 2006. Episodic growth of the Gondwana supercontinent from hafnium and oxygen isotopes in zircon. *Nature* 439, 580–583.
- Kemp, A.I.S., 2010. An isotopic roadmap of early Earth evolution – Progress and potholes. In: Tyler, I.M., Knox-Robinson, C.M. (Eds.), 5th International Archean Symposium, Abstracts. Geological Survey of Western Australia, Record, Perth, 18, pp. 3–4.
- Kendall, B., Creaser, R.A., Selby, D., 2006. Re-Os geochronology of post-glacial black shales in Australia: constraints on the timing of “Sturtian” glaciation. *Geology* 34, 729–732.
- Kendall, B., Reinhard, C.T., W., L.T., Kaufman, A.J., Poulton, S.W., Anbar, A.D., 2010. Pervasive oxygenation along late Archean ocean margins. *Nature Geoscience* 3, 647–652.
- Kennedy, M.J., Runnegar, B., Prave, A.R., Hoffmann, K.-H., Arthur, M.A., 1998. Two or four Neoproterozoic glaciations? *Geology* 26, 1059–1063.
- Kennedy, M.J., Christie-Blick, N., Sohl, L.E., 2001. Are Proterozoic cap carbonates and isotopic excursions a record of gas hydrate destabilization following Earth's coldest intervals? *Geology* 29, 443–446.
- Kennedy, M.J., Droser, M., Mayer, L.M., Pevear, D., Mrofka, D., 2006. Late Precambrian oxygenation; inception of the clay mineral factory. *Science* 311, 1446–1449.
- Kennedy, M.J., Mrofka, D., von der Borch, C., 2008. Snowball earth termination by destabilization of equatorial permafrost methane clathrate. *Nature* 453, 642–645.
- Kerrick, R., Goldfarb, R.J., Richards, J., 2005. Metallogenic provinces in an evolving geodynamic framework. *Economic Geology, 100th Anniversary Issue*: pp. 1097–1136.
- Kharcha, P., Kasting, J.F., Siefert, J.L., 2005. A coupled atmosphere-ecosystem model of the early Archean Earth. *Geobiology* 3, 53–76.
- Kholodov, V.N., Nedumov, R.I., 2009. Association of manganese ore and phosphorite-bearing facies in sedimentary sequences: Communication 2. Co-occurrence and paragenesis of P and Mn in Lower Paleozoic and Precambrian sediments. *Lithology and Mineral Resources* 44, 152–173.
- Kirschvink, J.L., 1992. Late Proterozoic low-latitude glaciation: the snowball Earth. In: Schopf, J.W., Klein, C. (Eds.), *The Proterozoic Biosphere*. Cambridge University Press, New York, pp. 51–52.
- Kirschvink, J.L., Gaidos, E.J., Bertani, L.E., Beukes, N.J., Gutzmer, J., Maepa, L.N., Steinberger, R.E., 2000. Paleoproterozoic snowball Earth: Extreme climatic and geochemical global change and its biological consequences. *Proceedings of the National Academy of Sciences, USA* 97, 1400–1405.
- Kiyokawa, S., Ito, T., Ikehara, M., Kitajima, F., 2006. Middle Archean volcano-hydrothermal sequence: Bacterial microfossil-bearing 3.2 Ga Dixon Island Formation, coastal Pilbara terrane, Australia. *GSA Bulletin* 118, 3–22.
- Klein, C., Beukes, N.J., 1989. Geochemistry and sedimentology of a facies transition from limestone to iron formation deposition in the Early Proterozoic Transvaal Supergroup, South Africa. *Economic Geology* 84, 1733–1774.
- Klein, C., Ladeira, E.A., 2000. Geochemistry and petrology of some Proterozoic banded iron-formation of the Quadrilátero Ferrífero, Minas Gerais, Brazil. *Economic Geology* 95, 405–428.
- Klein, C., 2005. Some Precambrian banded iron-formations (BIFs) from around the world: Their age, geologic setting, mineralogy, metamorphism, geochemistry, and origin. *American Mineralogist* 90, 1473–1499.
- Kleine, T., Mezger, K., Palme, H., Munker, C., 2004. The W isotope evolution of the bulk silicate Earth: constraints on the timing and mechanisms of core formation and accretion. *Earth and Planetary Science Letters* 228, 109–123.
- Kleine, T., Toubol, M., Bourdon, B., Nimmo, F., Mezger, K., Palme, H., Jacobsen, S.B., Yin, Q.-Z., Halliday, A.N., 2009. Hf-W chronology of the accretion and early evolution of asteroids and terrestrial planets. *Geochimica et Cosmochimica Acta* 73, 5150–5188.
- Knauth, L.P., Lowe, D.R., 2003. High Archean climatic temperature inferred from oxygen isotope geochemistry of cherts in the 3.5 Ga Swaziland Supergroup, South Africa. *Geological Society of America Bulletin* 115, 566–580.
- Knauth, L.P., Kennedy, M.J., 2009. The late Precambrian greening of the Earth. *Nature* 460, 728–732.
- Knoll, A.H., 1992. The early evolution of Eukaryotes: a geological perspective. *Science* 256, 622–625.
- Knoll, A.H., Carroll, S.B., 1999. Early animal evolution: emerging views from comparative biology and geology. *Science* 284, 2129–2137.
- Knoll, A.H., 2003. *Life on a Young Planet: The First Three Billion Years of Evolution on Earth*. Princeton University Press, Princeton, p. 277.
- Knoll, A.H., Walter, M.R., Narbonne, G.M., Christie-Blick, N., 2004. A new period for the geologic time scale. *Science* 305, 621–622.
- Kolodny, Y., Kaplan, I.R., 1970. Carbon and oxygen isotopes in apatite-CO₂ and co-existing calcite from sedimentary phosphorite. *Journal of Sedimentary Petrology* 40, 954–959.

- Konhauser, K.O., Hamade, T., Raiswell, R., Morris, R.C., Ferris, F.G., Southam, G., Canfield, D.E., 2002. Could bacteria have formed the Precambrian banded iron formations? *Geology* 30, 1079–1082.
- Konhauser, K.O., Amskold, L., Lalonde, S.V., Posth, N.R., Kappler, A., Anbar, A., 2007a. Decoupling photochemical Fe(II) oxidation from shallow-water BIF deposition. *Earth and Planetary Science Letters* 258, 87–100.
- Konhauser, K.O., Lalonde, S.V., Amskold, L., Holland, H.D., 2007b. Was there really an Archean phosphate crisis? *Science* 315, 1234.
- Konhauser, K.O., Pecoits, E., Lalonde, S.V., Papineau, D., Nisbet, E.G., Barley, M.E., Arndt, N.T., Zahnle, K., Kamber, B.S., 2009. Oceanic nickel depletion and a methanogen famine before the Great Oxidation Event. *Nature* 458, 750–753.
- Kontinen, A.T., 1987. An Early Proterozoic ophiolite – the Jormua mafic-ultramafic complex, northern Finland. *Precambrian Research* 35, 313–341.
- Kopp, R.E., Kirschvink, J.L., Hilburn, I.A., Nash, C.Z., 2005. The Paleoproterozoic snowball Earth: A climate disaster triggered by the evolution of oxygenic photosynthesis. *Proceedings of the National Academy of Sciences USA* 102, 11131–11136.
- Kositcin, N., Brown, S.J.A., Barley, M.E., Krapež, B., Cassidy, K.F., Champion, D.C., 2008. SHRIMP U-Pb zircon age constraints on the Late Archaean tectonostratigraphic architecture of the Eastern Goldfields Superterrane, Yilgarn Craton, Western Australia. *Precambrian Research* 161, 5–33.
- Kramers, J.D., 2007. Hierarchical Earth accretion and the Hadean Eon. *Journal of the Geological Society, London* 164, 3–17.
- Krapez, B., 1993. Sequence stratigraphy of the Archaean supracrustal belts of the Pilbara Block, Western Australia. *Precambrian Research* 60, 1–45.
- Kress, M.E., McKay, C.P., 2004. Formation of methane in comet impacts: Implications for Earth, Mars, and Titan. *Icarus* 168, 475–483.
- Krogh, T.E., Kamo, S.L., Sharpton, V., Marin, L., Hildebrand, A.R., 1993. U-Pb ages of single shocked zircons linking distal K/T ejecta to the Chicxulub crater. *Nature* 366, 731–734.
- Krogh, T.W., 1973. A low contamination method for hydrothermal decomposition of zircon and extraction of U and Pb for isotopic age determinations. *Geochimica et Cosmochimica Acta* 37, 485–494.
- Krogh, T.W., Davis, D.W., F., C., 1984. Precise U-Pb zircon and baddelyite ages for the Sudbury area. In: Pye, E.G., Naldrett, A.J., Giblin, P.E. (Eds.), *The Geology and Ore Deposits of the Sudbury Structure*. Ontario Geological Survey, Special vol. 1, pp. 431–446.
- Krogh, T.W., 1993. High precision U–Pb ages for granulite metamorphism and deformation in the Archean Kapuskasing Structural Zone, Ontario: Implications for structure and development of the lower crust. *Earth and Planetary Science Letters* 119, 1–18.
- Krogh, T.W., Moser, D.E., 1994. U-Pb zircon and monazite ages from the Kapuskasing uplift: age constraints on deformation within the Ivanhoe Lake fault zone. *Canadian Journal of Earth Sciences* 31, 1096–1103.
- Kröner, A., Byerly, G.R., Lowe, D.R., 1991. Chronology of early Archaean granite–greenstone evolution in the Barberton Mountain Land, South Africa, based on precise dating by single zircon evaporation. *Earth and Planetary Science Letters* 103, 41–54.
- Kröner, A., 2007. The Ancient Gneiss Complex of Swaziland and environs: record of early Archean crustal evolution in southern Africa. In: Van Kranendonk, M.J., Smithies, R.H., Bennet, V. (Eds.), *Earth’s Oldest Rocks*. *Developments in Precambrian Geology*, 15. Elsevier, Amsterdam, pp. 465–480.
- Krot, A.N., Amelin, Y., Bland, P., Ciesla, F.J., Connelly, J., Davis, A.M., Huss, G.R., Hutcheon, I.D., Makide, K., Nagashima, K., Nyquist, L.E., Russell, S.S., Scott, E.R.D., Thrane, K., Yurimoto, H., Yin, Q.-Z., 2009. Origin and chronology of chondritic components: A review. *Geochimica et Cosmochimica Acta* 73, 4963–4997.
- XKrull-Davatzes, A.E., Byerly, G.R., Lowe, D.R., 2010. Evidence for a low-O₂ Archean atmosphere from nickel-rich chrome spinels in 3.24 Ga impact spherules, Barberton greenstone belt, South Africa. *Earth and Planetary Science Letters* 296, 319–328.
- Krupp, R., Oberthur, T., Hirdes, W., 1994. The early Precambrian atmosphere and hydrosphere: thermodynamic constraints from mineral deposits. *Economic Geology* 89, 1581–1598.
- Kulikov, V.S., Bychkova, Y.V., Kulikova, V.V., Ernst, R., 2010. The Vetreny Poyas (Windy Belt) subprovince of southeastern Fennoscandia: An essential component of the ca.2.5–2.4 Ga Sumian large igneous province. *Precambrian Research* 183, 589–601.
- Kump, L.R., Barley, M.E., 2007. Increased subaerial volcanism and the rise of atmospheric oxygen 2.5 billion years ago. *Nature* 448, 1033–1036.
- Kyser, K.T., 2007. Fluids, basin analysis, and mineral deposits. *Geofluids* 7, 238–257.
- Laajoki, K., Saikkonen, R., 1977. On the geology and geochemistry of the Precambrian iron formations in Vayrylankyla South Puolanka area, Finland. *Geological Survey of Finland Bulletin* 292, p. 137.
- Labrosse, S., Jaupart, C., 2007. Thermal evolution of the earth: secular changes and fluctuations of plate characteristics. *Earth and Planetary Science Letters* 260, 465–481.
- Lamb, D.M., Awramik, S.M., Chapman, D.J., Zhu, S., 2009. Evidence for eukaryotic diversification in the ~1800 million-year-old Changzhougou Formation, North China. *Precambrian Research* 173, 93–104.
- Landuyt, W., Bercovici, D., 2009. Variations in planetary convection via the effect of climate on damage. *Earth and Planetary Science Letters* 277, 29–37.
- Lane, N., 2009. *Life Ascending: the ten great inventions of evolution*. Norton, New York, p. 344.
- Lange, M.A., Ahrens, T.J., 1982. The evolution of an impact-generated atmosphere. *Icarus* 51, 96–120.
- Le Hir, G., Donnadieu, Y., Goddés, Y., Pierrehumbert, R.T., Halverson, G.P., Macouin, M., Nédélec, A., Ramstein, G., 2009. The snowball Earth aftermath: exploring the limits of continental weathering processes. *Earth and Planetary Science Letters* 277, 453–463.
- Leather, J., Allen, P.A., Brasier, M.D., Cozzi, A., 2002. Neoproterozoic snowball Earth under scrutiny: Evidence from the Fiq glaciation of Oman. *Geology* 30, 891–894.
- Leckie, R.M., Bralower, T.J., Cashman, R., 2002. Oceanic anoxic events and plankton evolution: biotic response to tectonic forcing during the mid-Cretaceous. *Paleoceanography* 17, 1041. doi: 10.1029/2001PA000623.
- Lehtinen, M., Nurmi, P.A., Rämö, O.T., 2005. Precambrian geology of Finland: key to the evolution of the Fennoscandian Shield. *Developments in Precambrian Geology*, 14. Elsevier, Amsterdam, p. 736.
- Lenardic, A., Jellinek, A.M., Moresi, L.-N., 2008. A climate induced transition in the tectonic style of a terrestrial planet. *Earth and Planetary Science Letters* 271, 34–42.
- Lenton, T.M., Watson, A.J., 2004. Biotic enhancement of weathering, atmospheric oxygen and carbon dioxide in the Neoproterozoic. *Geophysical Research Letters* 31, L05202.

- Lepland, A., Arrhenius, G., Cornell, D., 2002. Apatite in Early Archean Isua supracrustal rocks, southern West Greenland: Its origin, association with graphite and potential as a biomarker. *Precambrian Research* 118, 221–241.
- Lepland, A., Van Zuilen, M.A., Arrhenius, G., Whitehouse, M.J., Fedo, C.M., 2005. Questioning the evidence for Earth's earliest life – Akilia revisited. *Geology* 33, 77–79.
- Lepland, A., Van Zuilen, M.A., Philippot, P., 2011. Fluid-deposited graphite and its geobiological implications in early Archean greiss from Akilia, Greenland. *Geobiology* 9, 2–9.
- Lepot, K., Benzerara, K., Brown Jr., G.E., Philippot, P., 2008. Microbially influenced formation of 2,724-million-year-old stromatolites. *Nature Geoscience* 1, 118–121.
- Lepot, K., Benzerara, K., Rividi, N., Cotte, M., Brown Jr., G.E., Philippot, P., 2009. Organic matter heterogeneities in 2.72 Ga stromatolites: Alteration versus preservation by sulfur incorporation. *Geochimica et Cosmochimica Acta* 73, 6579–6599.
- Li, Z.X., Bogdanova, S.V., Collins, A.S., Davidson, A., DeWaele, B., Ernst, R.E., Fitzsimons, C.W., Fuck, R.A., Gladkochub, D.P., Jacobs, J., Karlstrom, K.E., Lu, S., Natapov, L.M., Pease, V., Pisarevsky, S.A., Thrane, K., Vernikovsky, V., 2008. Assembly, configuration and break-up history of Rodinia: a synthesis. *Precambrian Research* 160, 179–210.
- Lindsay, J.F., Brasier, M.D., 2002. Did global tectonics drive early biosphere evolution? Carbon isotope record from 2.6 to 1.9 Ga carbonates of Western Australian basins. *Precambrian Research* 114, 1–34.
- Lindsay, J.F., Kruse, P.D., Green, O.R., Hawkins, E., Brasier, M.D., Cartledge, J., Corfield, R.M., 2005. The Neoproterozoic-Cambrian record in Australia: a stable isotope study. *Precambrian Research* 143, 113–133.
- Lindsay, J.F., 2008. Was there a late Archean biospheric explosion? *Astrobiology* 8, 823–839.
- Liu, L., 2004. The inception of the oceans and CO₂-atmosphere in the early history of the Earth. *Earth and Planetary Science Letters* 227, 179–184.
- Logan, W.E., 1857. On the division of the Azoic rocks of Canada into Huronian and Laurentian. *Proceedings of the American Association for the Advancement of Science* 1857, 44–47.
- Lompo, M., 2009. Geodynamic evolution of the 2.25–2.0 Ga Paleoproterozoic rocks in the Man-Leo Shield of the West Africa Craton. A model of subsidence of an oceanic plateau. In: Reddy, S.M., Mazumder, R., Evans, D.A.D., Collins, A.S. (Eds.), *Paleoproterozoic supercontinents and Global Evolution*. Geological Society, London, Special Publications, 323, pp. 231–254.
- Longkang, S., Zhendong, Y., 1988. The metamorphic petrology of the Susong Group and the origin of the Susong phosphorite deposits, Anhui province. *Precambrian Research* 39, 65–76.
- López-García, P., Moreira, D., 1999. Metabolic symbiosis at the origin of eukaryotes. *Trends in Biochemical Science* 24, 88–93.
- Love, G.D., 2006. Constraining the timing of basal metazoan radiation using molecular biomarkers and U-Pb isotope dating. *Geochimica et Cosmochimica Acta*, Goldschmidt Conference Abstracts supplement 70, A371.
- Love, G.D., Grosjean, E., Stalvies, C., Fike, D.A., Grotzinger, J.P., Bradley, A.S., Kelly, A.E., Bhatia, M., Meredith, W., Snape, C.E., Bowring, S.A., Condon, D.J., Summons, R.E., 2009. Fossil steroids record the appearance of Demospongiae during the Cryogenian period. *Nature* 457, 718–721.
- Lovley, D.R., Holmes, D.E., Nevin, K.P., 2004. Dissimilatory Fe(III) and Mn(IV) reduction. *Advances in Microbial Physiology* 49, 219–286.
- Lovley, D.R., 2004. Potential role of dissimilatory iron reduction in the early evolution of microbial respiration. In: Seckbach, J. (Ed.), *Origins, Evolution, and Biodiversity of Microbial Life*. Kluwer, Amsterdam, pp. 301–313.
- Lowe, D.R., 2007. A comment on “Weathering of quartz as an Archean climatic indicator” by N.H. Sleep and A.M. Hessler [Earth Planet. Sci. Lett. 241 (2006) 594–602]. *Earth and Planetary Science Letters* 253, 530–533.
- Lowe, D.R., Byerly, G.R., 2007. An overview of the geology of the Barberton greenstone belt and vicinity: implications for early crustal development. In: Van Kranendonk, M.J., Smithies, R.H., Bennett, V. (Eds.), *Earth's Oldest Rocks*. Developments in Precambrian Geology, 15. Elsevier, Amsterdam, pp. 481–526.
- Lyons, T.W., Luepke, J.J., Schreiber, M.E., Zeig, G.A., 2000. Sulfur geochemical constraints on Mesoproterozoic restricted marine deposition: lower Belt Supergroup, northwestern United States. *Geochimica et Cosmochimica Acta* 64, 427–437.
- Lyons, T.W., Reinhard, C.T., Scott, C., 2009. Redox Redux. *Geobiology* 7, 489–494.
- Macdonald, F.A., Schmitz, M.D., Crowley, J.L., Roots, C.F., Jones, D.S., Maloof, A.C., Strauss, J.V., Cohen, P.A., Johnston, D.T., Schrag, D.P., 2010. Calibrating the Cryogenian. *Science* 327, 1241–1243.
- Magaritz, M., 1989. $\delta^{13}\text{C}$ minima follow extinction events: A clue to faunal radiation. *Geology* 17, 337–340.
- Maheshwari, A., Sial, A.N., Chittora, V.K., Bhu, H., 1999. A positive $\delta^{13}\text{C}$ carb anomaly in Paleoproterozoic carbonates of the Aravalli Craton, Western India: Support for a global isotopic excursion. *Journal of Asian Earth Sciences* 2, 59–67.
- Maheshwari, A., Sial, A.N., Gaucher, C., Bossi, J., Bekker, A., Ferreira, V.P., Romano, A.W., 2010. Global nature of the Paleoproterozoic Lomagundi carbon isotope excursion: A review of occurrences in Brazil, India, and Uruguay. *Precambrian Research* 182, 274–299.
- Maier, W.D., Barnes, S.J., Campbell, I.H., Fiorentini, M.L., Peltonen, P., Barnes, S.-J., Smithies, R.H., 2009. Progressive mixing of meteoritic veneer into the early Earth's deep mantle. *Nature* 460, 620–623.
- Maloof, A.C., Rose, C.V., Beach, R., Samuels, B.M., Calmet, C.C., Erwin, D.H., Poirier, G.R., Yao, N., Simons, F.J., 2010. Possible animal-body fossils in pre-Marinoan limestones from South Australia. *Nature Geoscience* 3, 653–659.
- Manusco, J.J., Loughheed, M.S., Shaw, R., 1975. Carbonate-apatite in Precambrian cherty iron formation, Baraga county, Michigan. *Economic Geology* 70, 583–586.
- Margulis, L., 1970. *The origin of the eukaryotic cell*. Yale University Press, New Haven-London, p. 349.
- Margulis, L., Rambler, M., Walker, J.C.G., 1976. Reassessment of roles of oxygen and ultraviolet light in Precambrian evolution. *Nature* 264, 620–624.
- Margulis, L., Sagan, D., 1986. *Microcosmos: Four billion years of microbial evolution*. University of California Press, Berkeley, p. 300.
- Margulis, L., 1993. *Symbiosis in cell evolution*. W.H. Freeman, New York, p. 452.
- Marmo, J.S., Ojakangas, R.W., 1984. Lower Proterozoic glaciogenic deposits, eastern Finland. *Geological Society of America Bulletin* 95, 1055–1062.
- Marmont, S., 1987. Unconformity-type uranium deposits – ore deposits models #13. *Geoscience Canada* 14, 219–229.

- Marsh, J.S., 2006. The Dominion Group. In: Johnson, M.R., Anhaeusser, C.R., Thomas, R.J. (Eds.), *The Geology of South Africa*. Geological Society of South Africa & Council for Geoscience, Johannesburg & Pretoria, pp. 149–154.
- Marshall, C.P., Love, G.D., Snape, C.E., Hill, A.C., Allwood, A.C., Walter, M.R., Van Kranendonk, M.J., Bowden, S.A., Sylva, S.P., Summons, R.E., 2007. Structural characterization of kerogen in 3.4 Ga Archaean cherts from the Pilbara Craton, Western Australia. *Precambrian Research* 155, 1–23.
- Martin, D.M., Li, Z.X., Nemchin, A.A., Powell, C.M., 1998. A pre-2.2 Ga age for giant hematite ores of the Hamersley Province, Australia. *Economic Geology* 93, 1084–1090.
- Martin, D.M., 1999. Depositional setting and implications of Paleoproterozoic glaciomarine sedimentation in the Hamersley Province, Western Australia. *GSA Bulletin* 111, 189–203.
- Martin, D.M., 2004. Depositional environment and taphonomy of the ‘strings of beads’: Mesoproterozoic multicellular fossils in the Bagemall Supergroup, Western Australia. *Australian Journal of Earth Sciences* 51, 555–561.
- Martin, H., Moyen, J.-F., 2002. Secular changes in TTG composition as markers of the progressive cooling of the Earth. *Geology* 30, 319–322.
- Martin, H., Smithies, R.H., Rapp, R., Moyen, J.F., Champion, D., 2005. An overview of adakite, TTG and sanukitoid: relationships and some implications for crustal evolution. *Lithos* 79, 1–24.
- Martin, W., Müller, M., 1998. The hydrogen hypothesis for the first eukaryote. *Nature* 392, 37–41.
- Martin, W., Russell, M.J., 2007. On the origin of biochemistry at an alkaline hydrothermal vent. *Philosophical Transactions of the Royal Society of London, Series B* 362, 1887–1925.
- Mason, T.R., von Brunn, V., 1977. 3-Gyr-old stromatolites from South Africa. *Nature* 266, 47–49.
- Master, S., 1991. Stratigraphy, tectonic setting, and mineralization of the early Proterozoic Magondi Supergroup, Zimbabwe: a review. *EGRU Information Circular* 238, 75.
- [AU22] Matsui, T., Abe, Y., 1986a. Impact-induced atmospheres and oceans on Earth and Venus. *Nature* 322, 526–528.
- Matsui, T., Abe, Y., 1986b. Evolution of an impact-induced atmosphere and magma ocean on the accreting Earth. *Nature* 319, 303–305.
- Maurice, C., David, J., Bédard, J.H., Francis, D., 2009. Evidence for a widespread mafic cover sequence and its implications for continental growth in the northeastern Superior Province. *Precambrian Research* 168, 45–65.
- Mawson, D., 1949. The late Precambrian ice-age and glacial record of the Bibliando dome. *Journal of the Proceedings of the Royal Society of New South Wales* 82, 150–174.
- Mazumder, R., Bose, P.K., Sarkar, S., 2000. A commentary on the tectono-sedimentary record of the pre-2.0 Ga continental growth of India vis-a-vis a possible pre-Gondwana Afro-indian supercontinent. *Journal of African Earth Sciences* 30, 201–217.
- McArthur, J.M., Coleman, M.L., Bremner, J.M., 1980. Carbon and oxygen isotopic composition of structural carbonate in sedimentary francolite. *Journal of the Geological Society of London* 137, 669–673.
- McArthur, J.M., Benmore, R.A., Coleman, M.L., Soldi, C., Yeh, H.-W., O’Brien, G.W., 1986. Stable isotopic characterisation of francolite formation. *Earth and Planetary Science Letters* 77, 20–34.
- McCall, G.J.H., 2006. The Vendian (Ediacaran) in the geological record: Enigmas in geology’s prelude to the Cambrian explosion. *Earth-Science Reviews* 77, 1–229.
- McCarthy, T.S., 2006. The Witwatersrand Supergroup. In: Johnson, M.R., Anhaeusser, C.R., Thomas, R.J. (Eds.), *The Geology of South Africa*. Geological Society of South Africa & Council for Geoscience, Johannesburg & Pretoria, pp. 155–186.
- McCullom, T.M., 2003. Formation of meteorite hydrocarbons from thermal decomposition of siderite (FeCO₃). *Geochimica et Cosmochimica Acta* 67, 311–317.
- McCullom, T.M., Seewald, J.S., 2006. Carbon isotope composition of organic compounds produced by abiotic synthesis under hydrothermal conditions. *Earth and Planetary Science Letters* 243, 74–84.
- McCulloch, M.T., 1993. The role of subducted slabs in an evolving Earth. *Earth and Planetary Science Letters* 115, 89–100.
- McCulloch, M.T., Bennett, V.C., 1994. Progressive growth of the Earth’s continental crust and depleted mantle: geochemical constraints. *Geochimica et Cosmochimica Acta* 58, 4717–4738.
- McFadden, K.A., Huang, J., Chu, X., Jiang, G., Kaufman, A.J., Zhou, C., Yuan, X., Shuhai, X., 2008. Pulsed oxidation and biological evolution in the Ediacaran Doushantuo Formation. *Proceedings of the National Academy of Sciences* 105, 3197–3202.
- McKeegan, K.D., Kudryavtsev, A.B., Schopf, J.W., 2007. Raman and ion microscopic imagery of graphitic inclusions in apatite from older than 3830 Ma Akilia supracrustal rocks, west Greenland. *Geology* 35, 591–594.
- McSwiggen, P.L., Morey, G.B., Weiblen, P.W., 1986. Uranium in early Proterozoic phosphate-rich metasedimentary rocks of east-central Minnesota. *Economic Geology* 81, 173–183.
- Melezhik, V.A., Fallick, A.E., Makarikhin, V.V., Lubtsov, V.V., 1997. Links between Palaeoproterozoic palaeogeography and rise and decline of stromatolites: Fennoscandian Shield. *Precambrian Research* 82, 311–348.
- Melezhik, V.A., Fallick, A.E., Medvedev, P.V., Makarikhin, V.V., 1999a. Extreme ¹³Ccarb enrichment in ca. 2.0 Ga magnesite-stromatolite-dolomite-‘red beds’ association in a global context: a case for the worldwide signal enhanced by a local environment. *Earth-Science Reviews* 48, 71–120.
- Melezhik, V.A., Fallick, A.E., Filippov, M.M., Larsen, O., 1999b. Karelian shungite—an indication of 2.0 Ga-old metamorphosed oil-shale and generation of petroleum: geology, lithology and geochemistry. *Earth-Science Reviews* 47, 1–40.
- Melezhik, V.A., Filippov, M.M., Romashkin, A.E., 2004. A giant Palaeoproterozoic deposit of shungite in NW Russia: genesis and practical applications. *Ore Geology Reviews* 24, 135–154.
- Melezhik, V.A., Fallick, A.E., Hanski, E.J., Kump, L.R., Lepland, A., Prave, A.R., Strauss, H., 2005a. Emergence of the aerobic biosphere during the Archean-Proterozoic transition: Challenges of future research. *GSA Today* 15, 4–11.
- Melezhik, V.A., Fallick, A.E., Rychanchik, D.V., Kuznetsov, A.B., 2005b. Palaeoproterozoic evaporites in Fennoscandia: Implications for seawater sulfate, $\delta^{13}\text{C}$ excursions and the rise of atmospheric oxygen. *Terra Nova* 17, 141–148.
- Melezhik, V.A., 2006. Multiple causes of Earth’s earliest global glaciation. *Terra Nova* 18, 130–137.
- Melezhik, V.A., Huhma, H., Condon, D.J., Fallick, A.E., Whitehouse, M.J., 2007. Temporal constraints on the Paleoproterozoic Lomagundi-Jatuli carbon isotopic event. *Geology* 35, 655–658.
- Meyer, C., Williams, I.S., Compston, W., 1989. ²⁰⁷Pb/²⁰⁶Pb ages of zircon-containing rock fragments indicate continuous magmatism in the lunar crust from 4350 to 3900 million years. Abstracts from the 20th Lunar

- and Planetary Science Conference. Lunar & Planetary Institute, Houston, pp. 691–692.
- Miller, R.A., 1983. A progress report: uranium-phosphorous association in the Helikian Thelon Formation and sub-Thelon saprolite, central District of Keewatin. Geological Survey of Canada, Paper 83–1A, 449–456.
- Miller, A.R., Cumming, G.L., Krstic, D., 1989. U-Pb, Pb-Pb, and K-Ar isotopic study and petrography of uraniferous phosphate-bearing rocks in the Thelon Formation, Dubawnt Group, Northwest Territories, Canada. Canadian Journal of Earth Sciences 26, 867–880.
- Miller, S.L., 1953. A production of amino acids under possible primitive Earth conditions. Science 117, 528–529.
- Miller, S.L., Bada, J.L., 1988. Submarine hot springs and the origin of life. Nature 334, 609–611.
- Misi, A., Kaufman, A.J., Veizer, J., Powis, K., Azmy, K., Boggiani, P.C., Gaucher, C., Teixeira, J.B.G., Sanches, A.L., Iyer, S.S., 2006. Chemostratigraphic correlation of Neoproterozoic succession in South America. Chemical Geology 237, 143–167.
- Mojzsis, S.J., Arrhenius, G., McKeegan, K.D., Harrison, T.M., Nutman, A.P., Friend, C.R.L., 1996. Evidence for life on Earth before 3,800 million years ago. Nature 384, 55–59.
- Mojzsis, S.J., Harrison, T.M., Pidgeon, R.T., 2001. Oxygen-isotope evidence from ancient zircons for liquid water at the Earth's surface 4,300 Myr ago. Nature 409, 178–181.
- Mojzsis, S.J., 2007. Sulphur on early Earth. In: Van Kranendonk, M.J., Smithies, R.H., Bennett, V. (Eds.), Earth's Oldest Rocks. *Developments in Precambrian Geology*, 15. Elsevier, Amsterdam, pp. 923–970.
- Moorbath, S., 2005. Oldest rocks, earliest life, heaviest impacts, and the Hadean-Archaeon transition. Applied Geochemistry 20, 819–824.
- Moore, E.M., 1993. Neoproterozoic oceanic crustal thinning, emergence of continents, and origin of the Phanerozoic ecosystem: a model. Geology 21, 5–8.
- Morbidelli, A., Chambers, J., Lunine, J.I., Petit, J.M., Robert, F., Valsecchi, G.B., Cyr, E., 2000. Source regions and timescales for the delivery of water to the Earth. Meteoritic and Planetary Science 35, 1309–1320.
- Moreira, D., López-García, P., 1998. Symbiosis between methanogenic Archaea and δ -Proteobacteria as the origin of eukaryotes: The Syntrophic Hypothesis. Journal of Molecular Evolution 47, 517–530.
- Morris, R.C., Horwitz, R.C., 1983. The origin of the iron-formation-rich Hamersley Group of Western Australia – deposition on a platform. Precambrian Research 21, 273–297.
- Moser, D.E., Heaman, L.M., 1997. Proterozoic zircon growth in Archean lower crustal xenoliths, southern Superior craton – A consequence of Matachewan ocean opening. Contributions to Mineralogy and Petrology 128, 164–175.
- Moser, D.E., Bowman, J.R., Wooden, J., Valley, J.W., Mazdab, F., Kita, N., 2008. Creation of a continent recorded in zircon zoning. Geology 36, 239–242.
- Mossman, D.J., Dyer, B.D., 1985. The geochemistry of Witwatersrand-type gold deposits and the possible influence of ancient prokaryotic communities on gold dissolution and precipitation. Precambrian Research 30, 303–319.
- Mossman, D.J., Gauthier-Lafaye, F., Jackson, S.E., 2005. Black shales, organic matter, ore genesis and hydrocarbon generation in the Paleoproterozoic Franceville Series, Gabon. Precambrian Research 137, 253–272.
- Moyen, J.-F., Stevens, G., Kisters, A.F.M., Belcher, R.W., 2007. TTG plutons of the Barberton granitoid-greenstone terrain, South Africa. In: Van Kranendonk, M.J., Smithies, R.H., Bennett, V. (Eds.), Earth's Oldest Rocks. *Developments in Precambrian Geology*, 15. Elsevier, Amsterdam, pp. 607–668.
- Myers, J.S., Shaw, R.D., Tyler, I.M., 1996. Tectonic evolution of Proterozoic Australia. Tectonics 15, 1431–1446.
- Nagovitsin, K., 2009. *Tappania*-bearing association of the Siberian platform: biodiversity, stratigraphic position and geochronological constraints. Precambrian Research 173, 137–145.
- Naraoka, H., Ohtake, M., Maruyama, S., Ohmoto, H., 1996. Non-biogenic graphite in 3.8-Ga metamorphic rocks from the Isua district, Greenland. Chemical Geology 133, 251–260.
- Narbonne, G.M., 1998. The Ediacaran biota: a terminal Neoproterozoic experiment in the evolution of life. GSA Today 8, 1–6.
- Narbonne, G.M., 2005. The Ediacara biota: Neoproterozoic origin of animals and their ecosystems. Annual Reviews of Earth and Planetary Sciences 33, 421–442.
- Nelson, D.R., 1998. Granite-greenstone crust formation on Archaean Earth: a consequence of two superimposed processes. Earth and Planetary Science Letters 158, 109–119.
- Nemchin, A., Pidgeon, R.T., 1998. Precise conventional and SHRIMP baddeleyite U-Pb age for the Binneringie Dyke, near Narrogin, Western Australia. Australian Journal of Earth Sciences 45, 673–675.
- Nemchin, A., Timms, N., Pidgeon, R., Geisler, T., Meyer, C., 2009. Timing of crystallization of the lunar magma ocean by the oldest zircon. Nature Geoscience 2, 133–136.
- Nesbitt, H.W., Young, G.M., 1982. Early Proterozoic climates and plate motions inferred from major element chemistry of lutites. Nature 299, 715–717.
- Neuweiler, F., Turner, E.C., Burdige, D.J., 2009. Early Neoproterozoic origin of the metazoan clade recorded in carbonate rock texture. Geology 37, 475–478.
- Nikitina, A.P., Shchipskiy, A.A., 1987. Phosphorus resources in the early Proterozoic deposits of Belgorod district, KMA. Izvestiya Akademii Nauk SSSR, Seriya Geologicheskaya 2, 113–124.
- Nilsson, M.K., Söderlund, U., Ernst, R.E., Hamilton, M.E., Schersten, A., Armitage, P.E.B., 2010. Precise U-Pb baddeleyite ages of mafic dykes and intrusions in southern West Greenland and implications for a possible reconstruction with the Superior craton. Precambrian Research 183, 399–415.
- Nimmo, F., Hart, S.D., Korycansky, D.G., Agnor, C.B., 2008. Implications of an impact origin for the martian hemispheric dichotomy. Nature 453, 1220–1223.
- Nisbet, E.G., 1982. Definition of 'Archaean' – comment and a proposal on the recommendations of the International Precambrian subcommission on Precambrian stratigraphy. Precambrian Research 19, 111–118.
- Nisbet, E.G., 1991. Of clocks and rocks – The four aeons of Earth. Episodes 14, 327–330.
- Nisbet, E.G., 2000. The realms of Archaean life. Nature 405, 625–626.
- Nisbet, E.G., Sleep, N.H., 2001. The habitat and nature of early life. Nature 409, 1083–1091.
- Nisbet, E.G., Grassineau, N.V., Howe, C.J., Abell, P.I., Regelous, M., Nisbet, R.E.R., 2007. The age of Rubisco: the evolution of oxygenic photosynthesis. Geobiology 5, 311–335.
- Noble, S.R., Lightfoot, P.C., 1992. U-Pb baddeleyite ages of the Kerns and Triangle Mountain intrusions, Nipissing Diabase, Ontario. Canadian Journal of Earth Sciences 29, 1424–1429.

- Noffke, N., Hazen, R., Nhlenko, N., 2003. Earth's earliest microbial mats in a siliciclastic marine environment (2.9 Ga Mozaan Group, South Africa). *Geology* 31, 673–676.
- Noffke, N., Hazen, R.N., Eriksson, K.A., Simpson, E.L., 2006. A new window into early life: Microbial mats in siliciclastic early Archean tidal flat (3.2 Ga Moodies Group, South Africa). *Geology* 34, 253–256.
- Noffke, N., Beukes, N., Bower, D., Hazen, R.M., Swift, J.P., 2008. An actualistic perspective into Archean worlds – (cyano-)bacterially induced sedimentary structures in the siliciclastic Nhlazatse Section, 2.9 Ga Pongola Supergroup, South Africa. *Geobiology* 6, 5–20.
- Noffke, N., 2008. Turbulent lifestyles: Microbial mats on Earth's sandy beaches—Today and 3 billion years ago. *GSA Today* 18, 4–9.
- Norman, M., 2009. The Lunar cataclysm: Reality or “Mythconception”? *Elements* 5, 23–28.
- Notholt, A.J.G., Sheldon, R.P., 1986. Proterozoic and Cambrian phosphorites – regional review: world resources. In: Cook, P.J., Shergold, J.H. (Eds.), *Phosphate Deposits of the World*. vol. 1, Proterozoic and Cambrian Phosphorites. Cambridge University Press, Cambridge, pp. 9–19.
- Nutman, A.P., Friend, C.R.L., Baadsgaard, H., McGregor, V.R., 1989. Evolution and assembly of Archean gneiss terranes in the Godthåbsfjord region, southern West Greenland: Structural, metamorphic, and isotopic evidence. *Tectonics* 8, 573–589.
- Nutman, A.P., McGregor, V.R., Friend, C.R.L., Bennett, V.C., Kinny, P.D., 1996. The Itsaq gneiss complex of southern West Greenland; the world's most extensive record of early crustal evolution. *Precambrian Research* 78, 1–39.
- Nutman, A.P., Mojzsis, S.J., Friend, C.R.L., 1997. Recognition of ≥ 3850 Ma water-lain sediments in West Greenland and their significance for the early Archean Earth. *Geochimica et Cosmochimica Acta* 61, 2475–2484.
- Nutman, A.P., Bennett, V.C., Friend, C.R.L., Norman, C.D., 1999. Meta-igneous (non-gneissic) tonalites and quartz-diorites from an extensive ca. 3800 Ma terrain south of the Isua supracrustal belt, southern West Greenland: constraints on early crust formation. *Contributions to Mineralogy and Petrology* 137, 364–388.
- Nutman, A.P., Friend, C.R.L., Bennett, V.C., 2002. Evidence for 3650–3600 Ma assembly of the northern end of the Itsaq Gneiss complex, Greenland: implications for early Archean tectonics. *Tectonics* 21 (1005), p. 28.
- Nutman, A.P., Friend, C.R.L., Horie, K., Hidaka, H., 2007. The Itsaq Gneiss Complex of southern West Greenland and the construction of Eoarchean crust at convergent plate boundaries. In: Van Kranendonk, M.J., Smithies, R.H., Bennett, V. (Eds.), *Earth's Oldest Rocks*. Developments in Precambrian Geology, 15. Elsevier, Amsterdam, pp. 187–218.
- Nutman, A.P., Heiss, J., 2009. A granitic inclusion suite within igneous zircons from a 3.81 Ga tonalite (W. Greenland): Restrictions for Hadean crustal evolution studies using detrital zircons. *Chemical Geology* 261, 76–81.
- Nutman, A.P., Friend, C.R.L., Paxton, S., 2009. Detrital zircon sedimentary provenance ages for the Eoarchean Isua supracrustal belt southern West Greenland: Juxtaposition of an imbricated ca. 3700 Ma juvenile arc against an older complex with 3920–3760 Ma components. *Precambrian Research* 172, 212–233.
- Nyquist, L.E., Bogard, D.D., Shih, C.Y., Greshake, A., Stoffer, D., Eugster, O., 2001. Ages and geologic histories of Martian meteorites. *Space Science Reviews* 96, 105–164.
- Nyquist, L.E., Kleine, T., Shih, C.-Y., Reese, Y.D., 2009. The distribution of short-lived radioisotopes in the early solar system and the chronology of asteroid accretion, differentiation, and secondary mineralization. *Geochimica et Cosmochimica Acta* 73, 5115–5136.
- O'Brien, G.W., Veeh, H.H., 1980. Holocene phosphorite on the East Australian continental margin. *Nature* 288, 690–692.
- O'Neil, J., Maurice, C., Stevenson, R.K., Larocque, J., Cloquet, C., David, J., Francis, D., 2007. The geology of the 3.8 Ga Nuvvuagittuq (Porpoise Cove) greenstone belt, northeastern Superior Province, Canada. In: Van Kranendonk, M.J., Smithies, R.H., Bennet, V. (Eds.), *Earth's Oldest Rocks*. Developments in Precambrian Geology, 15. Elsevier, Amsterdam, pp. 219–250.
- O'Neil, J., Carlson, R.W., Francis, D., Stevenson, R.K., 2008. Neodymium-142 evidence for Hadean mafic crust. *Science* 321, 1828–1831.
- O'Neil, J., Francis, D., Carlson, R., 2011. Implications of the Nuvvuagittuq greenstone belt for the formation of Earth's early crust. *Journal of Petrology* 52, 985–1009.
- O'Neill, C., Lenardic, A., Moresi, L., Torsvik, T.H., Lee, C.-T.A., 2007. Episodic Precambrian subduction. *Earth and Planetary Science Letters* 262, 552–562.
- Ohmoto, H., Watanabe, Y., Kumazawa, K., 2004. Evidence from massive siderite beds for a CO₂-rich atmosphere before ~1.8 billion years ago. *Nature* 429, 395–399.
- Ohmoto, H., Watanabe, Y., Ikemi, H., Poulson, S.R., Taylor, B.E., 2006. Sulphur isotope evidence for an oxic Archean atmosphere. *Nature* 442, 908–911.
- Ojakangas, R.W., 1988. Glaciation: An uncommon “mega-event” as a key to intracontinental and intercontinental correlation of Early Proterozoic basin fill, North American and Baltic cratons. In: Kleinspehn, K.L., Paola, C. (Eds.), *New perspectives in basin analysis*. Springer, New York, pp. 431–444.
- Ojakangas, R.W., Marmo, J.S., Heiskanen, K.I., 2001. Basin evolution of the Paleoproterozoic Karelian Supergroup of the Fennoscandian (Baltic) Shield. *Sedimentary Geology* 141–142, 255–286.
- Okulitch, A.V., 2004. Geological time chart, 2004. Geological Survey of Canada.
- Olson, J.M., 2006. Photosynthesis in the Archean Era. *Photosynthesis Research* 88, 109–117.
- Ono, S., Eigenbrode, J.L., Pavlov, A., Kharecha, P., Rumble III, D., Kasting, J.F., Freeman, K.H., 2003. New insights into Archean sulphur cycle from mass-independent sulfur isotope records from the Hamersley Basin, Australia. *Earth and Planetary Science Letters* 213, 15–30.
- Ono, S., Beukes, N.J., Rumble, D., Fogel, M.L., 2006. Early evolution of atmospheric oxygen from multiple-sulfur and carbon isotope records of the 2.9 Ga Mozaan Group of the Pongola Supergroup, Southern Africa. *South African Journal of Geology* 107, 97–108.
- Ono, S., Beukes, N.J., Rumble, D., 2009. Origin of two distinct multiple-sulfur isotope compositions of pyrite in the 2.5 Ga Kleine Naute Formation, Griqualand West basin, South Africa. *Precambrian Research* 169, 48–57.
- Oparin, A.I., 1938. *The Origin of Life*. MacMillan, New York, p. 267.
- Pace, N.R., 1997. A molecular view of microbial diversity and the biosphere. *Science* 276, 734–740.
- Packer, B.M., 1990. Sedimentology, paleontology, and stable-isotope geochemistry of selected formations in the 2.7-billion-year-old Fortescue Group, Western Australia. Ph.D. thesis. University of California, Los Angeles, p. 187.
- Pahlevan, K., Stevenson, D.J., 2005. The oxygen isotope similarity between the Earth and Moon – source region or formation process? Abstract

- from the 36th Lunar and Planetary Science Conference. Lunar and Planetary Institute, abstract no. 2382, Houston.
- Pais, M.A., Le Mouél, J.L., Lambeck, K., Poirier, J.P., 1999. Late Precambrian paradoxical glaciation and obliquity of the Earth – a discussion of geodynamical constraints. *Earth and Planetary Science Letters* 174, 155–171.
- Papineau, D., Mojzsis, S.J., Schmitt, A.K., 2007. Multiple sulfur isotopes from Paleoproterozoic Huronian interglacial sediments and the rise of atmospheric oxygen. *Earth and Planetary Science Letters* 255, 188–212.
- Papineau, D., Purohit, R., Goldberg, T., Pi, D., Shields, G.A., Bhu, H., Steele, A., Fogel, M.L., 2009. High primary productivity and nitrogen cycling after the Paleoproterozoic phosphogenic event in the Aravalli Supergroup, India. *Precambrian Research* 171, 37–56.
- Papineau, D., 2010. Global biogeochemical changes at both ends of the Proterozoic: Insights from phosphorites. *Astrobiology* 10, 165–181.
- Parák, T., 1973. Rare Earths in the apatite iron ores of Lappland together with some data about the Sr, Th and U content of these ores. *Economic Geology* 68, 210–221.
- Parman, S.W., 2007. Helium isotopic evidence for episodic mantle melting and crustal growth. *Nature* 446, 900–903.
- Parnell, J., Boyce, A.J., Mark, D., Bowden, S., Spinks, S., 2010. Early oxygenation of the terrestrial environment during the Mesoproterozoic. *Nature* 468, 290–293.
- Partridge, M., Golding, S.D., Baublys, K.A., Young, E., 2008. Pyrite parageneses and multiple sulfur isotope distribution in late Archean and early Proterozoic Hamersley Basin sediments. *Earth and Planetary Science Letters* 272, 41–49.
- Passchier, S., Erukanure, E., 2010. Paleoenvironments and weathering regime of the Neoproterozoic Squantum ‘Tillite’, Boston: no evidence of a snowball Earth. *Sedimentology* 57, 1526–1544.
- Pavlov, A.A., Kasting, J.F., Brown, L.L., 2001a. UV-shielding of NH₃ and O₂ by organic hazes in the Archean atmosphere. *Journal of Geophysical Research* 106, 23267–23287.
- Pavlov, A.A., Kasting, J.F., Eigenbrode, J.L., Freeman, K.H., 2001b. Organic haze in Earth’s early atmosphere: Source of low-¹³C late Archean kerogens? *Geology* 29, 1003–1006.
- Pavlov, A.A., Kasting, J.F., 2002. Mass-independent fractionation of sulfur isotopes in Archean sediments: Strong evidence for an anoxic Archean atmosphere. *Astrobiology* 2, 27–41.
- Pavlov, A.A., Hurtgen, M.T., Kasting, J.F., Arthur, M.A., 2003. Methane-rich Proterozoic atmosphere? *Geology* 31, 87–90.
- Payne, J.L., Hand, M., Barovich, K.M., Reid, A., Evans, D.A.D., 2009. Correlations and reconstruction models for the 2500–1500 Ma evolution of the Mawson Continent. In: Reddy, S.M., Mazumder, R., Evans, D.A.D., Collins, A.S. (Eds.), *Paleoproterozoic supercontinents and Global Evolution*. Geological Society of London, Special Publications, 323, pp. 319–356.
- Payton, C.E., 1977. Seismic stratigraphy – applications to hydrocarbon exploration. *American Association of Petroleum Geology, Memoir* 26, 516.
- Pearson, D.G., Parman, S.W., Nowell, G.M., 2007. Events and continent growth seen in osmium isotopes. *Nature* 449, 202–205.
- Pease, V., Percival, J., Smithies, R.H., Stevens, G., Van Kranendonk, M.J., 2008. When did plate tectonics begin? Evidence from the orogenic record. In: Condie, K.C., Pease, V. (Eds.), *When did plate tectonics begin on Earth?* Geological Society of America, Special Paper, 440, pp. 199–228.
- Pecoits, E., Gingras, M., Aubet, N., Konhauser, K., 2007. Ediacaran in Uruguay: palaeoclimatic and palaeobiological implications. *Sedimentology* 55, 689–719.
- Percival, J.A., Sanborne-Barrie, M., Skulski, T., Stott, G.M., Helmstaedt, H., White, D.J., 2006. Tectonic evolution of the western Superior Province from NATMAP and Lithoprobe studies. *Canadian Journal of Earth Sciences* 43, 1085–1117.
- Percival, J.A., 2007. Eo- to Mesoarchean terranes of the Superior Province and their tectonic context. In: Van Kranendonk, M.J., Smithies, R.H., Bennet, V. (Eds.), *Earth’s Oldest Rocks*. Developments in Precambrian Geology, 15. Elsevier, Amsterdam, pp. 1065–1085.
- Perttunen, V., 1985. On the Proterozoic stratigraphy and exogenic evolution of the Peräpohja area, Finland. In: Laajoki, K., Paakkola, J. (Eds.), *Proterozoic Exogenic Processes and Related Metallogeny*. Geological Survey of Finland, Bulletin, 331, pp. 131–141.
- Peter, J., 2003. Ancient iron formations: their genesis and use in the exploration for stratiform base metal sulfide deposits, with examples from the Bathurst Mining Camp. In: Lentz, D.R. (Ed.), *Geochemistry of sediments and sedimentary rocks: evolutionary considerations to mineral deposit-forming environments*. Geological Association of Canada, *Geotext*, 4, pp. 145–176.
- Philippot, P., Van Zuilen, M., Lepot, K., Thomazo, C., Farquhar, J., Van Kranendonk, M.J., 2007. Early Archean microorganisms preferred elemental sulphur, not sulfate. *Science* 317, 1534–1537.
- Pickard, A.L., 2002. SHRIMP U-Pb zircon ages of tuffaceous mudrocks in the Brockman Iron Formation of the Hamersley Range, Western Australia. *Australian Journal of Earth Sciences* 49, 491–507.
- Pickard, A.L., 2003. SHRIMP U-Pb zircon ages for the Palaeoproterozoic Kuruman Iron Formation, Northern Cape Province, South Africa: evidence for simultaneous BIF deposition on Kaapvaal and Pilbara Cratons. *Precambrian Research* 125, 275–315.
- Pidgeon, R.T., Nemchin, A.A., Meyer, C., 2010. The contribution of the sensitive high-resolution ion microprobe (SHRIMP) to lunar geochronology. *Precambrian Research* 183, 44–49.
- Pierrehumbert, R.T., 2004. High levels of atmospheric carbon dioxide necessary for the termination of global glaciation. *Nature* 429, 646–649.
- Pirajno, F., Grey, K., 2002. Chert in the Paleoproterozoic Bartle Member, Killara Formation, Yerrida Basin, Western Australia: a rift-related playa lake and thermal spring environment? *Precambrian Research* 113, 169–192.
- Pirajno, F., Hocking, R.M., Reddy, S.M., Jones, A.J., 2009. A review of the geology and geodynamic evolution of the Palaeoproterozoic Earraheedy Basin, Western Australia. *Earth-Science Reviews* 94, 39–77.
- Pirajno, F., 2009. *Hydrothermal Mineral Systems*. Springer, Berlin, p. 1250.
- Planavsky, N., Rouxel, O., Bekker, A., Shapiro, R., Fralick, P., Knudsen, A., 2009. Iron-oxidizing microbial ecosystems thrived in late Paleoproterozoic redox-stratified oceans. *Earth and Planetary Science Letters* 286, 230–242.
- Plumb, K.A., James, H.L., 1986. Subdivision of Precambrian time: recommendations and suggestions by the submission on Precambrian stratigraphy. *Precambrian Research* 32, 65–92.
- Plumb, K.A., 1991. New Precambrian time scale. *Episodes* 14, 139–140.
- Polat, A., Hofmann, A.W., Rosing, M.T., 2002. Boninite-like volcanic rocks in the 3.7–3.8 Ga Isua greenstone belt, West Greenland: geochemical evidence for intra-oceanic subduction zone processes in the early Earth. *Chemical Geology* 184, 231–254.
- Polito, P.A., Kyser, T.K., Thomas, D., Marlatt, J., Drever, G., 2005. Re-evaluation of the petrogenesis of the Proterozoic Jabiluka

- unconformity-related uranium deposit, Northern Territory, Australia. *Mineralium Deposita* 40, 257–288.
- Pollack, G.D., Krogstad, E.J., Bekker, A., 2009. U-Th-Pb-REE systematic of organic-rich shales from the ca. 2.15 Ga Sengoma Argillite Formation, Botswana: Evidence for oxidative continental weathering during the Great Oxidation Event. *Chemical Geology* 260, 172–185.
- Pollack, H.N., 1997. Thermal characteristics of the Archaean. In: de Wit, M., Ashwal, L. (Eds.), *Greenstone belts*. Oxford University Press, Oxford, pp. 223–232.
- Polteau, S., Moore, J.M., Tsikos, H., 2006. The geology and geochemistry of the Palaeoproterozoic Makganyene diamictite. *Precambrian Research* 148, 257–274.
- Porter, S.M., 2004. The fossil record of early eukaryote diversification. *Paleontological Society Papers* 10, 35–50.
- Posth, N.R., Hegler, F., Konhauser, K.O., Kappler, A., 2008. Alternating Si and Fe deposition caused by temperature fluctuations in Precambrian oceans. *Nature Geoscience* 1, 703–708.
- Poulton, S.W., Frallick, P.W., Canfield, D.E., 2004. The transition to a sulphidic ocean ~1.84 billion years ago. *Nature* 431, pp. 179–178.
- Poulton, S.W., Frallick, P.W., Canfield, D.E., 2010. Spatial variability in oceanic redox structure 1.8 billion years ago. *Nature Geoscience* 3, 486–490.
- Powell, C.M., Li, Z.X., McElhinny, M.W., Meert, J.G., Park, J.K., 1993. Paleomagnetic constraints on timing of the Neoproterozoic breakup of Rodinia and the Cambrian formation of Gondwana. *Geology* 21, 889–892.
- Prasad, N., Roscoe, S.M., 1996. Evidence of anoxic to oxic atmospheric change during 2.45–2.22 Ga from lower and upper sub-Huronian paleosols, Canada. *Catena* 27, 105–121.
- Prave, A.R., 2002. Life on land in the Proterozoic: evidence from the Torridonian rocks of northwest Scotland. *Geology* 30, 811–814.
- Pufahl, P.K., Hiatt, E.E., Stanley, C.R., Nelson, G.J., Edwards, C.T., 2006. The iron to phosphorite oceanographic transition: a diachronous event along the Nunan continental margin as recorded in the ~1.8 billion year old Baraga group, Michigan and Ferriman Group, Labrador. *Geological Society of America Abstracts with Programs* 38 (7), 57.
- [AU23] Pufahl, P.K., Hiatt, E.E., Kyser, K., 2010. Does the Paleoproterozoic Aniakie Basin record the sulfidic ocean transition? *Geology* 38, 659–662.
- Rasmussen, B., 2000. Filamentous microfossils in a 3,235-million-year-old volcanogenic massive sulfide deposit. *Nature* 405, 676–679.
- Rasmussen, B., Bengston, S., Fletcher, I.R., McNaughton, N.J., 2002. Discoidal impression and trace-like fossils more than 1200 million years old. *Science* 296, 1112–1115.
- Rasmussen, B., Fletcher, I.R., 2002. Indirect dating of mafic intrusions by SHRIMP U–Pb analysis of monazite in contact metamorphosed shale: an example from the Paleoproterozoic Capricorn Orogen, Western Australia. *Earth and Planetary Science Letters* 197, 287–299.
- Rasmussen, B., Fletcher, I.R., Bengston, S., McNaughton, N.J., 2004. SHRIMP U–Pb dating of diagenetic xenotime in the Stirling Range Formation, Western Australia: 1.8 billion year minimum age for the Stirling biota. *Precambrian Research* 133, 329–337.
- Rautenbach, C.J.d., 2001. A hypothetical approach to determining the effect of palaeorotational rates on Earth's Neoproterozoic paleoclimate. *Journal of African Earth Sciences* 33, 463–473.
- Ray, J.S., Rainbird, R.H., Davis, W.J., 2008. U-Pb geochronology of authigenic xenotimes from Huronian Supergroup, Canada. *Goldschmidt Conference Abstracts. Geochimica et Cosmochimica Acta* 72 (12), A780.
- Reddy, S.M., Evans, D.A.D., 2009. Paleoproterozoic supercontinents and global evolution: Correlations from core to atmosphere. In: Reddy, S.M., Mazumder, R., Evans, D.A.D., Collins, A.S. (Eds.), *Paleoproterozoic supercontinents and Global Evolution*. Geological Society of London, Special Publications, 323, pp. 1–23.
- Rehtijärvi, P., Äikäs, O., Mäkelä, M., 1979. A middle Precambrian uranium- and apatite-bearing horizon associated with the Vihanti zinc ore deposit, Western Finland. *Economic Geology* 74, 1102–1117.
- Reinhard, C.T., Raiswell, R., Scott, C., Anbar, A., Lyons, T.W., 2009. A late Archean sulfidic sea stimulated by early oxidative weathering of the continents. *Science* 326, 713–716.
- Remane, J., 2003. Chronostratigraphic correlations: their importance for the definition of geochronologic units. *Palaeogeography, Palaeoclimatology, Palaeoecology* 196, 7–18.
- Rey, P.F., Philippot, P., Thébaud, N., 2003. Contribution of mantle plumes, crustal thickening and greenstone blanketing to the 2.75–2.65 Ga global crisis. *Precambrian Research* 127, 43–60.
- Rey, P.F., Houseman, G., 2006. Lithospheric scale gravitational flow: the impact of body forces on orogenic processes from Archaean to Phanerozoic. In: Butter, S.J.H., Schreurs, G. (Eds.), *Analogue and numerical modelling of crustal-scale processes*. Geological Society, London, Special Publications, 253, pp. 153–167.
- Rey, P.F., Coltice, N., 2008. Neoproterozoic lithosphere strengthening and the coupling of Earth's geochemical reservoirs. *Geology* 36, 635–638.
- Ribas, I., Guinan, E.F., Gudel, M., Audard, M., 2005. Evolution of the solar activity over time and effects on planetary atmospheres. I. High-energy irradiances (1–1700 angstrom). *Astrophysical Journal* 622, 680–694.
- Richter, F.M., 1988. A major change in the thermal state of the Earth at the Archean-Proterozoic boundary: Consequences for the nature and preservation of continental lithosphere. *Journal of Petrology, Special Lithosphere Issue* (1): pp. 39–52.
- Robb, L.J., Knoll, A.H., Plumb, K.A., Shields, G.A., Strauss, H., Veizer, J., 2004. The Precambrian: the Archean and Proterozoic Eons. In: Gradstein, F.M., Ogg, J.G., Smith, A.G. (Eds.), *A Geologic time Scale 2004*. Cambridge University Press, New York, pp. 129–140.
- Robert, F., Chaussidon, M., 2006. A palaeotemperature curve for the Precambrian oceans based on silicon isotopes in cherts. *Nature* 443, 969–972.
- Robock, A., Ammann, C.M., Oman, L., Shindell, D., Levis, S., Stenchikov, G., 2009. Did the Toba eruption of ~74 ka BP produce widespread glaciation? *Journal of Geophysical Research-Atmospheres* 114, D10107. doi:10.1029/2008JD011652.
- Rogers, J.J.W., Santosh, M., 2002. Configuration of Columbia, a Mesoproterozoic supercontinent. *Gondwana Research* 5, 5–22.
- Rollinson, H., 2008. Ophiolitic trondhjemites: a possible analogue for Hadean felsic 'crust'. *Terra Nova* 20, 364–369.
- Roscoe, S.M., 1973. The Huronian Supergroup: a Paleoproterozoic succession showing evidence of atmospheric evolution. *Geological Society of Canada, Special Paper* 12, 31–48.
- Roscoe, S.M., Card, K.D., 1993. The reappearance of the Huronian in Wyoming: Rifting and drifting of ancient continents. *Canadian Journal of Earth Sciences* 30, 2475–2480.
- Rose, N.M., Rosing, M.T., Bridgwater, D., 1996. The origin of metacarbonate rocks in the Archaean Isua Supracrustal Belt, West Greenland. *American Journal of Science* 296, 1004–1044.
- Rosing, M.T., Rose, N.M., Bridgwater, D., Thomsen, H.S., 1996. Earliest part of Earth's stratigraphic record: A reappraisal of the >3.7 Ga Isua (Greenland) supracrustal sequence. *Geology* 24, 43–46.

- Rosing, M.T., 1999. ^{13}C -depleted carbon microparticles in >3700 Ma sea-floor sedimentary rocks from West Greenland. *Science* 283, 674–676.
- Rosing, M.T., Frei, R., 2004. U-rich Archean sea-floor sediments from Greenland – indications of >3700 Ma oxygenic photosynthesis. *Earth and Planetary Science Letters* 217, 237–244.
- Rosing, M.T., Bird, D.K., Sleep, N.H., Glassley, W., Albarede, F., 2006. The rise of continents – an essay on the geologic consequences of photosynthesis. *Palaeogeography, Palaeoclimatology, Palaeoecology* 232.
- Rothschild, L.J., Mancinelli, R.L., 2001. Life in extreme environments. *Nature* 409, 1092–1101.
- Rouxel, O.J., Bekker, A., Edwards, K.J., 2005. Iron isotope constraints on the Archean and Paleoproterozoic ocean redox state. *Science* 207, 1088–1091.
- Roy, S., 2006. Sedimentary manganese metallogenesis in response to the evolution of the Earth system. *Earth-Science Reviews* 77, 273–305.
- Rubey, W.W., Poldervaart, A., 1955. Development of the hydrosphere and atmosphere, with special reference to probable composition of the early atmosphere. In: Poldervaart, A. (Ed.), *Crust of the Earth*. Geological Society of America, New York, pp. 631–650.
- Runnegar, B., 1991. Precambrian oxygen levels estimated from the biochemistry and physiology of early eukaryotes. *Palaeogeography, Palaeoclimatology, Palaeoecology* 71, 97–111.
- Russell, M.J., Hall, A.J., Cairns-Smith, A.G., Braterman, P.S., 1988. Submarine hot springs and the origin of life. *Correspondence*. *Nature* 336, 117.
- Russell, M.J., 1996. Life from the depths: The generation of life and ore deposits at hot springs. *Science Spectra* 1, 26–31.
- Russell, M.J., Hall, A.J., 2006. The onset and early evolution of life. In: Kesler, S.E., Ohmoto, H. (Eds.), *Evolution of Earth's atmosphere, hydrosphere, and biosphere – Constraints from ore deposits*. Geological Society of America, Memoir, 198, pp. 1–32.
- Russell, M.J., Hall, A.J., Martin, W., 2010. Serpentinization as a source of energy at the origin of life. *Geobiology* 8, 355–371.
- Ruttenberg, K.C., Berner, R.A., 1993. Authigenic apatite formation and burial in sediments from non-upwelling, continental margin environments. *Geochimica et Cosmochimica Acta* 57, 991–1007.
- Ryder, G., 2003. Bombardment of the Hadean Earth: Wholesome or deleterious? *Astrobiology* 3, 3–6.
- Rye, R., Kuo, P.H., Holland, H.D., 1995. Atmospheric carbon dioxide concentrations before 2.2 billion years ago. *Nature* 378, 603–605.
- Rye, R., Holland, H.D., 1998. Paleosols and the evolution of atmospheric oxygen: a critical review. *American Journal of Science* 298, 621–672.
- Safanova, I., Maruyama, S., Hirata, T., Kon, Y., Rino, S., 2010. LA ICP MS U–Pb ages of detrital zircons from Russia largest rivers: Implications for major granitoid events in Eurasia and global episodes of supercontinent formation. *Journal of Geodynamics* 50, 134–153.
- Sakurai, R., Ito, M., Ueno, Y., Kitajima, K., Maruyama, S., 2005. Facies architecture and sequence-stratigraphic features of the Tumbiana Formation in the Pilbara Craton, northwestern Australia: Implications for depositional environments of oxygenic stromatolites during the Late Archean. *Precambrian Research* 138, 255–273.
- Santosh, M., 2010. A synopsis of recent conceptual models on supercontinent tectonics in relation to mantle dynamics, life evolution and surface environment. *Journal of Geodynamics* 50, 116–133.
- Santosh, M., Wilde, S.A., Li, J.H., 2007. Timing of Paleoproterozoic ultra-high-temperature metamorphism in the north China Craton: Evidence from SHRIMP U–Pb zircon geochronology. *Precambrian Research* 159, 178–196.
- Sarangi, S., Gopalan, K., Kumar, S., 2004. Pb–Pb age of earliest megascopic, eukaryotic alga bearing Rohtas Formation, Vindhyan Supergroup, India: implications for Precambrian atmospheric oxygen evolution. *Precambrian Research* 132, 107–121.
- Saul, J.M., 2009. Did detoxification processes cause complex life to emerge? *Lethaia* 42, 179–184.
- Schaefer, L., Fegley, J.B., 2007. Outgassing of ordinary chondritic material and some of its implications for the chemistry of asteroids, planets, and satellites. *Icarus* 186, 462–483.
- Schidlowski, M., Eichmann, R., Junge, C.E., 1976. Carbon isotope geochemistry of the Precambrian Lomagundi carbonate province, Rhodesia. *Geochimica et Cosmochimica Acta* 40, 449–455.
- Schidlowski, M., Appel, P.W.U., Eichmann, R., Junge, C.E., 1979. Carbon isotope geochemistry of the 3.7x10⁹-yr-old Isua sediments, West Greenland – implications for the Archean carbon and oxygen cycles. *Geochimica et Cosmochimica Acta* 43, 189–199.
- Schidlowski, M., 1988. A 3,800-million-year isotopic record of life from carbon in sedimentary rocks. *Nature* 333, 313–318.
- Schmidt, M., Southgate, P.N., 1982. A phosphatic stromatolite (*Ilicia* cf. *composita* Sidorov) from the middle Cambrian, Northern Australia. *Alcheringa: An Australasian Journal of Palaeontology* 6, 175–183.
- Schneider, D.A., Bickford, M.E., Cannon, W.F., Schulz, K.J., Hamilton, M.A., 2002. Age of volcanic rocks and syndepositional iron formations, Marquette Range Supergroup: implications for the tectonic setting of Paleoproterozoic iron formations of the Lake Superior region. *Canadian Journal of Earth Sciences* 39, 999–1012.
- Schneiderhan, E.A., Gutzmer, J., Strauss, H., Mezger, K., Beukes, N.J., 2006. The chemostratigraphy of a Paleoproterozoic MnF–BIF succession – the Voëlwater Subgroup of the Transvaal Supergroup in Griqualand West, South Africa. *South African Journal of Geology* 109, 63–80.
- Schoenberg, R., Kamber, B.S., Collerson, K.D., Moorbath, S., 2002. Tungsten isotope evidence from ~3.8-Gyr metamorphosed sediments for early meteorite bombardment of the Earth. *Nature* 418, 403–405.
- Scholl, D.W., von Huene, R., 2007. Crustal recycling at modern subduction zones applied to the past – Issues of crustal growth and preservation of continental basement crust, mantle geochemistry, and supercontinent reconstruction. In: Hatcher Jr., R.D., Carlson, M.P., McBride, J.H., Martínez Catalán, J.R. (Eds.), *4-D Framework of Continental Crust*. Geological Society of America, Memoir, 20, pp. 9–32.
- Schopf, J.W., Walter, M.R., 1983. Archean microfossils: New evidence of ancient microbes. In: Schopf, J.W. (Ed.), *Earth's earliest biosphere: its origin and evolution*. Princeton University Press, pp. 214–239.
- Schopf, J.W., 1992. The oldest fossils and what they mean. In: Schopf, J.W., Klein, C. (Eds.), *Major events in the history of life*. Jones & Bartlett, Boston, pp. 29–64.
- Schopf, J.W., 1993. Microfossils of the early Archean Apex chert: New evidence of the antiquity of life. *Science* 260, 640–646.
- Schopf, J.W., Kudryavtsev, A.B., Agresti, D.G., Wdowiak, T.J., Czaja, A.D., 2002. Laser-Raman imagery of Earth's earliest fossils. *Nature* 416, 73–76.
- Schopf, J.W., 2004. Earth's earliest biosphere: status of the hunt. In: Eriksson, P.G., Altermann, W., Nelson, D.R., Mueller, W., Catuneanu, O. (Eds.), *The Precambrian Earth: Tempos and Events*. *Developments in Precambrian Geology*, 12, pp. 516–538.
- Schopf, J.W., Kudryavtsev, A.B., Czaja, A.D., Tripathi, A.B., 2007. Evidence of Archean life: Stromatolites and microfossils. *Precambrian Research* 158, 141–155.

- Schrag, D.P., Berner, R.A., Hoffman, P.F., Halverson, G.P., 2002. On the initiation of snowball Earth. *Geochemistry, Geophysics, Geosystems* 3, 1036. doi:10.1029/2001GC000219.
- Schröder, S., Bekker, A., Beukes, N.J., Strauss, H., van Nieker, H.S., 2008. Rise in seawater sulfate concentration associated with the Paleoproterozoic positive carbon isotope excursion: evidence from sulfate evaporites in the ~2.2–2.1 Gyr shallow-marine Lucknow Formation, South Africa. *Terra Nova* 20, 108–117.
- Schweitzer, J.K., Hatton, C.J., de Waal, S.A., 1995. Regional lithochemical stratigraphy of the Rooiberg Group, upper Transvaal Supergroup: A proposed new subdivision. *South African Journal of Geology* 98, 245–255.
- Scott, D.J., St-Onge, M.R., Lucas, S.B., Helmstaedt, H., 1991. Geology and chemistry of the Early Proterozoic Purtuniqu ophiolite, Cape Smith Belt, northern Quebec, Canada. In: Peters, T., Nicolas, A., Coleman, R. (Eds.), *Ophiolite Genesis and Evolution of the Oceanic Lithosphere*. Kluwer, Dordrecht, pp. 817–849.
- Scott, E.R.D., Sanders, I.S., 2009. Implications of the carbonaceous chondrite Mn-Cr isochron for the formation of early refractory planetismals and chondrules. *Geochimica et Cosmochimica Acta* 73, 5137–5149.
- Segura, A., Meadows, V.S., Kasting, J.F., Crisp, D., Cohen, M., 2007. Abiotic formation of O₂ and O₃ in high-CO₂ terrestrial atmospheres. *Astronomy and Astrophysics* 472, 665–679.
- Sethumadhav, M.S., Gunnell, Y., Ahmed, M.M., Chinnaiyah, 2010. Late Archean manganese mineralization and younger supergene manganese ores in the Anmod-Bisgod region, western Dharwar Craton, southern India: Geological characterization, paleoenvironmental history, and geomorphological setting. *Ore Geology Reviews* 38, 70–89.
- Sharma, M., Shukla, Y., 2009. Taxonomy and affinity of Early Mesoproterozoic megascopic helically coiled and related fossils from the Rohtas Formation, the Vindhyan Supergroup, India. *Precambrian Research* 173, 105–122.
- Shen, Y., Buick, R., Canfield, D.E., 2001. Isotopic evidence for microbial sulfate reduction in the early Archean era. *Nature* 410, 77–81.
- Shen, Y., Canfield, D.E., Knoll, A.H., 2002. Middle Proterozoic ocean chemistry: evidence from the McArthur basin, northern Australia. *American Journal of Science* 302, 81–109.
- Shen, Y., Knoll, A.H., Walter, M.R., 2003. Evidence for low sulfate and anoxia in a mid-Proterozoic marine basin. *Nature* 423, 632–634.
- Shields-Zhou, G., Och, L., 2011. The case for a Neoproterozoic oxygenation event: geochemical evidence and biological consequences. *GSA Today* 21, 4–11.
- Shields, G., Veizer, J., 2002. Precambrian marine carbonate isotope database: Version 1.1. *Geochemistry, Geophysics, Geosystems* 3, 1031. doi:10.1029/2001GC000266.
- Shields, G.A., Kasting, J.F., 2007. Evidence for hot early oceans? *Nature* 447, E1–E2.
- Shields, G.A., 2008. A normalized seawater strontium isotope curve and the Neoproterozoic–Cambrian chemical weathering event. *eEarth Discuss* 2, 69–84.
- Siebert, C., Kramers, J.D., Meisel, T., Morel, P., Nägler, T.F., 2005. PGE, Re-Os, and Mo isotope systematics in Archean and early Proterozoic sedimentary systems as proxies for redox conditions of the early Earth. *Geochimica et Cosmochimica Acta* 69, 1787–1801.
- Simonson, B.M., Schubel, K.A., Hassler, S.W., 1993. Carbonate sedimentology of the early Precambrian Hamersley Group of Western Australia. *Precambrian Research* 60, 287–335.
- Simonson, B.M., Sumner, D.Y., Beukes, N.J., Johnson, S., Gutzmer, J., 2009. Correlating multiple Neoproterozoic impact spherule layers between South African and Western Australia. *Precambrian Research* 169, 100–111.
- Sinha-Roy, S., Mohanty, M., Malhotra, G., Sharma, P., Joshi, D.W., 1993. Conglomerate horizons in south-central Rajasthan and their significance on Proterozoic stratigraphy and tectonics of the Aravalli and Delhi fold belts. *Journal of the Geological Society of India* 41, 331–350.
- Slack, J.F., Canon, W.F., 2009. Extraterrestrial demise of banded iron formations 1.85 billion years ago. *Geology* 37, 1011–1014.
- Slansky, M., 1986. Proterozoic and Cambrian phosphorites – regional review: West Africa. In: Cook, P.J., Shergold, J.H. (Eds.), *Phosphate Deposits of the World*. vol. 1, Proterozoic and Cambrian Phosphorites. Cambridge University Press, Cambridge, pp. 108–115.
- Sleep, N.H., Windley, B.F., 1982. Archean plate tectonics: Constraints and inferences. *The Journal of Geology* 90, 363–379.
- Sleep, N.H., Zahnle, K.J., Kasting, J.F., Morowitz, H.J., 1989. Annihilation of ecosystems by large asteroid impacts on the early Earth. *Nature* 342, 139–142.
- Sleep, N.H., 2005. Evolution of continental lithosphere. *Annual Review of Earth and Planetary Sciences* 33, 369–393.
- Sleep, N.H., Hessler, A.M., 2006. Weathering of quartz as an Archean climate indicator. *Earth and Planetary Science Letters* 241, 594–602.
- Sleep, N.H., Bird, D.K., 2007. Niches of the pre-photosynthetic biosphere and geologic preservation of Earth's earliest ecology. *Geobiology* 5, 101–117.
- Sleep, N.H., Bird, D.K., 2008. Evolutionary ecology during the rise of dioxygen in the Earth's atmosphere. *Philosophical Transactions of the Royal Society, Series B, Biological Sciences* 363, 2651–2664.
- Smith, A.J.B., Beukes, N.J., Gutzmer, J., Cochrane, J.M., 2010. Evidence for dissimilatory manganese reduction and availability of free molecular oxygen during deposition of Mesoarchean Witwatersrand-Mozaan strata. *Goldschmidt Conference Abstracts*. *Geochimica et Cosmochimica Acta* 74 (Suppl. 1), A973.
- Smithies, R.H., 2000. The Archean tonalite-trondhjemite-granodiorite (TTG) series is not an analogue of Cenozoic adakite. *Earth and Planetary Science Letters* 182, 115–125.
- Smithies, R.H., Champion, D.C., Cassidy, K.F., 2003. Formation of Earth's early Archean continental crust. *Precambrian Research* 127, 89–101.
- Smithies, R.H., Champion, D.C., Van Kranendonk, M.J., Howard, H.M., Hickman, A.H., 2005a. Modern-style subduction processes in the Mesoarchean: Geochemical evidence from the 3.12 Ga Whundo intra-oceanic arc. *Earth and Planetary Science Letters* 231, 221–237.
- Smithies, R.H., Van Kranendonk, M.J., Champion, D.C., 2005b. It started with a plume – early Archean basaltic proto-continental crust. *Earth and Planetary Science Letters* 238, 284–297.
- Solomon, S.C., Aharonson, O., Aurnou, J.M., Banerdt, W.B., Carr, M.H., Dombard, A.J., Frey, H.V., Golombek, M.P., Hauck, S.A., Head, J.W., Jakosky, B.M., Johnson, C.L., McGovern, P.J., Neumann, G.A., Phillips, R.J., Smith, D.E., Zuber, M.T., 2005. New Perspectives on Ancient Mars. *Science* 307, 1214–1220.
- Southgate, P.N., 1980. Cambrian stromatolitic phosphorites from the Georgina Basin, Australia. *Nature* 285, 395–397.
- Sproule, R.A., Leshner, C., Ayer, J.A., Thurston, P.C., Herzberg, C.T., 2002. Spatial and temporal variations in the geochemistry of komatiites and komatiitic basalts in the Abitibi greenstone belt. *Precambrian Research* 115, 153–186.

- Squire, R.J., Campbell, I.H., Allen, C.M., Wilson, C.J.L., 2006. Did the Transgondwanan Supermountain trigger the explosive radiation of animals on Earth? *Earth and Planetary Science Letters* 250, 116–133.
- Sreenivas, B., Das Sharma, S., Kumar, B., Patil, D.J., Roy, A.B., Srinivasan, R., 2001. Positive $\delta^{13}\text{C}$ excursion in carbonate and organic fractions from the Paleoproterozoic Aravalli Supergroup, Northwestern India. *Precambrian Research* 106, 277–290.
- Stein, M., Hofmann, A.W., 1994. Mantle plumes and episodic crustal growth. *Nature* 372, 63–68.
- Steiner, M., Zhu, M., Li, G., Qian, Y., Erdtmann, B.-D., 2004. New Early Cambrian bilateran embryos and larvae from China. *Geology* 32, 833–836.
- Steinhefel, G., Horn, I., von Blanckenburg, F., 2009. Micro-scale tracing of Fe and Si isotope signatures in banded iron formation using femto-second laser ablation. *Geochimica et Cosmochimica Acta* 73, 5343–5360.
- Stern, R.A., Bleeker, W., 1998. Age of the World's oldest rocks refined using Canada's SHRIMP: The Acasta Gneiss Complex, Northwest Territories, Canada. *Geoscience Canada* 25, 27–31.
- Stern, R.A., Machado, N., Syme, E.C., Lucas, S.B., David, J., 1999. Chronology of crustal growth and recycling in the Paleoproterozoic Amisk collage (Flin Flon Belt), Trans-Hudson Orogen, Canada. *Canadian Journal of Earth Sciences* 36, 1807–1827.
- Stern, R.J., 2005. Evidence from ophiolites, blueschists, and ultrahigh-pressure metamorphic terranes that the modern episode of subduction tectonics began in Neoproterozoic time. *Geology* 33, 557–560.
- Stetter, K.O., Gaag, G., 1983. Reduction of molecular sulfur by methanogenic bacteria. *Nature* 305, 309–311.
- Stetter, K.O., 1996. Hyperthermophiles in the history of life. In: Bock, G.R., Goode, J.A. (Eds.), *Evolution of hydrothermal systems on Earth (and Mars?)*. John Wiley & Sons, Chichester, pp. 1–10.
- Stockwell, C.H., 1961. Structural provinces, orogenies and time classification of rocks of the Canadian Shield. *Geological Survey of Canada, Paper 61*, 108–118.
- Stockwell, C.H., 1973. Revised Precambrian timescale for the Canadian Shield. *Geological Survey of Canada, Paper 72*, p. 4.
- Stockwell, C.H., 1982. Proposals for time classifications and correlations of Precambrian rocks and events in Canada and adjacent areas of the Canadian Shield: Part 1: A time classification of Precambrian rocks and events. *Geological Survey of Canada, Paper 80*, p. 135.
- Stöffler, D., Ryder, G., Ivanov, B.A., Artemieva, N.A., Contala, M.J., Grieve, R.A.F., 2006. Cratering history and Lunar chronology. *Reviews in Mineralogy and Geochemistry* 60, 519–596.
- Strik, G.M.H.A., Blake, T.S., Zegers, T.E., White, S.H., Langereis, C.G., 2003. Paleomagnetism of flood basalts in the Pilbara Craton, Western Australia: Late Archaean continental drift and the oldest known reversal of the geomagnetic field. *Journal of Geophysical Research* 108 (2551), p. 21.
- Sugitani, K., Grey, K., Allwood, A., Nagaoka, T., Mimura, K., Minami, M., Marshall, C.P., Van Kranendonk, M.J., Walter, M.R., 2007. Diverse microstructures from Archean chert from the Mount Goldsworthy – Mount Grant area, Pilbara Craton, Western Australia: Microfossils, dubiofossils, or pseudofossils? *Precambrian Research* 158, 228–262.
- Sugitani, K., Lepot, K., Nagaoka, T., Mimura, K., Van Kranendonk, M.J., Oehler, D.Z., Walter, M.R., 2010. Biogenicity of morphologically diverse carbonaceous microstructures from the ca. 3400 Ma Strelley Pool Formation, in the Pilbara Craton, Western Australia. *Astrobiology* 10, 899–920.
- Sumner, D.Y., Kirschvink, J.L., Runnegar, B.N., 1987. Soft-sediment paleomagnetic fold tests of late Precambrian glaciogenic sediments. *Eos* 68, 1251.
- Sumner, D.Y., Grotzinger, J.P., 2000. Late Archean aragonite precipitation: Petrographic, facies associations, and environmental significance. In: Grotzinger, J.P., James, N.P. (Eds.), *Carbonate sedimentation and diagenesis in the evolving Precambrian World*. Society for Sedimentary Geology, Special Publication, 67, pp. 123–144.
- Sumner, D.Y., Grotzinger, J.P., 2004. Implications for Neoproterozoic ocean chemistry from primary carbonate mineralogy of the Campbellrand-Malmani Platform, South Africa. *Sedimentology* 51, 1273–1299.
- Sun, S.F., Zhu, S.X., 1998. Discovery of micropaleophytes from the Doucun subgroup (about 2400 Ma), Hutuo Group of Wutai Mountain. *Acta Micropaleontologica Sinica* 15, 286–293.
- Sylvester, P.J., Attoh, K., 1992. Lithostratigraphy and composition of 2.1 Ga greenstone belts of the West African Craton and their bearing on crustal evolution and the Archean-Proterozoic boundary. *Journal of Geology* 100, 377–393.
- Syme, E.C., Lucas, S.B., Bailes, A.H., Stern, R.A., 1999. Contrasting arc and MORB-like assemblages in the Paleoproterozoic Flin Flon Belt, Manitoba, and the role of intra-arc extension in localizing volcanic-hosted massive sulfide deposits. *Canadian Journal of Earth Sciences* 36, 1767–1788.
- Takehara, M., Komure, M., Kiyokawa, S., Horie, K., Yokoyama, K., 2010. Detrital zircon SHRIMP U–Pb age of the 2.3 Ga diamictites of the Meteorite Bore Member in south Pilbara, Western Australia. 5th International Archean Symposium, abstracts.
- Taylor, S.R., 2007. The formation of the Earth and Moon. In: Van Kranendonk, M.J., Smithies, R.H., Bennett, V. (Eds.), *Earth's Oldest Rocks. Developments in Precambrian Geology*, 15. Elsevier, Amsterdam, pp. 21–30.
- Taylor, S.R., McLennan, S.M., 1985. *The Continental Crust: its Composition and Evolution*. Blackwell Scientific Publications, Oxford, p. 312.
- Tessalina, S.G., Bourdon, B., Van Kranendonk, M., Birck, J.-L., Philippot, P., 2010. Influence of Hadean crust evident in basalts and cherts from the Pilbara Craton. *Nature Geoscience* 3, 214–217.
- Thomazo, C., Ader, M., Philippot, P., 2011. Extreme ^{15}N -enrichments in 2.72-Gyr-old sediments: evidence for a turning point in the nitrogen cycle. *Geobiology* 9, 107–120.
- Tice, M.M., Lowe, D.R., 2004. Photosynthetic microbial mats in the 3,416-Myr-old ocean. *Nature* 431, 549–552.
- Tice, M.M., Lowe, D.R., 2006. The origin of carbonaceous matter in pre-3.0 Ga greenstone terrains: A review and new evidence from the 3.42 Ga Buck Reef Chert. *Earth-Science Reviews* 76, 259–300.
- Tomlinson, K.Y., Condie, K.C., 2001. Archean mantle plumes: Evidence from greenstone belt geochemistry. In: Ernst, R.E., Buchan, K.L. (Eds.), *Mantle plumes: Their identification through time*. Geological Society of America, Special Paper, 352, pp. 341–358.
- Toubol, M., Kleine, T., Bourdon, B., Palme, H., Wieler, R., 2007. Late formation and prolonged differentiation of the Moon inferred from W isotopes in lunar metals. *Nature* 450, 1206–1209.
- Towe, K.M., 1990. Aerobic respiration in the Archaean? *Nature* 348, 54–56.
- Trendall, A.F., Blockley, J.G., 1970. The iron formations of the Precambrian Hamersley Group, Western Australia. *Geological Survey of Western Australia, Bulletin* 119, p. 366.
- Trendall, A.F., 1972. Revolution in Earth history. *Journal of the Geological Society of Australia* 19, 287–311.


- Trendall, A.F., 1981. The Lower Proterozoic Meteorite Bore Member, Hamersley Basin, Western Australia. In: Hambrey, M.J., Harland, W.B. (Eds.), *Earth's pre-Pleistocene glacial record*. Cambridge University Press, New York, pp. 555–557.
- Trendall, A.F., Blockley, J.G., 2004. Precambrian Iron-Formation. In: Eriksson, P.G., Altermann, W., Nelson, D.R., Mueller, W.U., Catuneau, O. (Eds.), *The Precambrian Earth: Tempos and Events*. Developments in Precambrian Geology, 12. Elsevier, Amsterdam, pp. 403–421.
- Trendall, A.J., Compston, W., Nelson, D.R., de Laeter, J.R., Bennett, V.C., 2004. SHRIMP zircon ages constraining the depositional chronology of the Hamersley Group, Western Australia. *Australian Journal of Earth Sciences* 51, 621–644.
- Trindade, R.I.F., Macouin, M., 2007. Paleolatitude of glacial deposits and paleogeography of Neoproterozoic ice ages. *Comptes rendus: Geoscience* 339, 200–211.
- Trofimovs, J., Bavis, B.K., Cas, R.A.F., 2004. Contemporaneous ultramafic and felsic intrusive and extrusive magmatism in the Archaean Boorara Domain, Eastern Goldfields Superterrane, Western Australia, and its implications. *Precambrian Research* 131, 283–305.
- Tsiganis, K., Gomes, R., Morbidelli, A., Levison, H.F., 2005. Origin of the orbital architecture of the giant planets of the Solar System. *Nature* 435, 459–461.
- Tsikos, H., Matthews, A., Erel, Y., Moore, J.M., 2010. Iron isotopes constrain biogeochemical redox cycling of iron and manganese in a Paleoproterozoic stratified basin. *Earth and Planetary Science Letters* 298, 125–134.
- Turcotte, D.L., Morein, G., Malamud, B.D., 1999. Catastrophic resurfacing and episodic subduction on Venus. *Icarus* 139, 49–54.
- Twist, D., Cheney, E.S., 1986. Evidence for the transition to an oxygen-rich atmosphere in the Rooiberg Group, South Africa – A note. *Precambrian Research* 33, 255–264.
- Ueno, Y., Isozaki, Y., Yurimoto, H., Maruyama, S., 2001. Carbon isotopic signatures of individual Archean microfossils(?) from Western Australia. *International Geological Review* 40, 196–212.
- Ueno, Y., Yoshioka, H., Maruyama, S., Isozaki, Y., 2004. Carbon Isotopes and petrography of kerogens in ~3.5Ga hydrothermal silica dikes in the North Pole area, Western Australia. *Geochimica et Cosmochimica Acta* 68, 573–589.
- Ueno, Y., Yamada, K., Yoshida, N., Maruyama, S., Isozaki, Y., 2006. Evidence from fluid inclusions for microbial methanogenesis in the early Archean era. *Nature* 440, 516–519.
- Ullmer, E., 1981. A mid-Proterozoic phosphate occurrence in east-central Minnesota. *IGCP 156 Newsletter* 8, 22–25.
- Ullmer, E., 1985. The results of exploration for unconformity-type uranium deposits in east-central Minnesota. *Economic Geology* 80, 1425–1435.
- Upadhyay, D., Schere, E.E., Mezger, K., 2009. ^{142}Nd evidence for an enriched Hadean reservoir in cratonic roots. *Nature* 459, 1118–1121.
- Ushikubo, T., Kita, N.T., Cavosie, A.J., Wilde, S.A., Rudnick, R.L., Valley, J.W., 2008. Lithium in Jack Hills zircons: Evidence for extensive weathering of Earth's earliest crust. *Earth and Planetary Science Letters* 272, 666–676.
- Utsunomiya, S., Murakami, T., Nakada, M., Kasama, T., 2003. Iron oxidation state of a 2.45-Byr-old paleosol developed on mafic volcanics. *Geochimica et Cosmochimica Acta* 67, 213–221.
- Vaasjoki, M., Äikäs, O., Rehtijärvi, P., 1980. The age of mid-Proterozoic phosphatic metasediments in Finland as indicated by radiometric U-Pb dates. *Lithos* 13, 257–262.
- Valley, J.W., Peck, W.H., King, E.M., Wilde, S.A., 2002. A cool early Earth. *Geology* 30, 351–354.
- Valley, J.W., Lackey, J.S., Cavosie, A.J., Clechanko, C.C., J., S., Basei, M.A.S., Bindeman, I.N., Ferreira, V.P., Sial, A.N., King, E.M., Peck, W.H., Sinha, A.K., Wei, C.S., 2005. 4.4 billion years of crustal maturation: oxygen isotope ratios of magmatic zircon. *Contributions to Mineralogy and Petrology* 150, 561–580.
- Vallini, D.A., Cannon, W.C., Schulz, K.J., 2006. Age constraints for Paleoproterozoic glaciation in the Lake Superior region: detrital zircon and hydrothermal xenotime ages for the Chocoy Group, Marquette Range Supergroup. *Canadian Journal of Earth Sciences* 43, 571–591.
- Van Cappellen, P., Ingall, E.D., 1994. Benthic phosphorus regeneration, net primary production, and ocean anoxia: A model of the coupled marine biogeochemical cycles of carbon and phosphorus. *Paleoceanography* 9, 677–692.
- Van Hunen, J., van den Berg, A.P., 2008. Plate tectonics on the early Earth: Limitations imposed by strength and buoyancy of subducted lithosphere. *Lithos* 103, 217–235.
- Van Kranendonk, M.J., 1999. North Shaw, W.A. Western Australia Geological Survey, Geological Series 2755 scale 1:100 000.
- Van Kranendonk, M.J., 2004. Archaean tectonics 2004: a review. *Precambrian Research* 131, 143–151.
- Van Kranendonk, M.J., 2006. Volcanic degassing, hydrothermal circulation and the flourishing of early life on Earth: new evidence from the Warawoona Group, Pilbara Craton, Western Australia. *Earth-Science Reviews* 74, 197–240.
- Van Kranendonk, M.J., 2007a. Tectonics of early Earth. In: Van Kranendonk, M.J., Smithies, R.H., Bennet, V. (Eds.), *Earth's Oldest Rocks*. Developments in Precambrian Geology, 15. Elsevier, Amsterdam, pp. 1105–1116.
- Van Kranendonk, M.J., 2007b. A review of the evidence for putative Paleoproterozoic life in the Pilbara Craton. In: Van Kranendonk, M.J., Smithies, R.H., Bennet, V. (Eds.), *Earth's Oldest Rocks*. Developments in Precambrian Geology, 15. Elsevier, Amsterdam, pp. 855–896.
- Van Kranendonk, M.J., 2008. A chronostratigraphic division of the Precambrian: possibilities and challenges. 33rd International Geological Congress Oslo. Abstracts on CD-ROM available online at: <http://www.cprm.gov.br/33IGC/1339910.html>.
- Van Kranendonk, M.J., 2010a. Stromatolite morphology as an indicator of biogenicity for Earth's oldest fossils from the 3.5–3.4 Ga Pilbara Craton, Western Australia. In: Reitner, J., Queric, N.-V., Arp, G. (Eds.), *Advances in Stromatolite Geobiology*. Lecture Notes in Earth Sciences, 131, p. 200.
- Van Kranendonk, M.J., 2010b. Three and a half billion years of life on Earth: a transect back into deep time. *Geological Survey of Western Australia, Record* 2010/21, 93.
- Van Kranendonk, M.J., 2011. Two types of Archean continental crust: Plume and plate tectonics on early Earth. *American Journal of Science* 310, 1187–1209.
- Van Kranendonk, M.J., Smithies, R.H., Hickman, A.H., Champion, D.C., 2007a. Secular tectonic evolution of Archean continental crust: interplay between horizontal and vertical processes in the formation of the Pilbara Craton, Australia. *Terra Nova* 19, 1–38.
- Van Kranendonk, M.J., Hickman, A., Smithies, R.H., 2007b. The East Pilbara Terrane of the Pilbara Craton, Western Australia: formation of a continental nucleus through repeated mantle plume magmatism. In: Van Kranendonk, M.J., Smithies, R.H., Bennet, V. (Eds.), *Earth's Oldest*

- Rocks. *Developments in Precambrian Geology*, 15. Elsevier, Amsterdam, pp. 307–337.
- Van Kranendonk, M.J., Gehling, J., Shields, G., 2008a. Precambrian. In: Ogg, J.G., Ogg, G., Gradstein, F.M. (Eds.), *The Concise Geological Timescale*. Cambridge University Press, pp. 23–36.
- Van Kranendonk, M.J., Philippot, P., Lepot, K., Bodorkos, S., Pirajno, F., 2008b. Geological setting of Earth's oldest fossils in the c. 3.5 Ga Dresser Formation, Pilbara Craton, Western Australia. *Precambrian Research* 167, 93–124.
- Van Kranendonk, M.J., Kröner, A., Hegner, E., Connelly, J., 2009. Age, lithology and structural evolution of the c. 3.53 Ga Theespruit Formation in the Tjakastad area, southwestern Barberton Greenstone Belt, South Africa, with implications for Archean tectonics. *Chemical Geology* 261, 114–138.
- Van Kranendonk, M.J., Smithies, R.H., Hickman, A.H., Wingate, M.T.D., Bodorkos, S., 2010. Evidence for Mesoarchean (~3.2 Ga) rifting of the Pilbara Craton: The missing link in an early Precambrian Wilson cycle. *Precambrian Research* 177, 145–161.
- Van Zuilen, M.A., Lepland, A., Arrhenius, G., 2002. Reassessing the evidence for the earliest traces of life. *Nature* 418, 627–630.
- Van Zuilen, M.A., Lepland, A., Teranes, J., Finarelli, J., Wahlen, M., Arrhenius, G., 2003. Graphite and carbonates in the 3.8 Ga old Isua supracrustal belt, southern West Greenland. *Precambrian Research* 126, 331–348.
- Vantongeren, J.A., Mathez, E.A., Kelemen, P.B., 2010. A felsic end to Bushveld differentiation. *Journal of Petrology* 51, 1891–1912.
- Vargas, M., Kashefi, K., Blunt-Harris, E.L., Lovley, D.R., 1998. Microbiological evidence for Fe(III) reduction on early Earth. *Nature* 395, 65–67.
- Veeh, H.H., Burnett, W.C., Soutar, A., 1973. Contemporary phosphorite on the continental margin of Peru. *Science* 181, 844–845.
- Veizer, J., Compston, W., Clauer, N., Schidlowski, M., 1983. $^{87}\text{Sr}/^{86}\text{Sr}$ in Late Proterozoic carbonates: evidence for a “mantle” event at ~900 Ma ago. *Geochimica et Cosmochimica Acta* 47, 295–302.
- Veizer, J., Hoefs, J., Lowe, D.R., Thurston, P.C., 1989. Geochemistry of Precambrian carbonates II. Archean greenstone belts and Archean seawater. *Geochimica et Cosmochimica Acta* 53, 859–871.
- Veizer, J., Ala, D., Azmy, K., Bruckschen, P., Buhl, D., Bruhn, F., Carden, G.A.F., Diener, A., Ebner, S., Godderis, Y., Jasper, T., Korte, C., Pawellek, F., Podlaha, O.G., Strauss, H., 1999. $^{87}\text{Sr}/^{86}\text{Sr}$, $\delta^{13}\text{C}$ and $\delta^{18}\text{O}$ evolution of Phanerozoic seawater. *Chemical Geology* 161, 59–88.
- Vervoort, J.D., Blichert-Toft, J., 1999. Evolution of the depleted mantle: Hf isotope evidence from juvenile rocks through time. *Geochimica et Cosmochimica Acta* 63, 533–556.
- Viljoen, M.J., Viljoen, R.P., 1969. The geology and geochemistry of the lower ultramafic unit of the Onverwacht Group and a proposed new class of igneous rocks. *Geological Society of South Africa, Special Publication* 2, 55–86.
- Visser, J.N.J., 1971. The deposition of the Griquatown glacial member in the Transvaal Supergroup. *Transactions of the Geological Society of South Africa* 74, 187–199.
- Vlaar, N.J., 2000. Continental emergence and growth on a cooling Earth. *Tectonophysics* 322, 191–202.
- Vogel, D.C., James, R.S., Keays, R.R., 1998. The early tectono-magmatic evolution of the Southern Province: implications from the Agnew Intrusion, central Ontario, Canada. *Canadian Journal of Earth Sciences* 35, 854–870.
- Von Brunn, V., Gold, D.J.C., 1993. Diamictite in the Archaean Pongola Sequence of southern Africa. *Journal of African Earth Sciences* 16, 367–374.
- Vuollo, J., Huhma, H., 2005. Paleoproterozoic mafic dykes in NE Finland. In: Lehtinen, M., Nurmi, P.A., Ramo, O.T. (Eds.), *Precambrian geology of Finland – key to the evolution of the Fennoscandian Shield*. Elsevier, Amsterdam, pp. 193–235.
- Wacey, D., McLoughlin, N., Whitehouse, M.J., Kilburn, M.R., 2010. Two coexisting sulphur metabolisms in a ca. 3400 Ma sandstone. *Geology* 38, 1115–1118.
- Wächtershäuser, W., 2006. From volcanic origins of chemoautotrophic life to bacteria, archaean and eukarya. *Philosophical Transactions of the Royal Society of London, Series B* 361, 1787–1806.
- Wadhwa, M., Amelin, Y., Bogdanovski, O., Shukolyukov, A., Lugmair, G.W., Janney, P., 2009. Ancient relative and absolute ages for a basaltic meteorite: Implications for timescales of planetesimal accretion and differentiation. *Geochimica et Cosmochimica Acta* 73, 5189–5201.
- Waldbauer, J.R., Sherman, L.S., Sumner, D.Y., Summons, R.E., 2009. Late Archean molecular fossils from the Transvaal Supergroup record the antiquity of microbial diversity and aerobiosis. *Precambrian Research* 169, 28–47.
- Walker, J.C.G., 1977. *Evolution of the Atmosphere*. MacMillan, New York.
- Walker, J.C.G., Brimblecombe, P., 1985. Iron and sulfur in the pre-biologic ocean. *Precambrian Research* 28, 205–222.
- Walker, J.C.G., 1987. Was the Archaean biosphere upside down? *Nature* 329, 710–712.
- Walraven, F., Pape, J., 1994. Pb-Pb whole-rock ages for the Pongola Supergroup and the Usushwana Complex, South Africa. *Journal of African Earth Sciences* 18, 297–308.
- Walsh, M.M., Lowe, D.R., 1985. Filamentous microfossils from the 3,500-Myr-old Onverwacht Group, Barberton Mountain Land, South Africa. *Nature* 314, 530–532.
- Walsh, M.M., 1992. Microfossils and possible microfossils from the Early Archean Onverwacht Group, Barberton Mountain Land, South Africa. *Precambrian Research* 54, 271–293.
- Walter, M.J., Trönes, R.G., 2004. Early Earth differentiation. *Earth and Planetary Science Letters* 225, 253–269.
- Walter, M.R., Oehler, J.H., Oehler, D.Z., 1976. Megascopic algae 1300 million years old from the Belt Supergroup, Montana: a reinterpretation of Walcott's Helminthoidischniter. *Journal of Paleontology* 50, 872–881.
- Walter, M.R., Buick, R., Dunlop, J.S.R., 1980. Stromatolites 3400–3500 Myr old from the North Pole area, Western Australia. *Nature* 248, 443–445.
- Walter, M.R., 1983. Archean stromatolites: Evidence of the Earth's earliest benthos. In: Schopf, J.W. (Ed.), *Earth's earliest biosphere: its origin and evolution*. Princeton University Press, Princeton, pp. 187–213.
- Wang, J., Li, Z.-X., 2003. History of Neoproterozoic rift basins in South China: implications for Rodinia break-up. *Precambrian Research* 122, 141–158.
- Wang, J., Jiang, G., Xiao, S., Li, Q., Wei, Q., 2008. Carbon isotope evidence for widespread methane seeps in the ca. 635 Ma Doushantuo cap carbonate in south China. *Geology* 36, 347–350.
- Wang, X., Hu, S., Gan, L., Wiens, M., Müller, W.E.G., 2009. Sponges (Porifera) as living metazoan witnesses from the Neoproterozoic: biomineralization and the concept of their evolutionary success. *Terra Nova* 22, 1–11.

- Wang, Y., Xu, H., Merino, E., Konishi, H., 2009. Generation of banded iron formations by internal dynamics and leaching of oceanic crust. *Nature Geoscience* 2, 781–784.
- Wang, Z., Wilde, S.A., Wan, J., 2010. Tectonic setting and significance of 2.3–2.1 Ga magmatic events in the Trans-North China Orogen: New constraints from the Yanmenguan mafic-ultramafic intrusion in the Hengshan-Wutai-Fuping area. *Precambrian Research* 178, 27–42.
- Wanke, A., Melezhik, V.A., 2005. Sedimentary and volcanic facies recording the Neoproterozoic continent breakup and decline of the positive $\delta^{13}\text{C}_{\text{carb}}$ excursion. *Precambrian Research* 140, 1–35.
- Wardle, R.J., Gower, C.F., James, D.T., St-Onge, M.R., Scott, D.J., Garde, A.A., Culshaw, N.G., van Gool, J.A.M., Connelly, J.N., Perreault, S., Hall, J., 2002. Correlation chart of the Proterozoic assembly of the northeastern Canadian – Greenland Shield. *Canadian Journal of Earth Sciences* 39, 895.
- Whitehouse, M.J., Fedo, C.M., 2007a. Microscale heterogeneity of Fe isotopes in >3.71 Ga banded iron formation from the Isua Greenstone Belt, southwest Greenland. *Geology* 35, 719–722.
- Whitehouse, M.J., Fedo, C.M., 2007b. Searching for Earth's earliest life in southern West Greenland – History, current status, and future prospects. In: Van Kranendonk, M.J., Smithies, R.H., Bennet, V. (Eds.), *Earth's Oldest Rocks. Developments in Precambrian Geology*, 15. Elsevier, Amsterdam, pp. 841–854.
- Widdel, F., Schnell, S., Heising, S., Ehrenreich, A., Assmus, B., Schink, B., 1993. Ferrous iron oxidation by anoxygenic phototrophic bacteria. *Nature* 362, 834–836.
- Wiechert, U., Halliday, A.N., Lee, D.C., Snyder, G.A., Talyor, L.A., Rumble, D., 2001. Oxygen isotopes and the moon-forming giant impact. *Science* 294, 345–348.
- Wiggering, H., Beukes, N.J., 1990. Petrography and geochemistry of a 2000–2200-Ma-old hematitic paleo-alteration profile on Ongeluk Basalt of the Transvaal Supergroup, Griqualand West, South Africa. *Precambrian Research* 46, 241–258.
- Wilde, S.A., Valley, J.W., Peck, W.H., Graham, C.M., 2001. Evidence from detrital zircons for the existence of continental crust and oceans on the Earth 4.4 Gyr ago. *Nature* 409, 175–178.
- Wille, M., Kramers, J.D., Nägler, T.F., Beukes, N.J., Schröder, S., Meisel, T., Lacassie, J.P., Voegelin, A.R., 2007. Evidence for a gradual rise of oxygen between 2.6 and 2.5 Ga from Mo isotopes and Re-PGE signatures in shales. *Geochimica et Cosmochimica Acta* 71, 2417–2435.
- Williams, D.M., Kasting, J.F., Frakes, L.A., 1998. Low-latitude glaciation and rapid changes in the Earth's obliquity explained by obliquity-oblateness feedback. *Nature* 396, 453–455.
- Williams, G.E., 1975. Possible relation between periodic glaciation and the flexure of the galaxy. *Earth and Planetary Science Letters* 26, 361–369.
- Williams, G.E., 1993. History of the Earth's obliquity. *Earth Science Reviews* 112, 1–45.
- Williams, G.E., Schmidt, P.W., 1997. Paleomagnetism of the Paleoproterozoic Gowganda and Lorrain formations, Ontario: low paleolatitude for Huronian glaciation. *Earth and Planetary Science Letters* 153, 157–169.
- Williams, G.E., Schmidt, P.W., 2004. Paleomagnetism of the 1.88-Ga Sokoman Formation in the Schefferville-Knob Lake area, Québec, Canada, and implications for the genesis of iron oxide deposits in the central New Québec Orogen. *Precambrian Research* 128, 167–188.
- Williford, K.H., Van Kranendonk, M.J., Ushikubo, T., Kozdon, R., Valley, J.W., 2011. Constraining atmospheric oxygen and seawater sulfate concentrations during Paleoproterozoic glaciation: in situ sulfur three isotope microanalysis of pyrite from the Turee Creek Group, Western Australia. *Geochimica et Cosmochimica Acta* 75 (19), 5686–5705.
- Wilson, A.H., Shirey, S.B., Carlson, R.W., 2003. Archean ultra-depleted komatiites formed by hydrous melting of cratonic mantle. *Nature* 423, 858–861.
- Wilson, J.P., Fischer, W.W., Johnston, D.T., Knoll, A.H., Grotzinger, J.P., Walter, M.R., McNaughton, N.J., Simon, M., Abelson, J., Schrag, D.P., Summons, R., Alwood, A., Andres, M., Gammon, C., Garvin, J.S.R., Schweizer, M., Watters, W.A., 2010. Geobiology of the late Paleoproterozoic Duck Creek Formation, Western Australia. *Precambrian Research* 179, 135–149.
- Windley, B.F., Bridgwater, D., 1971. The evolution of Archean low- and high-grade terrains. *Geological Society of Australia, Special Publication* 3, 33–46.
- Windley, B.F., 1993. Proterozoic anorogenic magmatism and its orogenic connections. *Journal of the Geological Society of London* 150, 39–50.
- Windley, B.F., 1995. *The evolving continents*, third ed. John Wiley & Sons, Chichester, p. 526.
- Windley, B.F., Garde, A.A., 2009. Arc-generated blocks with crustal sections in the North Atlantic craton of West Greenland: Crustal growth in the Archean with modern analogues. *Earth-Science Reviews* 93, 1–30.
- Wingate, M.T.D., Giddings, J.W., 1999. Age and paleomagnetism of the Mundine Well dyke swarm, Western Australia: implications for an Australia-Laurentia connection at 755 Ma. *Precambrian Research* 100, 335–357.
- Wingate, M.T.D., 2000. Ion microprobe U-Pb zircon and baddelyite ages for the Great Dyke and its satellite dykes, Zimbabwe. *South African Journal of Earth Sciences* 103, 74–80.
- de Wit, M.J., Hart, R.A., 1993. Earth's earliest continental lithosphere, hydrothermal flux and crustal recycling. *Lithos* 30, 309–335.
- Wood, B.J., Nielsen, S.G., Rehkämper, M., Halliday, A.N., 2008. The effect of core formation on the Pb- and Tl-isotopic composition of the silicate Earth. *Earth and Planetary Science Letters* 269, 325–335.
- Wyche, S., 2007. Evidence of pre-3100 Ma crust in the Youanmi and South West Terranes, and Eastern Goldfields Superterrane, of the Yilgarn Craton. In: Van Kranendonk, M.J., Smithies, R.H., Bennet, V. (Eds.), *Earth's Oldest Rocks. Developments in Precambrian Geology*, 15. Elsevier, Amsterdam, pp. 113–124.
- Wyman, D.A., Kerrich, R., Polat, A., 2002. Assembly of Archean cratonic mantle lithosphere and crust: plume-arc interaction in the Abitibi-Wawa subduction-accretion complex. *Precambrian Research* 115, 37–62.
- Xiao, S., Zhang, Y., Knoll, A.H., 1998. Three-dimensional preservation of algae and animal embryos in a Neoproterozoic phosphorite. *Nature* 391, 553–558.
- Xiao, S., Hagadorn, J.W., Zhou, C., Yuan, X., 2007. Rare helical spheroidal fossils from the Doushantuo Lagerstätte: Ediacaran animal embryos come of age? *Geology* 35, 115–118.
- Yamaguchi, K.E., Johnson, C.M., Beard, B.L., Ohmoto, H., 2005. Biogeochemical cycling of iron in the Archean-Paleoproterozoic Earth: constraints from iron isotope variations in sedimentary rocks from the Kaapvaal and Pilbara Cratons. *Chemical Geology* 218, 135–169.
- Yang, W., Holland, H.D., Rye, R., 2002. Evidence for low or no oxygen in the late Archean atmosphere from the ~2.76 Ga Mt. Roe #2 paleosol, Western Australia: Part 3. *Geochimica et Cosmochimica Acta* 66, 3707–3718.

- Yang, W., Holland, H.D., 2003. The Hekpoort paleosol profile in Strata 1 at Gabarone, Botswana: soil formation during the Great oxidation Event. *American Journal of Science* 303, 187–220.
- Yanshin, A.L., 1986. Proterozoic and Cambrian phosphorites – regional review: Asian part of USSR and Mongolian People's Republic. In: Cook, P.J., Shergold, J.H. (Eds.), *Phosphate Deposits of the World*. vol. 1, Proterozoic and Cambrian Phosphorites. Cambridge University Press, Cambridge, pp. 63–69.
- Yin, L., Zhu, M., Knoll, A.H., Yuan, X., Zhang, J., Hu, J., 2007. Doushantuo embryos preserved inside diapause egg cysts. *Nature* 446, 661–663.
- Young, G.M., Gostin, V.A., 1991. Late Proterozoic (Sturtian) succession of the North Flinders Basin, South Australia: an example of temperate glaciation in an active rift setting. In: Anderson, J.B., Ashley, G.M. (Eds.), *Glacial marine sedimentation: paleoclimatic significance*. Geological Society of America, Special Paper, 261, pp. 207–223.
- Young, G.M., 1995. Are Neoproterozoic glacial deposits preserved on the margins of Laurentia related to the fragmentation of two supercontinents? *Geology* 23, 153–156.
- Young, G.M., von Brunn, V., Gold, D.J.C., Minter, W.E.L., 1998. Earth's oldest reported glaciation: physical and chemical evidence from the Archean Mozaan Group (~2.9 Ga) of South Africa. *Journal of Geology* 106, 523–538.
- Young, G.M., Nesbitt, H.W., 1999. Paleoclimatology and provenance of the glaciogenic Gowganda Formation (Paleoproterozoic), Ontario, Canada: a chemostratigraphic approach. *Geological Society of America Bulletin* 111, 264–274.
- Young, G.M., 2002. Stratigraphic and tectonic settings of Proterozoic glaciogenic rocks and banded iron-formations: relevance to the snowball Earth debate. *Journal of African Earth Sciences* 35, 451–466.
- Yuan, X., Xiao, S., Taylor, T.N., 2005. Lichen-like symbiosis 600 million years ago. *Science* 308, 1017–1020.
- Yuan, X., Chen, Z., Xiao, S., Zhou, C., Hua, H., 2011. An early Ediacaran assemblage of macroscopic and morphologically differentiated eukaryotes. *Nature* 470, 390–393.
- Yudin, N.I., 1996. Pre-Riphean phosphate genesis. *Lithology and Mineral Resources* 31, 286–292.
- Yueyan, L., 1986. Proterozoic and Cambrian phosphorites – regional review: China. In: Cook, P.J., Shergold, J.H. (Eds.), *Phosphate Deposits of the World*. vol. 1, Proterozoic and Cambrian Phosphorites. Cambridge University Press, Cambridge, pp. 42–62.
- Zahnle, K., Claire, M., Catling, D., 2006. The loss of mass-independent fractionation in sulfur due to a Palaeoproterozoic collapse of atmospheric methane. *Geobiology* 4, 271–283.
- Zahnle, K., Arndt, N., Cockell, C., Halliday, A., Nisbet, E., Selsis, F., Sleep, N.H., 2007. Emergence of a habitable planet. *Space Science Reviews* 129, 35–78.
- Zalasiewicz, J., Smith, A., Brenchley, P., Evans, J., Knox, R., Riley, N., Gale, A.S., Gregory, F.J., Rushton, A., Gibbard, P., Hesselbo, S.P., Marshall, J., Oates, M., Rawson, P., Trewin, N., 2004. Simplifying the stratigraphy of time. *Geology* 32, 1–4.
- Zhang, S., Jiang, G., Han, Y., 2008. The age of the Nantuo Formation and Nantuo glaciation in South China. *Terra Nova* 20, 289–294.
- Zhang, Y., 2002. The age and accretion of the Earth. *Earth-Science Reviews* 59, 235–263.
- Zhao, G., Cawood, P.A., Wilde, S.A., Sun, M., 2002. Review of global 2.1–1.8 Ga orogens: implications for a pre-Rodinia supercontinent. *Earth-Science Reviews* 59, 125–162.
- Zhao, G., Wilde, S.A., Sun, M., Li, S., Li, X., Zhang, J., 2008. SHRIMP U-Pb zircon ages of granitoid rocks in the Lülilian Complex: Implications for the accretion and evolution of the Trans-North China Orogen. *Precambrian Research* 160, 213–226.
- Zhu, S., Chen, H., 1995. Megascopic multicellular organisms from the 1700–Million-year-old Tuanshanzi Formation in the Jixian area, North China. *Science* 270, 620–622.

AUTHOR QUERY FORM

	<p>Book: GRADSTEIN-9780444594259</p> <p>Chapter: 16</p>	<p>Please e-mail your responses and any corrections to: E-mail: P.Wilkinson@Elsevier.com</p>
-----------------------------------------------------------------------------------	-----------------------------------------------------------------------	-----------------------------------------------------------------------------------------------------------------

Dear Author,

Any queries or remarks that have arisen during the processing of your manuscript are listed below and are highlighted by flags in the proof. (AU indicates author queries; ED indicates editor queries; and TS/TY indicates typesetter queries.) Please check your proof carefully and answer all AU queries. Mark all corrections and query answers at the appropriate place in the proof (e.g., by using on-screen annotation in the PDF file http://www.elsevier.com/framework_authors/tutorials/ePDF_voice_skin.swf) or compile them in a separate list, and tick off below to indicate that you have answered the query.

Please return your input as instructed by the project manager.

<p>Uncited reference: References that occur in the reference list but are not cited in the text. Please position each reference in the text or delete it from the reference list. NIL</p>		
<p>Missing reference: References listed below were noted in the text but are missing from the reference list. Please make the reference list complete or remove the references from the text. NIL</p>		
Location in Chapter	Query / Remark	
AU:1, page 319	“potassium-rich” might be a bit better	<input type="checkbox"/>
AU:2, page 360	Not in ref list; pls. supply	<input type="checkbox"/>
AU:3, page 363	I have no figure for this early fossil...MVK	<input type="checkbox"/>
AU:4, page 372	Not in ref list; pls. supply	<input type="checkbox"/>
AU:5, page 372	Not in ref list; pls. supply	<input type="checkbox"/>
AU:6, page 372	Not in ref list; pls. supply	<input type="checkbox"/>
AU:7, page 372	Not in ref list; pls. supply	<input type="checkbox"/>
AU:8, page 372	Not in ref list; pls. supply	<input type="checkbox"/>
AU:9, page 372	Föllmi 1996 Not in ref list; pls. supply	<input type="checkbox"/>
AU:10, page 372	Not in ref list; pls. supply	<input type="checkbox"/>

AU:11, page 372	Not in ref list; pls. supply	<input type="checkbox"/>
AU:12, page 372	Not in ref list; pls. supply	<input type="checkbox"/>
AU:13, page 376	Not in ref list; pls. supply	<input type="checkbox"/>
AU:14, page 376	Not in ref list; pls. supply	<input type="checkbox"/>
AU:15, page 376	Not in ref list; pls. supply	<input type="checkbox"/>
AU:16, page 376	Not in ref list; pls. supply	<input type="checkbox"/>
AU:17, page 377	Not in ref list; pls. supply	<input type="checkbox"/>
AU:18, page 377	Not in ref list; pls. supply	<input type="checkbox"/>
AU:19, page 377	Not in ref list; pls. supply	<input type="checkbox"/>
AU:20, page 377	Not in ref list; pls. supply	<input type="checkbox"/>
AU:21, page 387	Ref not cited in text; OK to delete?	<input type="checkbox"/>
AU:22, page 395	Ref not cited in text; OK to delete?	<input type="checkbox"/>
AU:23, page 399	Ref not cited in text; OK to delete?	<input type="checkbox"/>

Non-Print Items**Abstract:**

This chapter provides a review of events through Precambrian Earth history, with the aim of providing an up-to-date foundation on which to construct a chronostratigraphic revision of the Precambrian timescale. The guiding principles used to develop a revised Precambrian timescale follow Cloud's vision to "...seek trend-related events that have affected the entire Earth over relatively short intervals of time and left recognizable signatures in the rock sequences of the globe...", and apply Gould's historical principles of directionality and contingency.

Analysis of the Precambrian geological record reveals a series of linked, causative events over time that can be used as a basis for a more naturalistic timescale that better reflects our knowledge of events in the history of our planet and can be used as a template for further research. A revised Precambrian timescale envisages three eons:

- 1) A Hadean Eon, which extends from the time of formation of the solar system ($T_0 = 4567$ Ma), to the age of Earth's oldest rock (4030 Ma Acasta Gneiss);
- 2) An Archean Eon, extending from the top of the Hadean Eon to the time of the fundamental transition from an early, hotter, reducing Earth to a more modern, cooler, oxidized Earth, at c. 2420 Ma;
- 3) A Proterozoic Eon, from the c. 2420 Ma Archean-Proterozoic boundary to the base of the Phanerozoic Eon (542 Ma).

Each of the eons may be subdivided into a number of eras and periods that can each be marked by a chronostratigraphic Global Stratotype Section and Point (GSSP), excepting lowermost chronometric divisions of the Hadean Eon and Paleoproterozoic Era. Suggestions are presented for the age, name, and GSSP locality for each division.

Keywords: ■■■